Glucose oxidase induction and the modelling of gluconic acid production using *Aspergillus niger*

by

Kim Henry Silvanus Johnson

A thesis submitted in fulfilment of
the requirements of the degree of Master of Science
in Engineering in the Department of Chemical Engineering
University of Cape Town

Bioprocess Research Group
Department of Chemical Engineering
University of Cape Town

October 1995

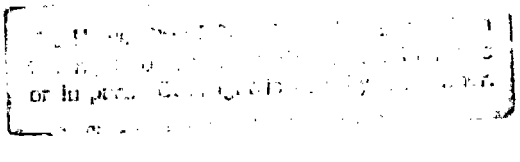

SYNOPSIS

The aim of this project is to establish and understand the production of glucose oxidase and gluconic acid using the *Aspergillus niger* bioprocess and predict its response to operating conditions. Glucose oxidase and gluconic acid are produced by a wide range of microbes and have a variety of applications. In this study *Aspergillus niger* was chosen as the microorganism as it has the "generally accepted as safe" (gras) status in the U.S.A. It is also the major industrial producer.

Glucose oxidase catalyses the conversion of glucose, oxygen and water to hydrogen peroxide and gluconic acid. This enzyme is used as a glucose and oxygen scavenger in the food industry and as a diagnostic tool in medicine for glucose determination.

Gluconic acid is an organic acid used as a sequestering agent with a broad spectrum of applications. The world market for gluconic acid and its various salts was 45 000 metric tonnes in 1985 (Bigelis cited by Markwell *et al.* 1989). Gluconic acid and its derivatives can be produced using three technologies: electrolysis, mild chemical oxidation and bioprocess. The first two technologies have not been proven to be commercially viable. The bioprocess offers diversity of feed and produces other products such as glucose oxidase.

Literature has shown that the production of gluconic acid involves two kinetic areas. Firstly, the glucose oxidase enzyme must be induced. Secondly, glucose is converted to gluconic acid by the enzyme glucose oxidase. The factors affecting the kinetics associated with the induction of glucose oxidase have only been described qualitatively. Glucose, oxygen and pH have been shown to affect the induction of glucose oxidase. The effect of pH has been studied by Roukas and Harvey (1989) who found that induction is maximal at a pH of between 5 and 6. The effect of glucose and oxygen have not been quantified. The kinetics of glucose oxidase conversion of glucose to gluconic acid have been well described by Atkinson and Lester (1974).

In order to quantify the effect of glucose and oxygen on the induction of glucose oxidase, a series of nine experiments were conducted. Inocula were grown in a non-inducing environment for three days and then transferred into a controlled inducing environment. The induction process of glucose oxidase and the formation of other related components were observed. The experiments were run at 50, 100 and 150 gl^{-1} glucose and 0.21, 0.75 and 1.00 atm oxygen forming a matrix of nine experiments.

It was found that at the three levels of oxygen used, glucose oxidase induction increased with increasing glucose concentration from 50 to 100 gl^{-1}. Further increase in glucose concentration to 150 gl^{-1} resulted in no further increase in glucose oxidase formation. It was also found that at each glucose level there was a corresponding optimum oxygen concentration for maximum glucose oxidase induction rate. Control of the dissolved oxygen level according to the glucose concentration during the bioprocess could result in higher glucose oxidase yields. Increasing the oxygen level from 0.21 atm to 1.00 atm oxygen, using an initial glucose concentration of 50 gl^{-1}, increased the glucose oxidase induction rate from 0.12 to 0.26 U/h and the final glucose oxidase activity from 1.3 U to 2.1 U. Similar increases were observed using as initial glucose concentration of 100 and 150 gl^{-1}. A maximum glucose oxidase induction rate of 0.34 U/h at 100 gl^{-1} and 1.00 atm oxygen and a maximum final glucose oxidase activity of 4.6 U at a glucose concentration of 100 gl^{-1} and 0.75 atm oxygen was observed.

The *A.niger* biosystem was modelled mechanistically accounting for subprocesses based on a comparison of their relaxation times with other subprocesses. The glucose oxidase enzyme kinetics were modelled using the Atkinson and Lester (1974) kinetic model. Oxygen mass transfer was modelled using two film theory. Biomass growth was modelled using logistic equation. The glucose oxidase induction was modelled using the gene operon theory (Imanaka *et al.* 1961).

A model using glucose oxidase induction as a function of glucose alone was fitted to a base case experiment at an initial glucose concentration of 100 gl^{-1} and 0.21 atm oxygen. The model includes glucose oxidase activity, gluconic acid concentration, dissolved oxygen concentration and biomass concentration profiles successfully. The parameters from this

model were then used to predict other experiments at different glucose concentrations. Prediction of glucose oxidase activity, gluconic acid production and dissolved oxygen concentration profiles at an initial concentration of 50 gl^{-1} glucose, and 0.21 atm oxygen was satisfactory. Prediction of the 150 gl^{-1} glucose experiment resulted in over-prediction of the glucose oxidase activity. It was postulated that the high glucose concentration caused an osmotic stress response and decreased the glucose oxidase production rate. This could be incorporated into the model by decreasing the mRNA production rate.

A second model based on glucose oxidase induction as a function of both glucose and oxygen was fitted to the same base case experiment and predictions made for the other eight inducing environments. This model could predict the glucose oxidase activity in the 50 gl^{-1} glucose experiments at 0.21 and 0.75 atm oxygen satisfactorily. Over-prediction of glucose oxidase activities at 150 gl^{-1} in all cases was observed although this could be corrected by decreasing the mRNA production rate. Gluconic acid production profiles were over-predicted at 0.75 atm oxygen experiments although the glucose oxidase activities were correctly predicted. The gluconic acid formation reaction may have been limited by diffusion resistances of glucose, oxygen or pH into the mycelial pellet. Glucose oxidase induction rates using 1.00 atm oxygen resulted in lower values than expected. This deviation was attributed to an oxygen toxicity effect.

ACKNOWLEDGEMENTS

I would like express my sincere thanks to the following people:

Dr S.T.L. Harrison, my M.Sc. supervisor for her support, guidance, training in research methodology and encouragement over the past two years.

The 'Biogroup' especially Jenny Löwenadler and Suzi Illing for teaching me biotechniques.

Dr. Ed. Merrifield and his team at Medical Biochemistry for help with HPLC work.

Laboratory manager Linda Harrower, Maria Josias and Jacqui Mshudulu for their help in the main laboratory.

Staff of the Chemical Engineering building: Granville de la Cruz, James Daniels, and John Jood for their job well done in cleaning and servicing our building.

Peter Tobias, Joachim Macke for help and patient assistance in the workshop.

The Beit Trust for their financial support over the past two years.

Family and friends for their continuous support.

GLOSSARY

Abs	Absorbance
Absorbance	A measure of the extent to which a beam of radiation, normally ultraviolet, visible and infrared, is attenuated by transmission through an absorbing medium, which can be a solid, liquid or solution, or gas. The absorbance (A) is defined as: $A = \log I_o/I$
ABTS	di-ammonium2,2'-azino-bis(3-ethylbenzothiazoline-6-sulfonate)
Active transport	The controlled movement of a solute across a biological membrane consuming energy.
Aeration	The introduction of air or oxygen into a liquid, fermenter, or activated sludge plant.
Agar	Also called agar-agar. A polysaccharide mixture isolated from certain agar bearing red algae, especially *Gelidium* and *Gracilaria* spp.
Air filter	A filter to remove microorganisms from an air stream connected to a fermenter, clean room or sterile cabinet.
Airlift reactor	Bioreactor designed for aerobic growth where agitation is provided solely by sparged air.
Antifoam agent	Surface-active agents used to reduce surface tension of foams formed on the surface of broths as a consequence of agitation and aeration.
Antioxidant	A substance that prevents or reduces oxidation especially of organic material. The mode of action depends on the mechanism involved. A chemical can be effective by being more easily oxidised than the product to be protected, or by deactivating catalysis of the reaction or by removal of oxygen. Examples glucose oxidase, long chain phenols, vitamin C and esters.
Asepsis	Freedom from contamination by undesirable or harmful microorganisms.
Aspergillus spp	A genus of filamentous fungi belonging to the Deuteromycotina. The fungi are used to produce a wide range of enzymes and metabolites.

Bead mill	A device for the rupturing of cells by using a ball-type mill loaded with glass or ceramic beads. Cooling is required to prevent denaturing.
Bioprocess	Any process that employs biological processes to perform chemical reactions.
Bioreactor	The vessel in which the biological reactions occur. Bioreactors are typically constructed from stainless steel.
C^*	Saturation concentration.
Chelating agent	A chemical capable of binding via two or more donor atoms to a metal ion. Chelates are used to solubilize metal ions.
Citric acid	An industrially used organic acid $C_6O_7H_8$. Traditionally produced from *Aspergillus niger* although more recently produced by yeasts. Citric acid is used as an acidulant in foods and esters used in plastics.
Corn steep liquor	A component of many bioprocess media. It is a byproduct of starch extraction from corn (maize). Although primarily used as a nitrogen source because of its amino acid content, it also contains vitamins, lactic acid and small amounts of reducing sugars and polysaccharides.
Corn syrup	A mixture of glucose, sugars, and dextrins; produced by the hydrolysis of starch and often referred to commercially as "glucose", whereas pure glucose is called dextrose.
CSTR	Continuously stirred tank reactor.
DO	Dissolved oxygen.
DNA	Deoxyribonucleic acid contains the genetic material of an organism. Sequences of bases in DNA eventually determine the sequences of amino acids incorporated into peptides. Since the form and function of proteins depend upon the amino acid sequences of their constituent polypeptide chains and these functions include the construction and regulation of other constituents. DNA in this way specifies the character of the organism.
Fed-batch culture	A system of intermediate between batch and continuous process. The term describes batch cultures that are fed continuously, or sequentially, with fresh medium without removal of culture fluid.

Fermentation	To the biochemist, a metabolic process whose main purpose is the conversion of free energy via ATP synthesis that uses substrate-level phosphorylation rather than oxidative phosphorylation. To the biotechnologist, any process that produces a useful product by the mass culture of microorganisms.
Fermenter	A vessel in which organisms can be grown under sterile controlled conditions that are optimum for product formation.
GA	Gluconic acid.
Glucose syrup	Purified, concentrated aqueous solutions of glucose and higher saccharides produced by the hydrolysis of maize (corn) or potato starch. Also referred to as corn syrup, corn starch hydrolysate, starch syrup, and confectioners glucose.
Glucose oxidase	An enzyme that converts ß-D-glucose, water and oxygen into gluconic acid and hydrogen peroxide. One glucose oxidase unit (U) is defined as 1 μmole of glucose converted per ml per min at pH 5.5, 25°C in excess glucose (0.5M) at 0.21 atm oxygen.
GO	Glucose oxidase.
GOD	Glucose oxidase.
GRAS organisms	Generally regarded as safe organisms. Selected strains of molds, bacteria and yeasts are currently used as sources of enzymes for the food industry. The most commonly used are *A.oryzae, A.niger* and *B.subtilis.* Inadvertent contamination of foods by these organisms or their products should not present a human health threat.
HPLC	High performance liquid chromatography.
Hyphae	The basic unit of a fungus.
Induction	The process by which an enzyme is synthesized in response to the presence of an external substance, the inducer.
k_la	Gas liquid mass transfer coefficient. It is a measure of the aeration capacity of a fermenter.
Malt	A term to describe barley grains that have been steeped in water, drained, allowed to germinate, and dried at defined temperatures in a kiln.

mRNA	Messenger RNA are molecules synthesised from a DNA template by an enzyme RNA polymerase.
Mycelium	The collective term for a network of hyphae.
ODE	Ordinary differential equation.
Operon	A group of functionally related genes.
OUR	Oxygen utilisation rate.
Peroxidase	An enzyme that breaks down hydrogen peroxide to oxygen and water.
POD	Peroxidase.
Promotor	A nucleotide sequence found upstream of a gene that acts as a signal for the binding of RNA polymerase.
Repressor	A protein that binds to DNA at a specific site (operator) to switch off a promotor and thus prevents transcription of the gene under the control of that promotor.
RNA	Ribonucleic acid.
Sequestering agent	Compounds that are able to form complexes with metal ions.
Std	Standard.
STR	Stirred tank reactor.

NOMENCLATURE

A	Gluconic acid (M)
$ß_G$	Group of glucose oxidase enzyme kinetic constants for glucose (M)
$ß_O$	Group of glucose oxidase enzyme kinetic constants for oxygen (M)
C_{O2}	Concentration of dissolved oxygen (mg^{-1}) or (ppm)
C^*_{O2}	Saturated dissolved oxygen concentration (mgl^{-1}) or (ppm)
E_I	Deactivated form of the glucose oxidase enzyme (M)
E_o	Oxidised form of glucose oxidase (M)
E_r	Reduced form of glucose oxidase (M)
G	Glucose (M)
G_{ex}	Extracellular glucose concentration (M)
G_{intra}	Intracellular glucose concentration (M)
G.A.	Gluconic acid (M)
GO_{ex}	Extracellular glucose oxidase activity (U)
GO_{intra}	Intracellular glucose oxidase activity (U)
L	Glucono-δ-lactone (M)
k_d	Oxygen deactivation rate of glucose oxidase (M/h)
k_i	Reaction rate constants
K_i	Reaction rate constants
K_m	Michaelis-Menten saturation constant (M)
K_la	Gas to liquid film mass transfer coefficient (1/h)
K_{SI}	Michaelis-Menten inhibition term (M)
M	Molarity (M)
P	Hydrogen peroxide (M)
r_a	Rate of production of gluconic acid ($mols/s/g_{glucose\ oxidase}$)
$r_{a,max}$	Maximum rate of production of gluconic acid ($mols/s/g_{glucose\ oxidase}$)
r_d	Rate of glucose oxidase deactivation (U/h)
s_i	Group of constants used in glucose oxidase enzyme kinetics (unitless)
S_g	Concentration of glucose substrate (M)
S_H	Concentration of hydrogen ion (M)

S_o	Concentration of oxygen substrate (M)
U	Activity of an enzyme (μmoles substrate/ml/min at controlled conditions)
U_G	Glucose mass transport coefficient (1/h)
U_{GO}	Glucose oxidase mass transport coefficient (1/h)
V_{max}	Michaelis-Menten maximum rate constant (M/h)
X	Cell mass (gl^{-1})
X_o	Initial cell mass (gl^{-1})
X_{max}	Maximum cell mass (gl^{-1})
Y	Yield (unitless)
μ_{max}	Maximum growth rate (1/h)
%m/m	Percentage mass on a mass basis i.e. x g/100g
%m/v	Percentage mass on a volume basis i.e. x g/100ml

TABLE OF CONTENTS

LIST OF FIGURES

LIST OF TABLES

1. INTRODUCTION

Glucose oxidase, also termed ß-D-glucose:oxygen 1-oxidoreductase, (EC 1.1.3.4), is an enzyme that catalyses the oxidation of ß-D-glucose to gluconic acid. Oxygen is used as the electron acceptor with the simultaneous production of hydrogen peroxide. The enzyme is highly specific to ß-D-glucose while other electron acceptors can be used. Glucose oxidase, sourced from *Aspergillus niger*, has a molecular weight of 19200 and has "generally regarded as safe" (GRAS) status in the U.S.A. The enzyme is composed of two identical subunits, each consisting of 583 amino acids. It contains 8 potential sites for N-linked glycosylation (Friderick 1990). Industrial producers of glucose oxidase use either *Aspergillus niger* or *Gluconobacter.*

Glucose oxidase has wide ranging applications, the majority in the consumer food industry. These are listed below (Richter 1983):

- antioxidant to replace ascorbic acid, used in fruit juices
- trace glucose removal
- mild biocide in fruit mashes
- sterile yoghurt and cottage cheese production with glucose oxidase and lactonase
- toothpastes
- glucose measurement in medical diagnostic tools for hypoglycaemia, diabetes, adrenal and pituitary disorders (Lockwood 1979).

Gluconic acid and hydrogen peroxide formation is catalysed from ß-D-glucose, oxygen and water by glucose oxidase :

$$Glucose + O_2 \xrightarrow{glucose\ oxidase} Gluconic\ acid + H_2O_2 \qquad (1.1)$$

Gluconic acid is used in many diverse fields and in different ways. Some of the applications are listed below:

- pickling agent for metal surfaces prior to welding
- wall cleaner prior to painting
- sequestering agent in alkaline detergent glass bottle washing
- control of water resistance and settling time of cement.
- carrier for the delivery of trace metals and drugs into the human body

Sodium and calcium gluconate production has increased from 3 700 metric tonnes in 1974 to 45 000 metric tonnes in 1985 (Bigelis 1985 cited by Markwell *et al.* 1989). Glucono-δ-lactone, gluconic acid, and its various salts can be made using three different technologies: electrolysis, mild chemical oxidation and bioprocess. The electrolysis process uses bromine. It requires a very high purity of the raw materials and has high capital and running costs. The mild chemical oxidation system, using hypobromite, has not proven to be economically viable although the initial capital cost is the lowest of the three processes. The bioprocess can use cheap raw materials but has a high capital cost. Bioprocess can also be used to produce the enzyme glucose oxidase as well as gluconic acid. Simultaneous production of gluconic acid and glucose oxidase was part of the motivation for this project. Both fungi and bacteria can be used to produce gluconic acid. Fungi include *Aspergillus niger, Penicillium, Gliocladium, Scopulariopsis, Gonatobotyrys* and *Endomycopsis*. Bacteria include *Pseudomonas, Vibrio* and *Gluconobacter*. *A.niger* and *Gluconobacter* are the most commonly used organisms with *A.niger* accounting for the larger volume (Lockwood 1979).

The main aim of this work is to explore the simultaneous production of glucose oxidase and gluconic acid in *A.niger*. This is broken down into the following sub-objectives:

1) to find optimum operating conditions for glucose oxidase and gluconic acid production
2) to estimate yields obtainable for both glucose oxidase and gluconic acid at the industrial scale
3) to understand and quantify the induction of glucose oxidase in *A.niger*
4) to develop a kinetic model of glucose oxidase induction and gluconic acid formation in the *A.niger* bioprocess

In chapter 2 of the thesis, the literature pertaining to glucose oxidase and gluconic acid production by *A.niger* is reviewed. The location and induction system of glucose oxidase is discussed and a detailed explanation of the glucose oxidase enzyme kinetics is presented. A brief description of media and reactor configurations reported in the literature is included.

Chapter 3 covers the philosophy for the design of the experiments to determine the effect of glucose and oxygen on the induction of glucose oxidase. Experimental conditions for the growth of inocula, fermentations and media are then discussed. Analytical techniques are described briefly in the body of the thesis with a detailed explanation, experimental procedure and validation being given as an Appendix for each technique.

Chapter 4 presents and discusses the experimental results of the induction of glucose oxidase over the range of glucose and oxygen conditions.

In chapter 5, the development of a mechanistic model of the *A.niger* bioprocess is presented. A brief comparison with other models cited in literature for the glucose oxidase and gluconic acid system is given. The model is then derived by combining models of the sub-processes mechanisms. The glucose oxidase induction is modelled using the gene operon model in which only glucose acts as an inducer. The components of the model are derived step by step and then joined together using the species balance equations.

Chapter 6 describes the implementation of the model equations and the integration technique used in a Turbo Pascal computer program. Initial conditions and parameter estimates are then discussed. Parameters are optimised by simplex search technique using the least squares error on a single experiment as the objective function. Near optimal model parameters are then given with the fitted profiles. The model is validated by the comparison of the prediction of the model and measured profiles under other conditions. A sensitivity analysis is conducted to describe the relative error attached to parameters and limitations of the model are discussed.

In chapter 7, the extension of the *A.niger* bioprocess system is presented by including the effect of oxygen, as well as glucose, on the induction of glucose oxidase. Again initial

conditions and parameter estimates are given and the near optimal parameters are calculated using the simplex search algorithm. The model is again validated by prediction at other conditions and comparison to measured profiles. Limitations of this extended model are then discussed.

In chapter 8, the conclusions are drawn from throughout the thesis.

2. LITERATURE REVIEW

Many microbes produce glucose oxidase and gluconic acid. This chapter focuses on the factors affecting the production of glucose oxidase and gluconic acid in *A.niger*, the major industrial producer.

2.1 Glucose oxidase and gluconic acid

2.1.1 Glucose oxidase and its uses

Glucose and oxygen in the presence of glucose oxidase react to form gluconic acid and hydrogen peroxide as shown below:

$$\beta\text{-}D\text{-}glucose + O_2 \xrightarrow{GOD} gluconic\ acid + H_2O_2$$

Diagnostic tool for determining glucose concentration

The prosthetic group of the enzyme is alloxazine-adenine dinucleotide or flavine-adenine dinucleotide and the enzyme is a dehydrogenase as opposed to an oxidase (Kirk-Othmer 1980). Glucose oxidase can be used as a diagnostic tool for determining the concentration of glucose in blood and urine (Hugget *et al.* 1957). By quantifying the H_2O_2 formed, the amount of glucose present is determined. The peroxide formed can be measured directly using U.V. absorption or used as the limiting reactant in a coupled reaction to oxidise a dye in the presence of excess catalase (Loyd *et al.* 1969 cited by Fiedurek *et al.* 1986). The oxidised dye is quantified colorimetrically. Alternatively oxygen utilisation rate may be monitored.

Antioxidant

Glucose oxidase is used as an antioxidant in the food industry. It provides an alternative to harsh antioxidants such as ascorbic acid and sulphur dioxide. The formation of peroxides in

fruit juices in the presence of dissolved oxygen and sunlight may be avoided by the addition of 20-200 glucose oxidase units/l. It is important that cellulase is not present in the glucose oxidase preparation as the cloud stability of the juice is achieved using cellulose (Richter 1983). The enzyme is also added to emulsion products that need a long shelf life such as mayonnaise and salad dressings. The natural oxygen present in the product is removed to prevent off-flavour, broken emulsions and faded colours. The enzyme can also be used to preserve dried food such as coffee, cake mixtures, milk powders, dried soups, dried yeast and concentrated aroma compounds which are very susceptible to oxidation.

Removal of glucose

Glucose oxidase is also used by the food industry to remove glucose from dried powder products such as dried egg whites, thereby preventing the Maillard reaction. It is used to improve the stability of colour and flavour in tinned foods, beer and soft drinks (Lockwood 1975) and is added to flour in the baking industry to improve the doughing characteristics (Markwell *et al.* 1989).

The principle of removing glucose from a system has also been implemented in the production of fructo-oligosaccharide syrups. Sucrose is converted to fructo-oligosaccharide and glucose by fructosyltransferase. This reaction is inhibited by glucose due to feedback inhibition. The addition of glucose oxidase converts glucose to gluconic acid removing the inhibitory byproduct and thus increasing the level of conversion. Jung *et al.* (1993) report an increase in the yield of fructo-oligosaccharide from 55% to 90%.

The enzyme can also be used to transform lignin and lignocellulose complexes. These are major waste products from the paper industry (Rogalski *et al.* 1988). It can also be used to separate similar sugars from one another due to its high specificity. Fructose and glucose, for example, cannot be separated easily on an industrial scale. Glucose oxidase oxidises the non-ionic glucose into gluconic acid (ionic) which can be separated from the non-ionic fructose by precipitation or ion exchange (Doeppner *et al.* 1984). Doeppner points out the need for immobilisation of the enzyme as using glucose oxidase as a raw material is extremely costly.

Other uses

A further use of glucose oxidase is the conversion of glucose to gluconic acid and gluconate salts. The potential uses of these products are described in Section 2.1.2.

Future development of the use of the enzyme include addition to toothpastes with amyloglucosidase. The enzymes increase the natural level of hydrogen peroxide in the mouth to kill the bacteria which produce acids that demineralise and weaken teeth (Richter 1983). A trial toothpaste has been developed under the name Zendium.

2.1.2 Use of gluconic acid

The formation of gluconic acid from glucose proceeds via the intermediate glucono-δ-lactone. This non-acidic product has a limited market in baking powders. The derivatives of major interest are the final product gluconic acid and its salts sodium gluconate and calcium gluconate.

Gluconic acid is used as a mild acidulant in the food and tanning industries (Lockwood 1975). The acid is a sequestering agent (forming metal ion complexes) and is used to remove rust and to clean metallic surfaces prior to welding. The acid is also used as a metal carrier for patients suffering from metal deficiencies by forming gluconate salts. These salts are readily absorbed into the human body compared to inorganic carriers. Sodium gluconate is used to prevent water hardness by forming complexes with the calcium and magnesium ions. It is used extensively in the bottle washing industry.

It is possible to produce gluconate using an electrolytic process (Shah *et al.* 1993). This is highly energy intensive and requires a pure form of glucose monohydrate as its feed which accounts for 70% of the raw material costs. The process is patent protected. Mild oxidation of glucose syrups using hypobromite solutions is an alternative process to the electrolysis process. However it has not proven to be economically viable although the capital cost is lower. The bioprocess offers advantages over the electrolytic and chemical oxidation process. These include the presence of side products e.g. lactonase, glucose oxidase and the ability to use a variety of low purity raw materials. In addition, to this it is an environmentally

responsible process compared to the large electricity requirements of the electrolytic process.

2.2 Cultivation of *A.niger* for glucose oxidase and gluconic acid production

Aspergillus niger is used to produce a wide variety of industrial products. These include organic acids such as citric acid, gluconic acid, oxalic acid and α-ketoglutarate, and enzymes including amylases, hemicelluloses, pectinase and glucose oxidase. In this review only glucose oxidase and its product gluconic acid will be considered. Glucose oxidase is produced by a wide range of microbes : *Aspergillus niger, Bacillus mutants, Gluconobacter, Penicillium purpurogenum, Penicillium vitale and Zymomona mobilis*. *A.niger* is the major industrial producer (Atkinson and Mavituna 1991, Fogarty 1983).

2.2.1 *A.niger* product formation

A variety of products are produced by *A.niger*. The type of product is dependent on the pH and composition of the media. Citric acid is produced exclusively at a pH below 2 and in a manganese deficient media. Kisser *et al.* (1980) showed a 50% drop in citric acid production when increasing the manganese concentration from 0 to 1E-6M. Gluconic acid is produced predominately above pH 5. Oxalic acid may be produced concomitantly with gluconic acid in some strains of *Aspergillus niger* in the presence of sodium ions (Lockwood 1979).

2.2.2 Media

A.niger can convert a variety of carbohydrate sources into gluconic acid. Impure liquid glucose, sucrose, maize gur (hydrol), tapioca and molasses have been explored as alternative carbon sources. Due to the metabolic requirements of *A.niger*, some of these substitutes are supplemented with salts and nitrogen sources.

Baig (1987) compared three substrates at various concentrations in the production of calcium gluconate. He found that maize gur resulted in a higher gluconic acid yield than liquid

glucose. This was attributed to the presence of amino acids, minerals and vitamins in the maize gur. Maize gur produced similar yields to pure commercial glucose. The calcium gluconate conversions are shown in the Table 2.1.

Maximum conversion of the glucose source occurred at 15% equivalent glucose concentration using both maize gur and commercial glucose. It has been shown that increasing the carbohydrate concentration above 15% inhibits the production rate of calcium gluconate (Qadeer 1975, Baig 1987). Table 2.2 shows the effect of liquid glucose concentration on the rate of gluconate formation.

Table 2.1 Comparison of calcium gluconate yield on liquid glucose and maize gur (Baig 1987)

	15% Liquid Glucose	15% Maize Gur (Hydrol)	15% Commercial Glucose
Calcium gluconate at 48h (g/l) 22°C	72.6	80.8	78.1

Table 2.2 Effect of liquid glucose concentration on gluconate production rate (Baig 1987)

	10% liquid glucose	15% liquid glucose	20% liquid glucose
Gluconate formed at 24h (g/l)	94.6	130.8	61.8

Tapioca starch hydrolysate supplemented with corn steep liquor was proposed by Shah (1993) as an economical substrate for the production of tablet grade calcium gluconate. The media is detailed in Table 2.3 and produces an almost quantitative amount of gluconate from the carbohydrate source in 22 to 26h of fermentation. Table 2.3 compares the various media used. All values are on a mass percentage basis.

Munk *et al.* (1963) cited by Elnaughy *at al.* (1975) found that a decrease in the magnesium concentration increased the production of glucose oxidase. This was attributed to the stimulation of riboflavin synthesis. Glucose oxidase is a flavin enzyme. Elnaughy (1975) studied media formulated for gluconic acid production by *Penicillium puberulum*. It was found that the best source of nitrogen was peptone. This resulted in larger cell masses than inorganic nitrogen sources. The optimum conditions are contained in Table 2.3.

Table 2.3 : Comparison of media used for the production of gluconic acid by *A.niger*. Quantities given as mass %

Author	Carbon source	% Carbon source	$MgSO_4$ $7H_2O$	KH_2PO_4	Nitrogen source		Trace elements	Buffers	Other	Antifoam
(Witteveen *et al.* (1990)	Glucose	10	0.020	0.050	0.12 KNO_3	0.05 Yeast.	0.0004 Trace			0.01 Antifoam
Fiederek (1986)	Glucose	8	0.016	0.018	0.04 $(NH_4)_2HPO_4$	0.3 Peptone		3.4 $CaCO_3$		
(Mischak et al. 1985)	Sucrose	22.6	0.11	0.015			0.00015 $ZnSO_4 7H_2O$		0.055 $CaCl_2$ 0.015 KCl	
Anderson (1980)	Sucrose	14	0.025	0.020	0.25 NH_4NO_3					
Ishimori (1982)	Sucrose	3	0.030	0.100	0.20 KNO_3	0.5 Yeast.	0.001 $FeSO_4 7H_2O$		0.05 KCl	
Shah (1993)	Tapioca	20	0.010	0.010	0.02 $(NH_4)_2HPO_4$	0.04 Urea				0.05 Antifoam
Paresh (1982)	Molasses	15	0.015	0.02	0.12 NH_4Cl			3.2 $CaCO_3$		
Elnaughy (1975) [*Penicillium puberulum*]	Glucose	8	0.005	0.005	1.0					
Blom (1957)	Glucose	24	0.017	0.002	0.04 $(NH_4)_2HPO_4$	0.01 Urea				1% octadecanol
Moyer (1937)	Glucose	15	0.0156	0.0188	0.0388 $(NH_4)_2HPO_4$			10 $CaCO_3$		

2.2.3 Factors affecting the morphology of *A.niger*

A.niger is a filamentous fungus. Filaments with a high degree of branching and the production of gel layers become entangled and form pellets. Filaments with a low degree of branching and the absence of gel layers remain isolated filament strands. Hence *A.niger* may grow in filamentous or pellet form in submerged culture. The environment in which the fungus is grown determines the degree of branching and gel layer formation, and hence its morphology. Shear stress environments and manganese level have been cited to affect the type of morphology.

Hydrodynamic forces

Low shear environments in shake flask cultures allow mycelial pellets to form up to 1cm in diameter (Kobayashi *et al.* 1973). High shear environments in a STR allow small pellets or pulpy filamentous mycelial growth (Traeger *at al.* 1989). Konig *et al.* (1982) observed that the morphology of the inocula can define the morphology of the growth in airlift bubble columns. The pellet morphology is only stable in an airlift column if the inoculum is grown under defined conditions.

Trace metals

The effect of trace metals on growth type has been studied by Clark (1966). The elements Al^{3+}, Ca^{2+}, Co^{2+}, Cu^{2+}, Fe^{2+}, Mg^{2+}, Ni^{2+}, Zn^{2+} were found not to affect the growth type. Mn^{2+}, Al^{3+},Fe^{2+} and Zn^{2+} affected both the morphology and the citric acid yield in the range of 5-25 ppm. Table 2.4 summarises these findings. The manganese concentration apparently controls the formation of a slime mucilage surrounding the mycelium (Kisser *et al.* 1980). This mucilage is found in the presence of manganese and is absent under manganese deficient conditions. The influence manganese on the location of glucose oxidase is described in Section 2.5.

Table 2.4 Trace metal effect on *A.niger* morphology (Clark *et al.* 1966)

Metal ion	Amount added [ppm]	Citric acid yield (%) after 8 hours	Morphology
None	-	8.8	Pellet
Al^{3+}	5.0	7.3	Pellet
Fe^{2+}	100.0	7.5	Pellet
Zn^{2+}	5.0	7.5	Pellet
Mn^{2+}	1.0	1.5	Filamentous

Temperature

A.niger can sporulate in plate and submerged cultures. Sporulation is inhibited by high temperatures. Temperatures between 38 and 43°C will prevent sporulation and induce mycelial growth (Muller 1986a, Meiberg and Spa 1983).

2.3. Gluconic acid formation within the metabolism of *A.niger*

In studying the microbial formation of gluconic acid, it is advantageous to understand the value of this organic acid to the microorganism. The following competitive advantages of gluconic acid have been proposed:

- The conversion of glucose to gluconic acid lowers the pH of the environment, increasing the chances of survival for the microorganism as most of the gluconic acid forming organisms can survive in the pH 2 region.
- With the production of gluconic acid, hydrogen peroxide is also produced which may act as a biocide removing all organisms unable to degrade hydrogen peroxide.
- The conversion of glucose to gluconic acid may provide an intermediate storage compound which cannot be consumed by other organisms.

Gluconate can be formed from D-ß-glucose by three routes : glucose oxidase conversion, glucose dehrogenase conversion and hexokinase conversion using glucose-6-phosphate as an intermediate. The glucose oxidase route has been identified as the major route in *A.niger* (Muller 1986).

2.3.1. Synthesis of glucose oxidase

The enzyme glucose oxidase consists of 2 identical subunits. The production of the enzyme follows a multiple step process:

a) Phosphorylation (James *et al.* 1981 cited by Markwell *et al* 1989)

b) Sequential glycosidation (Hayashi and Nakamur 1981 cited by Markwell *et al* 1989)

c) Coordinate synthesis of the flavin adenine dinucleotide cofactor (Markwell *et al.* 1989)

2.3.2. Conversion of glucose to gluconic acid by glucose oxidase

Glucose oxidase is specific for ß-D-glucose: hence it does not convert the α-D-glucose present in glucose monohydrate. However, the α form is in equilibrium with the ß form. Maintenance of this equilibrium is accelerated by the presence of mutarotase in the *A.niger* system.

Glucose oxidase is a flavoprotein catalysing the removal of 2 hydrogen atoms from glucose to form D-glucono-δ-lactone while being reduced itself. The reduced form of the protein is oxidised by molecular oxygen to produce hydrogen peroxide. In *A.niger*, catalases are present to decompose the hydrogen peroxide formed (Wittiveen *et al.* 1993).

$$D\text{-}glucose + O_2 \rightarrow D\text{-}glucono\text{-}\delta\text{-}lactone + H_2O_2 \qquad (2.2)$$

Glucono-δ-lactone is converted to gluconic acid spontaneously at high pH values (Lockwood 1979). The presence of lactonase accelerates the conversion of the lactone to gluconic acid. Accumulation of glucono-δ-lactone inhibits the conversion of glucose. The spontaneous

conversion of the intermediate by moderately high pH values means it is necessary to control the pH by base addition e.g $CaCO_3$ or NaOH for maximum gluocse conversion.

2.3.3. Utilisation of gluconic acid in *A.niger*

Figure 2.1 shows three possible routes for the metabolism of gluconate. Growth of cultures on gluconate only occurs in the low pH range. Gluconate catabolism is maximal at pH 1-3. In gluconate accumulating media, the prevailing pH or excess gluconate may inhibit gluconate catabolism (Muller 1986).

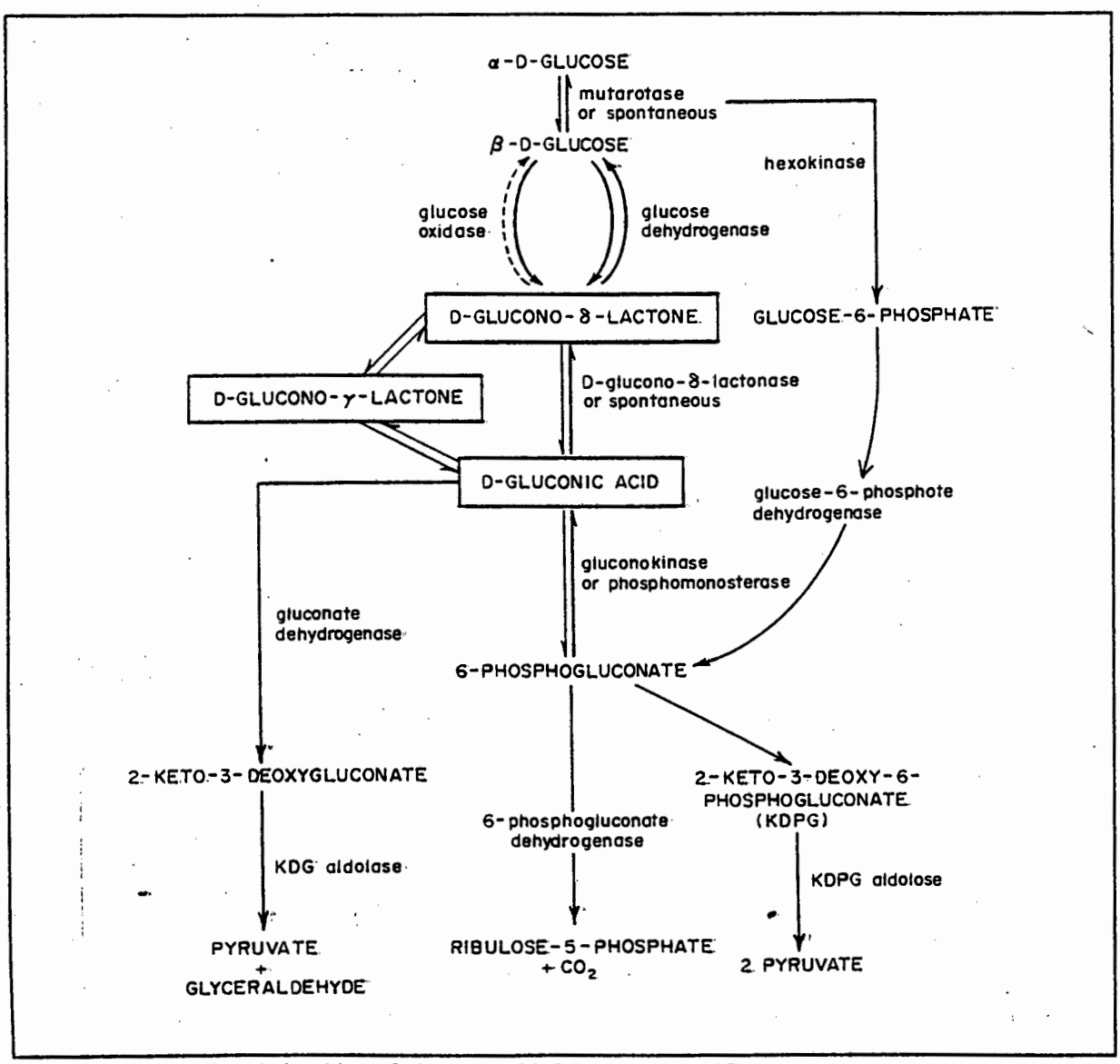

Figure 2.1 Metabolic relationships of gluconic acid (Moo-Young 1985)

2.4 The induction of glucose oxidase production in *A.niger*

The induction of glucose oxidase is influenced by a variety of external factors. Rohr (1983) identifies the main factors as glucose concentration, dissolved oxygen concentration and pH. These will be discussed in turn.

2.4.1. The effect of glucose

Glucose oxidase is induced by high levels of glucose and glucose-6-phosphate (Mischak *et al.* 1985). The enzyme is not induced by glycerol. A minimum glucose concentration is required before glucose oxidase is induced. Markwell *et al.* (1989) found this level to be 0.2M in plate cultures, while Witteveen *et al.* (1990) determined the level to be 0.002M in plate cultures. Witteveen's detection system used o-dianisidine which detects the presence of hydrogen peroxide, (a singular product of glucose oxidase) whereas Markwell used a methyl red indicator which detects general acid production. Thus Witteveen's results are more specific.

There are two kinetic factors that affect the overall production rate of gluconic acid:

- glucose oxidase induction kinetics
- glucose oxidase enzyme kinetics

Lee (1987) reports the combined optimum glucose concentration for gluconic acid production to be between 10 and 15 % glucose. Hatzininkoloy and Macris (1995) showed that increasing the sucrose and molasses concentration from 10 gl^{-1} to 120 gl^{-1} resulted in an increase and a flattening off of induced glucose oxidase activity with increasing glucose.

2.4.2. The effect of dissolved oxygen

A minimum dissolved oxygen concentration is required for glucose oxidase induction. *A.niger* does not produce glucose oxidase at oxygen concentrations below 7% of air saturation (Witteveen 1990,1992). Further supplementation beyond the minimum requirement augments glucose oxidase production. Traeger *et al.* (1991) increased the glucose oxidase activity from 1 unit ml^{-1} using air to 4 units ml^{-1} using pure oxygen.

Traeger *et al.* (1992) investigated the effect of an oscillating oxygen supply on glucose oxidase production. Cultures were run with an oscillating dissolved oxygen concentration between 70 and 130% of saturation with frequencies varying from 90 to 200s. Table 2.5 summaries the results of glucose oxidase activity at a fermentation time of 20h. It can be seen that the oscillatory dissolved oxygen concentration induces a higher glucose oxidase concentration than the equivalent sustained average level. It also shows that there is an optimal frequency of oscillation for maximum induction and the location of the enzyme is also affected. Traeger *et al.* (1992) attribute the increase in glucose oxidase to a "bio-resonance" effect in the enzymes that control the mRNA in the cell. The time period of these enzymes is of the order of minutes. Hence an undamped oscillatory behaviour is possible in the feedback response to an oscillating external condition.

Table 2.5 Effect of period of oscillating dissolved oxygen concentration on intra- and extracellular glucose oxidase activity at 20 hours (Traeger *et al.* 1992).

Average oxygen % of sat. 1bar air	Period [s]	Extracellular glucose oxidase [U/ml]	Glucose oxidase ante [U/ml]
100	0	1.1	4.0
100	90	2.2	3.2
100	140	2.2	5.0
100	200	2.4	3.2

The oscillating conditions are similar to those found in airlift reactors where the culture cycles through regions of varying oxygen concentration in the reactor. The dissolved oxygen concentration is high at the base due to hydrostatic pressure. Airlift reactors may be ideal for glucose oxidase fermentation due to the cyclical dissolved oxygen concentration and increased level. However the control of the dissolved oxygen concentration is easier compared to a stirred tank reactor (Oosterhuis *et al.* 1983).

2.4.3. The effect of pH

It is commonly known that glucose oxidase is produced by *A.niger* in the pH range of 4 to 7 (Mischak *et al.* 1985). Roukas and Harvey (1988) varied the pH conditions of the feed in a continuous culture and measured the glucose oxidase production rate. Beet molasses treated with hot ferrocyanide to remove trace metals was fed at a dilution rate of 0.012 hr^{-1}. Figure 2.2 shows the glucose oxidase production as a function of pH under the conditions above. The enzyme was assayed as total activity of the whole culture (disrupted by sonication).

However gluconate production has been observed in fixed bed and stirred fermenter cultures once the nitrate source has been consumed, below a pH of 2.5 (Heinrich *et al.* 1982) . This was attributed to the high manganese concentration. Witteveen *et al.* (1990) also found that glucose oxidase was produced in cultures at a pH of 2.8, although the induction was lagged.

For optimal production of gluconic acid, a pH of 5.5 is required for the following reasons:

- Optimal glucose oxidase induction occurs at a pH around 5.
- Glucose oxidase activity is optimal at pH of 5.6 and falls to 35% at pH 3 and 5% at pH 2 (Franke *et al.* 1963).

2.4.4. The effect of nitrogen concentration

A low nitrogen level has been reported as a prerequisite for glucose oxidase induction (Muller 1966, cited by Muller 1986).

2.4.5. The effect of manganese

Lockwood (1975) states that manganese is essential for industrial glucose oxidase production. However, Mischak *et al* (1985) showed that glucose oxidase and gluconic acid production are not affected by manganese concentration. Mischak *et al.* reported glucose oxidase production as extracellular if the manganese concentration is less than 10^{-6}M and intracellular if the manganese is greater than 10^{-5}M. Lockwood's industrial process flowsheet only extracts glucose oxidase from the cell matter and hence would require high levels of manganese to ensure cell associated location of glucose oxidase.

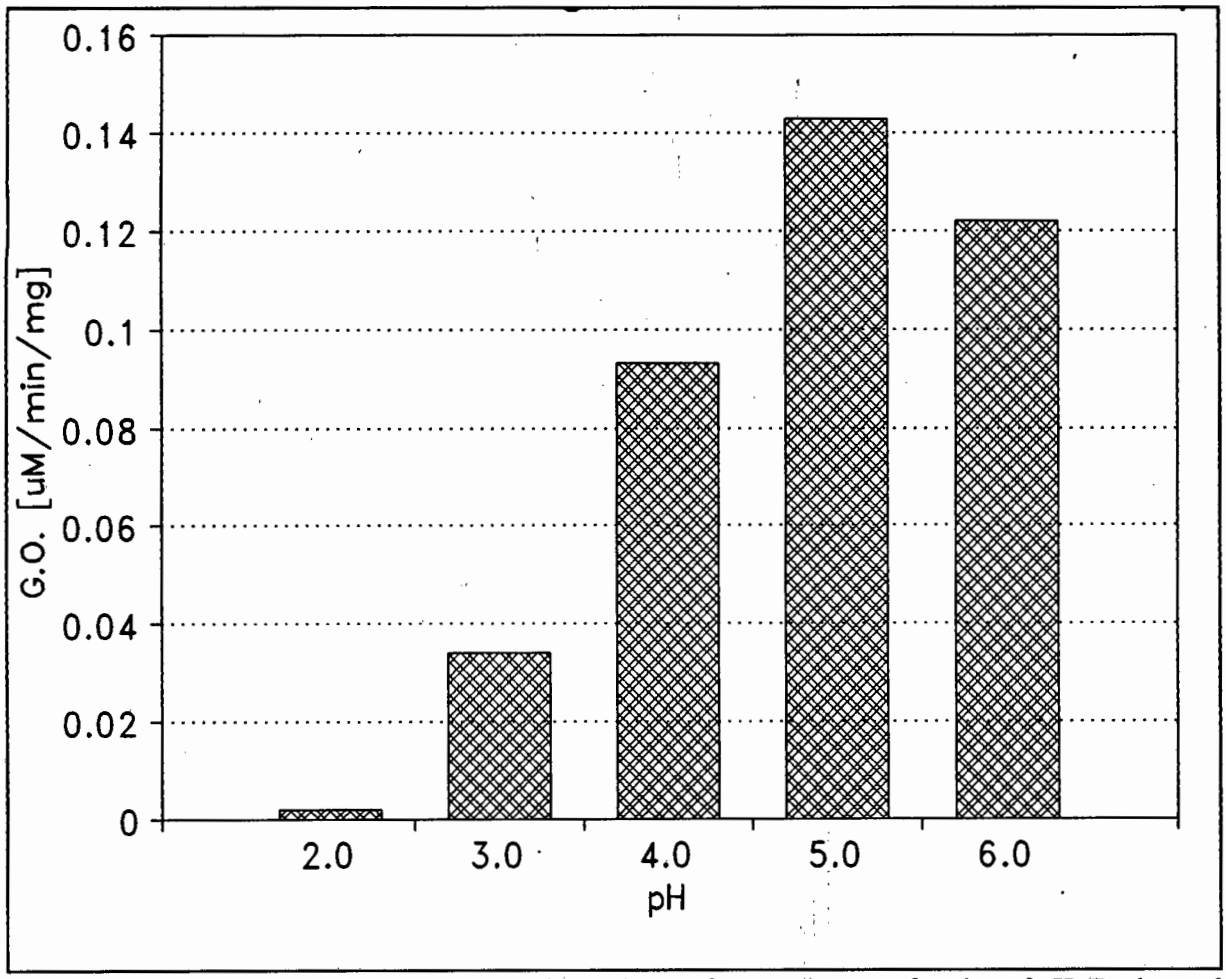

Figure 2.2 Production rates of glucose oxidase in continuous fermentation as a function of pH (Roukas and Harvey 1988).

Leaching of manganese from stainless steel can be significant. Heinrich and Rehm (1982) has reported manganese levels of 0.2E-7 M before sterilisation, 0.55E-7 M after sterilisation and increasing to 0.76E-7 M after 6 days incubation. The increase in levels is due to contamination from the stainless steel fermenter used. Mischak *et al.* (1985) reported that the stainless steel fermenter could be pacified with 5% (w/v) $K_2Cr_2O_7$ acidified to a pH of 3.0 with H_2SO_4 and a voltage of 1.0 V for 3 hours to avoid manganate leaching.

2.4.6. The effect of antifoams

Blom *et al.* (1952) reported the use of soya and lard as an antifoam at an industrial scale to be detrimental to glucose oxidase and to glucose utilisation. Replacement with 1% ocatadecyl alcohol was preferred.

2.4.7. The effect of particulate matter

Hatzinikolaou and Macris (1995) found that calcium carbonate increases the level of glucose oxidase induced. Furthermore, an optimum concentration of between 4-5% calcium carbonate was found. The role of insoluble calcium carbonate in media is to control the pH at about 5.5.

2.5. Location of glucose oxidase in *A.niger*

From an industrial point of view it is necessary to determine the location of glucose oxidase for the design of downstream separation. However, "There are still contradictory reports in the literature regarding the localisation of the enzyme (glucose oxidase)" (Traeger *et al.* 1991). In order to understand this contradictory literature, it is necessary to look at the location of glucose oxidase from the cellular point of view and factors which affect the cell.

2.5.1. Location of glucose oxidase from the cell's point of view

2.5.1.1. Design of the glucose oxidase enzyme

The following features of glucose oxidase suggest that glucose oxidase is intrinsically an extracellular enzyme by its design:

1) The DNA sequence for glucose oxidase contains the typical secretion peptide sequence (Frederick 1990 cited by Witteveen *et al.* 1992).
2) Glucose oxidase is also highly glycosylated which suggests an extracellular enzyme (Pazur *et al.* 1965).
3) Other fungi such as *Penicillium* produce glucose oxidase extracellularly.

2.5.1.2 Intracellular conditions required for intracellular gluconic acid production

Glucose oxidase may be contained inside the cells, on the exterior cell walls, caught up in a slime mucilage or in the culture fluid. By examining the environmental conditions required for the conversion of glucose to gluconic acid by glucose oxidase, the location of the enzyme may be postulated.

Firstly, gluconic acid production requires high levels of glucose and oxygen and an optimum pH to maximise the production rate based on enzyme kinetics. It is difficult to measure the intracellular glucose concentration, but it is possible to infer an upper level of 0.001M. This is derived from an analysis of hexokinase kinetics. The enzyme is controlled by other metabolites and hence cannot operate at this maximum level (Mischak *et al.* 1985). For the observed production rates of gluconic acid, much higher glucose concentrations are required and therefore it is apparent that the majority of the gluconic acid is produced extracellularly.

Secondly, during the production of gluconic acid, an equal amount of hydrogen peroxide is produced. Witteveen *et al.* (1992) quote a production rate of 0.05-0.1 mols of hydrogen peroxide produced per hour per gram of mycelia in industrial cultures . A group of catalases are produced as a protective system for degrading hydrogen peroxide. Witteveen *et al.* (1992) determined for the location of various types of catalase during the production of gluconic acid. Four types of catalase were found, two being constitutive (one intracellular, one extracellular) and two being present on induction of glucose oxidase. One induced enzyme was intracellular and the other extracellular. The catalase location shows that glucose oxidase could be present both intracellularly and extracellularly.

2.5.2. The effect of manganese on glucose oxidase location

The location of glucose oxidase is reported to be dependent on the concentration of manganese present. It is suggested that this results from the presence or absence of a slime mucilage as a function of manganese concentration (Kisser *et al.* 1980). This mucilage may entrap glucose oxidase on excretion from the cell, causing it to remain associated with the mycelium and thus appear intracellular.

It has been observed that the inclusion of manganese in a synthetic media is essential for the production of glucose oxidase (Lockwood 1975). Lockwood's flowsheet for the industrial production of glucose oxidase, however, shows recovery of the enzyme only from the mycelia. This indicates that glucose oxidase is not present in the supernatant at an economically recoverable level when manganese is present in the culture medium.

Mischak *et al.* (1985) showed that the total amount of glucose oxidase produced is not dependent on the concentration of manganese ions. It was found however that the location of the enzyme changed. At low manganese levels the enzyme was extracellular and at high levels intracellular, as shown in Table 2.6. Mischak confirmed that the extracellular levels were not a result of autolysis by checking the concentration of the intracellular malate dehydrogenase enzyme present in the supernatant. It was found that the extracellular malate dehydrogenase enzyme accounted for 17% of the entire malate dehydrogenase concentration (Table 2.6), confirming the low cell lysis.

Table 2.6 Variation in location of glucose oxidase with manganese concentration (Mischak *et al.* 1985)

Mn^{2+} [M]	G.O. U/ml				%		
	Supernatant	Cell debris	Culture fluid	Total	Supernatant	Cell debris	Culture fluid
-	.01	.04	.11	0.16	6	25	69
10E-6	.05	.04	.08	0.17	29	24	47
10E-5	.10	.05	.04	0.19	53	26	21

2.5.3. The effect of oxygen on glucose oxidase location

Dissolved oxygen has an effect on both the level and location of glucose oxidase (Traeger *et al.* 1991). Traeger found that aeration with pure oxygen in place of air increased the intracellular glucose oxidase concentration from 1 unit using air to 4 units. The extracellular glucose oxidase only increased marginally from 0.5 units to 1.0 units under the same change. Traeger concluded that glucose oxidase is predominantly an intracellular enzyme and that a controlled excretion of the enzyme into the fluid occurred up to a certain concentration in the fluid. Traeger's method of glucose oxidase analysis would have detected glucose oxidase trapped in a mucilage layer as "intracellular". Traeger's hypothesis is supported by the active excretion of glucose oxidase into fresh medium when the mycelium is resuspended. However, this secretion may also be due to diffusion from a slime layer into the fluid.

Traeger *et al.* (1992) found that an oscillating dissolved oxygen concentration between 30% of air saturation and saturation at 1 bar caused an increase in extracellular glucose oxidase activity.

2.5.4. The effect of ultrasound on glucose oxidase location

Ishimori *et al.* (1982) found that by constantly irradiating growing mycelia with ultrasound at 20kHz from a probe at a power input of 15W per 80ml, glucose oxidase can be moved from the cell wall region into the culture fluid. The enzyme is deactivated by ultrasound waves above 15W. Continuous liberation of glucose oxidase from living cells using ultrasound implies that the glucose oxidase is not a truly intracellular enzyme but may be associated with the cell membrane through a mucilage.

2.6. Reactor type and configuration used to produce glucose oxidase and gluconic acid

Several types of reactors that can be used in industrial fermentations. The most common and versatile is the stirred tank reactor. However the airlift reactor finds increased application. It does not have an impeller, has a reduced power input and a reduced risk of contamination (Traeger *et al.* 1989). Each type of reactor has certain inherent advantages in optimising a specific bioprocess. These include modifications in gas transfer, shear rate and mixing.

2.6.1. Stirred tank reactor (STR)

STRs consist of a single vessel with impeller and baffles. Air is sparged at the base of the reactor and broken up by the impeller. The reactors are usually associated with high shear forces required to mix and break bubbles to achieve high oxygen transfer.

STR can be configured a variety of ways. A single STR can be used for simple batch reaction, fed batch, draw and fill or continuous operation. Simple batch operation allows formation of products that require a long residence time and are only produced at the end of a batch. Fed batch operation allows the conversion of a high amount of substrate while

avoiding substrate inhibition by maintaining a constant concentration of raw materials by feeding at the substrate utilisation rate. In draw and fill operation the fermenter is run in simple batch or fed batch mode first. Once a product has formed, part of the culture is harvested. The remainder is diluted with fresh medium and growth continues. This minimises the sterilisation and lag times associated with restarting a fermentation.

2.6.2. Airlift column

The airlift column consists of a vertical cylinder with a concentric draft tube in it. The liquid level just covers the draft tube. Air is sparged at the base of the column either inside or outside the draft tube. The density difference that forms between the aerated and non-aerated regions due to the entrained air causes circulation of the culture. To achieve adequate circulation the height to diameter ratio should be about 10:1 (Onken *et al.* 1983) and the ratio of the inner and outer cylinder diameters should be between 0.6-0.9 (Weiland 1984). The airlift column does not contain an impeller and thus uses about one third of the energy requirements of a STR (Traeger *et al.* 1989). Low shear forces are exerted on cultures. However there is enough turbulence to suspend solid particles with a density of 2800 kgm^{-3} (Heck *et al.* 1987).

Traeger *et al.* (1989) compared the growth of *A.niger* in STR and airlift reactors. He found good mass transfer and growth as small pellets in airlift reactors. Similar mass transfer in the STR required high shear forces and ensured filamentous growth. Gbewonyo *et al.* (1983) reported that the oxygen transfer coefficient increased by a factor of 4 in changing from filamentous growth to small pellets in *Penicillium chrysogenum*.

2.6.3. Reactor configurations used with *A.niger*

The choice of reactor configuration depends on the type of product to be produced. The following reactor configurations are reported in literature for gluconic acid and glucose oxidase production:

a) Batch (Blom *et al.* 1957)

b) Draw and fill, fed batch reusing mycelia (Sakurai *et al.* 1989)

c) Reuse of mycelia (Mattey 1992)

d) Continuous disc fermenter (Anderson *et al.* 1980)

e) Airlift (Traeger *et al.* 1992)

2.6.3.1 Fed batch culture

Glucose concentrations above 15% by mass inhibit the production of gluconic acid (Lee 1987). In order to produce gluconic acid above 15%, the glucose must be added during the course of the fermentation. This is done by continuous or discrete addition of glucose powder or concentrated glucose solutions. Sakura (1989) added powdered glucose to fermentations to achieve to achieve a concentration of $150gl^{-1}$ at 0h, 3h, 6h and 10h. A final gluconic acid concentration of $550gl^{-1}$ was achieved at 30h. The fermenter was run at 6 atmospheres and aerated with a pure oxygen feed to satisfy the oxygen requirements.

2.6.3.2 Reuse of mycelia from batch cycles

If the fermentation is aimed at producing gluconic acid, reuse of the mycelia with fresh media is preferred. The *A.niger* suspension may be allowed to settle out at the end of a batch fermentation, the supernatant drawn off and fresh feed added to the cell mass (Mattey 1992). Alternatively the mycelia may be immobilised on a support to aid reuse of the cell mass. Supports for the immobilization of *A.niger* include polyurethane foam (Vassilev *et al.* 1993), calcium alginate (Moresi *et al.* 1991), glutaraldehyde, nonwoven fabric (Sakurai *et al.* 1989) and immobilization onto a rotating discs (Anderson *et al.* 1980).

Sakura (1989) compares the use of filamentous mycelia, the pellet form and mycelia immobilised onto nonwoven fabric for gluconic acid production. The pellet form could be reused four times whereas the filamentous form could only be reused three times. The longer life of the pellet form is attributed to its robustness. However, when an immobilised system was used, the mycelia could be reused as many as fourteen times with one addition of powdered glucose per use. Table 2.7 summarises the productivity of the various configurations. It can be seen that the time based productivity of the immobilised system is far less than the free format. This is due to slow reaction rates caused by diffusion limitations and can be reduced by the use of a different support.

Table 2.7 Comparison of durability of different morphologies and immobilisation *A.niger*

Configuration	Reaction time	Number of cycles	Total gluconic acid produced (g)	Average rate of gluconic acid production (g/h)
Filamentous	32	3	900	28
Pellet	29	4	980	34
Immobilized on nonwoven fabric	1100	15	3300	3

2.7 Enzyme kinetics of glucose oxidase

The kinetics of the enzyme catalysed conversion of glucose to gluconic acid are affected by the relative substrate, products and enzyme concentrations, the reaction kinetics and the deactivation kinetics of the enzyme.

2.7.1 Application of Michaelis-Menten kinetics to glucose oxidase

Glucose oxidase has been found to follow typical Michaelis-Menten saturation kinetics (Atkinson and Lester 1974). The oxidation of glucose to gluconic acid can be modelled by classical enzyme reactions involving the following species and combination intermediates:

G	the ß form of glucose
E_o	the oxidised form of glucose oxidase {E-FAD}
E_r	the reduced form of glucose oxidase {E-$FADH_2$}
L	glucono-δ-lactone an intermediate product
P	hydrogen peroxide
A	gluconic acid

S_G Glucose concentration

S_O Oxygen concentration

A reaction network has been described by Gibson *et al.* (1964), Bright and Gibson (1967) and Duke *et al.* (1969). These models are subsets of the most general model shown below (Atkinson and Lester 1974) :

$$E_o + G \underset{k_{-1}}{\overset{k_{+1}}{\rightleftarrows}} E_oG \qquad (2.3)$$

$$E_oG \overset{k_{+6}}{\rightarrow} E_rL \qquad (2.4)$$

$$E_rL \overset{k_{+2}}{\rightarrow} E_r + L \qquad (2.5)$$

$$E_r + O_2 \overset{k_{+3}}{\rightarrow} E_oP \qquad (2.6)$$

$$E_oP \overset{k_{+4}}{\rightarrow} E_o + P \qquad (2.7)$$

$$E_rL + G \overset{k_{+5}}{\rightarrow} E_r + L + G \qquad (2.8)$$

$$L \overset{k_h}{\rightarrow} A \qquad (2.9)$$

The reaction pathways can also be represented by the flow diagram in Figure 2.3.

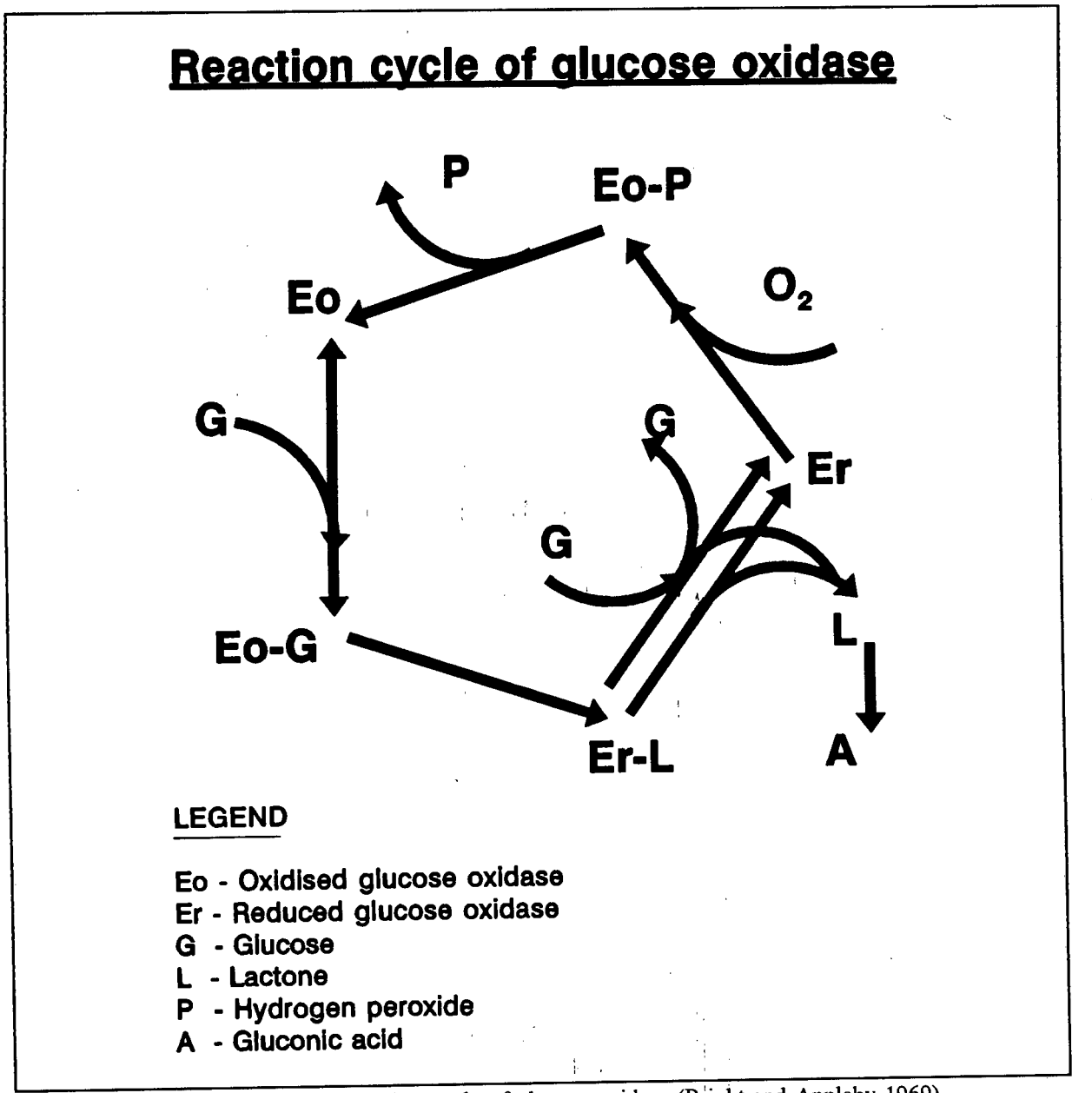

Figure 2.3 Diagram showing the reaction cycle of glucose oxidase (Bright and Appleby 1969)

The overall rate of gluconic acid formation, r_a, can be found by applying algebra to the reaction sequence. This is shown below:

$$\frac{1}{r_a} = \frac{k_{+1}+k_{+6}}{k_{+1}k_{+6}S_G} + \frac{1}{k_{+3}S_O} + \frac{1}{k_{+2}+k_{+5}S_G} + \frac{1}{k_{+4}} + \frac{1}{k_{+6}} \qquad \textbf{(2.10)}$$

This general model can be simplified by the following observations:

1. There are 2 routes for the breakdown of the reduced enzyme lactone complex. These are by glucose combination (Equation 2.8) and by spontaneous breakdown (Equation 2.5). As glucose does not combine readily with the complex, k_5 can be assumed to be 0.

2. Once the enzyme has bonded to the glucose, there is a rapid oxidation and formation of the oxidised enzyme lactone complex. Thus k_6 can be assumed to be infinity.

Thus the simplified kinetic model is given in Equation 2.11.

$$\frac{1}{r_a} = \frac{1}{k_{+1}S_G} + \frac{1}{k_{+3}S_O} + \frac{k_{+2} + k_{+4}}{k_{+2}\,k_{+4}} \qquad \textbf{(2.11)}$$

As the glucose and oxygen concentration tend to infinity, the rate tends to the maximum rate. The maximum rate is given by Equation 2.12. The rate of reaction can be represented as a ratio of the maximum rate to the actual rate shown in Equation 2.13:

$$r_{a,\max} = \frac{k_{+2}k_{+4}}{k_{+2}+k_{+4}} \qquad \textbf{(2.12)}$$

$$\frac{r_{a,\max}}{r_a} = \frac{\beta_G}{S_G} + \frac{\beta_O}{S_O} + 1 \qquad \textbf{(2.13)}$$

where,

$$\beta_G = \frac{k_{+2}k_{+4}}{k_{+1}(k_{+2}+k_{+4})} \qquad \textbf{(2.14)}$$

$$\beta_O = \frac{k_{+2}k_{+4}}{k_{+3}(k_{+2}+k_{+4})} \qquad \textbf{(2.15)}$$

2.7.2 Extension of glucose oxidase kinetics to include pH effect

Bright and Appleby (1969) have determined the effect of pH on rate. The proposed effect of hydrogen ions on the enzyme is shown in Figure 2.4 and in the following reactions given in Equations 2.17 to 2.21, the modified rate expression is given in Equation 2.21.

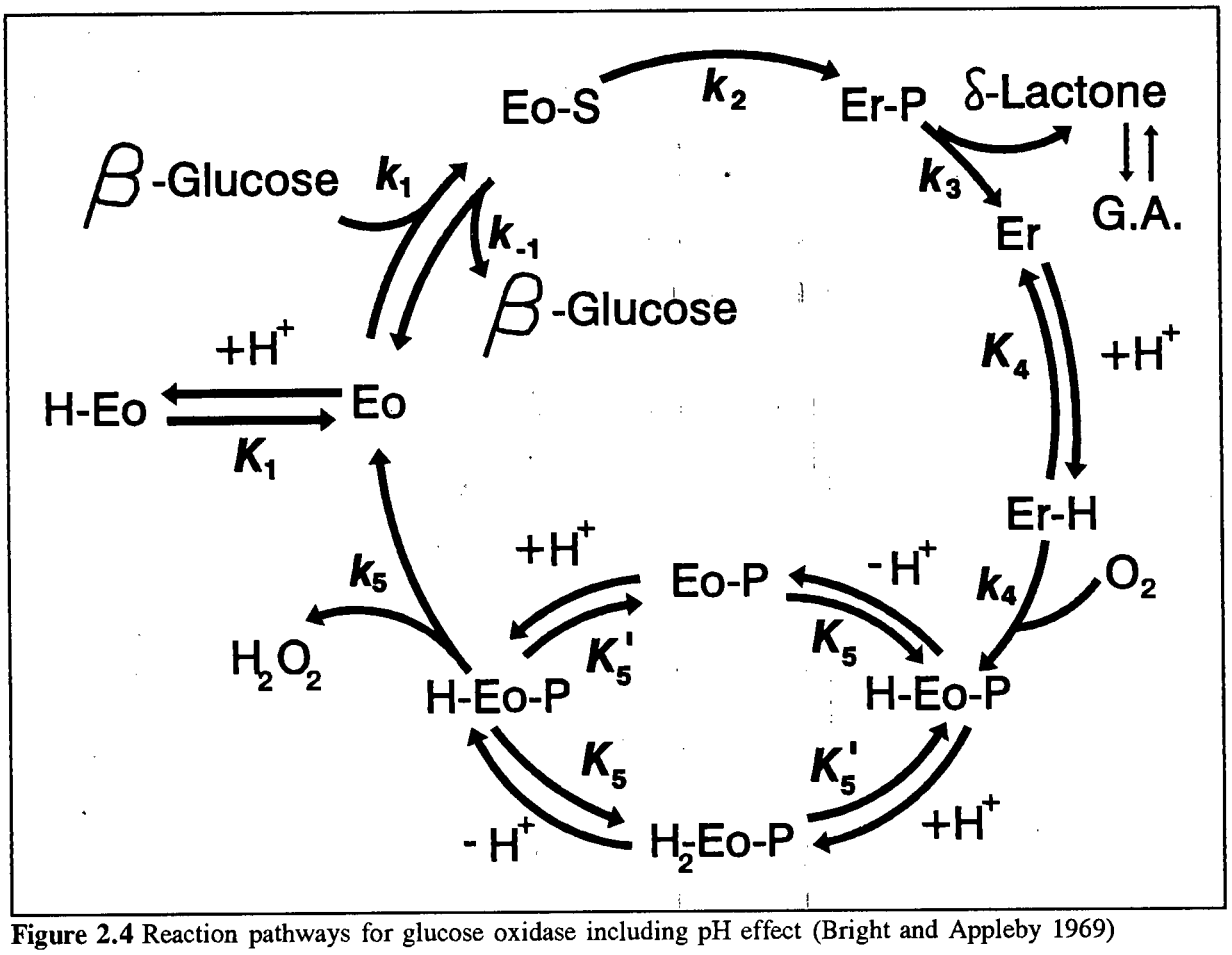

Figure 2.4 Reaction pathways for glucose oxidase including pH effect (Bright and Appleby 1969)

where:

H Hydrogen ions

S_H Hydrogen ion concentration

$$H + E_o \overset{K_1}{\rightleftarrows} E_o + H^+ \quad (2.16)$$

$$E_oPH^+ \overset{K_5}{\rightleftarrows} E_oP + H^+ \quad (2.17)$$

$$\downarrow\uparrow K_5' \qquad \downarrow\uparrow K_5' \quad (2.18)$$

$$H^+E_oPH^+ \overset{K_5}{\rightleftarrows} H^+E_oP \quad (2.19)$$

$$H^+ + E_r \overset{K_4}{\rightleftarrows} E_rH^+ \quad (2.20)$$

$$\frac{r_{a,\max}}{r_a} G_I(s_H) = \frac{\beta_G G_g(s_H)}{S_G} + \frac{\beta_O G_O(s_H)}{S_O} + 1 \quad (2.21)$$

where :

$$G_I(s_H) = \frac{1}{1 + s_3 + s_4} \quad (2.22)$$

$$G_g(s_H) = (1 + s_1)G_I \quad (2.23)$$

$$G_o(s_H) = (1 + s_2)G_I \quad (2.24)$$

$$s_1 = \frac{s_H}{K_1} \quad (2.25)$$

$$s_2 = \frac{K_4}{s_H} \quad (2.26)$$

$$s_3 = \frac{k_2}{k_2+k_4}\frac{s_H}{K_5} \quad (2.27)$$

$$s_4 = \frac{k_2}{k_2+k_4}\frac{K_5}{s_H} \quad (2.28)$$

The constants for these reactions have been determined by Atkinson and Lester (1975). These are shown in Table 2.8. Figures 2.5 to 2.7 show the modelled effects of pH, glucose and oxygen concentration on rate of gluconic acid formation.

Table 2.8 Constants and units for glucose oxidase kinetic model

Coefficient	Dimension	Correlation Coefficient	# of points	Value @ 25°C
k_1	1 $mol^{-1}s^{-1}$	0.904	12	11944
k_2	s^{-1}	.807	5	5093
k_3	1 $mol^{-1}s^{-1}$	.906	12	2.15E6
k_4	s^{-1}	.979	12	1171
K_1	mol l^{-1}			1.00E-4
K_4	mol l^{-1}			1.26E-7
K_5	mol l^{-1}			7.94E-5
K_5'	mol l^{-1}			4.00E-8

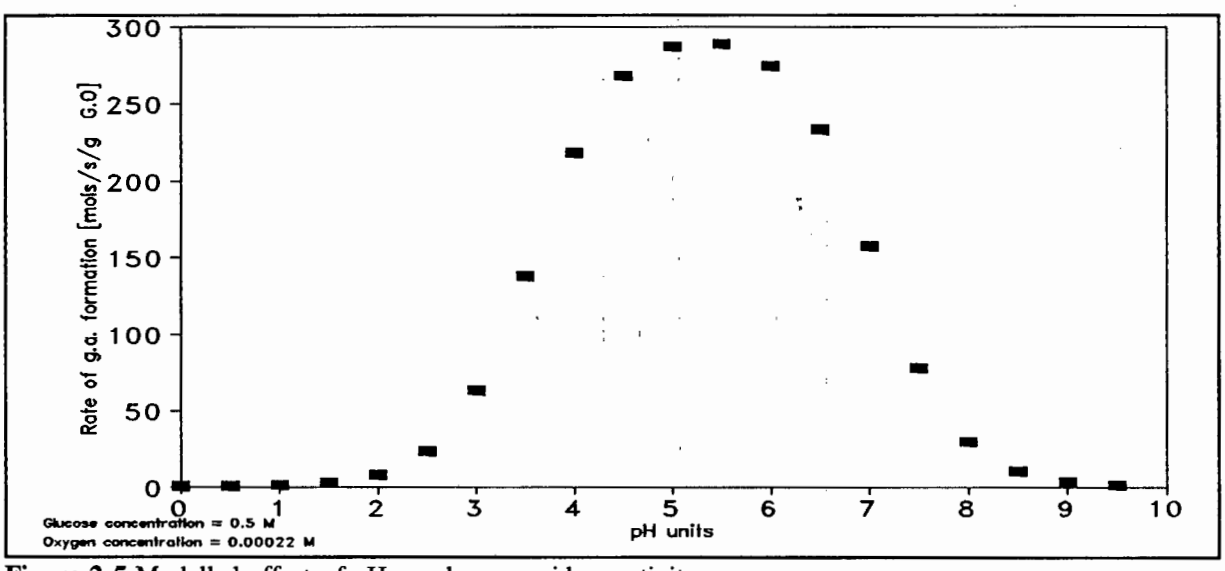

Figure 2.5 Modelled effect of pH on glucose oxidase activity

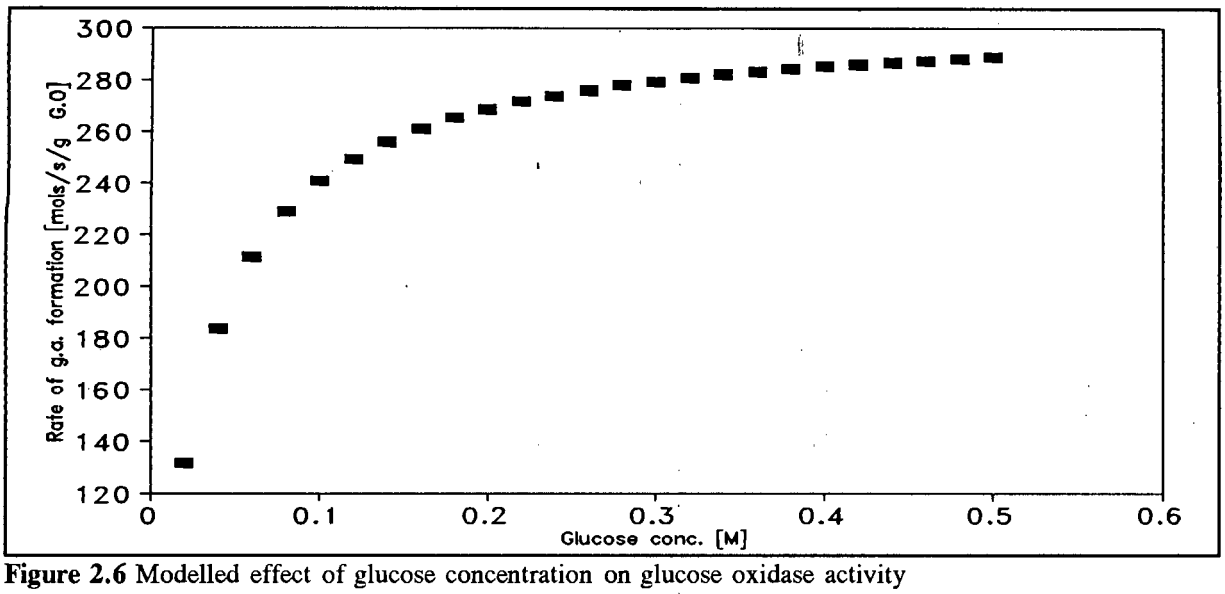

Figure 2.6 Modelled effect of glucose concentration on glucose oxidase activity

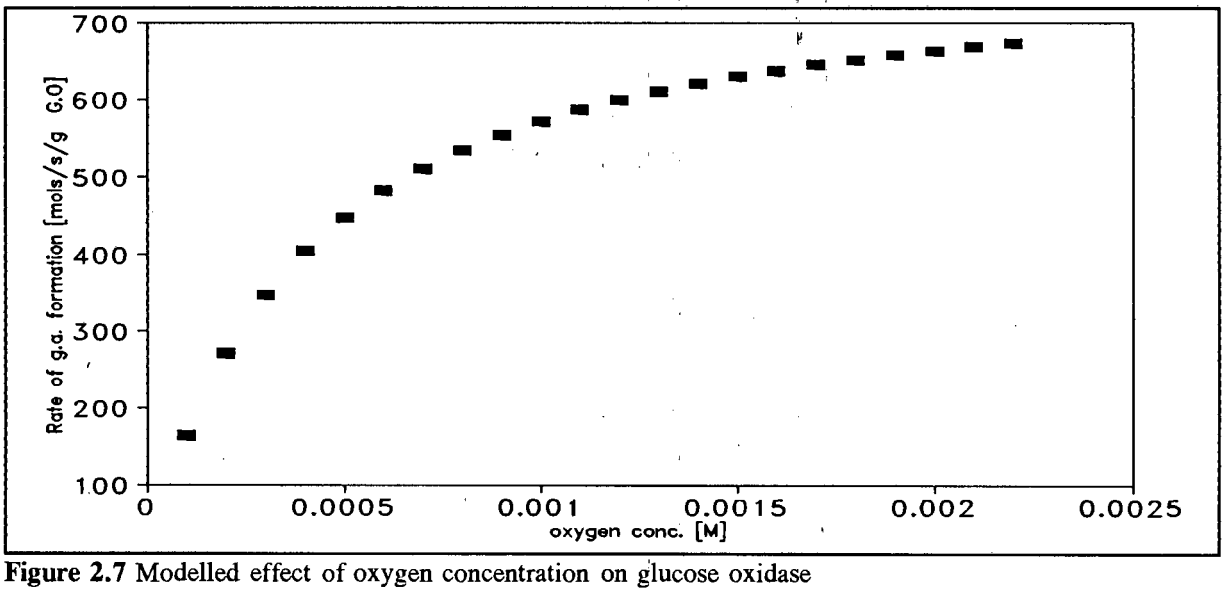

Figure 2.7 Modelled effect of oxygen concentration on glucose oxidase

2.7.3 Deactivation kinetics of glucose oxidase

Glucose oxidase can be deactivated by heavy metal poisons such as mercury and copper (Nakamatsu 1975). The kinetics of this process has not been studied in detail. The enzyme is also deactivated by oxygen and heat. These factors are covered in the next two sections.

2.7.3.1 Oxygen substrate inhibition

Glucose oxidase is deactivated by oxygen. The precise kinetics of the inhibition are not well understood. Venugopal and Saville (1993) have fitted a Michaelis-Menten kinetic model for substrate inhibition and have obtained a correlation coefficient of 0.95. The deactivation was modelled using a first order reaction shown in Equation 2.29.

$$E + S \underset{k_{-1}}{\overset{k_1}{\rightleftharpoons}} E\text{-}S \xrightarrow{k_2} E_I + S \qquad (2.29)$$

where:

E is the uncombined glucose oxidase enzyme (activity)

S is the oxygen concentration as the partial pressure (kPa)

E_I is the deactivated form

Using the equilibrium assumption, the deactivation rate is of the following form

$$r_d = \frac{k_d K_m E\, S}{S + K_m} \qquad (2.30)$$

$$k_d = \frac{k_1 k_2}{k_{-1} + k_2} \qquad (2.31) \qquad K_m = \frac{k_{-1} + k_2}{k_1} = \frac{k_2}{k_d} \qquad (3.1)$$

where:

r_d	Rate of deactivation of enzyme (U/h)
k_d	2.70 E-3 kPa/h
K_m	22.0 kPa
S	Oxygen partial pressure 0-100 kPa
E	Initial enzyme activity (U)

Figure 2.8 shows the half life of the deactivation rate constant as a function of oxygen concentration.

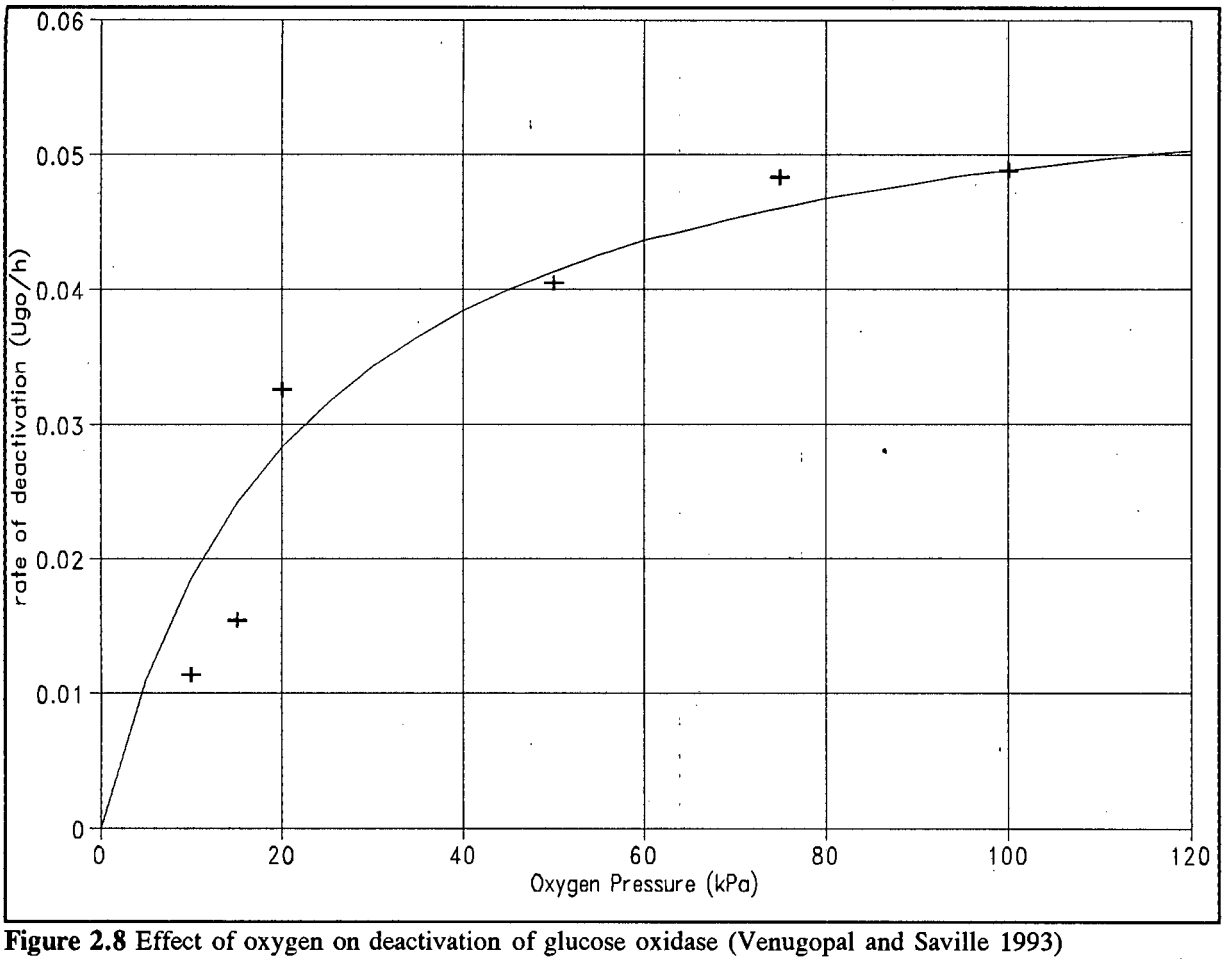

Figure 2.8 Effect of oxygen on deactivation of glucose oxidase (Venugopal and Saville 1993)

2.7.3.2 Temperature deactivation of glucose oxidase

Glucose oxidase activity shows a typical dependence on temperature. Icho *et al.* (1989) showed that the free enzyme denatured at 66.7°C and the enzyme immobilised on super fine fibres denatured at 70°C.

2.7.4 Mass transfer effects on glucose oxidase in a pelleted culture

When *A.niger* grows in pellet form, diffusion within the pellets may cause one of the substrate to become limiting or the product to become inhibiting. In the conversion of glucose

to gluconic acid by glucose oxidase, the first substrate to become limiting will be oxygen. This can be seen from analysis of the kinetics of the enzyme shown in Figure 2.7. Maximum oxidation rate as a function of glucose is readily achieved by using glucose concentrations above 0.2M ($36gl^{-1}$). To maximise the oxidation rate as a function of oxygen, a minimum oxygen concentration of 0.002M is required (Figure 2.7). When the dissolved oxygen concentration is limited by air saturation at atmospheric conditions, oxygen concentrations below 0.0002M or 6.4ppm are found. The slope of the enzyme activity increases as the dissolved oxygen decreases. Hence a small change at low concentrations in oxygen concentration affects the rate dramatically. Any further decrease in oxygen concentration in the pellet due to diffusion limitation will influence the rate of reaction more strongly than a similar decrease in glucose concentration.

Traeger (1991) demonstrates this oxygen limitation in pellets. He compared rates of gluconate conversion per unit of enzyme activity in the supernatant and in the pellet and found that their ratio changed from a ratio 47:53 to 22:78 when the pellet diameter increased from approximately 1mm to 2mm.

The last step in the formation of gluconic acid is the conversion of glucono-δ-lactone to gluconic acid. Above a pH of 5.5, the enzyme lactonase catalyses this reaction (Heinrich *et al.* 1986). Below this pH an accumulation of glucono-δ-lactone could shift equilibria preceding this final reaction. Heinrich *et al.* (1986) points out that in pelleted processes the glucono-δ-lactone could accumulate in a mycelial layer and inhibit glucose oxidase activity on the surface of mycelia.

2.7.5 Chemical effects on glucose oxidase

Several chemicals permanently inhibit the activity of glucose oxidase and some increase the activity. Table 2.9 shows the effect of some chemicals on glucose oxidase activity (Nakamatsu *et al.* 1975).

Table 2.9 Chemicals that enhance and inhibit glucose oxidase activity

Substance	Concentration	Effect
Ethanol	16% m/v	Increase the activity by 300 %
NaCl	4% m/v	Reduces the activity by 40%
$HgCl_2$	1mM	Inhibits glucose oxidase
$CuSO_4$	1mM	Inhibits glucose oxidase
$NaHSO_4$	1mM	Inhibits glucose oxidase
Phenylhydrazine	1mM	Inhibits glucose oxidase
p-hydroxymercuribenzoate	1mM	No effect
EDTA	1mM	No effect
hydroxylamine	1mM	No effect
dimedone	1mM	No effect

2.7.6 Specificity of glucose oxidase

An important aspect of industrial application of glucose oxidase is its high degree of specificity. This allows the enzyme to be used in diagnostic work where interference from other carbohydrates must be reduced to a minimum level. Table 2.10 shows the activity of glucose oxidase on various carbon sources (Rogalski 1988):

Table 2.10 Comparison of glucose oxidase activity on different carbohydrates

Substrate	Activity (%)
Glucose	100
2-Deoxy-δ-glucose	30
Cellobiose	0.1
Xylose	0.9
Galactose	0.6
Mannose	0.9
Fructose	0.1
Arabinose	0.2

2.8 Conclusion

The production of gluconic acid from *A.niger* is affected by two kinetic areas. The first is the kinetics of the induction of the glucose oxidase enzyme and the second is the conversion of glucose to gluconic acid catalysed by glucose oxidase. The glucose oxidase catalysed reaction is well understood in terms of enzyme kinetics, whereas the glucose oxidase induction kinetics is only understood in qualitative terms and no mechanism or quantification has been proposed or investigated.

The location of the enzyme appears to be affected by two process conditions - manganese concentration and dissolved oxygen concentration. It is important that the location of the enzyme is understood in these terms so that the bioprocess conditions can be engineered to complement efficient downstream processes.

3. EXPERIMENTAL PROCEDURE

3.1 Experimental philosophy

Literature has shown that there are 2 kinetic areas in the *A.niger* glucose oxidase and gluconic acid system: enzyme kinetics of glucose oxidase enzyme and induction kinetics of glucose oxidase. The first area has been well understood and documented. In the second area, there is considerable debate over the influence of glucose and oxygen and no quantification of the effects has been noted. In order to investigate the glucose oxidase induction system of *A.niger* with respect to glucose and oxygen it is necessary to choose an appropriate experimental system. The system must operate under conditions that will allow the inductive process of glucose oxidase to be observed. Mischak *et al.* (1985) used a pH shift from pH 2 (non-inducing range) to 5 (inducing range) to induce glucose oxidase. This method was implemented by growing inocula in the pH 2 range and introducing them into a variety of inducing environments, monitoring the induction of glucose oxidase.

3.2 Choice of induction environment

To explore the induction of glucose oxidase formation with respect to glucose and oxygen concentration, three concentrations of each were chosen to generate 9 different reaction conditions. The specific values chosen were based on literature findings.

Witteveen (1990) observed the minimum glucose concentration for glucose oxidase induction to be $36gl^{-1}$ or 0.2M. It has also been noted that $250gl^{-1}$ or 1.38M glucose fermentation becomes inhibiting (Lee *et al.* 1987). These concentrations serve as a guide for the choice of glucose concentrations. Three equi-spaced glucose concentrations of 50, 100 and 150 gl^{-1} were chosen.

Traeger (1991) found that increasing the partial pressure of oxygen from 7.7ppm to 27.1ppm, the glucose oxidase activity increased from 1 unit/ml to 4 units/ml. A minimum oxygen concentration for glucose oxidase induction was found to be 0.5ppm. Oxygen levels chosen

for this study range from 7.7ppm (0.21 atm) to 36.7ppm (1.0 atm) using pure oxygen. This extends the range reported by Traeger (1991).

3.3 Growing *A.niger*

3.3.1 The choice of a batch or a continuous process

In order to investigate the effect of glucose and oxygen on the induction of glucose oxidase in *A.niger*, batch experiments were performed at different glucose concentrations and dissolved oxygen partial pressures. Batch culture was chosen over continuous culture as it is experimentally difficult to implement a reproducible continuous protocol with pelleted mycelia. Selective harvesting of the liquid phase with respect to the biomass results. Thus after extended periods of time in continuous culture the cell mass in the reactor increases. Batch culture avoids this problem although it does not yield kinetic data directly and the results need to be deconvoluted to see the underlying mechanisms.

3.3.2 Inoculum growth conditions

The growth stage of the inoculum was chosen not to be in the exponential growth stage, as is done in industrial bioprocesses where the lag phase is to be avoided. Instead a stationary phase inoculum was employed to allow the induction process of the enzymes to be observed during the lag phase of batch culture.

The inoculum was prepared in two stages to ensure a reproducible morphology. A spore preparation was transferred from malt extract agar or potato dextrose agar plate culture into 50ml of 10% malt extract broth in a 125ml conical flasks via a flame sterilised Nichrome loop. The flasks were then incubated on a shaker at 30°C and 95 r.p.m. for 24h. The resulting pre-inoculum culture, containing many small regular pellets, was then used to inoculate the inoculum.

The 10% inoculum by volume was prepared using the fermentation media containing the same glucose levels as the experiment. The inoculum was grown in 3.0ℓ conical flasks at 30°C and 95 r.p.m. in a shaker for 3 days. The large conical flasks ensured good mixing and aeration. This prevented clumping of pellets in dead zones and ensured small regular pellets. Inocula were grown up for three days to ensure that the fungal pellets were in the stationary phase and all the inducible enzymes were in a relaxed state i.e. all processes had reached completion and were not in a transient state. In addition, the pH of the culture dropped to below the inducing range of glucose oxidase due to the formation of gluconic acid. Citric acid formation is, however, inhibited by the presence of manganese contained in the trace metal solution. The inocula were pumped into the reactor using a peristaltic pump.

3.3.3 Reactor media and conditions

In order to investigate the influence of glucose and oxygen on glucose oxidase formation, all other conditions in the reactor must remain constant. The set of operating conditions chosen for the experimental system were based on the pilot studies of Blom (1952). Table 3.1 summarises the conditions chosen.

The media was chosen to be suitable for industrial fermentation. The criterion was that the majority of nitrogen should come from an inorganic sourceas organic sources are usually more expensive than inorganic sources. The media was also chosen so that the cell mass formed was low to prevent excessively high viscosities associated with filamentous and pelleted fungi at high biomass levels.

To avoid foaming 0.2ml/l Sigma antifoam 289 was added to the reactor. A 20% m/m NaOH solution was used for base control. Figure 3.1 shows the equipment layout for the experiments and the data logging facility. A 7.0ℓ Chemapec laboratory fermenter with a working volume of 5.5ℓ was used. Agitation was achieved by two equispaced 90mm OD, 20x20mm 4 bladed rushton turbines driven by a central base shaft. The temperature was controlled to within $\pm$½°C by cooling and heating a 0.7 $lmin^{-1}$ water stream passing through two stainless steel heat transfer coils. pH was controlled by a UCT pH controller driving a

UCT peristaltic dosing pump. The base was drawn from a reservoir suspended on a logged scale pan. This allowed the base addition profile to be followed. A sterilisable Phoenix dissolved oxygen probe connected to a UCT amplifier was used to measure the dissolved oxygen. The air supply was passed through a de-mister and pressure regulation unit and then through a rotameter and carbon filter before entering the reactor. The carbon filter ensured that no biological contaminant entered with the air. The exhaust gases left the top of the fermenter via a condenser cooled with tap water and through a carbon filter to prevent contaminating the laboratory with *A.niger*. A steam sterilised sample port at the base of the vessel enables samples to be taken monoseptically. Dissolved oxygen and pH were logged onto a computer using a analogue to digital converter and the scale pan readings were logged digitally via RS-232C communication.

Table 3.1 Comparison of reactor conditions used in this study and by Blom (1952)

Condition	Blom (1952)	Setting used in this study
Temperature	30°C	30°C
Aeration	1-1.5 vvm	1.5 vvm
Agitation	100-200 r.p.m	600 r.p.m.
pH	6.0-6.5	5.5
Impeller type	single propeller	2x80mm rushton equispaced
Fermenter	Pilot plant 5701	Chemap bench 7.01

The media described by Witteveen *et al.* (1990) satisfied all of the above criteria, hence it was used as the reaction medium. It is detailed in Table 3.2.

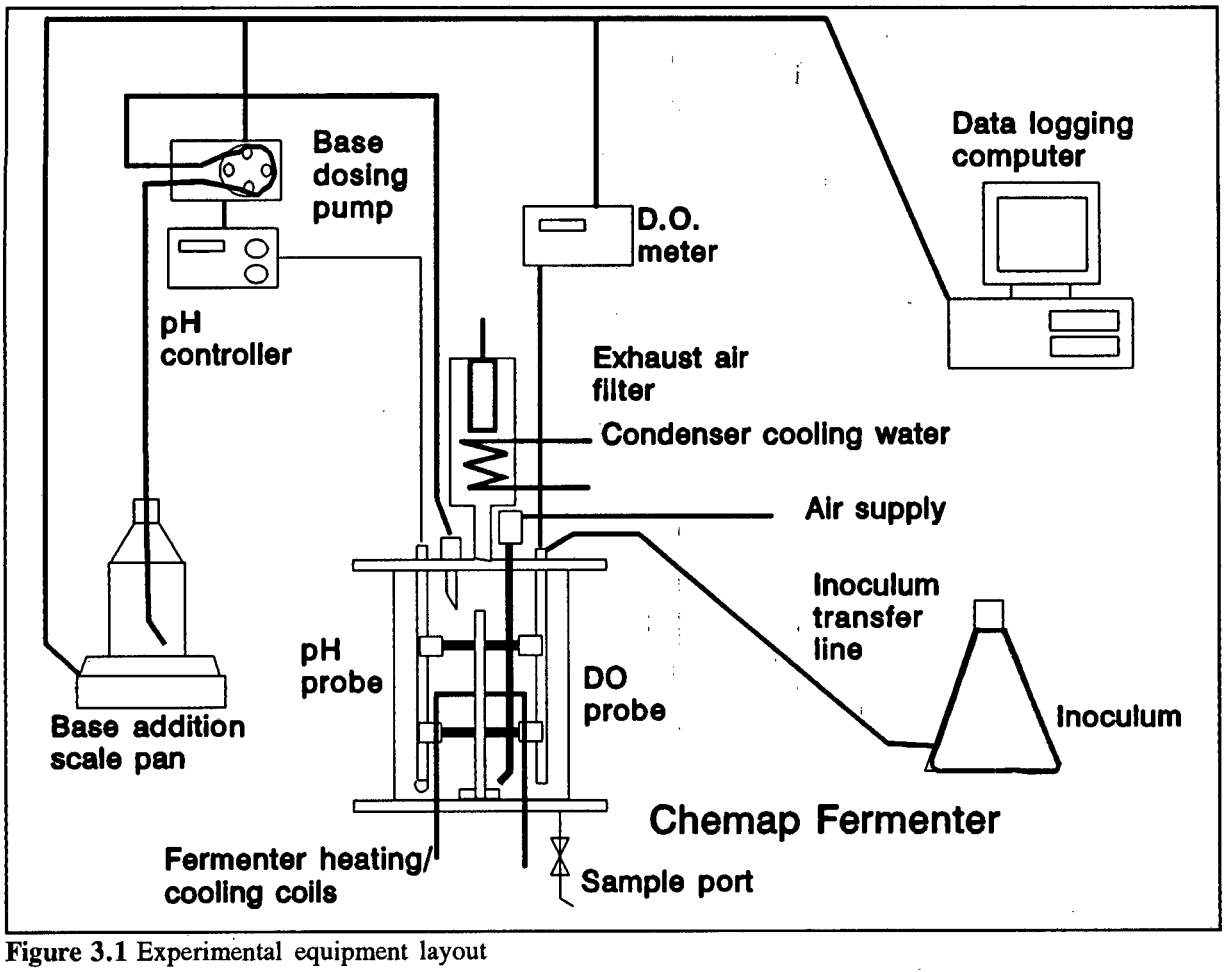

Figure 3.1 Experimental equipment layout

3.4 Experimental assay methods

It is necessary to set up a suite of analytical methods that quantitatively measure the properties and composition of the experimental system. The quality of these techniques determine the level of understanding of the underlying mechanisms. Quantitative assessment of the following parameters is detailed below: enzyme activity, oxygen utilisation rate, cell disruption, gluconic acid, sodium hydroxide addition, dissolved oxygen concentration, mass transfer coefficient K_la, dry cell mass, pellet size distribution and glucose concentration.

Table 3.2 Witteveen et al. (1990) media for gluconic acid fermentation and chemical specifications

Substance	Specification of chemicals used in this study	Concentration (g/l)
$NaNO_3$	UnivAR SARChem	1.20
KH_2PO_4	UnivAR SARChem	0.50
$MgSO_4 \cdot 7H_2O$	H.K. C.P.	0.20
Yeast extract	Oxoid CM19	0.50
Trace metal solution Vishniac and Santer (1957)	EDTA: 50gl^{-1}, $ZnSO_4 \cdot 7H_2O$: 22.0gl^{-1} $CaCl_2$: 5.54 gl^{-1}, $MnCl_2 \cdot 4H_2O$: 5.06gl^{-1} $FeSO_4 \cdot 7H_2O$: 4.99gl^{-1} $(NH_4)_6MoO_{24} \cdot 7H_2O$: 1.1gl^{-1} $CuSO_4 \cdot 5H_2O$: 1.57 gl^{-1} $CoCl_3 \cdot 6H_2O$: 1.61 gl^{-1} adjusted to pH 6.0	0.04 ml

3.4.1. Glucose oxidase activity

In order to measure the kinetics of the induction of glucose oxidase, it is necessary to be able to measure the activity of the enzyme. A variety of methods used in the literature each with its advantages and disadvantages. Two methods namely o-dianisidine and oxygen utilisation rate methods are described and compared here. In this study, glucose oxidase activity has been determined by the quantification of oxygen consumption. The glucose oxidase activity unit has been defined here as the number of μmoles of oxygen (O) consumed or glucose consumed or gluconic acid produced per ml per minute at pH 5.5 and at 30°C. The hydrogen peroxide produced by the glucose oxidase is degraded to oxygen and water by the peroxidase which has been shown to be produced concomitantly with glucose oxidase (Witteveen 1993). The net reaction in the glucose oxidase/peroxidase system is given in Equation 3.1.

$$glucose + O \xrightarrow{GOD/POD} gluconic\ acid \qquad (3.1)$$

3.4.2 Oxygen Utilisation method

This method measures the oxygen depleted as a result of the enzyme converting an excess of glucose (0.5M) in a 0.1M phosphate buffered media at pH 5.5. The method can measure enzyme activity in the presence of particulate matter such as cell debri. This method was chosen over the o-dianisidine method as it can measure total activity of disrupted cells and is inexpensive to operate. The method does, however, assume that peroxidase is induced at the same time as glucose oxidase. This assumption is appropriate as otherwise *A.niger* would deteriorate in the fermentation due to excess H_2O_2. Witteveen *et al.* (1993) has shown that glucose oxidase and peroxidase are induced at the same time. The assay is specific to oxygen utilisation and hence the oxygen utilisation of the disrupted mycelia is included in the measurement. The oxygen utilisation rate of 1:100 diluted disrupted cells has been found to be insignificant compared to typical glucose oxidase activities. A detailed description of the method and assay procedure is contained in Appendix A. The method is accurate to within 5% in samples diluted 1:120 and accurate to within 2% in samples diluted 1:24. The method can detect activity as low as 0.1 GO units.

3.4.3 O-dianisidine photometric method

This method is based on the coupled reaction of the oxidation of o-dianisidine to an orange coloured dye. The reaction occurs at pH 7.0 and an excess of peroxidase is added to ensure the hydrogen peroxide formed by the glucose oxidase oxidation reaction is decomposed quantitatively oxidising the o-dianisidine. This allows samples that may not have peroxidase present to be analyzed. The method is restricted to filtered samples. It cannot be used on disrupted whole cells which may have the enzyme attached to membranes.

3.4.4 Method of Cell disruption

In order to liberate the glucose oxidase formed within the mycelia or trapped in the pellets, the culture broth must be disrupted before the total enzyme activity can be assayed. Four methods of disruption were compared : French press, Al_2O_3 in a waring blender, bead mill and ultrasonication. The comparison is shown in Appendix B. From the data in Appendix B,

it is clear that the French press liberates all of the glucose oxidase after a single passes. This method was used to enable total glucose oxidase analysis.

3.4.5 Gluconic acid

Gluconic acid is the product of the glucose oxidase reaction. The acid can be measured using HPLC. In this case, a 0.1M H_2SO_4 solution was used as the solvent at a flow of 0.6ml/min in an ion exclusion emulsion column HPX-87H (300x7.8mm) [Catalogue number 125 0140 serial # 027 439]. Gluconic acid was detected by 215nm U.V. beam using a Beckman system gold. Gluconic acid has a residence time of about 8.3 minutes using a 25μl injection at 10gl^{-1} concentration. The HPLC is accurate to within 2% using injection volumes greater than 25μl. Injection volumes less than 10μl can have an error of $\pm$20%.

3.4.6 Sodium hydroxide addition

20% m/m sodium hydroxide was used to control the pH of the fermentations. Sodium hydroxide addition can be correlated to the amount of gluconic acid produced during the fermentation as gluconic acid is the only acid produced. The base addition was monitored using a scale pan. Correlation between the base added and the gluconate measured by HPLC was good, illustrating that 93% of base added formed gluconate (see Figure 4.5). Conversion has been quoted in the literature range from 85% to 100%.

3.4.7 Dissolved oxygen concentration

During the course of a fermentation the dissolved oxygen concentration shows the rate at which oxygen is being consumed. In the *A.niger* system the majority of oxygen consumed is used to oxidise glucose to gluconic acid.

Dissolved oxygen was measured using the polarographic Phoenix sterilisable dissolved oxygen electrode. This has a platinum anode and a silver cathode. It is fitted with a teflon membrane and KCl in glycerol electrolyte solution. The anode is polarised with +0.6V relative to the silver cathode. A resulting current is proportional to the dissolved oxygen

concentration. The probe had a time constant of 10s.

3.4.8 Oxygen utilisation rate

Oxygen utilisation rate gives the sum of oxygen used by respiration and oxygen consumed in gluconic acid formation. The rate is measured by turning the aeration off, lowering the agitation to 100 r.p.m. to minimise surface aeration and following the dissolved oxygen concentration with time. The slope of the dissolved oxygen profile gives the oxygen utilisation rate. Correlation coefficient, greater than 0.995 were attained and reproducibility was within 10%.

3.4.9 $K_l a$ mass transfer coefficient measurement

$K_l a$ measurements were taken before fermentations started in the pure media and at the end of the fermentation to show the effect of cell mass on the transfer coefficient. Table 3.3 shows the results obtained, Appendix D contains the method used.

Table 3.3 $k_l a$ variation with glucose concentration and media

glucose concentration (gl^{-1})	$k_l a$ (s^{-1}) (%error)	
	Media	Culture
Water	0.0728 (16%)	
50 gl^{-1}	0.0485 (7%)	0.0502 (4%)
100 gl^{-1}	0.0347 (5%)	0.0359 (3%)
150 gl^{-1}	0.0401 (2%)	0.0263 (1%)

3.4.10 Dry cell mass

The measurement of cell mass is difficult in *A.niger* due to the very low cell masses, low

density and pelleted nature of the fungus. Samples cannot be centrifuged down in an ordinary 10 000g lab centrifuge due to the low density of the cell mass. Dry weight must be measured using filtration techniques. 0.45μm millipore membrane (pre-dried in an oven at 100°C for 24h and pre-weighed) are used in order not to loose any of the filaments during filtration. The volume of sample used is increased from 1ml used in gravity settling assays to 20ml. This increased the cell mass measured and improves representative filtering of the pellet suspension. The wet cell masses were washed 3 times to remove entrained glucose/gluconate.

The dry cell mass method is described and validated in Appendix E, is accurate to within 5% and uses 30ml sample volumes. The method is most inaccurate at cell masses below $1gl^{-1}$.

3.4.11 Pellet size distribution

The pellet size distribution of a standard 10% glucose fermentation was measured to record the typical distribution of pellets during the course of the fermentation. Three 1.0ml broth samples were spread on slides and the image captured by a video camera. The resulting image was processed on a Joyce Loebel image processing package and the number and size of the pellets recorded. A description of the method used is contained in Appendix F.

This technique allows the hydrodynamic stress of the Chemap fermenter to be compared with other geometries of bioreactor.

3.4.12 Glucose

Glucose concentration was monitored using the Boehringer Mannheim glucose/GOD-Perid kit (CAT# MPR 3 124 036). The method and standard curve are detailed in Appendix G. Samples must be diluted into the 0 to 0.6 gl^{-1} glucose range to ensure the linear relationship between absorbance and glucose concentration. The assay technique is 2% accurate without dilution. The maximum error results from dilution and the method is accurate to within 7% at 1:1000 dilution.

3.5 Conclusions

An experimental system to observe and quantify the induction of glucose oxidase in *A.niger* with respect to glucose and oxygen has been described. The media was chosen to be appropriate for an industrial bioprocess so that results could be used for pilot plant development. Experimental apparatus and conditions were defined to allow glucose oxidase induction. Growth conditions of the inoculum were also defined to allow the glucose oxidase induction to be observed by a pH shift and *denovo* synthesis of glucose oxidase under controlled conditions.

A suite of experimental analytical techniques were formulated together with descriptions of the methods and error analysis for the following:

- Cell disruption
- Glucose oxidase activity
- Gluconic acid concentration
- Sodium hydroxide addition and its correlation to gluconic acid concentration
- Dissolved oxygen concentration
- Oxygen utilisation rate
- Gas mass transfer coefficient $k_l a$
- Dry cell mass
- Pellet size distribution
- Glucose concentration

4. RESULTS AND DISCUSSION

Aspergillus niger produces glucose oxidase in response to glucose and oxygen when cultured in the pH range of 3 to 7. Once glucose oxidase is produced, glucose present in the media is converted to gluconic acid at a rate depending on the enzyme kinetics of the glucose oxidase. One of the main aims of this study is to map out and demonstrate typical yields of glucose oxidase, gluconic acid and biomass under a set of base case conditions. Product profiles of glucose oxidase and gluconic acid give indications of typical fermentation times required for their production. Adequate aeration and agitation conditions can be evaluated from the base case for the design of larger scale reactors.

The induction kinetics of glucose oxidase has been described qualitatively in the literature but quantification of glucose oxidase induction has not been reported. The second main objective of this thesis is to study and quantify the trends and levels of glucose oxidase induction under a range of glucose and oxygen concentrations. In order to do this, 9 experiments were run with varying glucose and oxygen concentrations. Chapter 3 has set out motivation for the experimental conditions used and choice of media to observe the induction of glucose oxidase in batch culture. The glucose oxidase induction profiles generated enable the effect of glucose and oxygen and their interactions to be evaluated.

This section presents and discusses the results of a typical base case experiment for the production of glucose oxidase and gluconic acid. The effects of glucose and oxygen on the induction of glucose oxidase are then presented and discussed with a view for production of glucose oxidase and gluconic acid.

4.1. Glucose oxidase and gluconic acid formation at 100gl^{-1} glucose and 0.21 atm oxygen

In the base case experiment, 100 gl^{-1} glucose and air sparging (0.21 atm oxygen) were used. The setup of the bioreactor and the experimental conditions used are given in Section 3.3. Analytical techniques are describe in Section 3.4.

4.1.1 Substrate and oxygen utilisation

Glucose is converted by glucose oxidase to gluconic acid with the concomitant consumption of oxygen. The glucose concentration decreases at the same rate as the gluconic acid is produced. The final yield of gluconic acid produced at 24 hours is 94% on a basis of the initial glucose concentration (mole for mole). This is unusually high for a biological process and is achieved by ensuring that the cell mass is extremely low (± 2.5 gl^{-1}) resulting in a growth yield of 0.026g/g. Low biomass concentrations can be maintained where the production process is a biotransformation reaction and not a product of metabolism as in citric acid production.

The predicted glucose concentration using sodium hydroxide addition (as a measure of gluconic acid formation) and a mass balance fits the glucose profile well (Figure 4.1) as the majority of glucose is converted to gluconic acid and only a small fraction to cell mass. Section 4.1.4 describes and validates the correlation of gluconic acid and sodium hydroxide addition.

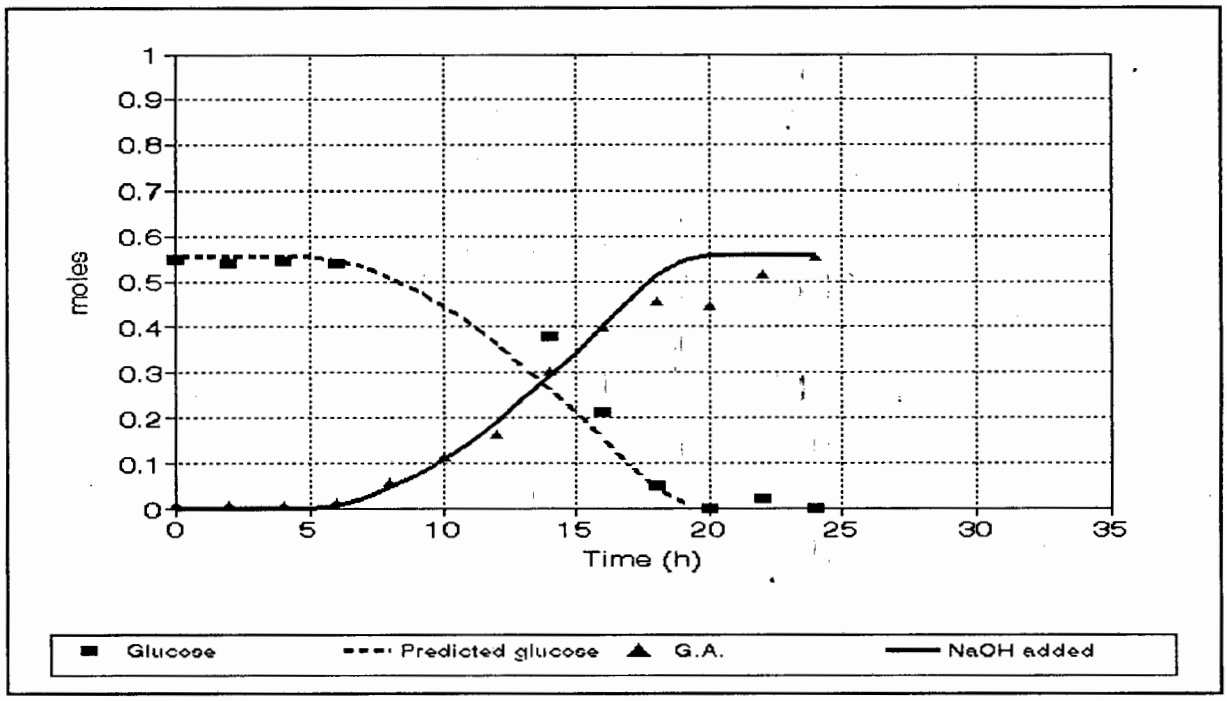

Figure 4.1 Glucose and gluconic acid concentrations as a function of time, using an in initial glucose concentration of 100 gl^{-1} at 0.21 atm oxygen

The utilisation of oxygen is undetectable during the 5 hour lag phase. Thereafter the oxygen utilisation rate (OUR) increases to ±300 ppm/min during glucose oxidation and then falls to ±110 ppm/min on depletion of the glucose. The final OUR is presumably due to cell respiration and maintenance.

The dissolved oxygen profile shows a minimum dissolved oxygen concentration corresponding to the time of maximum glucose oxidation. Table 4.1 shows the variation of minimum dissolved oxygen concentration with initial glucose concentration. The minimum dissolved oxygen levels follow same inverted trends as the maximum glucose oxidase activity. The experiment conducted at an initial glucose concentration of 100 gl^{-1} has the lowest minimum dissolved oxygen concentration of 2.3ppm followed by the 150 gl^{-1} experiment at 3ppm.

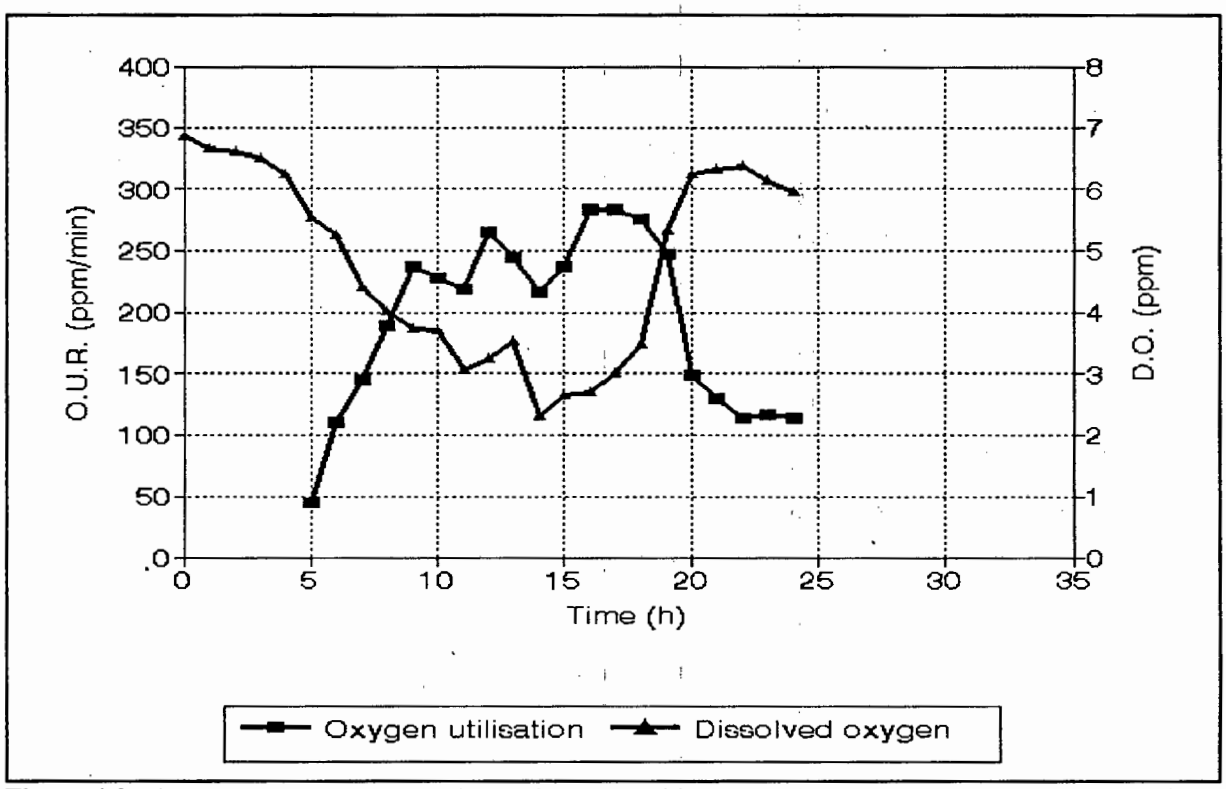

Figure 4.2 Dissolved oxygen concentration and oxygen utilisation rate profile for 100 g/l air fermentation

Table 4.1 Variation of minimum dissolved oxygen concentration with glucose level

Fermentation	50 g/l	100 g/l	150 g/l
D.O. (ppm)	5.5	2.3	3

4.1.2 Growth and cell mass profile

The biomass profile is shown in Figure 4.3. It can be seen that the profile is sigmoidal. This can be described by the logistic equation. Equation 4.1 and 4.2 describe the logistic equation and the nomenclature used. Explanation of the equation is also found in Section 5.3.2. The logistic equation was fitted to the data as shown in Figure 4.3 and the parameters are given in Table 4.2.

The logistic equation indicates the rate of change of cell mass as follows

$$\frac{dX}{dt} = \mu_{max} X\left(1 - \frac{X}{X_{max}}\right) \qquad \textbf{(4.1)}$$

and in its integrated form

$$X = \frac{X_o e^{\mu_{max} t}}{1 - \frac{X_o}{X_{max}}\left(1 - e^{\mu_{max} t}\right)} \qquad \textbf{(4.2)}$$

X, X_o Cell mass, initial cell mass (gl^{-1})

X_{max} Asymptotic maximum cell mass (gl^{-1})

μ_{max} Maximum growth rate (s^{-1})

The biomass yield of 0.0262 g/g was obtained when grown in the STR bioreactor under controlled conditions. This is higher than the biomass yield in the shake flask experiments (Table 4.2). The increase in yield could be due to the maintenance of a controlled pH in the

reactor compared with the decreasing pH in the shake flask or to the improved oxygen transfer in the reactor. In addition considerable pellet diffusion could result in the shake flasks due to the larger pellets formed in comparison to the relatively high mass transfer conditions resulting from small pellet sizes in the fermenter.

Table 4.2 Logistic equation parameters for dry cell mass measured in 100 g/l initial glucose concentration at 0.21 atm oxygen experiment

X_o (g/l)	X_{max} (g/l)	μ_{max} (h^{-1})	$Y_{x/s\ shake\ flask}$	$Y_{x/s\ fermenter}$
0.1651	2.6424	0.2311	0.0182	0.0262

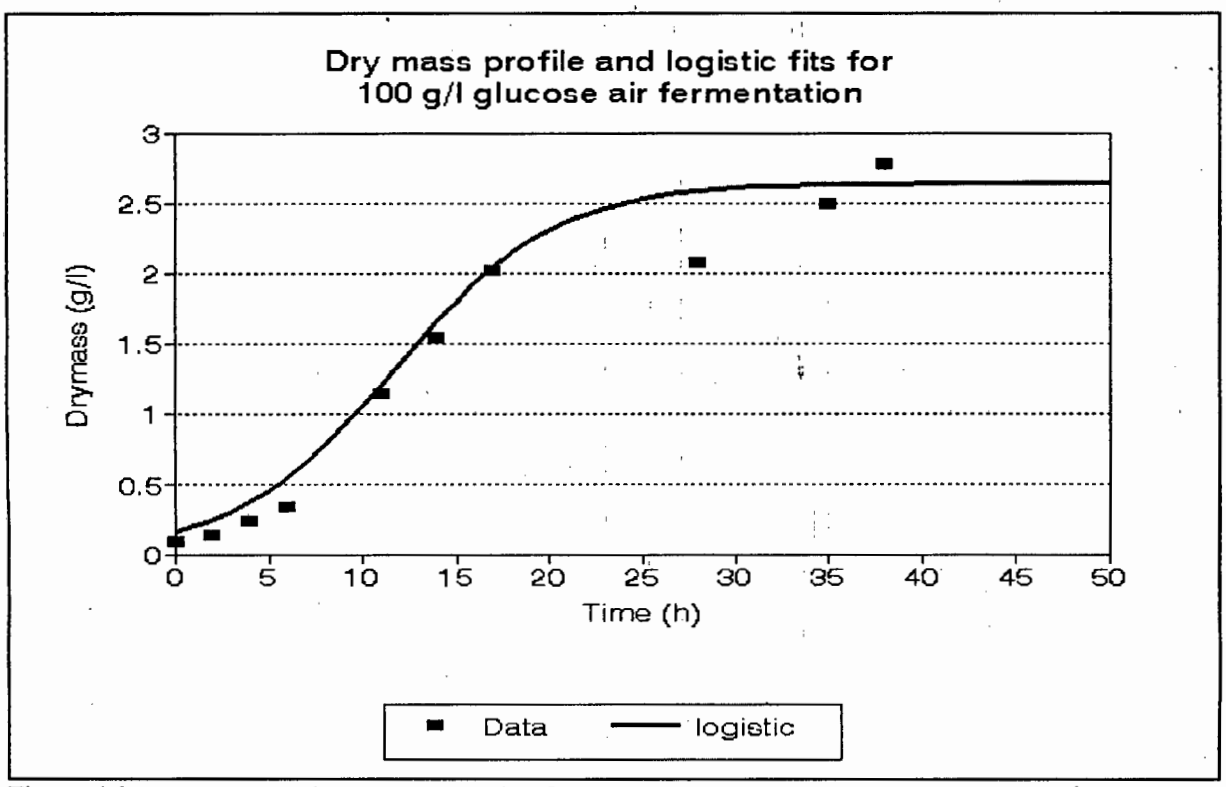

Figure 4.3 Biomass formation profile resulting from an initial glucose concentration of 100 gl^{-1} at 0.21 atm oxygen and its representation by the logistic equation

4.1.3 Appearance of glucose oxidase

Figure 4.4 illustrates the glucose oxidase activity as a function of time. Glucose oxidase activity is not observed during the initial 5h. The total glucose oxidase activity of the culture increases while glucose is present and remains constant when the glucose is depleted at 19 hours. The extracellular glucose oxidase activity increases after 5 hours to a plateau of 1 GO unit at 35 hours. Increase in the extracellular glucose oxidase activity may be due to diffusion of the enzyme out of the mycelial pellets or to active transport of the enzyme out of the cell envelope. Diffusion would result an extracellular glucose oxidase activity equal to the level in the pellet once steady state is reached. The actual location of glucose oxidase associated with the mycelial pellets is under debate in the literature. It has been reported in two locations: totally intracellular (Pazur 1966, van Dijken and Veenhuis 1990) or associated with a gel layer on the outer cell wall (Mischak 1985). Active transport would result in a controlled ratio of extracellular and intracellular glucose oxidase activities.

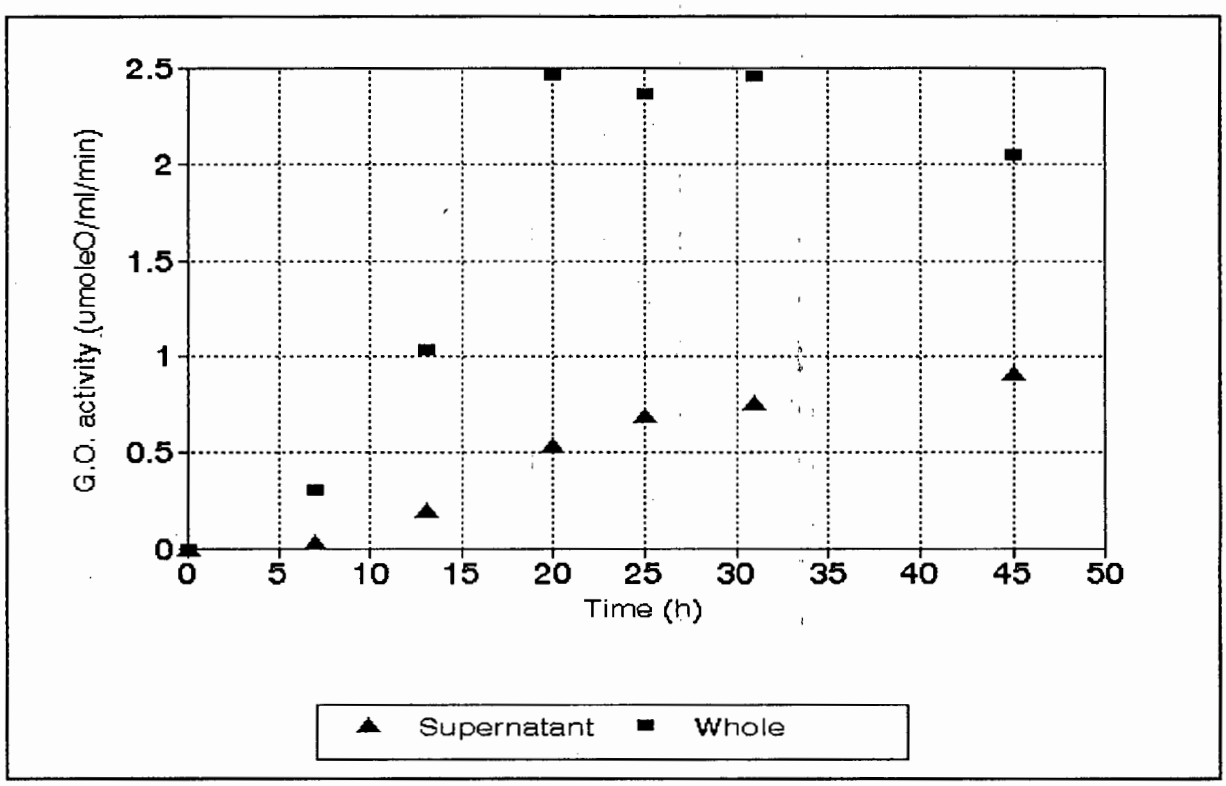

Figure 4.4 Glucose oxidase activity for 100 g/l fermentation in air

4.1.4 Gluconic acid production and sodium hydroxide consumption

Gluconic acid forms after a 6 hour lag, conversion halts after 19 hours. Figure 4.5 shows the correlation of gluconic acid formed and sodium hydroxide added. Table 4.3 shows the correlation coefficients and slopes of the regressions for the 100 gl^{-1} and 150gl^{-1} glucose experiments in air. It can be seen that the sodium hydroxide added follows the gluconic acid production well at low gluconic acid levels. It is possible that other organic acids are produced, however this is unlikely as the HPLC profile shows only a single peak for gluconic acid. Although most strains of *Aspergillus niger* can form mixtures of gluconic, citric and oxalic acid during gluconic acid production (Lockwood 1979), strain NRRL 3 has been shown to produce gluconic acid alone using manganese to inhibit citric acid formation (Blom 1952). Manganese is present at this inhibitory level in this study.

Table 4.3 Regression of sodium hydroxide addition and gluconic acid formed

Glucose (gl^{-1})	Correlation coefficient	Intercept (molesOH)	Slope (MolesOH/ MoleG.A)
100	0.977	-0.007	1.097
150	0.998	0.011	1.070

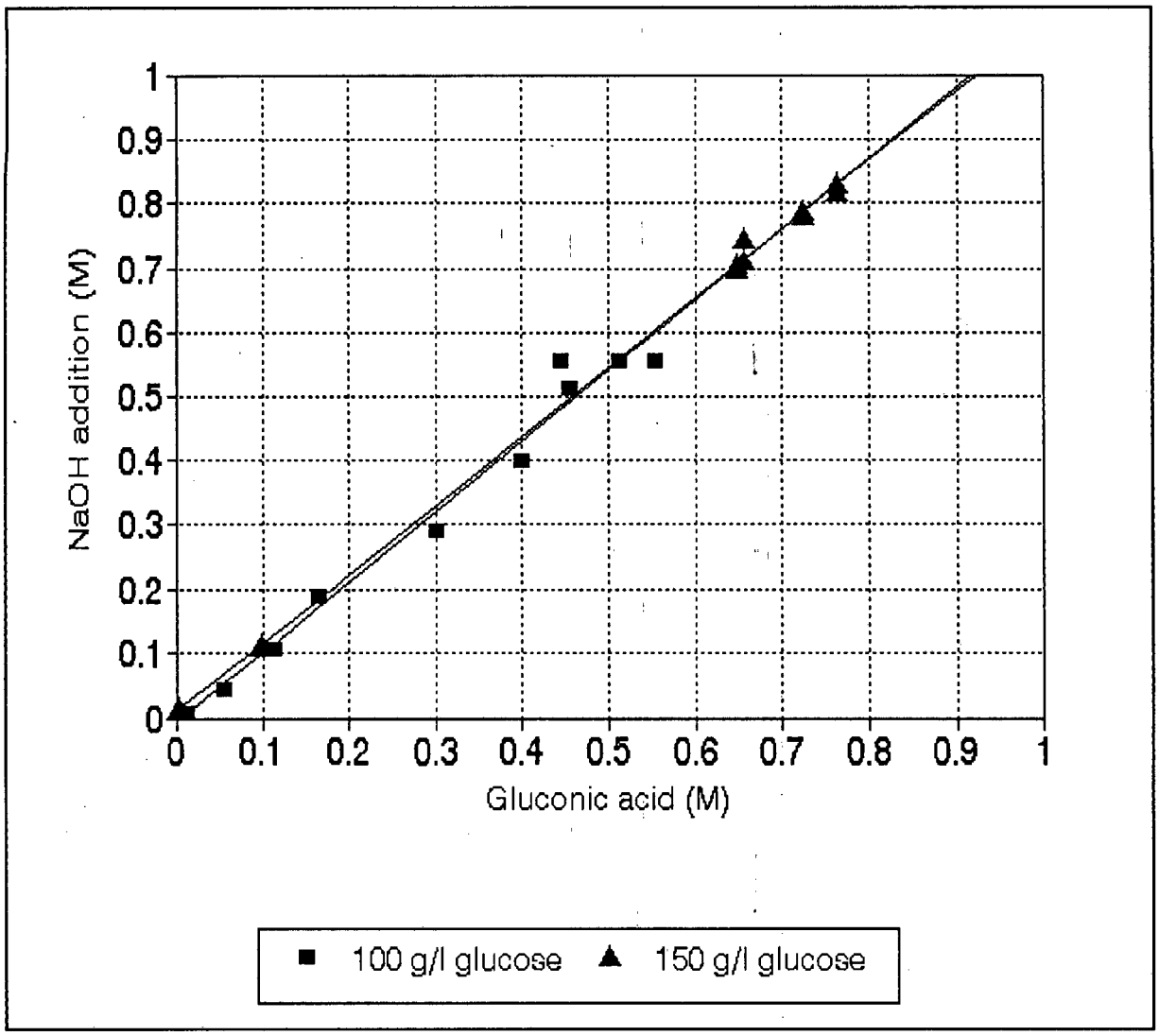

Figure 4.5 Correlation of sodium hydroxide addition and gluconate formed in air experiments

4.1.5 Morphology

Image analysis was used to determine pellet size distributions in whole fermentation samples. The size distributions of the 100 gl^{-1} initial glucose concentration at 0.21 atm oxygen experiment are shown in Figures 4.6-4.11 as a function of time.

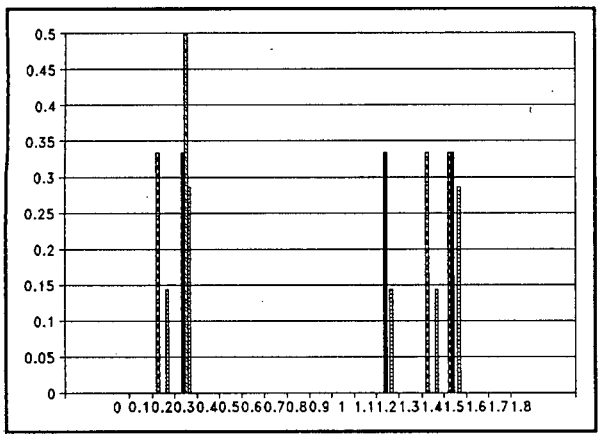

Figure 4.6 Pellet size distribution at 5 hours

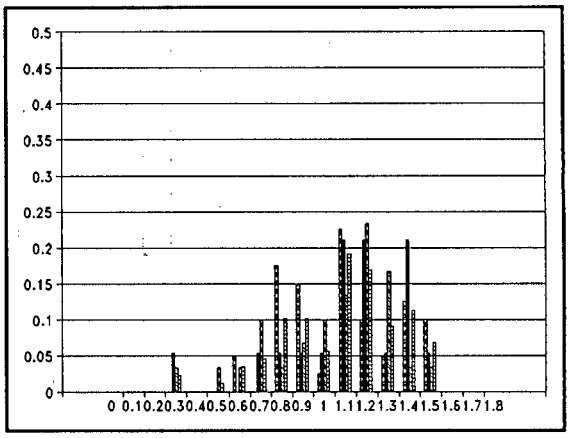

Figure 4.7 Pellet size distribution at 11 hours

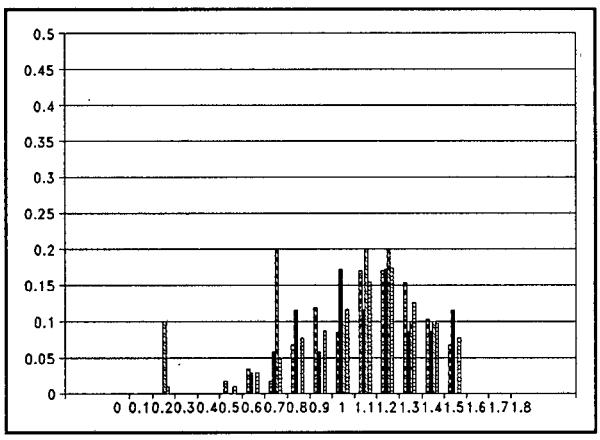

Figure 4.8 Pellet size distribution at 19 hours

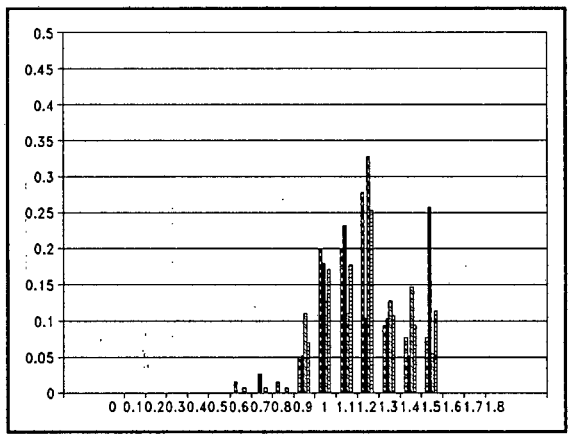

Figure 4.9 Pellet size distribution at 24 hours

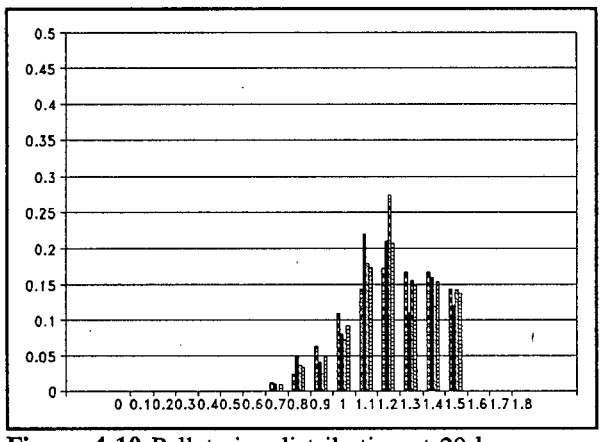

Figure 4.10 Pellet size distribution at 29 hours

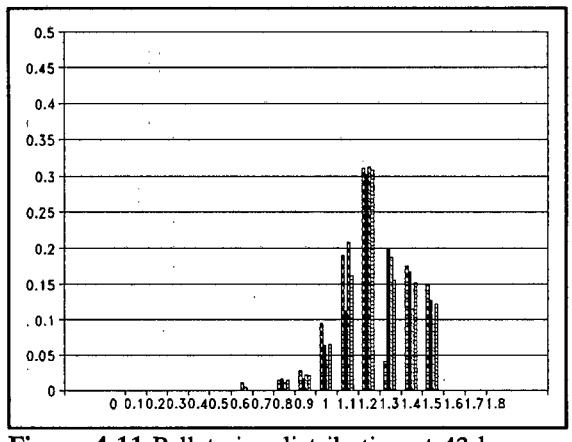

Figure 4.11 Pellet size distribution at 43 hours

The pellet size distribution profiles show that the inoculum has a bi-modal distribution. This corresponds to the presence of the filamentous and pelleted form. As fermentation progresses, the two distributions move together to form a unimodal distribution. It appears that the hydrodynamic forces in the reactor allow only a narrow size band of pellets to exist. The larger pellets fragment and the filaments aggregate as time progresses. The size of the

final average pellet may give an indication to the hydrodynamic forces present in the bioreactor. The inoculum is grown under low shear and forms very large soft pellets. These are instantly broken down in the fermenter and more compact smaller pellets are produced.

4.1.6 Glucose oxidase production and location

In Section 4.1.3, it was illustrated that glucose oxidase is located in the culture fluid and within the pellets. The glucose oxidase located within the pellet can be exposed to a micro-environment caused by diffusion resistances of either reactants or products. The micro-environment within the pellet is not homogeneous but has composition varying with radial position. The overall reaction rate is decreased because the glucose oxidase operates with a substrate concentration gradient which is lower than bulk substrate concentration. Differential mass balance equations can be set up for the pellet to predict the concentration profiles and the average rate of reaction for the whole pellet. This can be expressed as an effectiveness factor which is defined as the ratio of the average reaction rate of the pellet to the rate of reaction in the pellet if there were no diffusion resistances. Appendix H shows the calculation of the effectiveness factor for oxygen diffusion within the pellets in the *A. niger* system, based on the work by Kobayashi *et al.* (1973).

Oxygen, glucose and hydroxyl ions diffuse into the pellet and are converted to glucono-δ-lactone. There is a maximum rate at which each of the reactants can diffuse into the mycelial pellets. The glucose oxidase catalysed reaction rate cannot exceed the diffusion rate. Thus at high glucose oxidase activities diffusion may limit the overall rate of reaction within the pellet. Traeger (1991) observed that glucose oxidase associated with the pellet operates at 47% of the rate of the extracellular enzyme. The lower value indicates that the overall rate of reaction is limited by the rate of diffusion of reactants into the pellet. Diffusion effects can limit oxygen, glucose and hydroxyl ion concentrations in the pellets. Glucose and oxygen concentrations affect the overall rate as they are reactants. Hydroxyl ions affect the reaction in two ways. Firstly, the pH will decrease from the optimum pH of 5.5 due to gluconic acid formation. Secondly, the hydrolysis of glucono-δ-lactone will be inhibited by the shortage of hydroxyl ions.

Consideration of oxygen diffusion alone, according to the approach of Kobayashi *et al.* (1973) (Appendix H), predicts that the intracellular enzyme operates at 52% of maximum efficiency in the experiment conducted at an initial glucose concentration of 100 gl^{-1} at 0.21 atm oxygen. Glucose and hydroxyl ion diffusion effects have not been measured or modelled for mycelial pellets.

Figure 4.12 shows that the extracellular glucose oxidase only accounts for ±30% of the total enzyme produced at the end of 30h. During the conversion of glucose to gluconic acid (6-19h) the enzyme is predominantly intracellular. This implies that the majority of the gluconate formed is catalysed within the mycelial pellet.

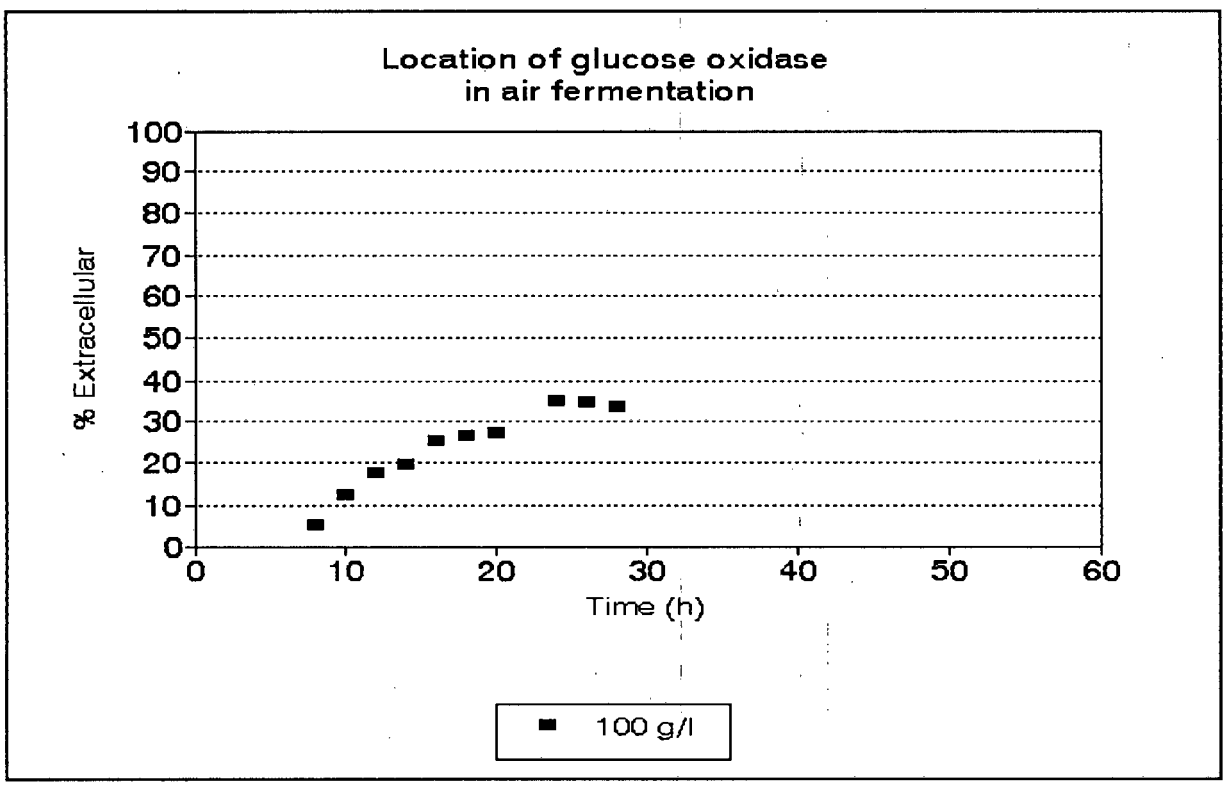

Figure 4.12 Percentage extracelular glucose oxidase of total glucose oxidase for experiment conducted at an initial glucose concentration of 100 gl^{-1} at 0.21 atm oxygen

4.2 The role of glucose in the induction of glucose oxidase

Experiments were conducted at an initial glucose concentration of 50 and 150 gl^{-1} in air to observe the effect of glucose on the induction of glucose oxidase. The experimental conditions were identical to those described in Section 3.3.

4.2.1 Substrate and oxygen utilisation

Figures 4.13 and 4.14 show the dissolved oxygen, glucose, gluconic acid concentration and sodium hydroxide additions for the 50 and 150 gl^{-1} experiments. The reactions have a 5 to 8 hour lag phase before induction of glucose oxidase and subsequent conversion of glucose to gluconic acid. The conversion times of glucose to gluconic acid and rates of glucose oxidase oxidation are given in Table 4.4. It can be seen that the sodium hydroxide addition is generally over predicting the gluconic acid level. As stated earlier this may be due to dilution error in HPLC.

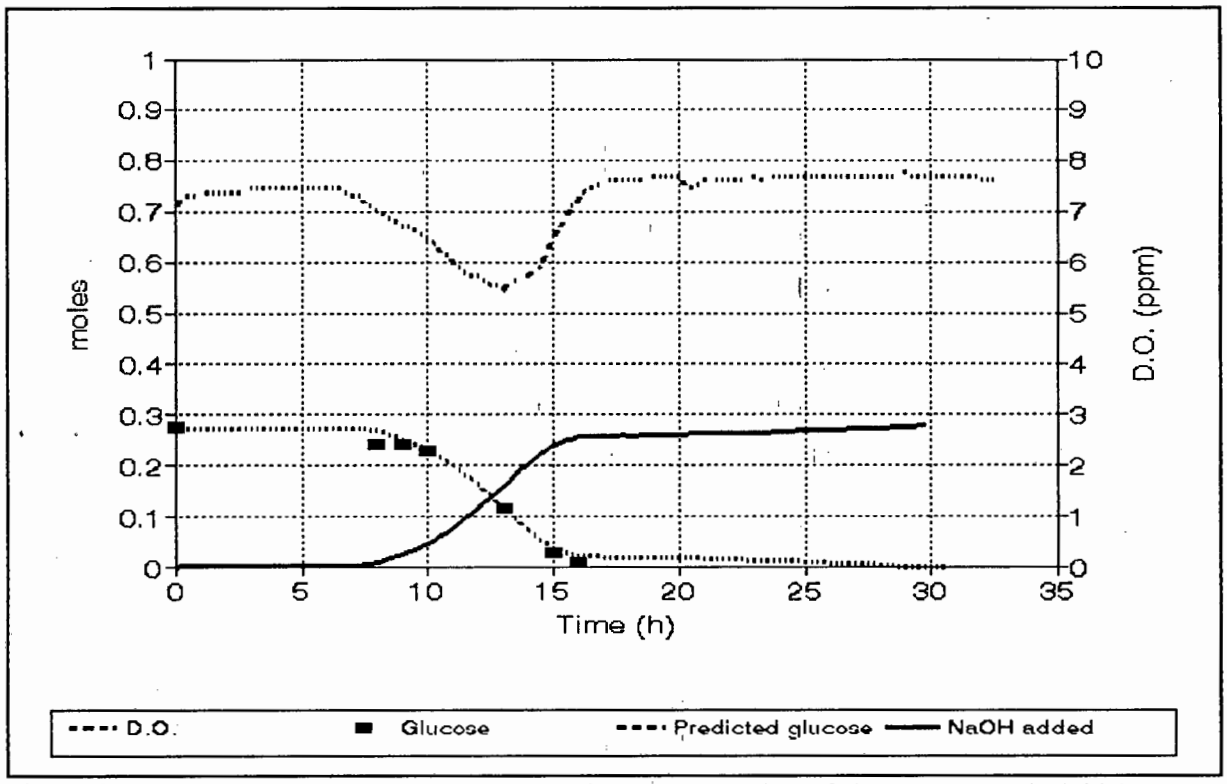

Figure 4.13 Glucose and gluconic acid concentrations as a function of time, using an in initial glucose concentration of 50 gl^{-1} at 0.21 atm oxygen

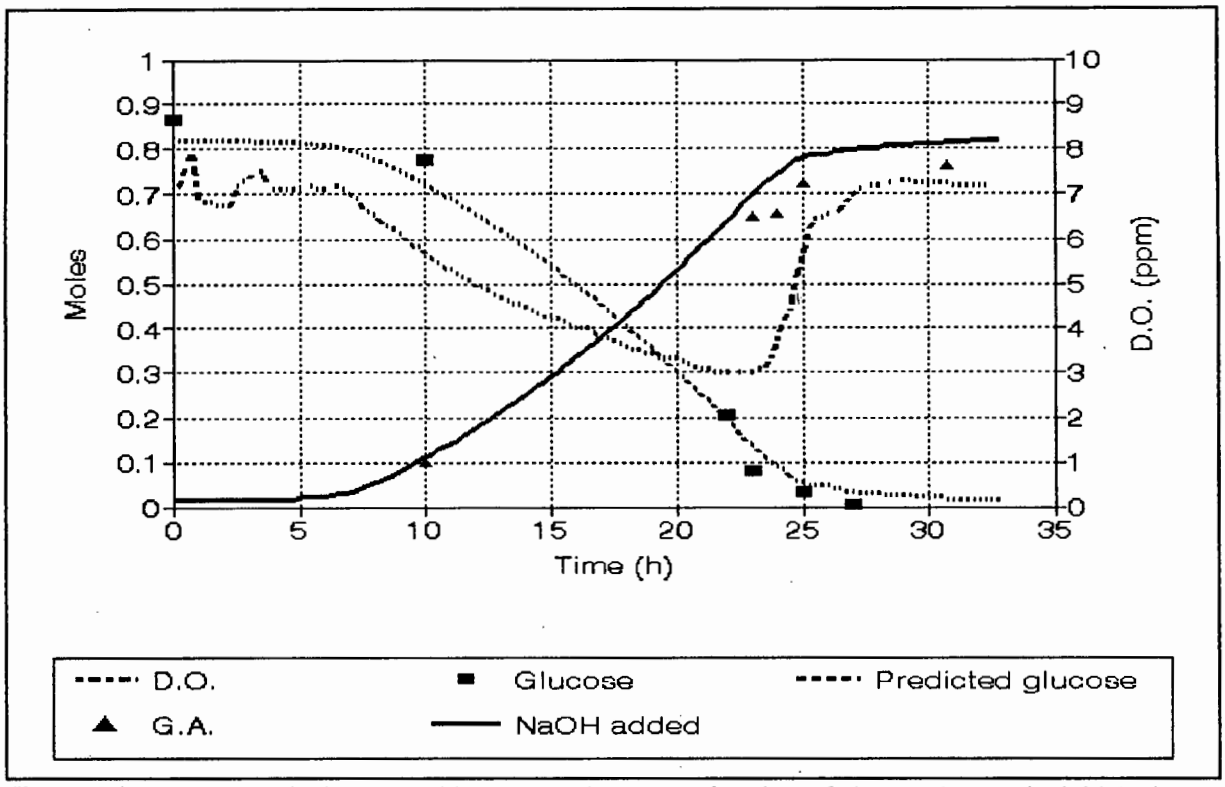

Figure 4.14 Glucose and gluconic acid concentrations as a function of time, using an in initial glucose concentration of 150 gl^{-1} at 0.21 atm oxygen

Table 4.4 Lag time, conversion times of gluconic acid and rates for air fermentations

(h)	50 g/l glucose	100 g/l glucose	150 g/l glucose
Lag time (h)	7	6	6
Conversion time (h)	9	13	20
Conversion rate g/h_{cnv}	5.6	7.7	7.5
Conversion rate g/h_{total}	3.1	5.3	5.8

4.2.2 Growth and dry mass results

The dry mass profiles obtained with initial glucose concentration of 50, 100 and 150 gl^{-1} are shown in Figure 4.15. The logistic equation has been fitted to those profiles (Figure 4.15) Experimental biomass concentrations and yields as well as logistic equation parameters are summarised in Table 4.5. It can be seen that the initial glucose concentration has a marginal effect on the initial and final cell masses and maximum growth rate. The 50 gl^{-1} glucose

fermentation produces the lowest final cell mass followed by the 150 gl^{-1} case. The final biomass concentration of the 50 gl^{-1} glucose experiment is lower than the 100 and 150 gl^{-1} glucose experiments at the 95% confidence interval. Calculation of the glucose required for biomass using a typical yeast biomass composition $CH_{1.75}N_{0.15}O_{0.5}$ (Atkinson and Mavituna 1983) shows that 3.1 gl^{-1} glucose is used in biomass synthesis showing that the culture is not carbon limited. It is important to note that the biomass is not a function of the glucose concentration as the culture is nitrogen limited i.e. the initial nitrogen concentration in the medium determines the final biomass concentration. Once the nitrogen source has been depleted, proteins and nucleic acids cannot be synthesised and growth halts. The biomass glucose yield $Y_{x/s}$ shows that the biomass does not increase with the increasing glucose concentration. It shows a decreasing yield as the biomass remains constant compared to the changing glucose concentration. Again this illustrates that the gluconic acid is not growth associated and that the culture is not limited by glucose.

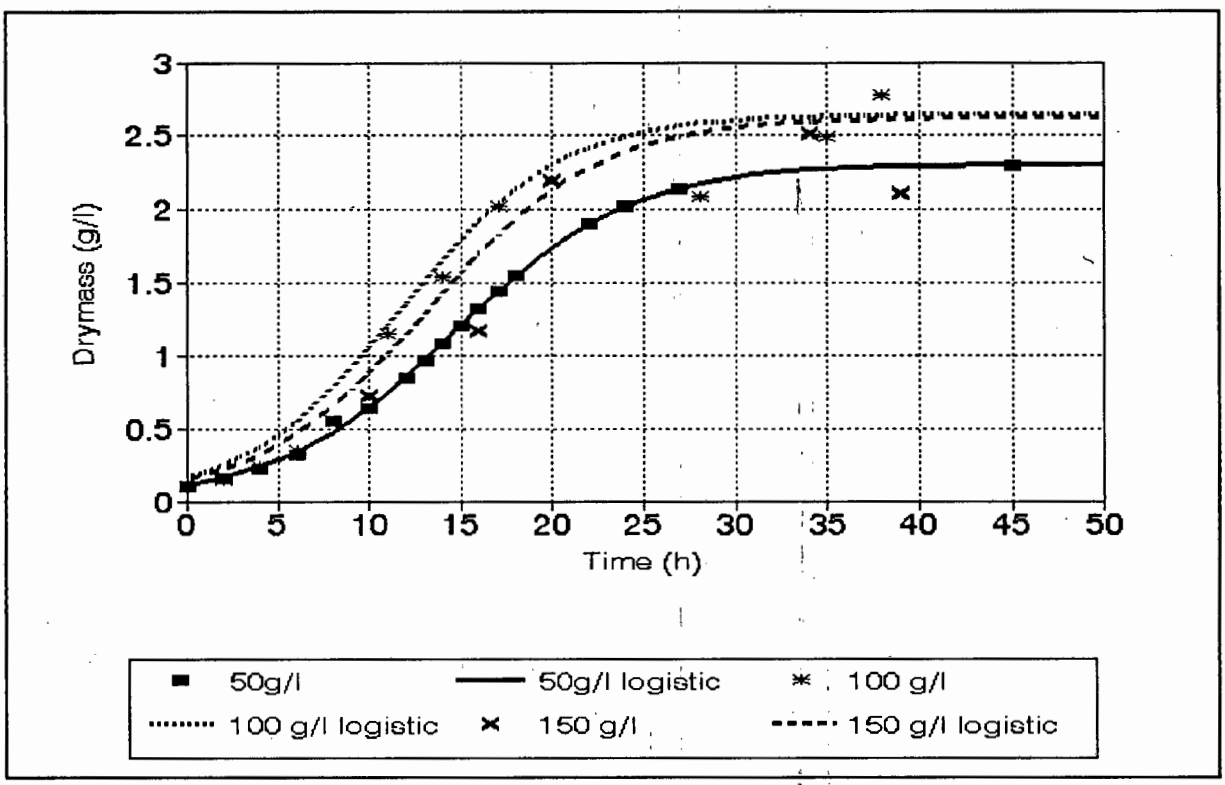

Figure 4.15 Dry mass and logistic fit profiles for glucose fermentations in air

Table 4.5 Logistic parameters for glucose fermentations in air

	50 g/l	100 g/l	150 g/l
X_o (g/l)	0.1110	0.1651	0.1503
X_{max} (g/l)	2.3095	2.6424	2.624
μ_{max} (h^{-1})	0.2053	0.2311	0.2136
$Y_{x/s\ shaker}$	0.0244	0.0181	0.0110
$Y_{x/s\ fermenter}$	0.0462	0.0264	0.0175

4.2.3 Appearance of glucose oxidase

The effect of glucose on the glucose oxidase profile for air fermentations is shown in Figure 4.16. It can be seen that the enzyme is induced between 5 and 7 hours after inoculation and reaches a plateau once all of the glucose is consumed.

In order to quantify differences in the rate of induction under varying glucose and oxygen conditions, the initial induction rate is used. Once glucose oxidase production has been initiated, glucose and oxygen are consumed lowering the levels in the environment. Thus, in the later stages of the reaction glucose oxidase is produced as a function of the resultant glucose and oxygen levels. Before the formation of glucose oxidase, the rate of reaction is zero and thus the pellet is homogeneous. The pellet conditions are the same as in the bulk medium. In the presence of glucose oxidase, a profile of dissolved oxygen, glucose and pH is set up within the pellet. The concentration of glucose, oxygen and OH^- ions are then lower than the bulk level. This affects the future induction of glucose oxidase and the gluconic acid reaction rate.

The initial rates of glucose oxidase production together with final glucose oxidase activities are shown in Figure 4.17. The slopes were calculated from linear regression of the first 3 data points. In the range of 50 to 150 gl^{-1} glucose in air, the 100 gl^{-1} glucose case has maximal induction rate and final level of glucose oxidase activity (Table 4.6).

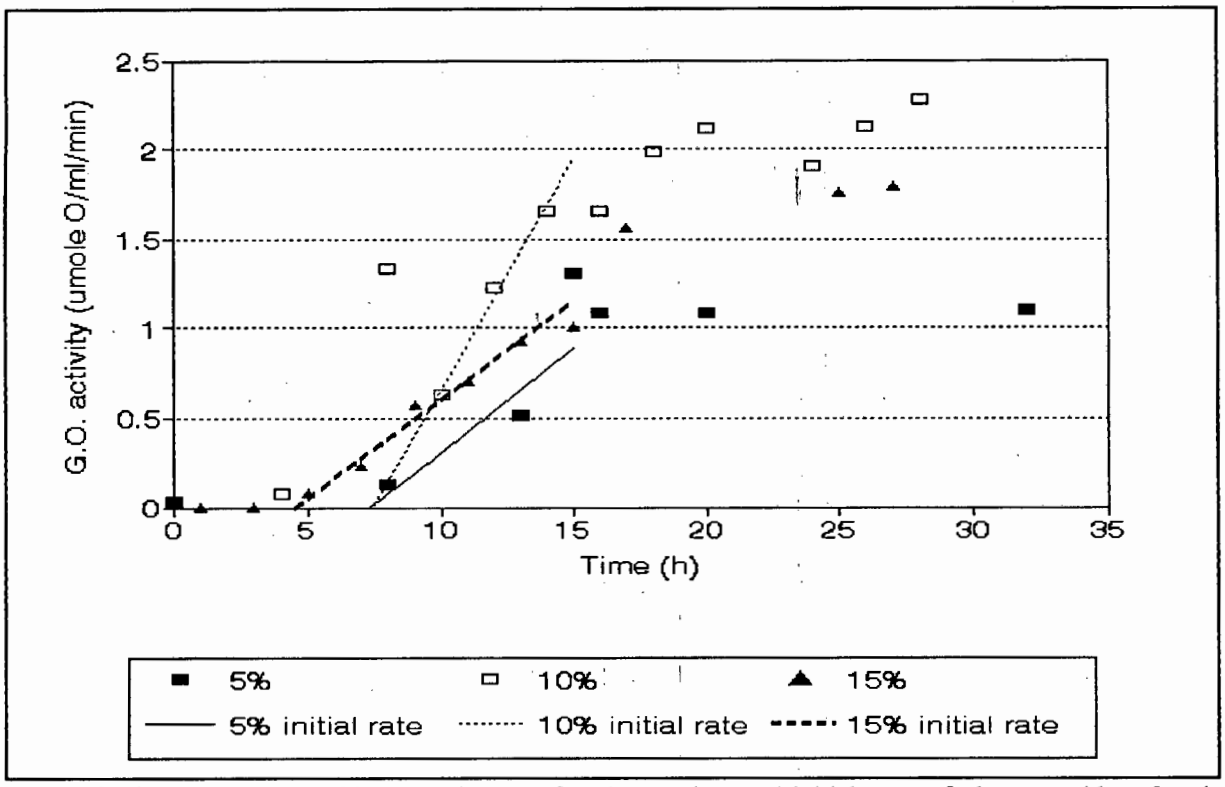

Figure 4.16 Total glucose oxidase activity as a function of time and initial rates of glucose oxidase for air experiments

In Figure 4.17 it is seen that the effect of glucose at atmospheric conditions shows a concave downwards profile with an optimum between 50 and 150 gl^{-1}. This information shows that there is some inhibitory effect of glucose above 100 gl^{-1} on the initial rate of production of glucose oxidase. This is borne out when comparing the initial rate to the final total levels of glucose oxidase produced i.e. the final 150gl^{-1} glucose experiment has a lower final glucose oxidase level than the 100 gl^{-1} experiment despite the longer induction window in the 150 gl^{-1} case.

Table 4.6 Initial glucose oxidase induction rates w.r.t glucose and oxygen concentrations

	50 g/l glucose	100 g/l glucose	150 g/l glucose
Initial glucose oxidase induction rate (μmole O/ml/min/h)	0.116	0.258	0.111
Final Glucose oxidase activity (μmole O/ml/min)	1.31	2.28	1.79

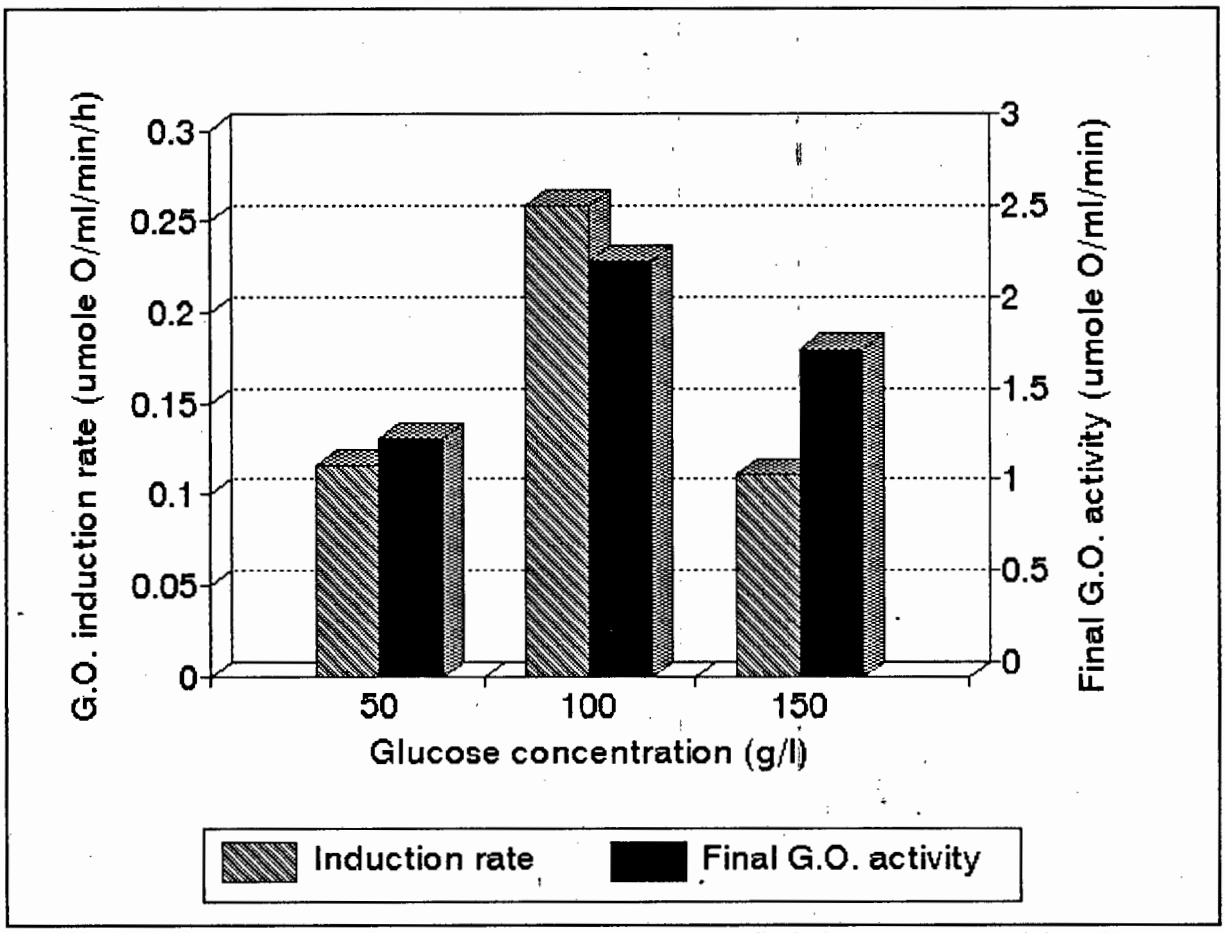

Figure 4.17 Variation of initial glucose oxidase induction rate and final glucose oxidase activity with glucose concentration in atmospheric experiments

4.2.4 Industrial production

Gluconic acid and glucose oxidase are produced using a batch or fed batch process. Efficient production design must take into account the time required for sterilisation, the lag phase,

the induction phase, the conversion phase and thereafter the clean out time. From the batch experiments conducted with varying glucose concentration at 0.21 atm oxygen, it can be seen that there is a compromise between low product concentration with short formation times and high product concentrations with long production times. In order to compare the performance of different glucose concentration experiments, the total gluconic acid production rates must be compared. Table 4.7 compares the lag times, product formation times, absolute product formation rate and effective production rate (total product over total time taken) for the 0.21 atm oxygen experiments.

Table 4.7 Lag time, conversion times of gluconic acid and rates for air fermentations

(h)	50 g/l glucose	100 g/l glucose	150 g/l glucose
Lag time (h)	7	6	6
Conversion time (h)	9	13	20
Conversion rate g/h_{cnv}	5.6	7.7	7.5
Conversion rate g/h_{total}	3.1	5.3	5.8

The 100 gl^{-1} fermentation is the most efficient in conversion excluding the lag phase. The 150 gl^{-1} has the highest overall conversion rate including the lag phase. Comparison of the initial glucose oxidase induction rates as a function of glucose concentration, the rates of conversion and the molar yields of gluconic acid as a function of substrate available suggest that the optimum production configuration is the fed-batch mode. Here induction rate may be optimised at 100 gl^{-1} glucose. In addition, the absolute rate of conversion and final product concentrations may be maximized by the feeding of glucose to maintain a constant glucose concentration of 100 gl^{-1}. Furthermore cleaning, preparation and sterilisation and lag times are minimised.

4.3. The role of glucose and oxygen in the induction of glucose oxidase

A matrix of nine experiments over the glucose range of 50 to 150 gl^{-1} and oxygen range of 0.21 atm to 1.00 atm were performed. The profiles of each experiment show similar trends to the base case fermentation. However glucose oxidase activities, conversion rates of glucose to gluconic acid and dissolved oxygen concentrations vary as a function of the initial experimental conditions.

4.3.1 Substrate and oxygen utilisation

The 9 fermentations show similar substrate and oxygen utilisation profiles. All have a lag phase varying between 5 and 8 hours. Figures 18 to 23 show the glucose concentration, predicted gluconic acid concentration (from sodium hydroxide addition profiles) and dissolved oxygen profiles for the six oxygenated experiments as a function of time.

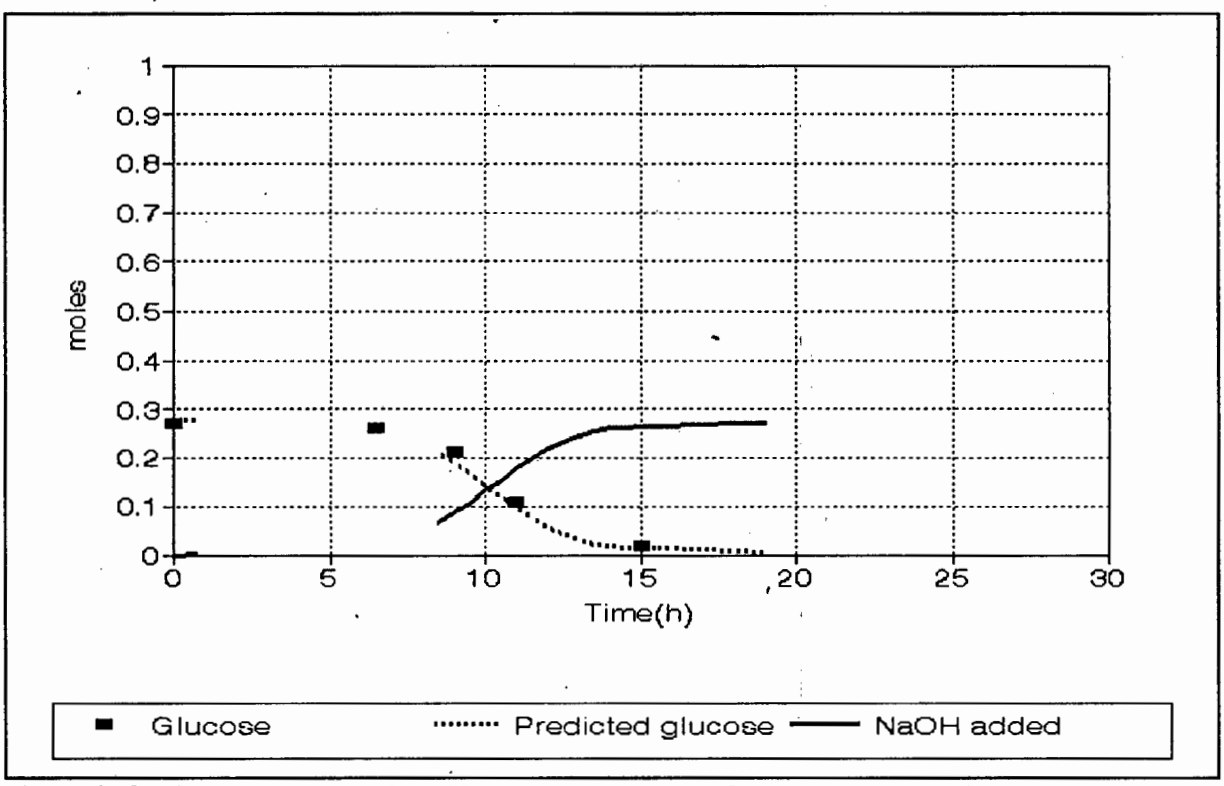

Figure 4.18 Glucose and gluconic acid concentrations as a function of time, using an initial glucose concentration of 50 gl^{-1} at 0.75atm oxygen

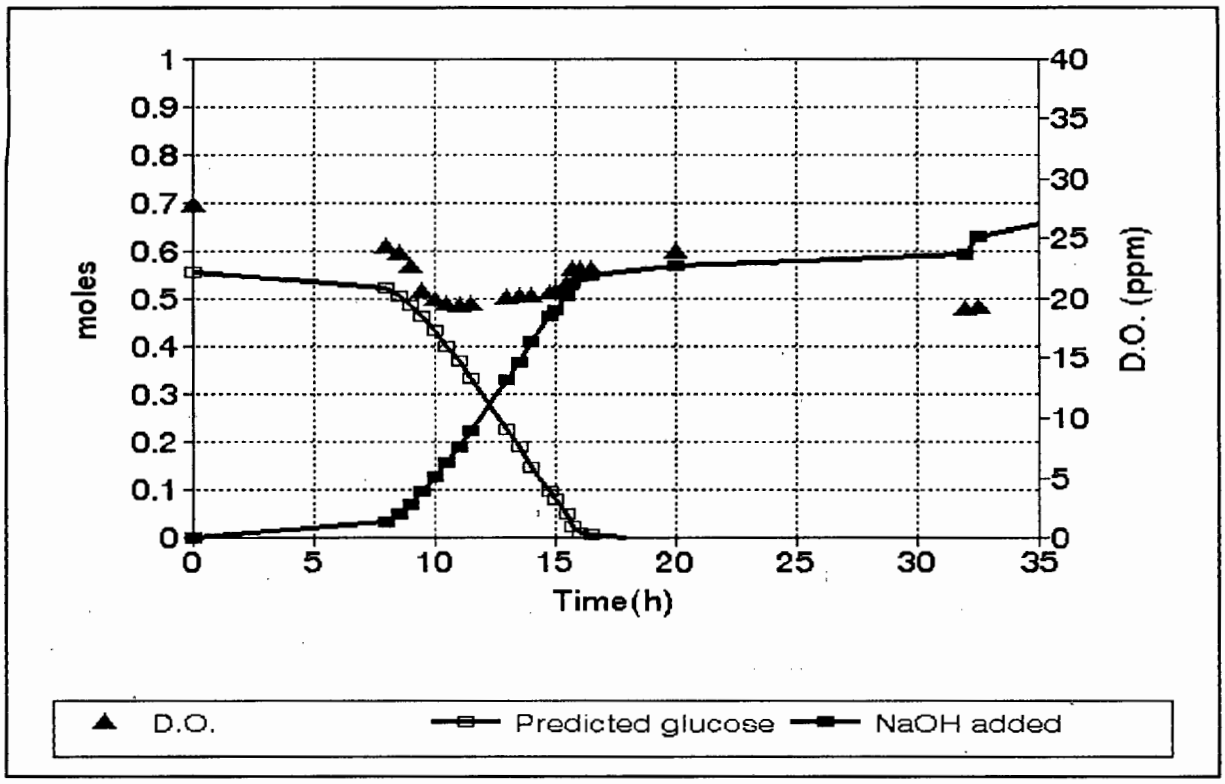

Figure 4.19 Glucose and gluconic acid concentrations as a function of time using an initial glucose concentration of 100 gl^{-1} at 0.75 atm oxygen

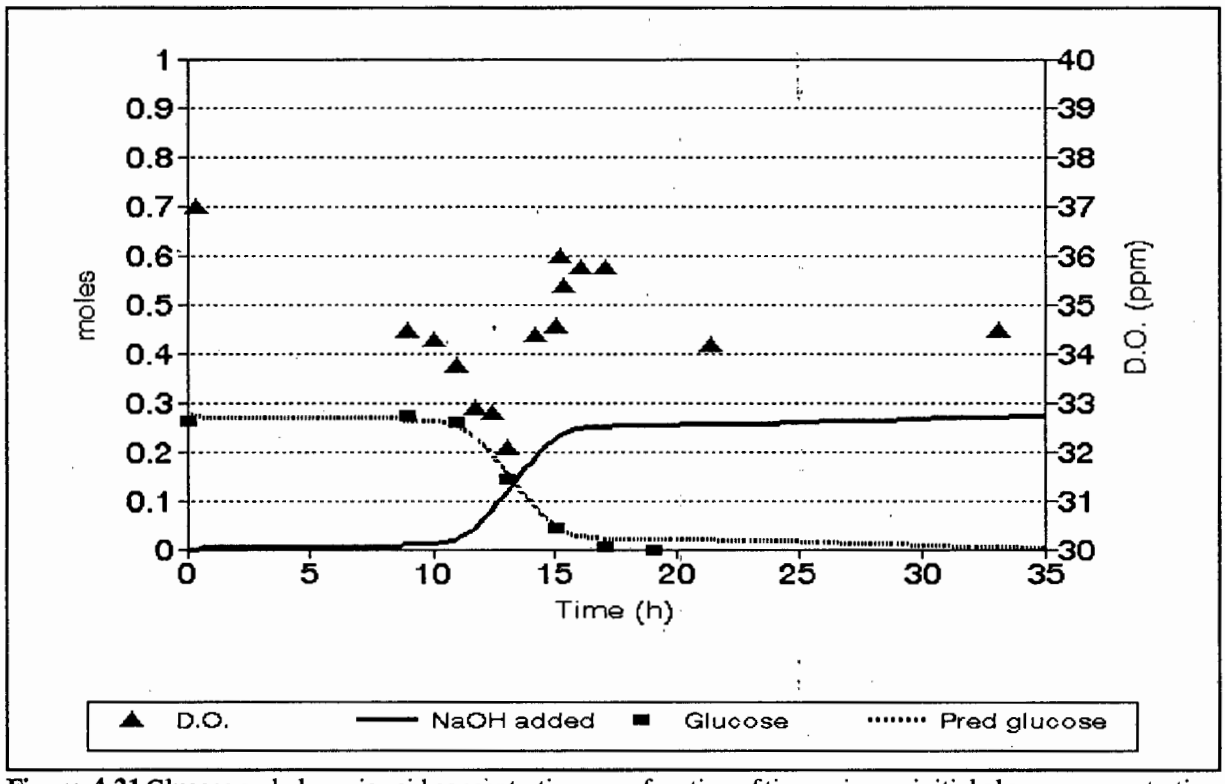

Figure 4.21 Glucose and gluconic acid concentrations as a function of time using an initial glucose concentration of 50 gl^{-1} at 1.00 atm oxygen

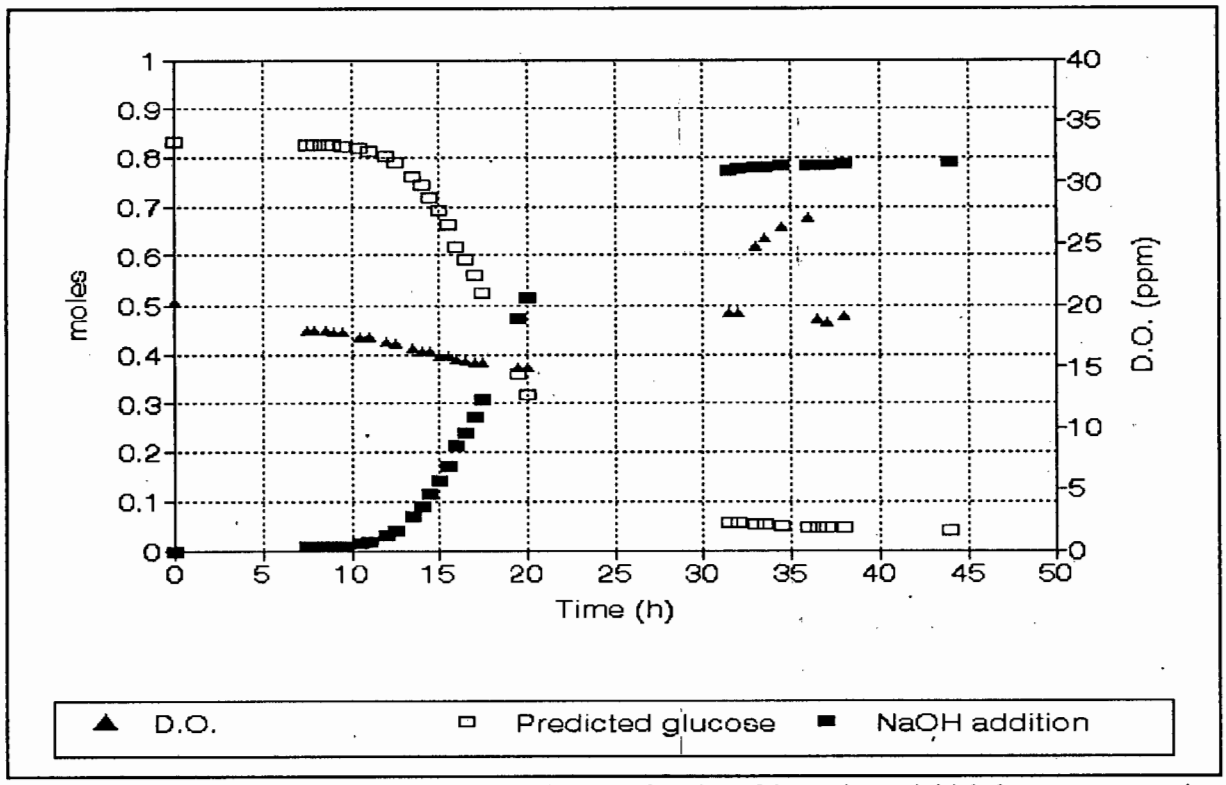

Figure 4.20 Glucose and gluconic acid concentrations as a function of time using an initial glucose concentration of 150 gl^{-1} glucose 0.75 atm oxygen

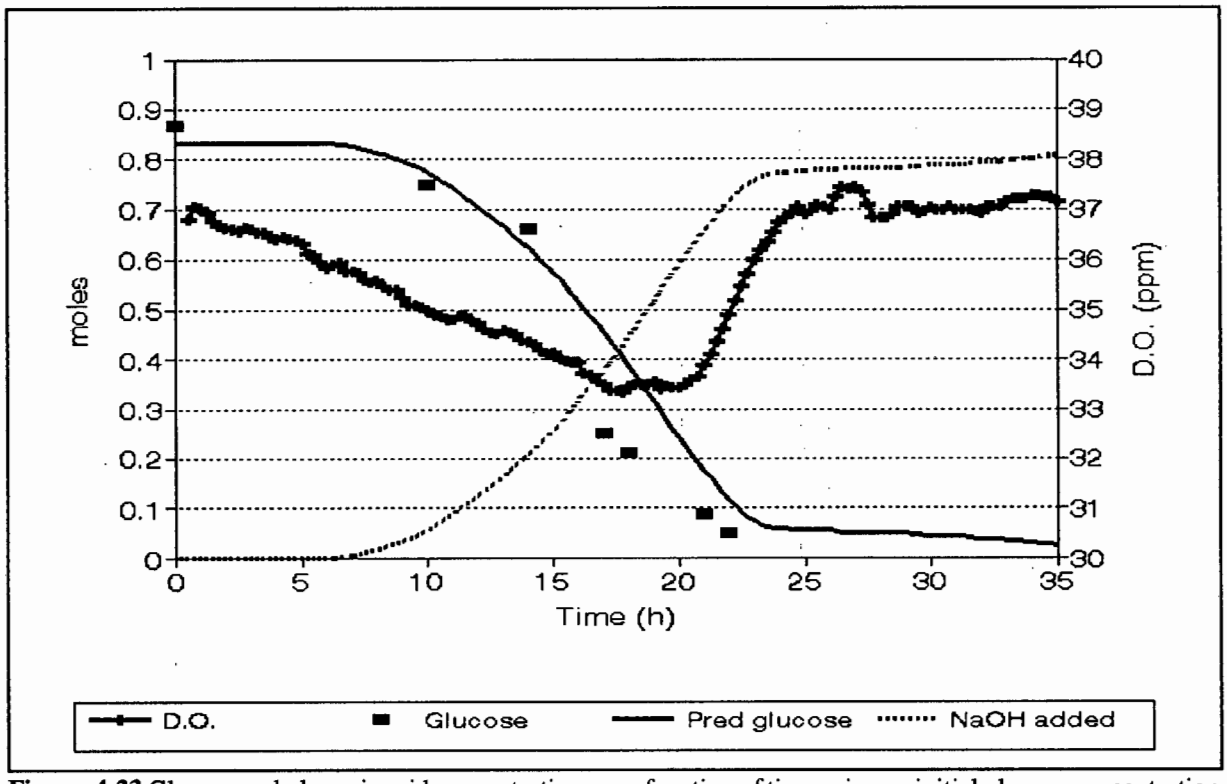

Figure 4.23 Glucose and gluconic acid concentrations as a function of time using an initial glucose concentration of 150 gl^{-1} glucose 1.00 atm oxygen

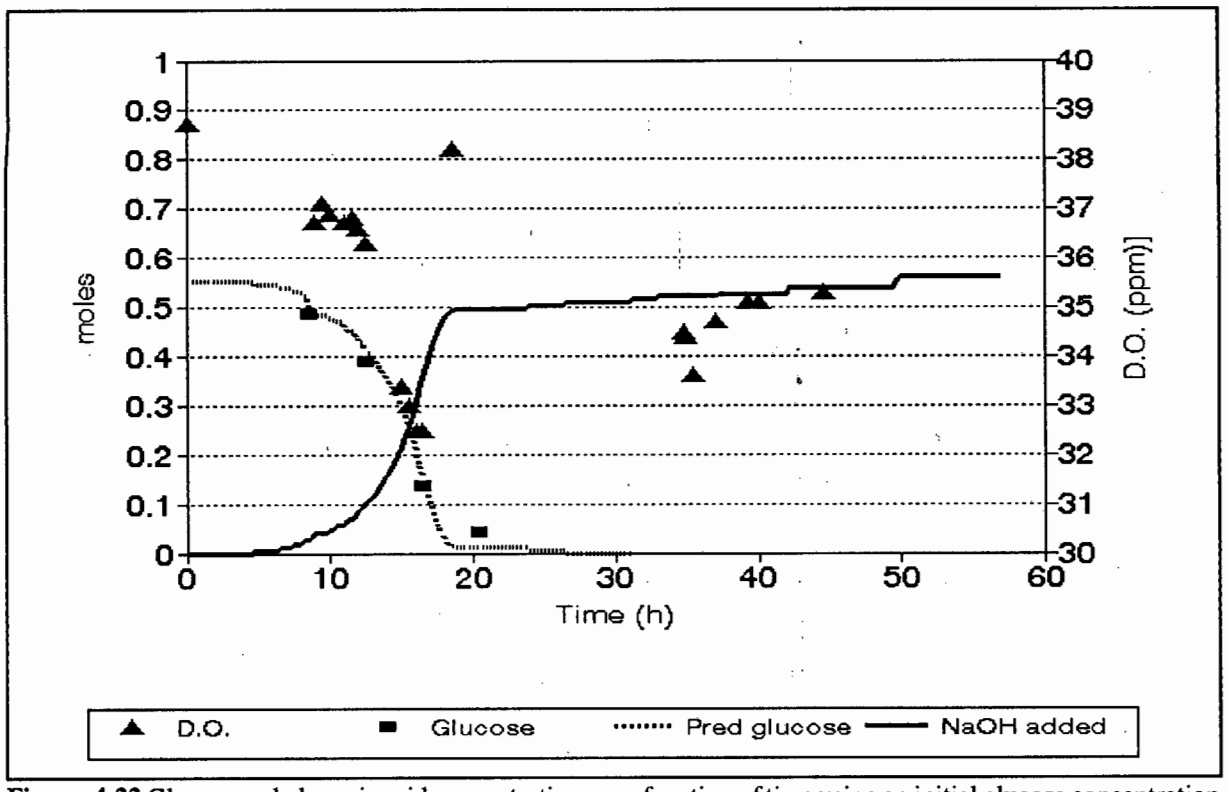

Figure 4.22 Glucose and gluconic acid concentrations as a function of time using an initial glucose concentration of 100 gl^{-1} glucose 1.00 atm oxygen

4.3.1 Biomass formation

Dry mass profiles for 0.21 atm and 0.75 atm oxygen over the three glucose ranges (Figures 4.15 and 4.24) follow similar trends. The logistic parameters, given in Table 4.8, are similar. Figure 4.24 and 4.25 show the biomass profiles resulting at 0.75 and 1.00 atm oxygen respectively. It appears that high oxygen levels, 1.00 atm oxygen, the biomass is inhibited in the 50 gl^{-1} case while this is not seen in the 150 gl^{-1} case. Table 4.8 shows the logistic fits for the 0.21, 0.75 and 1.00 atm oxygen biomass results.

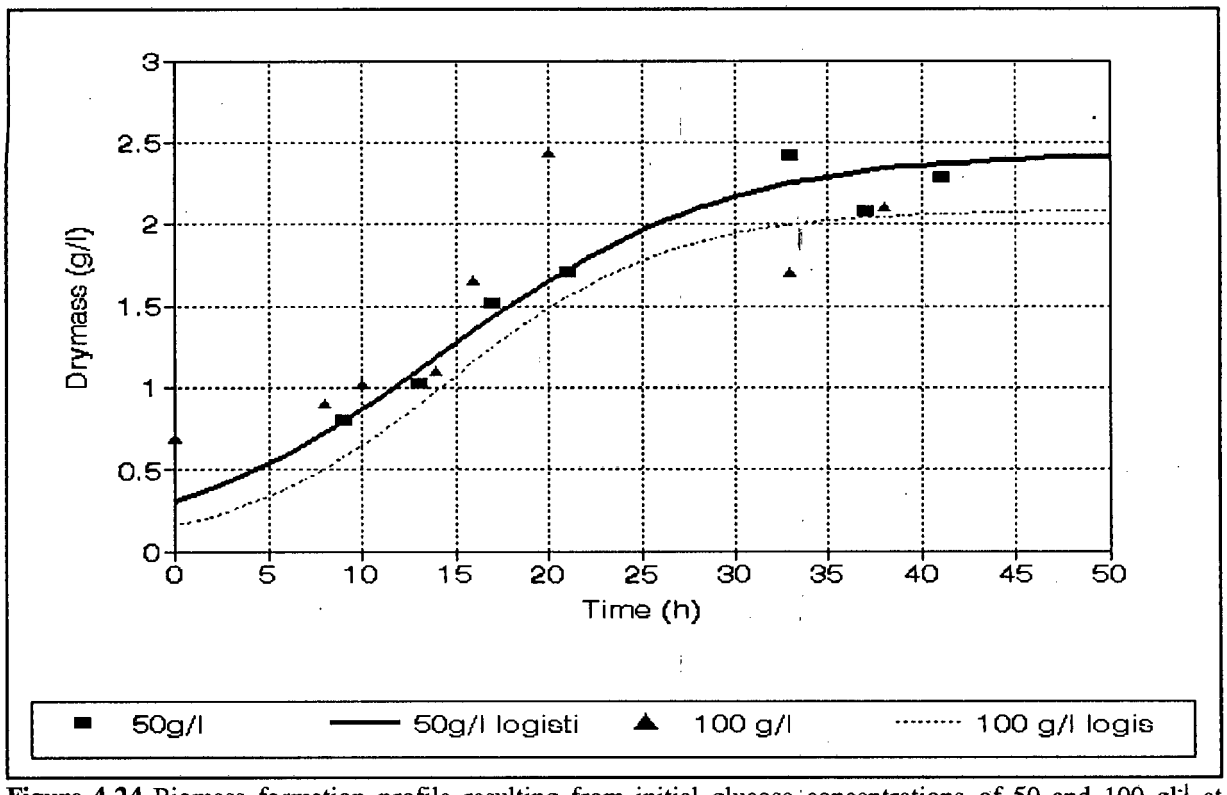

Figure 4.24 Biomass formation profile resulting from initial glucose concentrations of 50 and 100 gl^{-1} at 0.75atm oxygen and representation by the logistic equation

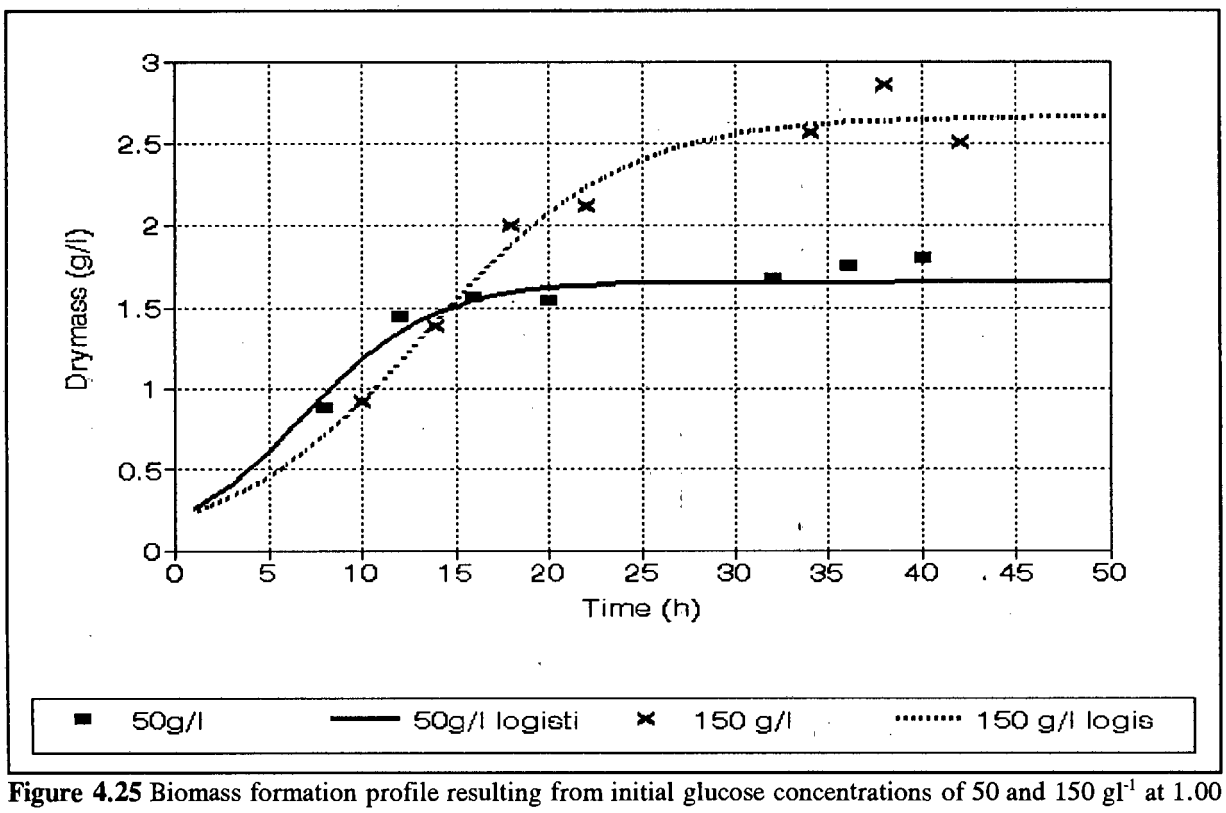

Figure 4.25 Biomass formation profile resulting from initial glucose concentrations of 50 and 150 gl^{-1} at 1.00 atm oxygen and representation by the logistic equation

Table 4.8 Logistic parameters for experiments with varying glucose and oxygen

Glucose (gl^{-1})	50 g/l			100 g/l			150 g/l		
Oxygen level (atm)	0.21	0.75	1.00	0.21	0.75	1.00	0.21	0.75	1.00
X_o (g/l)	0.1110	0.3092	0.2013	0.1651	0.1596	-	0.1503	-	0.1993
X_{max} (g/l)	2.3095	2.4344	1.6558	2.6424	2.0846	-	2.624	-	2.6638
μ_{max} (h^{-1})	0.2053	0.1337	0.2887	0.2311	0.1696	-	0.2136	-	0.1887
$Y_{X/S\ shaker}$	0.00222	0.00618	0.00618	0.00165	0.00159	-	0.00100	-	0.00133
$Y_{X/S\ reactor}$	0.04619	0.04869	0.03312	0.02642	0.02085	-	0.01749	-	0.01775

4.3.2 Glucose oxidase

The effect of glucose concentration on the initial glucose oxidase induction rate and final glucose oxidase activity illustrates similar features at all three oxygen levels. Figures 4.26 and 4.27 and Table 4.9 show that the profiles are all concave down with a maximum induction rate occurring between 50 and 150 gl^{-1} glucose. Initial induction rates at all three glucose concentrations are enhanced by increasing the oxygen level from 0.21 atm to 0.75 atm oxygen (Figures 4.26 to 4.29 and Table 4.8). This is in agreement with Traeger *et al.* (1991) who observed a 4 fold increase in glucose oxidase level by increasing the oxygen from 0.21 atm to 0.74 atm. Increasing the oxygen level to 1.00 atm increases the 50 gl^{-1} induction rate by 25%. Little effect on the induction rate at 100 gl^{-1} glucose is seen. The 150 gl^{-1} induction rate is decreased by the further increase in oxygen supply from 0.75 atm to 1.00 atm. This implies that there is not a single, independent optimum glucose and oxygen concentration for the induction of glucose oxidase. Hence for each glucose concentration there is an optimum oxygen concentration. This may find application through dissolved oxygen control of batch fermentations to achieve a maximum or improved final glucose oxidase level by altering the dissolved oxygen concentration as a function of the remaining glucose as the glucose is consumed or vice versa in fed batch culture. The maximum initial

rate of induction for the 150 gl^{-1} glucose case is between 0.21 atm oxygen and 1.00 atm oxygen. The 50 and 100 gl^{-1} cases have optimum initial production rates above 1.00 atm oxygen.

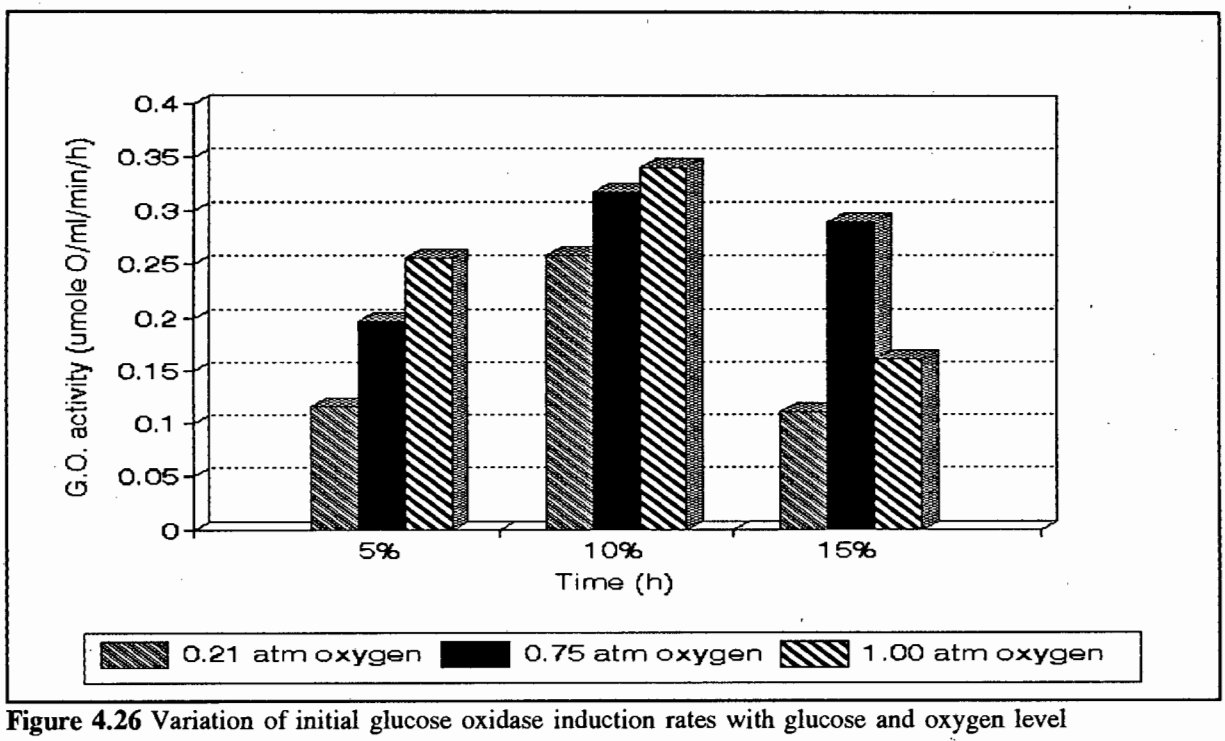

Figure 4.26 Variation of initial glucose oxidase induction rates with glucose and oxygen level

Table 4.9 Initial glucose oxidase induction rates w.r.t glucose and oxygen concentrations

	50 g/l glucose initial rate (U/h)	100 g/l glucose initial rate (U/h)	150 g/l glucose initial rate (U/h)
0.21 atm O_2	0.116	0.258	0.111
0.75 atm O_2	0.196	0.317	0.290
1.00 atm O_2	0.255	0.340	0.160

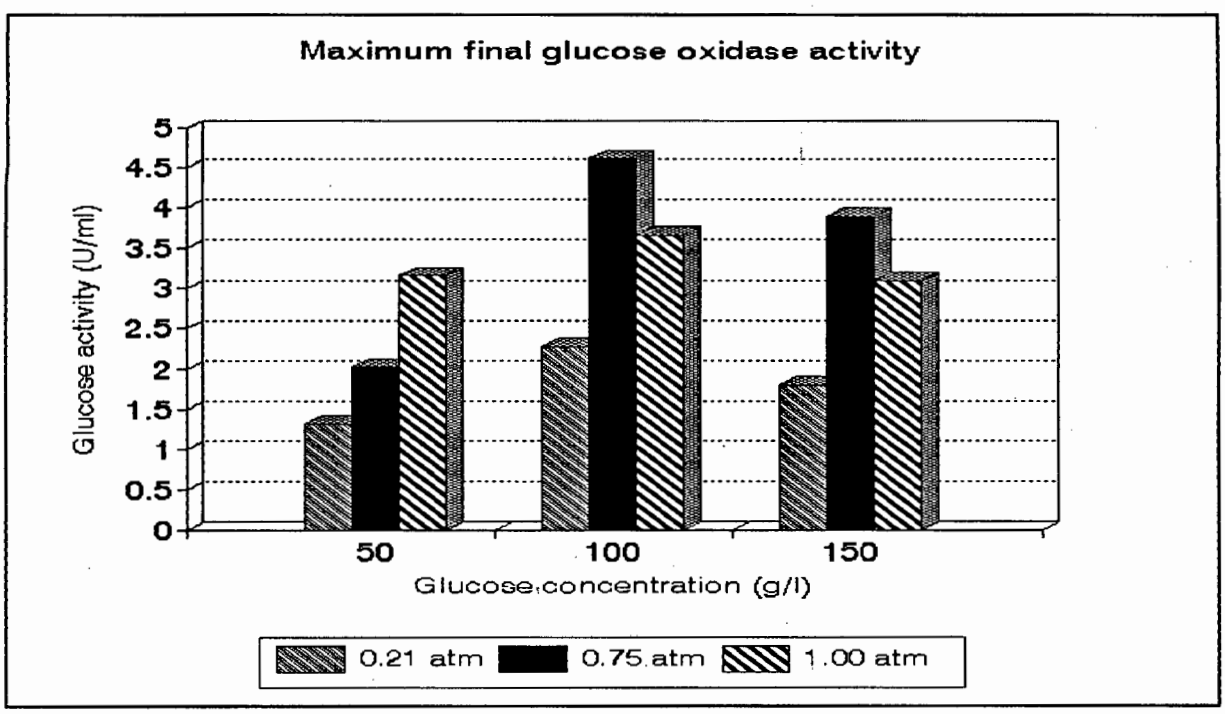

Figure 4.27 Effect of glucose and oxygen on maximum glucose oxidase levels

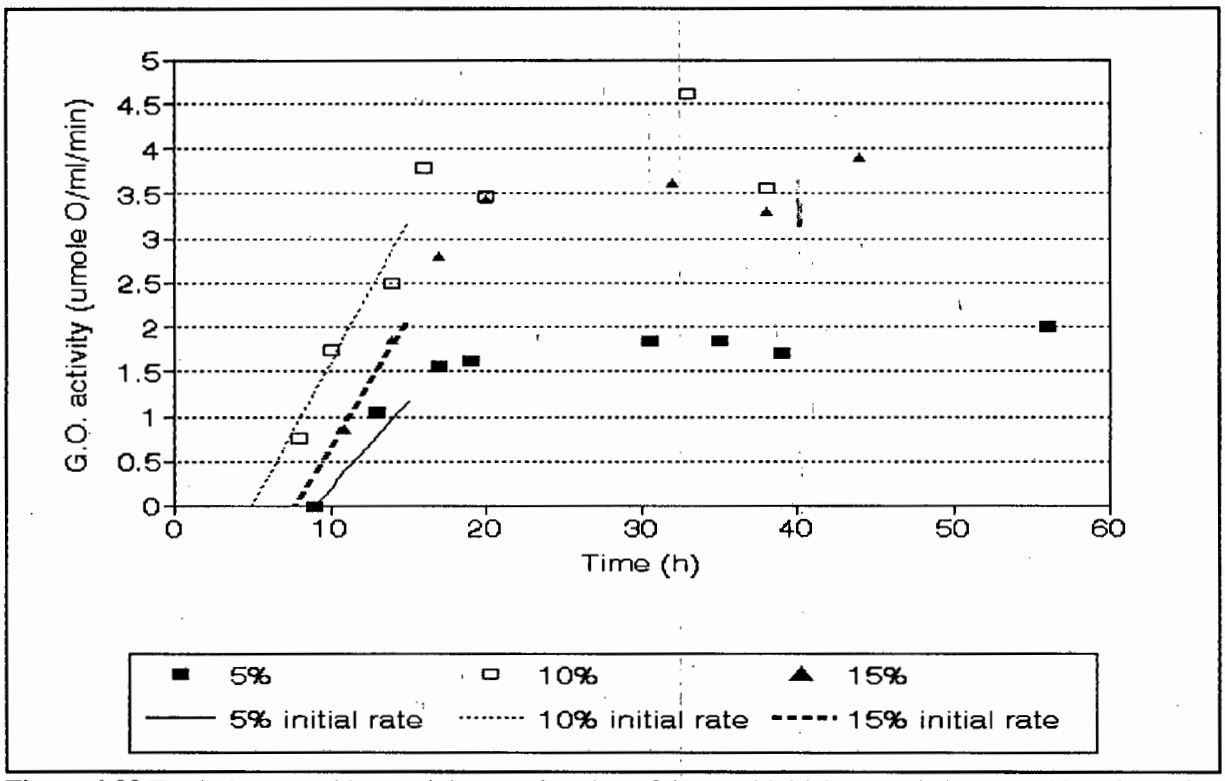

Figure 4.28 Total glucose oxidase activity as a function of time and initial rates of glucose oxidase formation for 0.75atm oxygen experiments

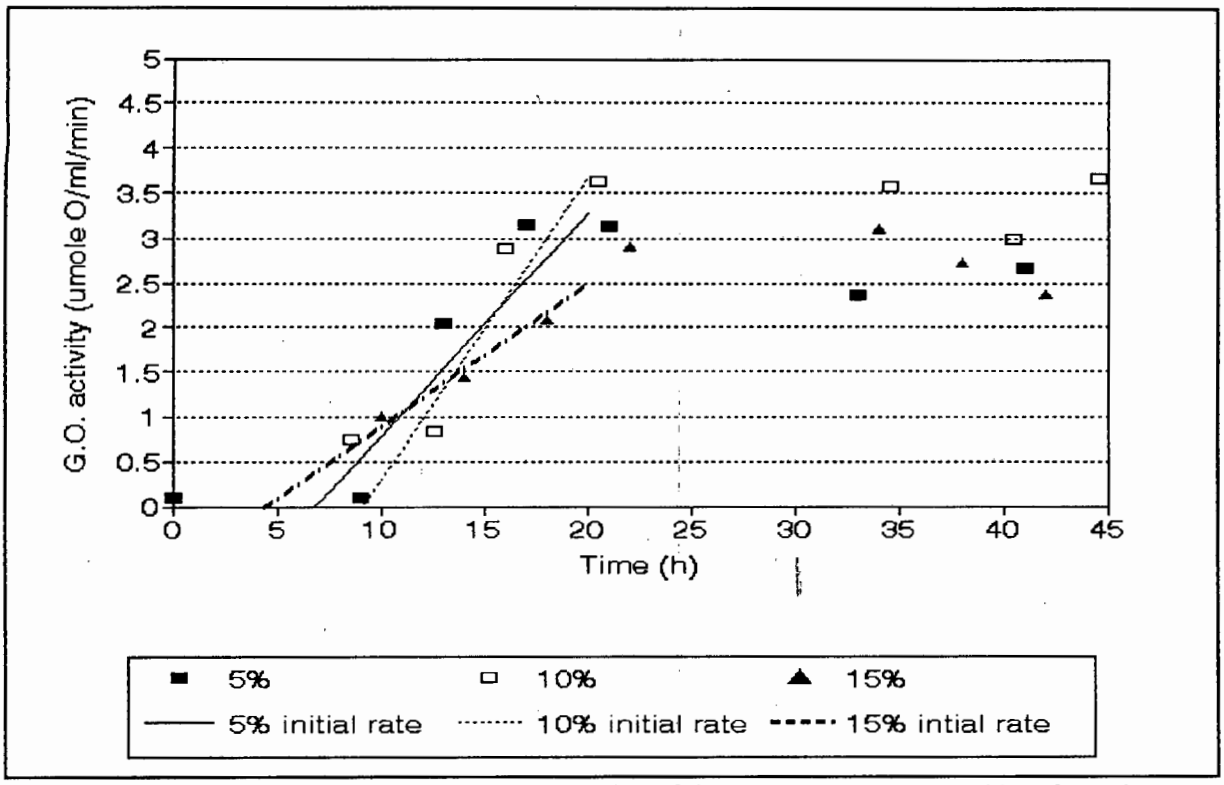

Figure 4.29 Total glucose oxidase activities as a function of time and initial glucose oxidase formation rates for 1.00 atm oxygen experiments

4.4 Conclusions

1) Biomass is not affected by glucose concentration as the culture is not limited by carbon.

2) Biomass is not affected by oxygen concentration in the 0.21 to 1.00 atm oxygen range. However a decrease in biomass was observed at an initial glucose concentration of 50 gl^{-1} at 1.00 atm oxygen.

3) Biomass formation has been established by the logistic equation. Typical values of μ_{max} range between 0.2 and 0.3 h^{-1} and the final biomass levels range between 2.3 to 3.0 gl^{-1}

4) Gluconic acid production can be correlated to sodium hydroxide addition (0.94 moles G.A per mole NaOH) with a correlation coefficient of 0.998.

5) 149 gl^{-1} gluconic acid was produced from 150 gl^{-1} glucose solution with 94% $Y_{P/S}$.

6) Glucose conversion is best at initial glucose concentrations of 100 and 150 gl^{-1}.

7) Glucose oxidase is induced by both glucose and oxygen. The final glucose oxidase level shows a maximum at 100gl^{-1} with oxygen varying from 0.21 atm to 1.00 atm. Increasing oxygen from 0.21 atm to 0.75 atm increases the final glucose oxidase levels. Further increasing oxygen concentration above 0.75 atm to 1.00 atm does not increase the final level of glucose oxidase produced. A global maximum of 4.6 U was obtained at an initial glucose concentration of 100 gl^{-1} and 0.75 atm oxygen.

8) The initial rate of glucose oxidase induction has an optimum between 50 and 100 gl^{-1} glucose for oxygen ranging from 0.21 atm to 1.00 atm. Each glucose concentration appears to have an independent optimum oxygen concentration for maximal glucose oxidase induction rate. At 50 and 100 gl^{-1} glucose levels oxygen above 1.00 atm is required for maximum glucose oxidase induction rate. At 150 gl^{-1}

the optimum oxygen level lies between 0.21 and 1.00 atm.

9) Glucose and oxygen effect on glucose oxidase induction is not independent therefore a combined optimum must be determined.

10) Glucose oxidase is associated with the bulk media (extracellular) and with the mycelial pellet. Diffusion limitations are observed at high glucose oxidase activities.

11) Shake flask cultures have lower biomass yields than controlled reactor experiments.

5. MODEL DEVELOPMENT OF *A.NIGER* SYSTEM AND GLUCOSE OXIDASE INDUCTION BY GLUCOSE ALONE

The following chapter outlines the motivation and level of detail required for the development of bioprocess models. The development of a model of the *A.niger* system, glucose oxidase formation and activity based on a gene operon model to describe the induction of glucose oxidase due to glucose alone is discussed. The final model equations and solution strategy are then presented.

5.1. Bioprocess models

There are two types of bioprocess models. The first type is an empirical model which is not based on mechanism. Empirical models are often used to describe complex systems where the number of mechanisms is great or the mechanisms are not well understood. The second type of model is the mechanistic model. These models are based on the fundamental processes of the system. A system can often be broken down into its component subprocesses which can be modelled on the mechanistic level.

Bioprocesses are built up out of a number of fundamental processes. To gain an understanding of the system as a whole, it is necessary to identify and understand each area on its own. Once this has been done a model can be formed out of the component processes. The model can be used in a variety of ways in the research and design of bioprocesses and bioreactors.

A model allows processes that are well understood in isolation to be coupled and their interactions observed. Models can be used as important tools in testing out hypotheses of processes that are not well understood. Typically these hypotheses cannot be tested on their own as they interact with a large number of other processes. A model comprised of the well

understood areas and a hypothesis of an unknown process allows observed experiments to be deconvoluted or compared with predicted results. An example of this is the induction kinetics of the glucose oxidase system which is hypothesised to follow the gene operon induction model.

Models are also used in the design of bioreactors and bioprocesses. Large scale processes can be built up from modelled data obtained from laboratory scale bioreactors e.g. prediction of process profiles under decreased k_la due to scale up and utility requirements for cooling and pH control. Mechanistic models are advantageous over empirical models as they can predict the performance of bioprocesses in different reactor configurations allowing an optimal configuration to be chosen for large scale production. Empirical models are limited to the conditions under which they were developed. The design of model predictive controllers can utilise simplified models to obtain robust and stable controllers. Figure 5.1 demonstrates the components and uses of models in bioprocess design.

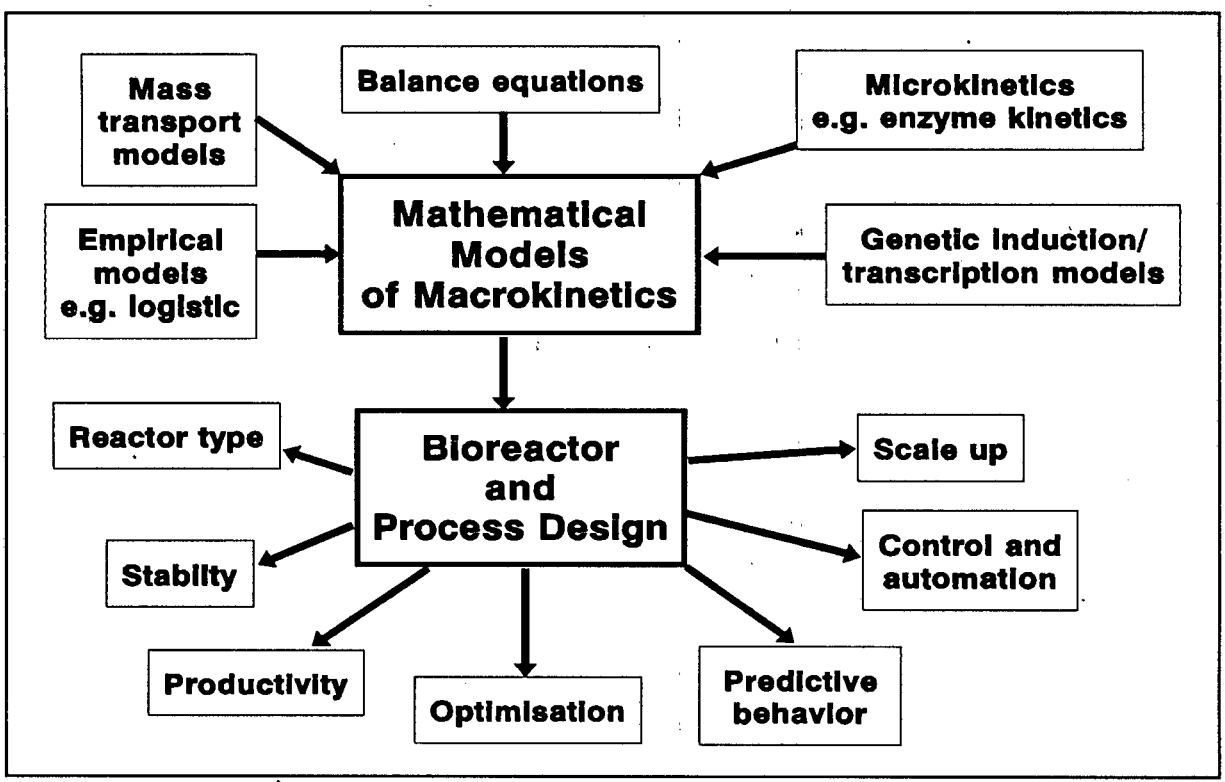

Figure 5.1 Diagram showing the components of bioprocess models and use in process design (modified from J.A.Roels (1982))

5.2 Existing models of gluconic acid and glucose oxidase production

In the *A.niger* glucose oxidase and gluconic acid system little modelling has been found in the literature. Most of the models tend to be empirical and are not tested for their predictive power in varied process environments.

Miura *et al.* (1970) modelled the production of gluconic acid in *Aspergillus niger* and assumed that the entire oxidation of glucose to gluconic acid occurred inside the cell. The model was based on the assumption that the active uptake of glucose was rate limiting to the oxidation reaction. The active uptake was modelled using Monod kinetics. The oxidation of glucose to gluconic acid cannot occur within the cell as the glucose concentration for the observed rate of oxidation is too low and that the peroxidase inside the cell could not break down the hydrogen peroxide at the rate it is generated. Miura *et al.* did not model the effect of glucose oxidase induction and oxygen consumption was not modelled or included in the rate of gluconic acid production. The model was only tested under one set of conditions and no predictive behaviour was shown.

Modelling of gluconic acid production by *pseudomonas ovalis* has received some attention by Koga *et al.* (1967) and Tanner and Merk (1970). Koga *et al.* (1967) assumed that the gluconic acid is a growth associated product and that the rate of gluconate production is limited to the hydrolysis of glucono-δ-lactone intermediate. The model is based on Monod kinetics for cell growth and glucono-δ-lactone intermediate production. Oxygen consumption and glucose oxidase enzyme kinetics were not used in the model.

Tanner and Merk (1970) modelled the production of gluconic acid using the gene operon model to model the production of glucose oxidase. The glucose oxidase production of gluconic acid was modelled using a Monod equation (which an empirical equation based on Michaelis-Menten kinetics using glucose as sole substrate) and not the enzyme kinetic equation of Atkinson and Lester (1974) which include the effects of glucose, oxygen and pH. The induction kinetics of glucose oxidase with respect to glucose and oxygen was not considered as the model was only fitted to one set of data.

Takamtsu (1981) uses a two floc model of the system. Gluconic acid production is described as a growth associated product and the glucose oxidase enzyme production is not modelled.

5.3 Level of model detail

5.3.1 Level of detail in bioprocess models

The level of detail used in building a model is entirely dependent on the knowledge of the underlying mechanisms and computation power to handle large numbers of state variables. The number of processes that must be considered to represent the system can be found by comparing relaxation times of the biological process with the relaxation times of environmental factors. Three possible situations arise from the comparison. These are shown in Figure 5.2.

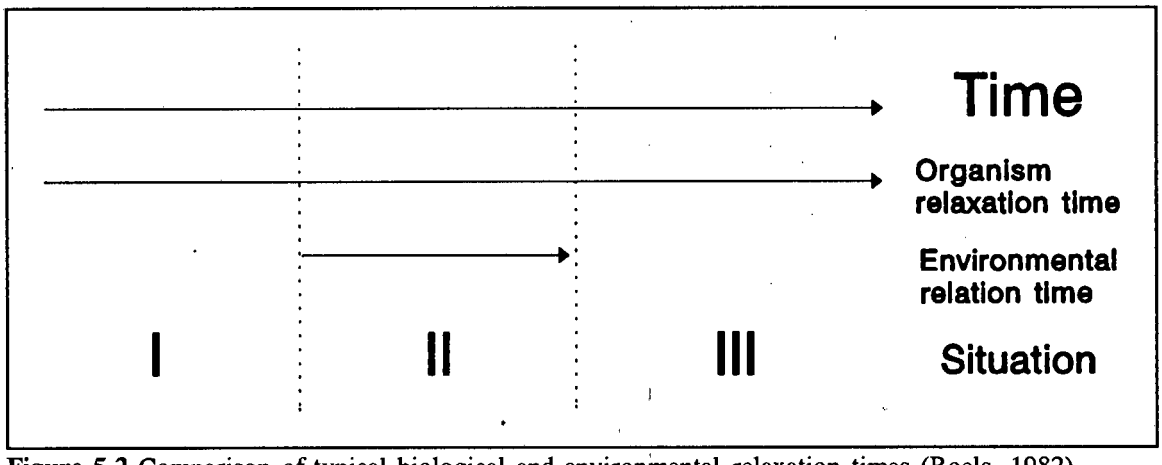

Figure 5.2 Comparison of typical biological and environmental relaxation times (Roels, 1982)

Situation I The organism time constant is much shorter than the environment. This results in pseudo steady state i.e. the organisms is always adapted to the environment and its condition is dictated by the environment

Situation II The organism and environmental time constants are similar. This results in a dynamic interaction where lag, overshoot and oscillation are possible. The environment does not dictate the organism's condition and a dynamic model

is required to represent the system.

Situation III The time constant of the organism is much longer than the environment: the organism is observed as being frozen and its state is a function only of its initial conditions and not of the environment.

Roels (1982) describes 6 types of biological processes, classified on a basis of time constant:

- Mass action of chemical reactions (less than 10^{-4}s)
- Allosteric enzyme regulation (between 10^{-5} and 10^{1}s)
- Gene operon induction of enzymes (between 10^{1} and 10^{4}s)
- Genetic mutation of single cells (above 10^{3}s)
- Population adaption in mixed cultures (above 10^{5}s)
- Evolutionary changes (above 10^{6}s)

Figure 5.2 compares the biological relaxation times with typical relaxation times occurring in the environment

5.3.2 Level of detail required for modelling the *A.niger* system

The *A.niger* system contains several sub processes. Each biological process is discussed with respect to the environmental changes that affect it.

a) Gluconic acid formation is catalysed by glucose oxidase. The reaction follows a typical enzyme cycle between reduced glucose oxidase complex and an oxidised form. The reaction is in the mass action regime. The concentration of the reactants does not change as fast as the cyclic reactions and therefore the components of the cyclic reaction can be regarded as at equilibrium when evaluating the rate of glucose oxidation at any position in time. The pH is assumed to be sufficiently high to allow both spontaneous and lactonase-catalysed conversion of gluconic-δ-lactone intermediate into gluconic acid.

b) Glucose oxidase induction has a 5-7h lag associated with it. Glucose, oxygen and pH have been identified as factors affecting the induction process (Section 2.4). These factors have similar or shorter relaxation times compared to the lag time. Hence a transient description of the induction process is required.

c) The dissolved oxygen utilisation rate is of the same order of magnitude as the transfer rate. Therefore the mass transfer process from the bubble to the media has to be modelled if the transient profile of the dissolved oxygen concentration is to be modelled.

d) The mixing time in the reactor is shorter than any other process except for the cyclic reactions of glucose oxidase (assumed to be instantaneous). Hence the overall production of gluconic acid is dominated by the glucose oxidase, glucose and oxygen environmental conditions. The mixing time does not have to be modelled as the reactor can be assumed to be homogeneous in the bulk.

e) Pellet diffusion times may be slower than the conversion time of glucose to gluconic acid and thus may interfere with the reaction. In this model pellet diffusion is ignored.

f) Cell growth does not remain constant. It is varied by the changes in environmental conditions of glucose, oxygen and nitrogen. Thus the growth is transient and must be modelled.

g) pH control is achieved via sodium hydroxide addition based on the pH measured by an *in situ* electrode. The dynamics of the system are assumed to be much faster than any reaction that is affected by pH. Thus the dynamics of the pH control system is ignored.

h) *A.niger* mutation and population selection would only occur long after one batch fermentation has finished. Inocula are prepared from a standard stock culture maintained at 4°C. The stock culture is transferred once a month on to fresh agar

alternating between potato dextrose agar and malt extract agar. Thus the process of genetic variation can be ignored in this model.

5.4. Development of a model to describe glucose induction of glucose oxidase in *A.niger*

There are two separate kinetic processes in the formation of gluconic acid by *A.niger*. Firstly, glucose oxidase is induced by three factors - glucose, oxygen and pH. The second process is the enzymatic oxidation of glucose by glucose oxidase to form gluconic acid. This process is also affected by glucose, oxygen and pH. Figure 5.3 illustrates the two kinetic processes. The first area is not well understood and is described qualitatively in terms of the factors affecting the induction. The aim of this study is to quantify and model the induction effect with respect to glucose and oxygen and to propose a mechanism by which the enzyme is induced.

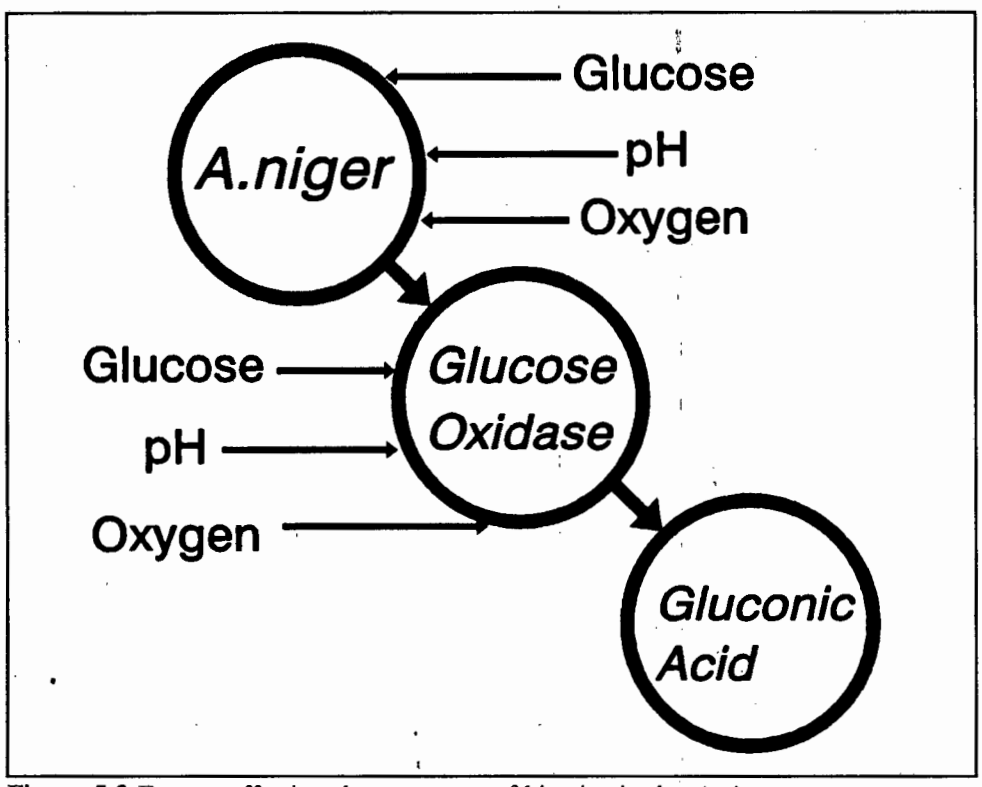

Figure 5.3 Factors affecting the two areas of kinetics in the *A.niger* system

The *A.niger* system also contains many other well understood chemical engineering processes. The system is modelled by setting up equations for all the known subprocesses and

including equations for the induction of glucose oxidase based on a hypothesis and mechanism. The hypothesis used is based on the gene operon model for enzyme production first described by Jacob and Monod (1961). It has been used by Imanaka *et al.* (1972) to model the induction of α-galactosidase in *Monascus sp.* Initially a model based on glucose induction of glucose oxidase alone is presented. In Section 7, this is expanded to include the effect of oxygen on the induction kinetics.

The model consists of 3 phases: gas bubbles, liquid media and cellular contents bounded by a cell wall. Several processes allow the interaction and reaction of the chemical species present. The processes involved are illustrated in Figure 5.4. Each process will be described in turn and the model equations derived.

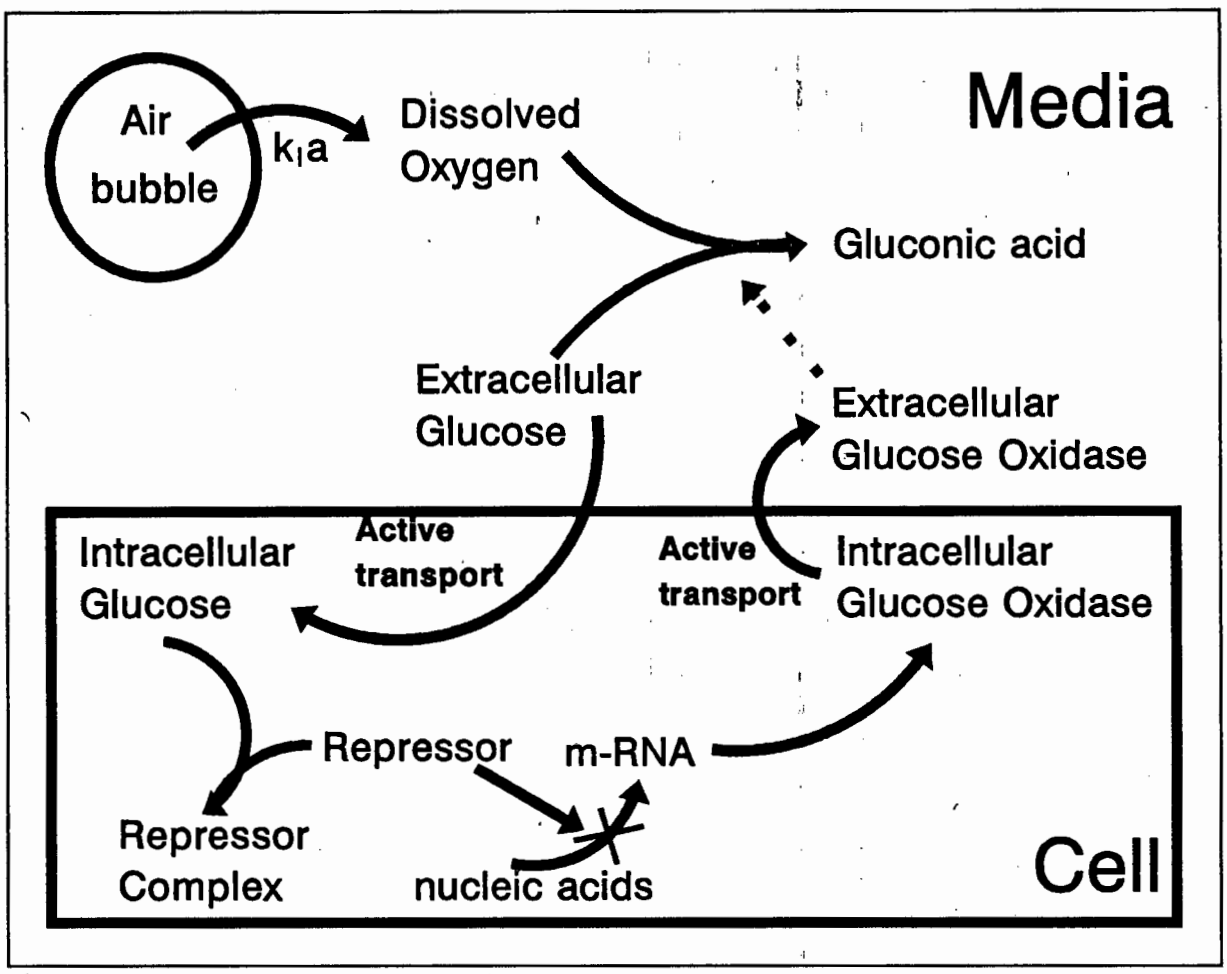

Figure 5.4 Dominant processes occurring in *A.niger* system

5.4.1. Oxygen mass transfer

Oxygen is transferred from the interior surface of the gas bubble to the bulk media. The interior surface of the bubble is assumed to be in constant equilibrium with the gas sparged. The surface dissolved oxygen concentration is therefore the saturated dissolved oxygen concentration for the medium in contact with the partial pressure of oxygen present in the bubble. Dissolved oxygen is transferred convectively from the interfacial film into the bulk media. This process is modelled by a convective mass transfer coefficient k_l. The rate of oxygen transfer is given by the following equation:

$$\frac{dC_{O_2}}{dt} = k_l a(C^*_{O_2} - C_{O_2}) \qquad (5.1)$$

where

C_{O2}	Dissolved oxygen concentration (ppm)
C^*_{O2}	Saturated dissolved oxygen concentration (ppm)
k_l	Gas mass transfer coefficient (mh^{-1})
a	Total air bubble surface area per unit volume (m^{-1})

5.4.2 Biomass

The biomass composition is complex. Modelling the growth of each component is not possible and so an empirical representation of the biomass formation observed is used. The logistic curve was chosen to describe the formation of biomass as it has an initial cell mass at time zero, a sigmoidal shape and an asymptotic final cell mass associated with stationary phase. The logistic equation assumes an exponential growth rate derived from elemental binary fission and superimposes an inhibitory effect as the cell mass increases. Thus the maximum and final cell mass occurs when the growth and inhibitory effect balance out.

The logistic equation indicates the rate of change of cell mass as follows

$$\frac{dX}{dt} = \mu_{max} X\left(1 - \frac{X}{X_{max}}\right) \qquad (5.2)$$

This is integrated to yield:

$$X = \frac{X_o e^{\mu_{max} t}}{1 - \frac{X_o}{X_{max}}\left(1 - e^{\mu_{max} t}\right)} \qquad (5.3)$$

where:

X, X_o Cell mass, initial cell mass (gl^{-1})

X_{max} Asymptotic maximum cell mass (gl^{-1})

μ_{max} Maximum growth rate (s^{-1})

5.4.3 Overall activity of glucose oxidase

The overall activity of glucose oxidase is affected by the amount of active enzyme present, the available substrate concentrations and the environmental conditions such as pH and temperature.

Glucose oxidase follows typical Michaelis-Menten enzyme kinetics predicted from the reaction sequence shown in Figure 5.5. The reaction sequence accounts for the effects of glucose, oxygen and pH on the activity of the enzyme. The final rate equation, based on the previously mentioned species, was derived by Atkinson and Lester (1974). The relevant equations are presented in Section 2.7 and the final rate expression is given below.

$$\frac{r_{a,max}}{r_a} G_I(s_H) = \frac{\beta_G G_g(s_H)}{S_G} + \frac{\beta_O G_O(s_H)}{S_O} + 1 \qquad (5.4)$$

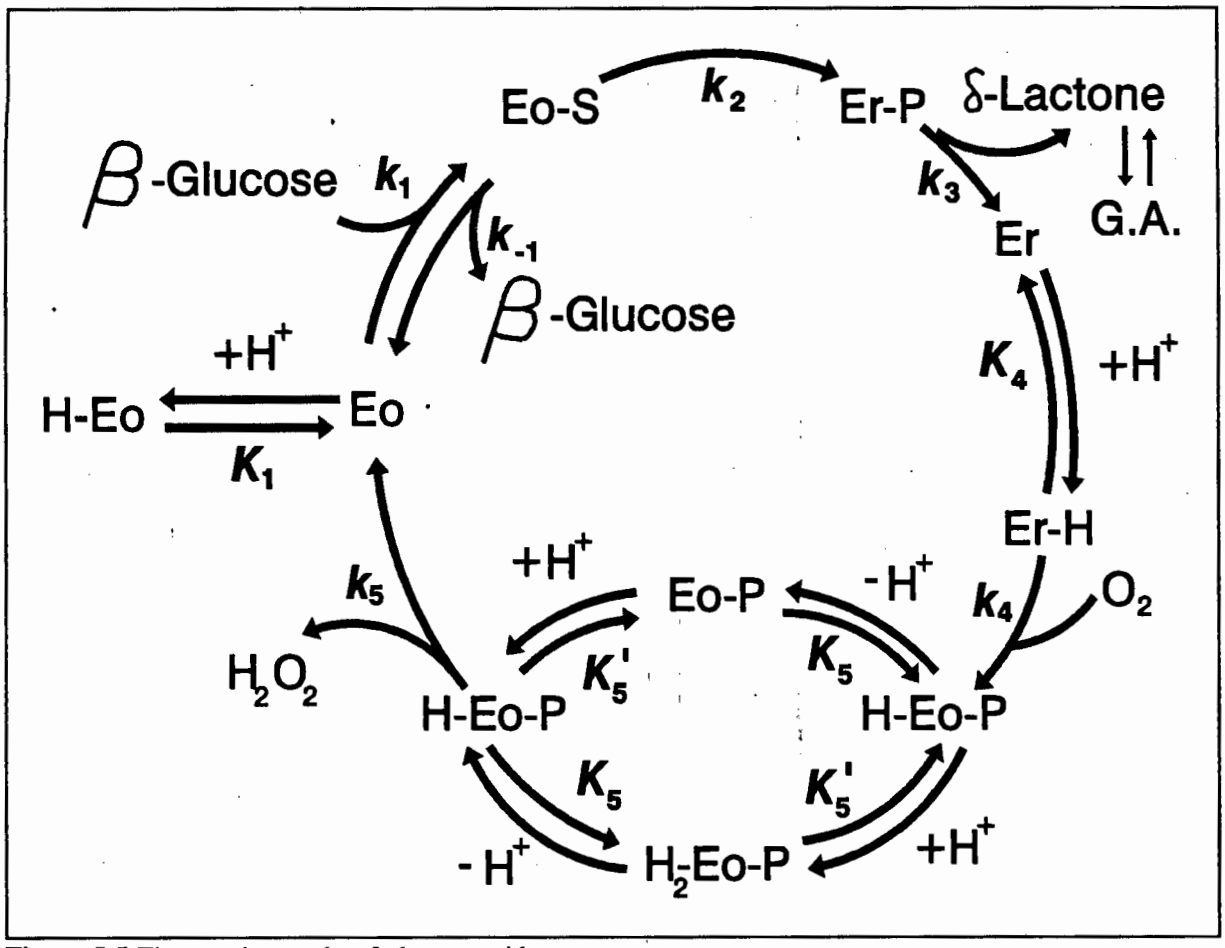

Figure 5.5 The reaction cycle of glucose oxidase enzyme

The deactivation of the enzyme results from protein turnover, heat degradation and exposure to oxygen.

Venugopal and Saville (1993) have shown that oxygen deactivates glucose oxidase during glucose oxidation. The deactivation follows the kinetics predicted by an irreversible reaction of the enzyme with dissolved oxygen. Half-lives range from 14.2 to 60.6 h at oxygen concentrations ranging from 3.7 to 37.7ppm.

Glucose oxidase is deactivated in the presence of certain substances that bind to the enzyme irreversibly. Heavy metals such as mercury and copper have been identified (Nakamatsu 1975). Oxygen combined irreversibly with glucose oxidase. The precise kinetics of the process are not understood well. Michaelis-Menten kinetics have been applied to the reaction of glucose oxidase in the reduced form with oxygen. Venugopal and Saville (1993) fitted this

model and obtained a 0.95 correlation. Equation 5.5 shows the result.

$$r_d = \frac{k_d K_m E_t ppO_2}{(ppO_2 + K_m)} \quad (5.5)$$

Ichijo *et al.* (1989) investigated the thermal stability of free and immobilised glucose oxidase. It was found that the denaturing temperature increased as the pH decreased to pH 4.3 (the isoelectric point of glucose oxidase). The maximum denaturing temperature was found to be 66.7°C. Glucose oxidase immobilised on polyvinyl alcohol superfine fibres (SFF) denatured at 70°C at a pH of 5.4 and at an enzyme loading above 0.2 g enzyme/g SFF. As the temperature is kept constant at 30°C, this factor is not modelled.

Table 5.1 Constants for the oxygen deactivation of glucose oxidase

Constant	Unit	Value
K_d	kPa/h	2.70E-3
K_m	kPa	22.0
ppO_2	kPa	0 - 100

5.4.4 Glucose uptake by *A.niger* cells

The intracellular glucose concentration within *A.niger* cells cannot be the same as the external glucose concentration. Mischak *et al.* (1985) shows that the intracellular glucose concentration must lie below 1mM at all times so that hexokinase does not operate at its maximum rate rendering it unsusceptible to fine metabolic control.

Imanaka *et al.* (1972) used an active transport model for glucose uptake to model α-galactosidase induction in *Monascus sp.* The active uptake model was originally described by Cohen and Monod (1957). Cohen and Monod (1957) observed saturation of the glucose uptake rate when the glucose concentration was increased above certain levels. The active transport model predicts an equilibrium glucose concentration on the interior of the cell wall that follows a Michaelis-Menten saturation curve with exterior glucose concentration.

$$G_{int} = \frac{V_{\max}^{G_{act}} G_{ext}}{K_S^{G_{act}} + G_{ext}} \qquad (5.6)$$

where: V_{max} Michaelis-Menten maximum rate constant

G_{ext} Extracellular glucose concentration

G_{int} Intracellular glucose concentration

K_s^G Michaelis-Menten saturation constant

From the results of glucose oxidase production at varied glucose concentrations, glucose appears to have an inhibiting effect on the production of glucose oxidase above 100 gl^{-1} (Section 4). This effect is modelled using an inhibition term in the active transport of glucose. The active transport expands to include substrate inhibition of the membrane-associated permease enzyme:

$$G_{int} = \frac{V_{\max}^{G_{act}} G_{ext}}{K_S^{G_{act}} + G_{ext} + \frac{G_{ext}^2}{K_{SI}}} \qquad (5.7)$$

where

$$G_{\max}^{int} = \sqrt{K_S^{G_{act}} K_{SI}} \qquad (5.8)$$

$$Initial\ slope = \frac{V_{\max}^{G_{act}}}{K_S^{G_{act}}} \qquad (5.9)$$

K_{SI} Michaelis-Menten inhibition constant

5.5. Gene operon model

The induction of groups of enzymes and proteins in response to environmental stimulation has been modelled at the mRNA induction level by Jacob and Monod (1961). Microorganisms are able to utilise a variety of substrates. The enzymes associated with each substrate are only produced in response to that unique substrate. *A.niger* is able to utilise a wide range of substrates using inducible enzymes e.g. α-glucosidase, α-amylase and amyloglucosidase (Tan *et al.* 1984). Glucose oxidase has been reported to be induced by glucose and oxygen. The gene operon model describes the control system that expresses the correct genetic information for the substrate when present. The hypothesis that is tested in this work is that glucose oxidase is induced following the gene operon induction model.

There are two types of control system in the gene operon model: induction and repression. Both systems control the expression of genes at the transcription level and use a repressor to inhibit the transcription process. The model developed here assumes that glucose oxidase is induced by glucose alone and the induction process follows the gene operon model. In Section 7, the model is extended to consider induction by glucose and oxygen.

5.5.1 Induction control

Induction control is typically used to express a set of enzymes which are required for utilisation of a specific substrate. A repressor is a constitutive enzyme and is maintained at a constant level within the cell. When the substrate or environmental condition exist to require induction, the chemical causing the induction combines with the repressor and inactivates it, allowing the enzyme to be synthesised. Once the conditions have changed and the enzymes concerned are no longer required, the repressor accumulates and prevents enzyme production. This is modelled by a repressor pool. The repressor can exist either as free or complexed with glucose. The reaction between intracellular glucose and the free repressor is modelled by a first order reversible reaction.

$$R + G \underset{k_{-1}}{\overset{k_1}{\rightleftarrows}} R\text{-}G \tag{5.10}$$

where:

R Repressor

G Intracellular glucose

R-G Repressor glucose complex

Figure 5.6 and 5.7 illustrate the induction control in an inducing and non-inducing environment respectively.

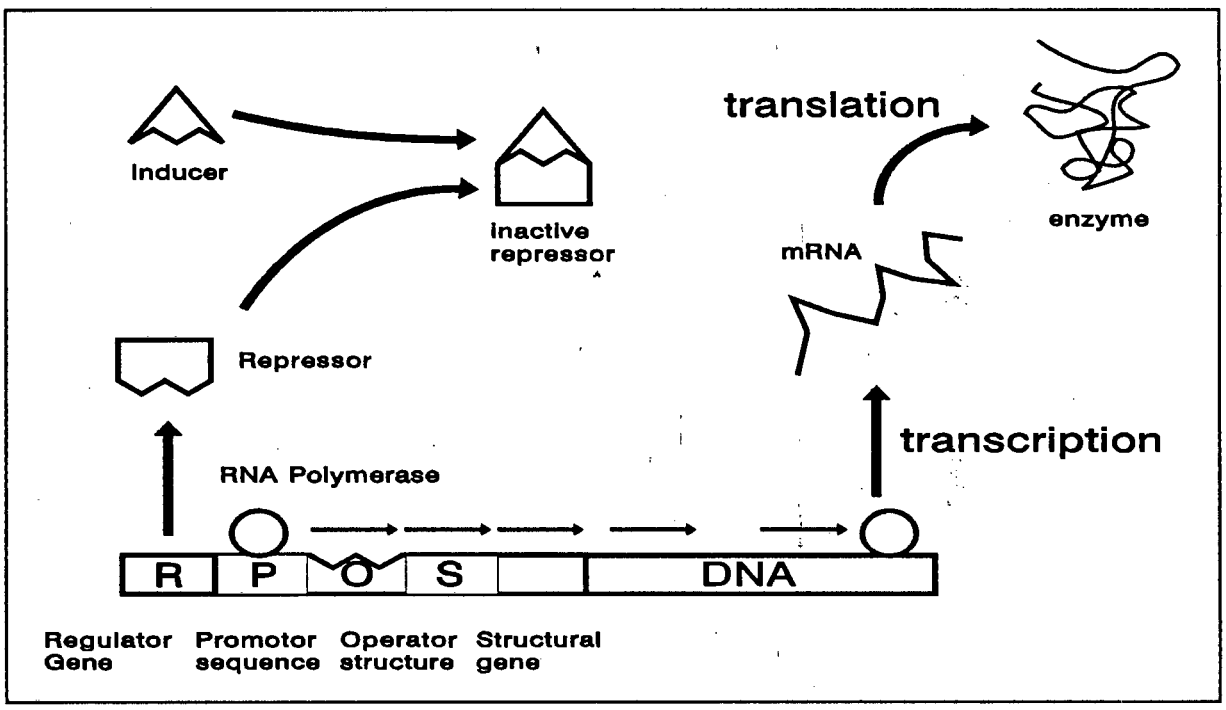

Figure 5.6 Gene operon model of induction control in an inducing environment

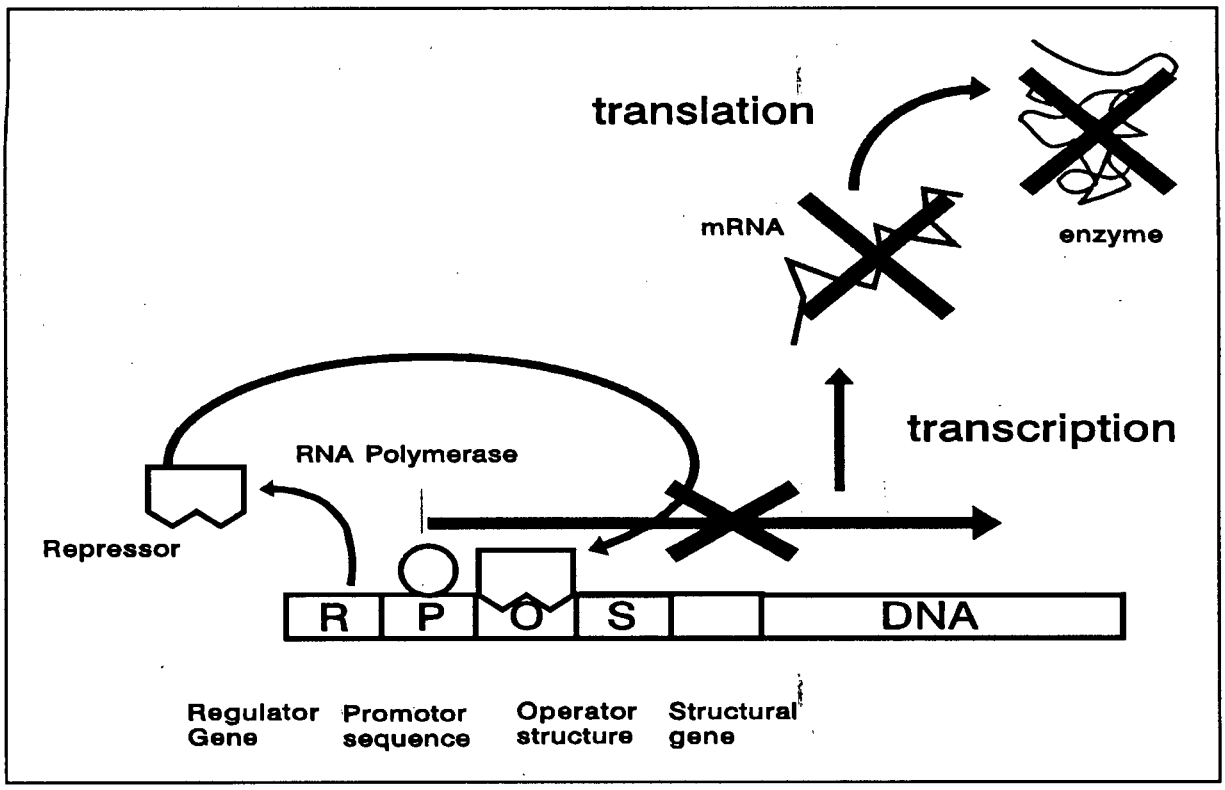

Figure 5.7 Gene operon model of induction control in a non-inducing conditions

5.5.2 Transcription

RNA polymerase converts the genetic information contained in the DNA into mRNA by matching the nucleic acids in the DNA with nucleotides according to pairing rules. The RNA polymerase enzyme binds to the promoter sequence on the DNA. If a repressor is present, this binds to the operator sequence which immediately follows the promoter sequence. This prevents the RNA polymerase from moving along the DNA strand and synthesising mRNA. If the repressor is not present, the mRNA is formed as the RNA polymerase moves down the DNA.

The production of mRNA is therefore dependent on the concentration of the repressor. The process is modelled by assuming the repressor binds to the promoter site under a probability mechanism. Above a critical threshold level, the repressor is assumed to be bound to the operator at all times. As the concentration of the repressor drops below this value, the probability of the repressor not binding to the operator increases to 1 when the repressor concentration is zero. The number of mRNA molecules produced is determined by the number of passes that the mRNA polymerase makes across the DNA which in turn is

determined by the probability or chance that the operator is free of bound repressor so that RNA polymerase binding at the promotor site may transcribe the DNA. Thus the production of mRNA when the repressor concentration is below the critical level is described as follows:

$$\frac{d[mRNA][X]}{dt} = k_3(R_{crit} - R)[X] - k_4[mRNA][X] \qquad (5.11)$$

When the repressor concentration is higher than the threshold level the mRNA production rate:

$$\frac{d[mRNA][X]}{dt} = - k_4[mRNA][X] \qquad (5.12)$$

where:

- k_3 Production rate of mRNA
- k_4 The natural decay rate of mRNA
- R Repressor concentration
- R_{crit} Critical repressor concentration

5.5.3 Translation

Proteins and enzymes are built from the mRNA template using tRNA to order the amino acid. tRNA molecules consist of two parts - an anticodon and a uniquely corresponding amino acid group. Ribosomes bind at the start of the mRNA at a binding site. The ribosome joins correct codon pairs with the mRNA. A peptide bond then forms between adjoining amino acids to link them in the same order as the codons forming the enzyme or protein.

The translation process is modelled by a first order reaction with respect to the mRNA concentration. This assumes that no other process is limiting.

5.5.4 Limitations and assumptions in the gene operon model

Several assumptions are made within the operon model. These are made explicit below:

- The concentrations of operons and repressors within cells are extremely low. For such low concentrations, the idea of macroscopic averaging of the individual units and thermodynamic equilibria becomes uncertain.
- The total amount of repressor within the cell i.e. repressor-glucose complex and free repressor is always proportional to the cell mass.
- The repressor-glucose complex is assumed to form and to decay by first order kinetics.
- The production and natural decay of mRNA is assumed to be first order and constant respectively.

5.6 Balance equation development

Using these models, species balance equations can be generated. These are detailed below:

1) Dissolved oxygen [O_2] balance :

$$\frac{d[O_2]}{dt} = k_l a(C^* - [O_2]) - \frac{[GO_{ex}]r_{max}}{1 + \frac{\beta_g}{[G_{ex}]} + \frac{\beta_O}{[O_2]}} \qquad \textbf{(5.13)}$$

Rate of increase of dissolved oxygen concentration = bubble film to bulk transfer - rate for oxygen used in gluconic acid production

2) Extracellular glucose [G_{ex}] balance :

$$\frac{d[G_{ex}]}{dt} = -\frac{[GO_{ex}]r_{max}}{1 + \frac{\beta_g}{[G_{ex}]} + \frac{\beta_O}{[O_2]}} - U_g[X]\left[\frac{G_g[G_{ex}]}{K_{sg} + [G_{ex}]} - [G_{int}]\right] \qquad \textbf{(5.14)}$$

Rate of increase in extracellular glucose = - rate for glucose used in gluconate production - rate glucose transfer into cell

3) Intracellular glucose [G_{int}] balance :

$$\frac{d[G_{int}][X]}{dt} = U_g[X]\left[\frac{G_g[G_{ex}]}{K_{sg}+[G_{ex}]} - [G_{int}]\right] - k_1[R][X][G_{int}] + k_2[R-G][X] \quad (5.15)$$

Rate of increase of intracellular glucose concentration = rate of glucose transfer into cell - rate of repressor complex formation + rate of complex breakdown

4) Repressor glucose complex [R-G] balance:

$$\frac{d[R-G][X]}{dt} = k_1[R][X][G_{int}] - k_2[R-G][X] \quad (5.16)$$

Rate of increase of repressor complex concentration = rate of repressor complex formation - rate of complex breakdown

5) mRNA balance:
If [R] < r_{crit} then

$$\frac{d[mRNA][X]}{dt} = k_3(R_{crit} - R)[X] - k_4[mRNA][X] \quad (5.17)$$

Rate of increase in mRNA concentration = production rate of mRNA - natural decay rate of mRNA

If [R] > r_{crit} then

$$\frac{d[mRNA][X]}{dt} = - k_4[mRNA][X] \quad (5.18)$$

Rate of increase in mRNA concentration = - natural decay rate

6) Intracellular glucose oxidase balance:

$$\frac{d[GO_{int}][X]}{dt} = k_5[m\text{-}RNA][X] - U_{go}[X]\left[\frac{G_{GO}[GO_{int}]}{K_{sgo}+[GO_{int}]} - [GO_{ex}]\right] \quad (5.19)$$

Rate of increase in intracellular glucose oxidase concentration = production rate of glucose oxidase from mRNA - rate of export out of cell

7) Extracellular glucose oxidase balance:

$$\frac{d[GO_{ex}]}{dt} = U_{go}[X]\left[\frac{G_{GO}[GO_{int}]}{K_{sgo}+[GO_{int}]} - [GO_{ex}]\right] \quad (5.20)$$

Rate of increase in extracellular glucose oxidase concentration = rate of export out of cell

8) Gluconic acid balance:

$$\frac{d[G.A.]}{dt} = \frac{[GO_{ex}]r_{max}}{1+\frac{\beta_g}{[G_{ex}]}+\frac{\beta_O}{[O_2]}} \quad (5.21)$$

Rate of increase in gluconic acid concentration = glucose oxidase enzyme kinetics rate

9) Cell biomass balance: (Based on logistic equation)

$$\frac{d[X]}{dt} = k_x[X](1-\beta_x[X]) \quad (5.22)$$

5.7 Conclusions

1) Analysis of the *A.niger* bioprocess system shows that the glucose oxidase induction process can be modelled mechanistically. This is because glucose oxidase induction is not a growth associated product. A mechanistic model has an inherent structure and should be valid over a wider range than an empirical model.

2) Analysis of the relative relaxation times show the areas that need to modelled:

   Cell mass growth
   Dissolved oxygen mass transfer
   Gluconic acid production rate as a function of glucose, oxygen and glucose oxidase.
   Glucose oxidase induction
   Glucose oxidase export
   Glucose uptake

3) Balance equations have been generated for the various species contained in the state vector. These equations describe 3 areas of kinetics:

   a) Cell growth
   b) Gluconic acid production
   c) Glucose oxidase induction

   and 3 areas of mass transfer:

   a) Glucose oxidase export
   b) Glucose uptake
   c) Oxygen bubble to media transfer

6. FITTING *A.NIGER* MODEL, BASED ON INDUCTION BY GLUCOSE ALONE

6.1 Methodology

Modelling of the *A.niger* glucose oxidase and gluconic acid production requires cell growth, enzyme production kinetics and gluconic acid production kinetics to be modelled and linked. In the previous chapter, the derivation of the various mechanisms known to occur or hypothesised to occur were presented. A series of ordinary differential species balance equations (ODE's) in time were developed (Section 5.6). These equations can be integrated in time using initial conditions and appropriate parameters. Experimental data and modelled profiles can be compared, the parameters adjusted and the process repeated until experimental results are suitably represented by the model.

Initially glucose oxidase induction was modelled to be dependent on glucose concentration alone. Thus the air experiments at various glucose concentrations served as the data pool. The 100 gl^{-1} glucose experiment in air was used first and the parameters gained from optimisation were used to predict the 50 and 150 gl^{-1} air experiments. The predictions were compared to experimental data. Validation and limitations of the model were then made.

6.2 Integration of the ordinary differential equations (O.D.E.)

The integration problem is an initial condition problem containing eleven state variables listed in Table 6.2 together with units.

The fourth order Runge-Kutta technique was used to integrate the system of O.D.E.'s. The initial values of the various state variables were deduced from experimental conditions at the start of the experiments. Intracellular concentrations of repressor, repressor glucose complexes and mRNA were assumed to be at equilibrium in the non-inducing state as the inoculum was in the 'relaxed' state and all processes were assumed to be a steady state.

The fourth order Runge-Kutta was implemented as detailed by Chapra and Canale (1989) for a system of O.D.E.:

$$\overline{y_{i+1}} = \overline{y_i} + \left[\frac{1}{6}(\overline{k_1} + 2\overline{k_2} + 2\overline{k_3} + \overline{k_4})\right]h \qquad \textbf{(6.1)}$$

$$\overline{k_1} = f(x_i\ ,\ \overline{y}) \qquad \textbf{(6.2)}$$

$$\overline{k_2} = f\left[x_i+\frac{h}{2}\ ,\ \overline{y_i}+\frac{h}{2}\overline{k_1}\right] \qquad \textbf{(6.3)}$$

$$\overline{k_3} = f\left[x_i+\frac{h}{2}\ ,\ \overline{y_i}+\frac{h}{2}\overline{k_3}\right] \qquad \textbf{(6.4)}$$

$$\overline{k_4} = f\left[x_i+h\ ,\ \overline{y_i}+h\overline{k_3}\right] \qquad \textbf{(6.5)}$$

where symbols are given in Table 6.1.

Table 6.1 Description of variables used in Runge-Kutta algorithm

Variable	Description
X	Time
$\mathbf{Y_t}$	State variable at time t
$\mathbf{Y_{t+1}}$	State variable at time t+1
$\mathbf{k_{1\text{-}4}}$	O.D.E. evaluated at different state vectors and times calculated by Runge-Kutta algorithm
f[X,Y]	O.D.E. function evaluated at state vectors **Y** and **X**

6.3 Optimisation strategy

Initial estimates of parameters were made from literature (Imanaka *et al.* 1973) and experimental conditions. These parameters were then optimised using a simplex search strategy. The algorithm was taken from Press *et al.* (1986). The objective function was formed out of the sodium hydroxide addition profiles (equivalent to gluconic acid formed). This objective function effectively includes glucose oxidase activity (affected by glucose and oxygen concentration) and oxygen transfer as these factors interrelate to the product formed. The function does not however include glucose oxidase induction after the glucose has been converted to gluconic acid.

The step size was chosen to be smaller than the smallest process time constant to ensure stable integration. The $k_l a$ mass transfer coefficient was of the order of 100 h^{-1} ($t_{½}$ = 25s) so the time step was chosen to be 0.001h or 3.6 seconds.

6.3.1 Initial parameter estimates

Parameters used in the model fall into three areas. The first area contains well understood constants documented in the literature for processes such as glucose oxidase catalysed conversion of glucose to gluconic acid. The second area contains parameters which are measurable in the experimental system such as $k_l a$ and biomass growth rate and maximum cell mass. The third area covers the unknown parameters in the induction model of glucose oxidase. These parameters contain equilibrium constants for reactions of glucose uptake and of glucose complexing with repressor.

Initial estimates of the parameters can be taken from literature. Table 6.3 compares the time constants for the optimised 100 gl^{-1} air experiment to a gene operon model used by Imanaka *et al.* (1973) to model α-galactosidase production in a mold *Monascus* sp. The time constants are of similar order of magnitude.

Table 6.4 contains the near optimal parameter estimates from the simplex search in the 100 gl^{-1} glucose case.

Table 6.2 State variables,units and initial conditions for the model of glucose induction of glucose oxidase at 100 gl^{-1}

State Variable	Unit	Initial 100gl^{-1} value
Biomass	(gl^{-1})	0.1651
Extracelluar glucose	(M)	0.556
Intracellular glucose	(mole g^{-1}_{cell})	0.2E-3
Repressor	(mole g^{-1}_{cell})	1E-3
Repressor glucose complex	(mole g^{-1}_{cell})	1E-8 ≡ 0
m-RNA	(mole g^{-1}_{cell})	1e-8 ≡ 0
Intracellular glucose oxidase	($Uml^{-1}g^{-1}_{cell}$)	0
Extracelluar glucose oxidase	(U/ml)	0
Extracelluar gluconic acid	(M)	0
Dissolved oxygen	(ppm)	7.7
Time	(h)	0

Table 6.3 Comparison of half-life time constants for *Monascus* sp. and *A.niger*

Bioprocess	*Monascus* sp.	*A.niger*
Glucose repressor complex reaction	±1.0 h	±0.8 h
mRNA production	±1.0 h	±2.3 h
Glucose uptake	±25 s	±50 s
Glucose oxidase export	-	±50 s

Table 6.4 Near optimal parameters for the model of glucose induction of glucose oxidase at 100 gl^{-1} model

Parameter	Symbol	Near optimal value	Sensitivity (%change in error after a 10% parameter change)	Units
Glucose mass transport coefficient	U_g	50		h-1
Glucose Michaelis Menten saturation	G_g	1E-3		Mg^{-1}_{cell}
Glucose Michaelis menten rate	Ks_g	0.0965		Mg^{-1}_{cell}
Repressor-glucose complex formation rate	k_1	18000	76	$g_{cell}h^{-1}M^{-1}$
Repressor-glucose destruction rate	k_2	0.87	16	h^{-1}
Repressor threshold level	R_{crit}	4.0 E-4	107	Mg^{-1}_{cell}
mRNA natural destruction rate	k_4	0.30	46	h^{-1}
mRNA induction rate	k_3	8.0 E-3	136	h^{-1}
glucose oxidase formation rate	k_5	300	325	$UM^{-1}h^{-1}$
mass transfer coefficient	k_la	450	55	h^{-1}
Logistic biomass growth rate	μ_{max}	0.231	20	h^{-1}
Maximum cell mass	X_{max}	2.624	1	gl^{-1}

6.4 Model profiles and experimental results

The parameters of the model were optimised to minimise the squared error between the measured sodium hydroxide addition and the predicted addition using an initial glucose concentration of 100 gl^{-1}. The initial extracellular glucose conditions of the model were then altered for the 50 and 150 gl^{-1} cases. The model was run to predict the profiles of glucose oxidase, sodium hydroxide addition (equivalent to gluconic acid) and dissolved oxygen under these conditions. These were compared to experimental profiles.

6.4.1 Initial glucose concentration of 100 gl^{-1}

The profile of sodium hydroxide addition can be split into four sections: a 6h lag phase, a section of increasing slope, a short decreasing section and a flat plateau. The lag phase is modelled by the inductive process of glucose oxidase. The repressor is consumed once the inoculum is placed in an inducing environment. When the repressor reaches the critical threshold level, the mRNA is produced. Glucose oxidase is then produced from the mRNA and exported into the bulk phase. The glucose oxidase then catalyses the conversion of glucose to gluconic acid. The slow increasing section occurs as glucose oxidase is accumulating in the media. Once the glucose falls below ± 0.05M, the Michaelis-Menten glucose oxidase enzyme kinetics predict a rate proportional to the glucose concentration. Thus the rate of conversion slows down and stops once the glucose is consumed. Experimental data as well as the model fitted to NaOH addition for an initial glucose concentration of 100 gl^{-1} are shown in Figure 6.1.

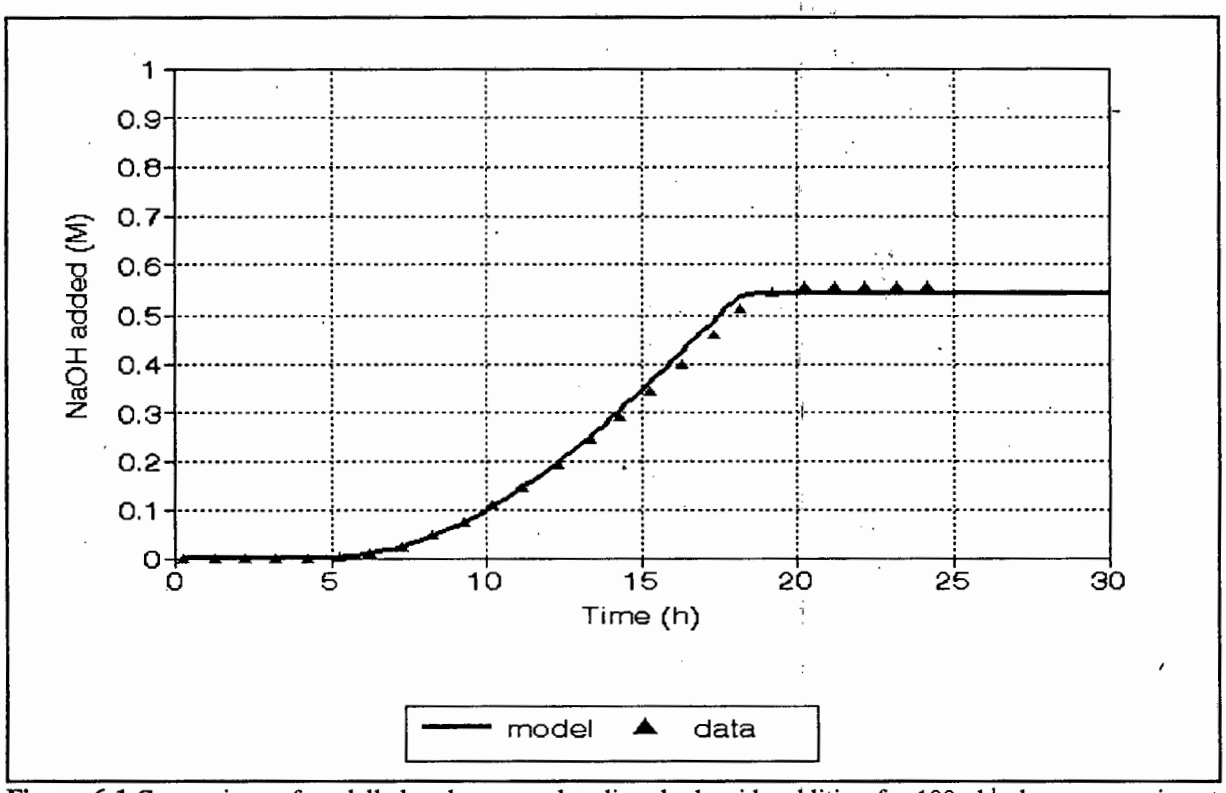

Figure 6.1 Comparison of modelled and measured sodium hydroxide addition for 100 gl^{-1} glucose experiment

The glucose oxidase profile shown in Figure 6.2 is matched well by the model. The lag phase, production shape and final value are matched.

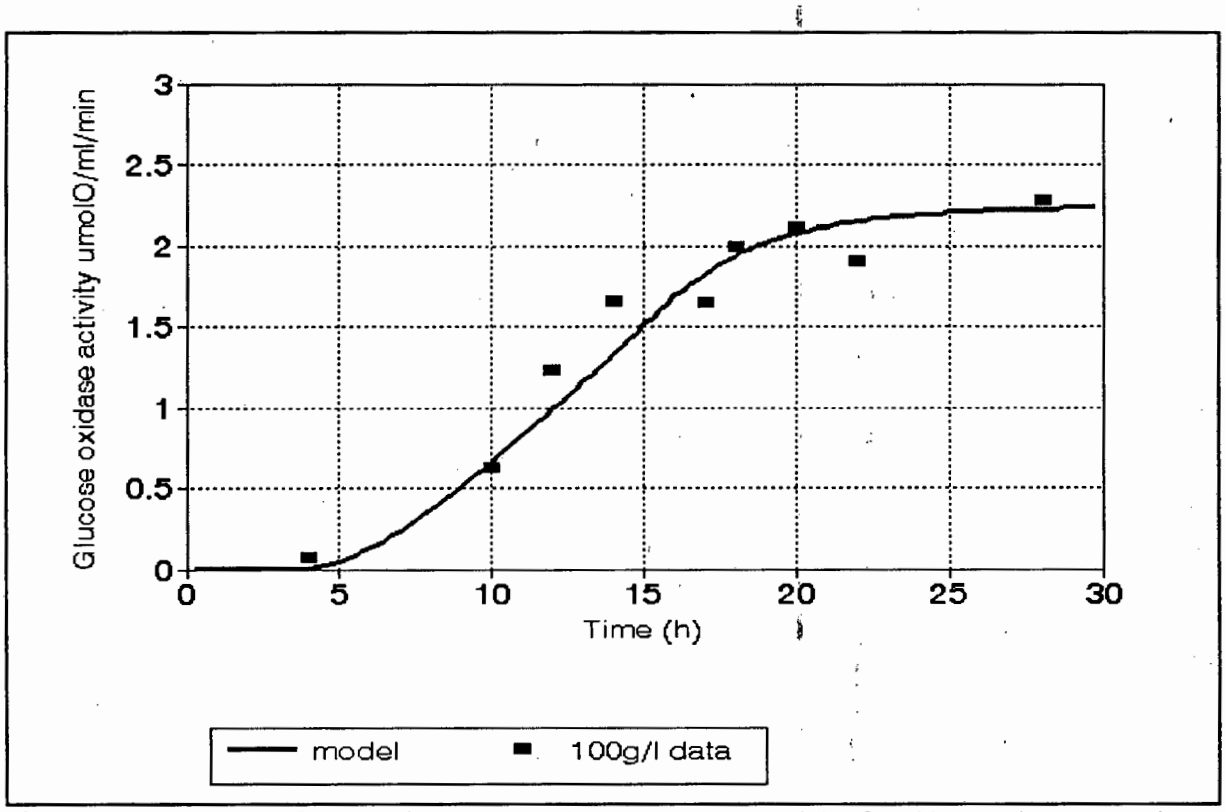

Figure 6.2 Comparison of modelled and measured glucose oxidase activity for 100 gl-1 glucose experiment

The dissolved oxygen profile is predicted from the balance between oxygen consumption due to glucose conversion and oxygen transfer via the mass transfer resistance k_la. The profile shown in Figure 6.3 is matched well by the model using measured values of k_la.

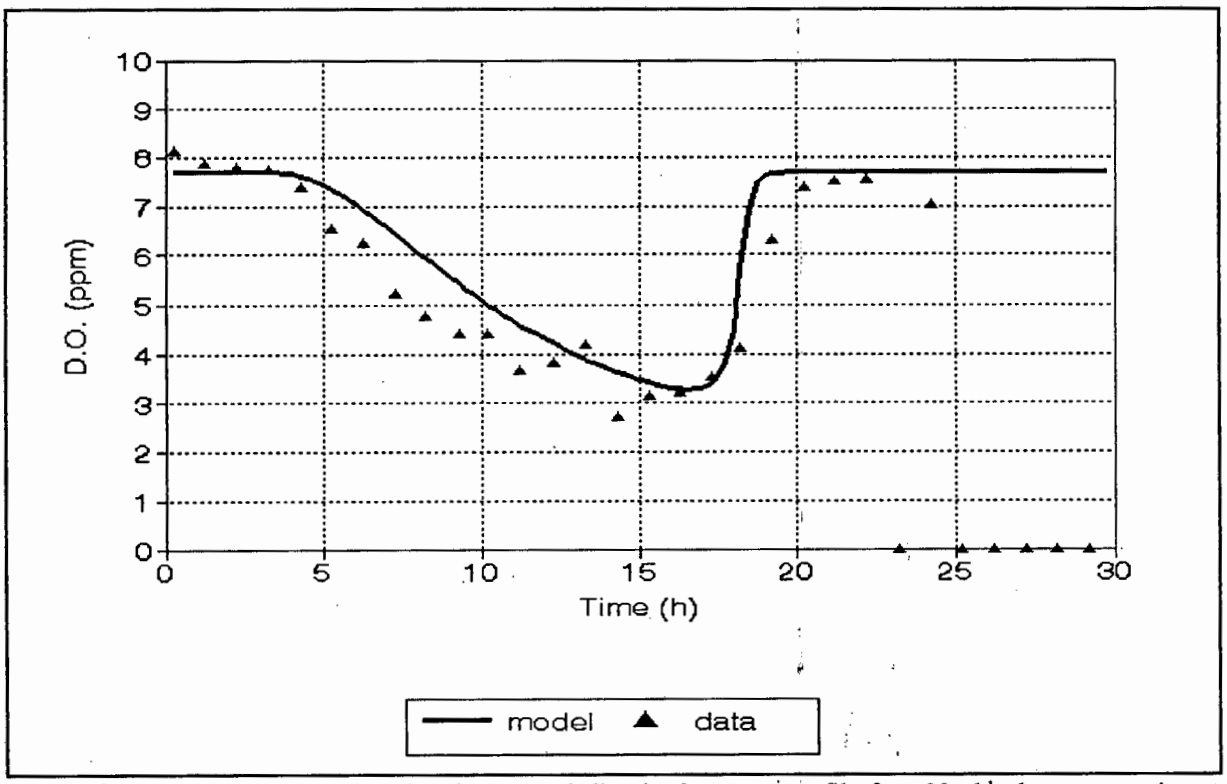

Figure 6.3 Comparison of modelled and measured dissolved oxygen profile for 100 gl^{-1} glucose experiment

The profiles of the intracellular induction system are given in the Figure 6.4. The graph shows the decline in the repressor concentration as it combines with glucose present due to the inducing environment. The repressor-glucose complex increases at the same time. The mRNA synthesis begins as soon as the repressor concentration is less than the threshold level of 4 10^{-4}M. The mRNA continues to be produced until the glucose has been consumed and then production slows as the repressor concentration rises to the non-inducing level.

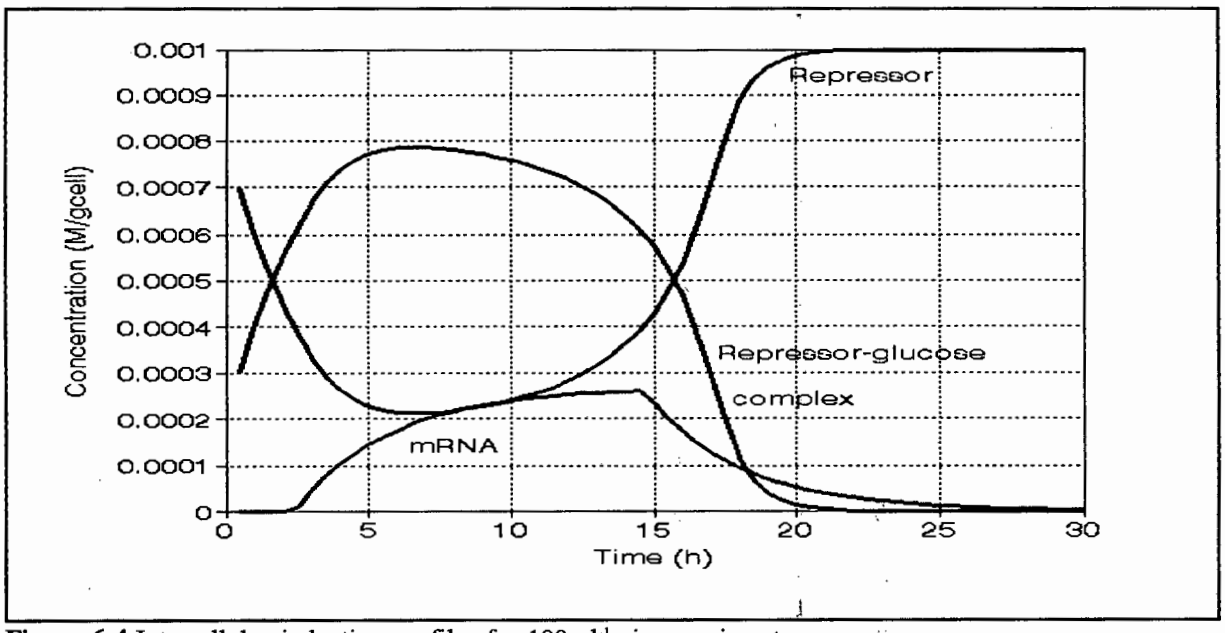

Figure 6.4 Intracellular induction profiles for 100 gl^{-1} air experiment

6.4.2 50 and 150 gl^{-1} glucose predicted profiles

The predicted profiles for the 50gl^{-1} reaction compare well to the experimental profiles for sodium hydroxide addition, dissolved oxygen concentration and glucose oxidase activity (Figures 6.5 to 6.7). The model prediction of the 150gl^{-1} reaction is less satisfactory when compared to experimental results (Figures 6.8 to 6.10). Whilst the shape and trends of the profiles are correct, the model predicts that the glucose oxidase production, for the 150 gl^{-1} case, exceeds the 100gl^{-1} case whilst inhibition is observed experimentally in the 150 gl^{-1} case (Figure 6.11). Glucose oxidase activities are similar in the presence of 100 gl^{-1} and 150 gl^{-1} glucose. The mechanism of glucose oxidase induction is not understood well enough to include inhibitory terms in the model.

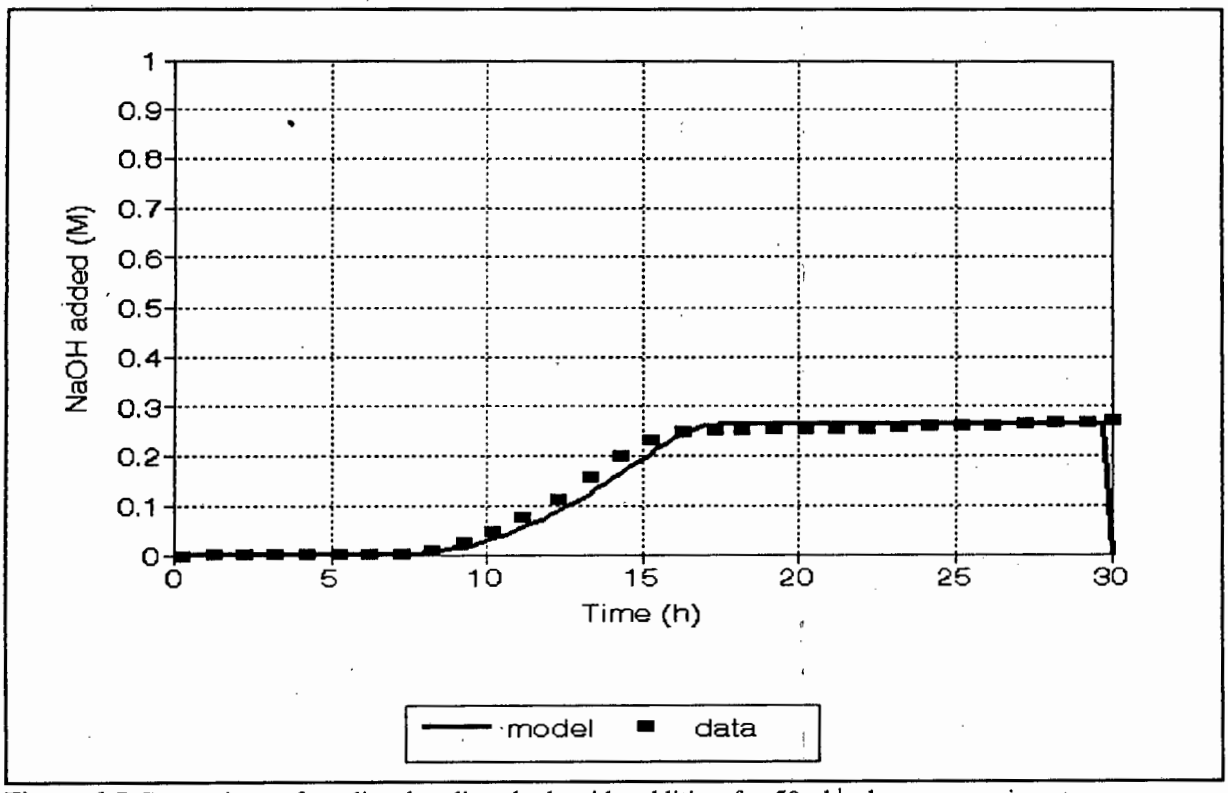

Figure 6.5 Comparison of predicted sodium hydroxide addition for 50 gl^{-1} glucose experiment

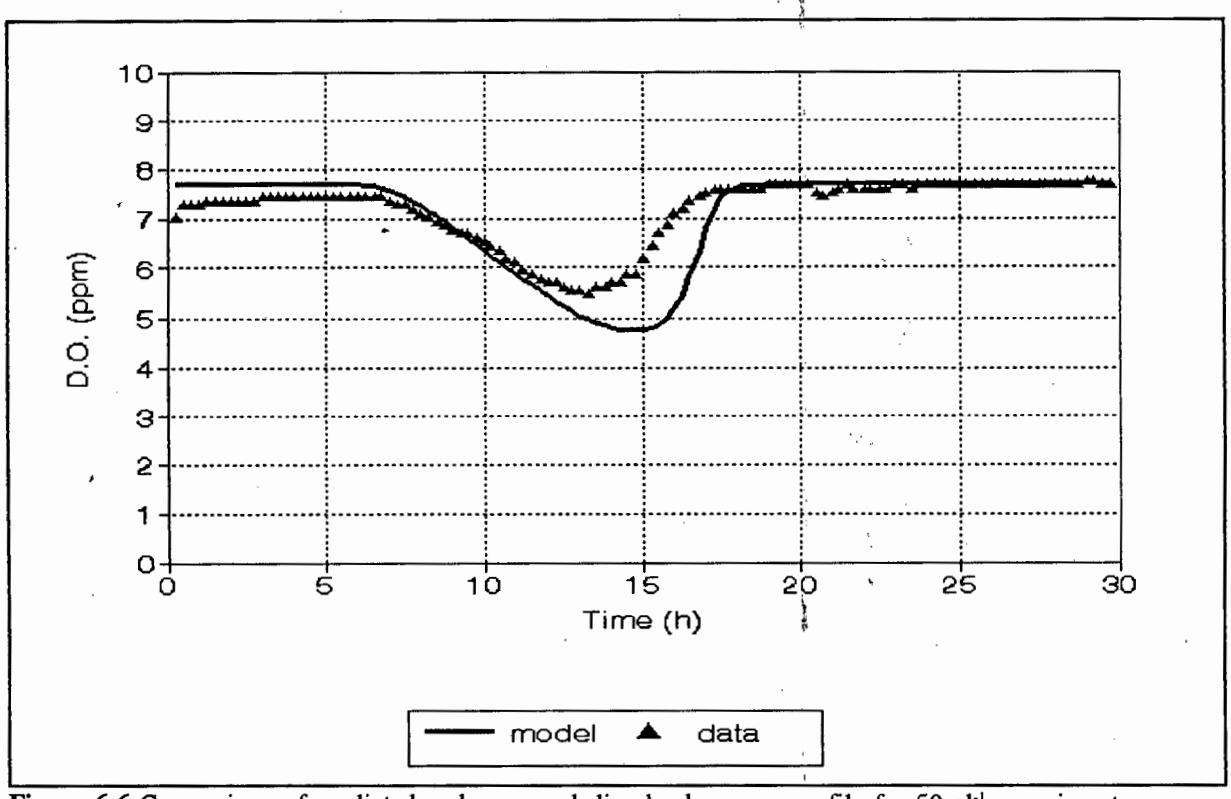

Figure 6.6 Comparison of predicted and measured dissolved oxygen profile for 50 gl^{-1} experiment

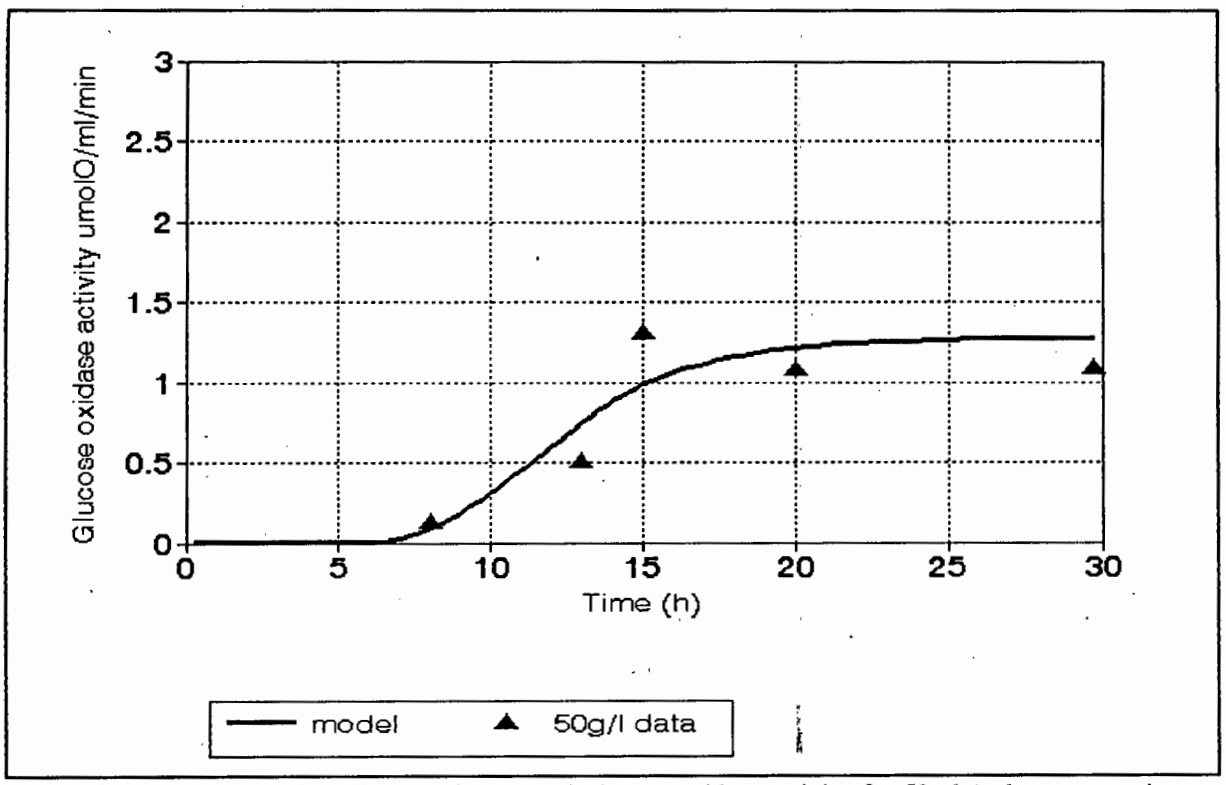

Figure 6.7 Comparison of predicted and measured glucose oxidase activity for 50 gl-1 glucose experiment

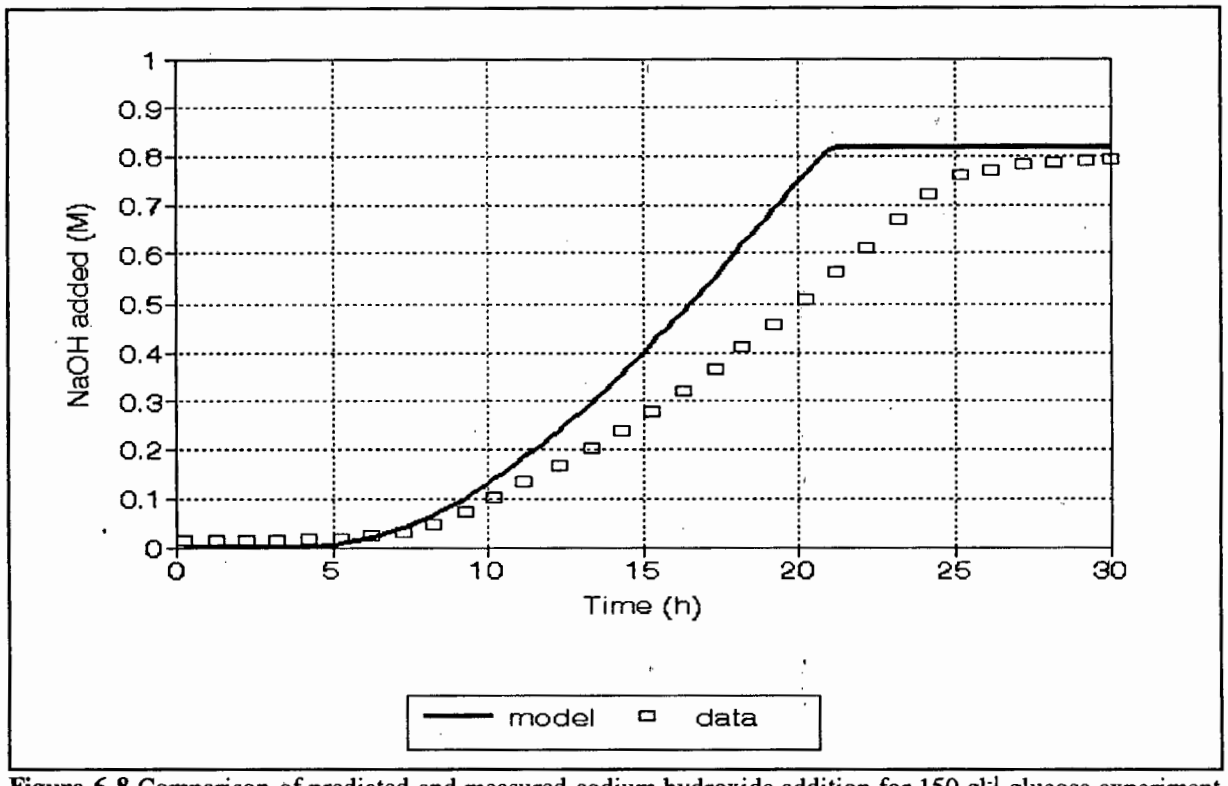

Figure 6.8 Comparison of predicted and measured sodium hydroxide addition for 150 gl^{-1} glucose experiment

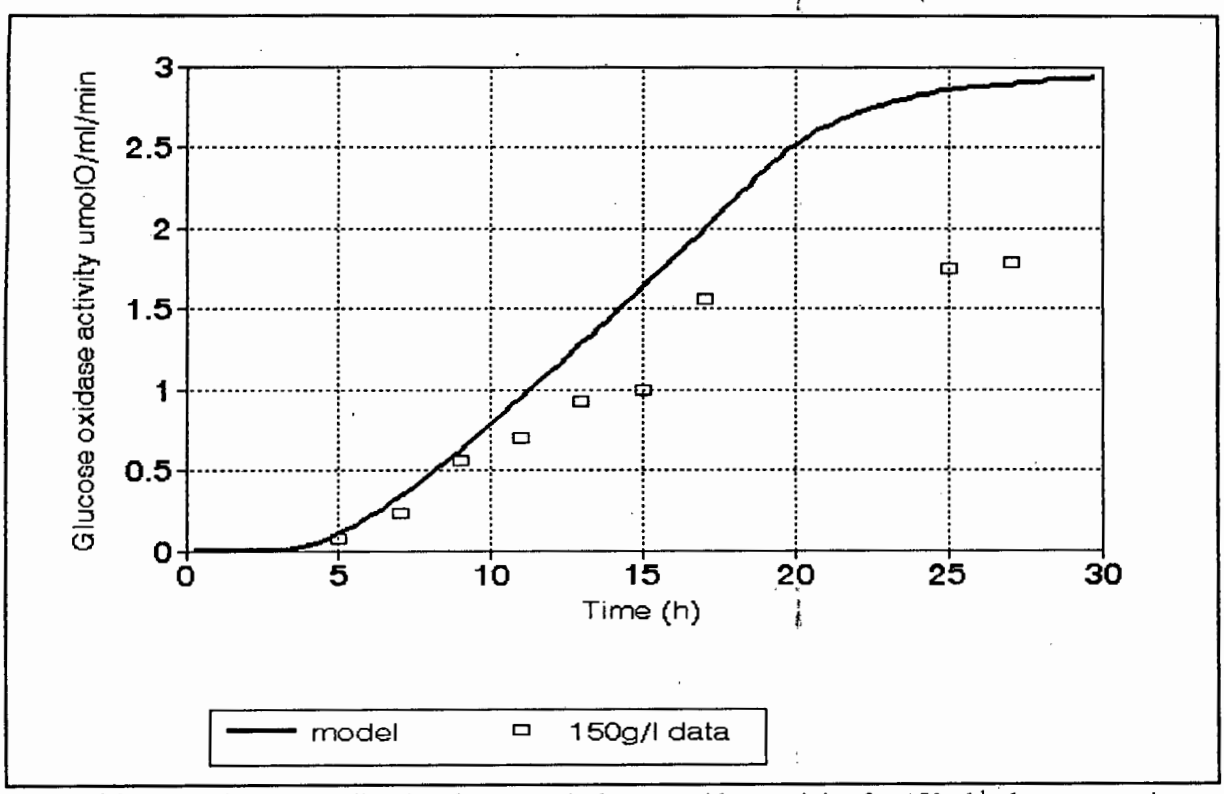

Figure 6.9 Comparison of predicted and measured glucose oxidase activity for 150 gl^{-1} glucose experiment

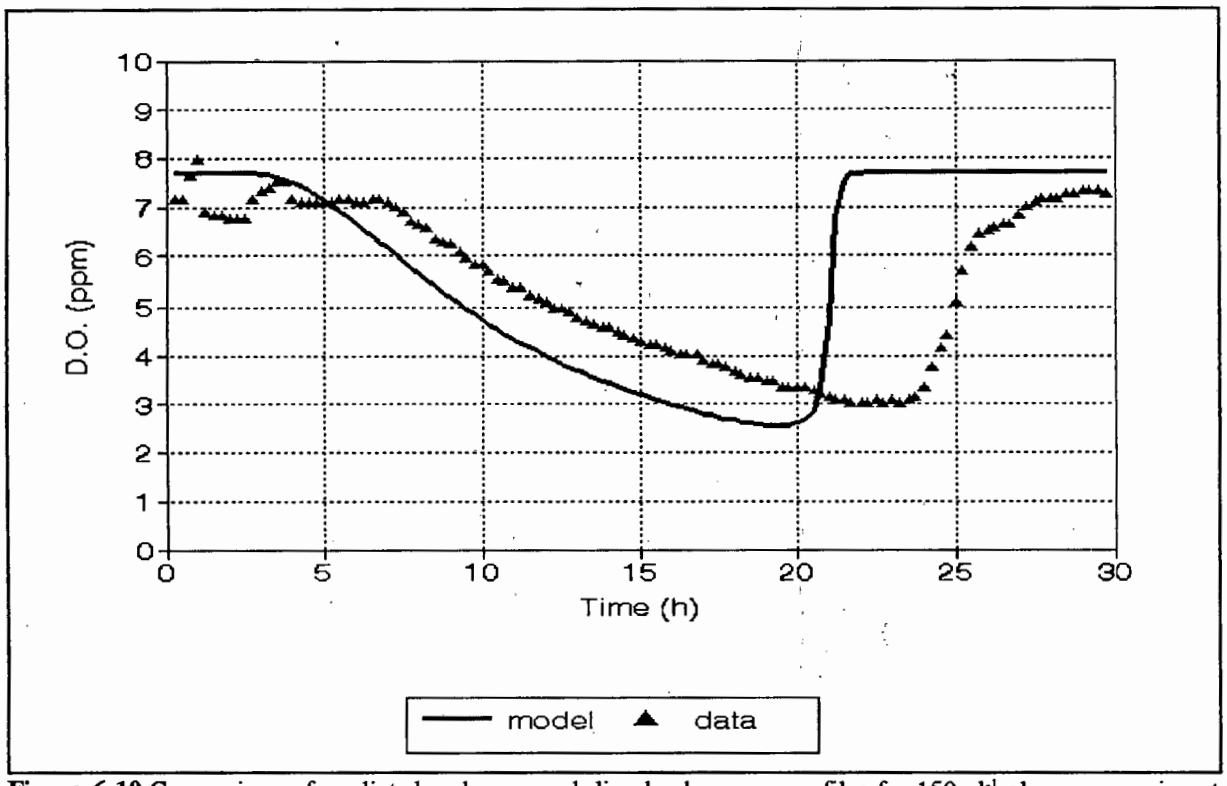

Figure 6.10 Comparison of predicted and measured dissolved oxygen profiles for 150 gl^{-1} glucose experiment

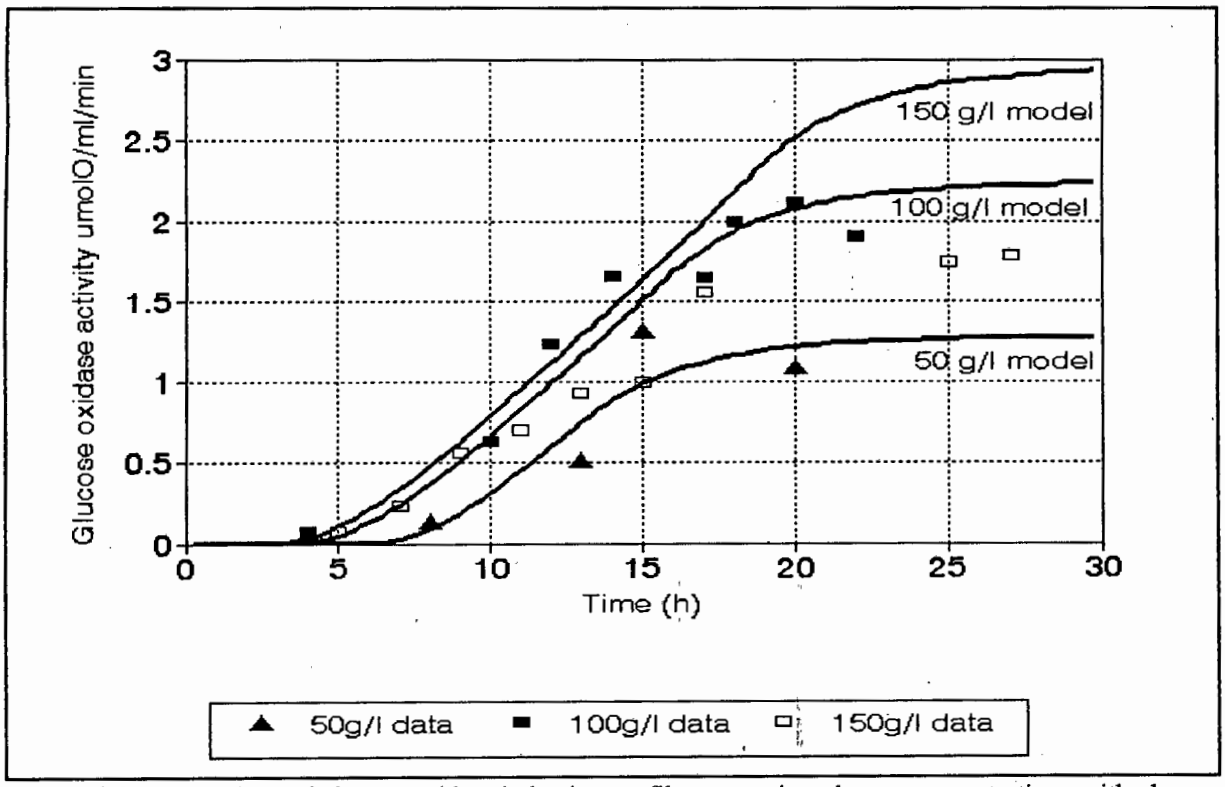

Figure 6.11 Comparison of glucose oxidase induction profiles at varying glucose concentrations with glucose induction model

6.4.3 Osmotic stress

Microorganisms respond to osmotic stress in two basic ways. Firstly, the cell expends energy in maintaining the new osmotic pressure to prevent plasmolysis (Gervais *et al.* 1992). Secondly, osmosensory proteins embedded in the cell envelope respond to high osmotic stress and trigger off a regulatory cascade of genes (Rudulier *et al.* 1984). These genes can control the production of chemicals such as glycine betaine and proline betaine which have been shown to be induced by high NaCl concentrations in higher plants (Aspinall *et al.* 1981). The regulatory effects have been shown to either increase enzyme synthesis (Edgley and Brown 1983), decrease enzyme synthesis (Davis and Baudon 1986) or selectively increase and decrease enzyme synthesis e.g. an increase in the 2-ketogluconate pathway and a decrease in the glucose-6-phosphate pathway has been observed by Prior and Kenyon (1980). Osmoregulation has been observed in both fungal and bacterial systems, operating on both intracellular and extracellular enzymes (Davis and Baudon 1987).

Following the experimental observation of reduced glucose oxidase formation at increased glucose concentration, it has been postulated that this results from the increase in osmotic stress at high glucose concentration.

6.4.4 Modified model

The mRNA production rate was decreased by 63% to simulate the reduced glucose oxidase production at 150 gl^{-1}. The resultant profiles, shown in Figures 6.12 to 6.14, illustrate that the reduced rate and extent of glucose oxidase formation can be modelled in this way satisfactorily. The mechanism in which the cell controls the rate of induction as a function of osmotic pressure is not understood.

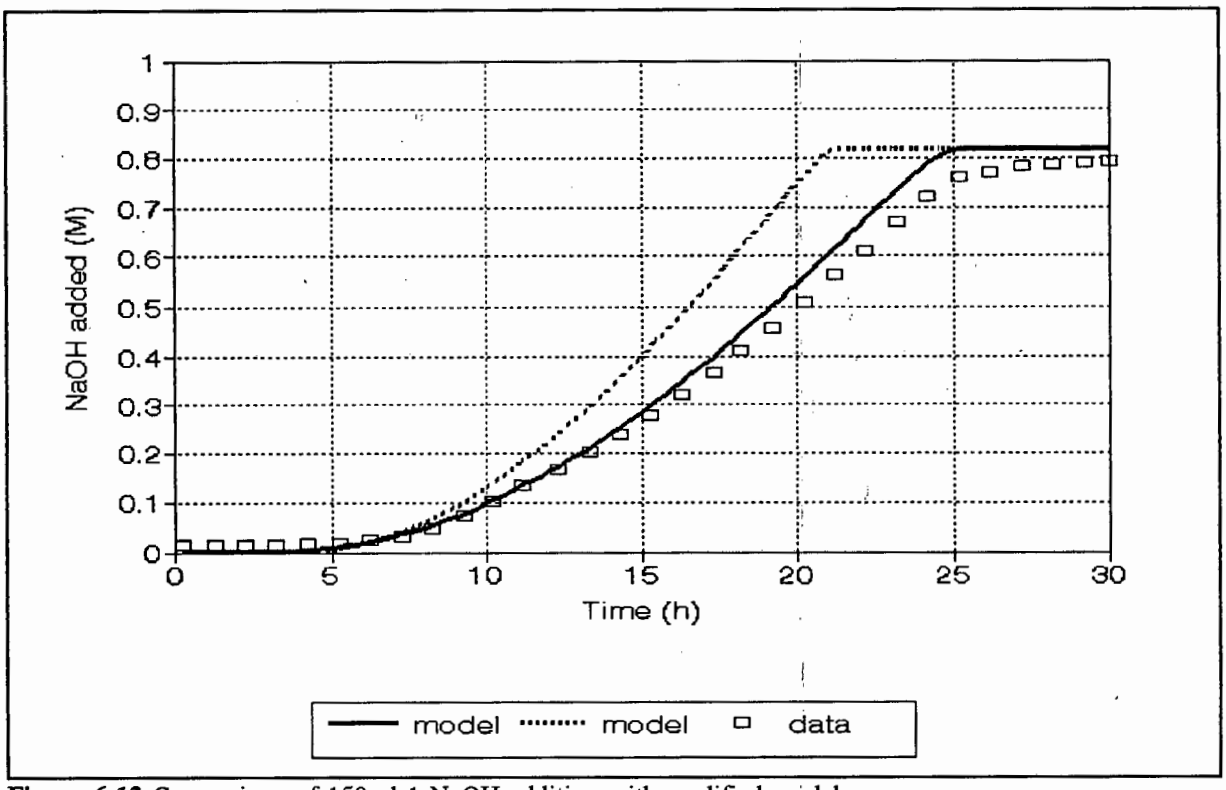

Figure 6.12 Comparison of 150 gl-1 NaOH addition with modified model

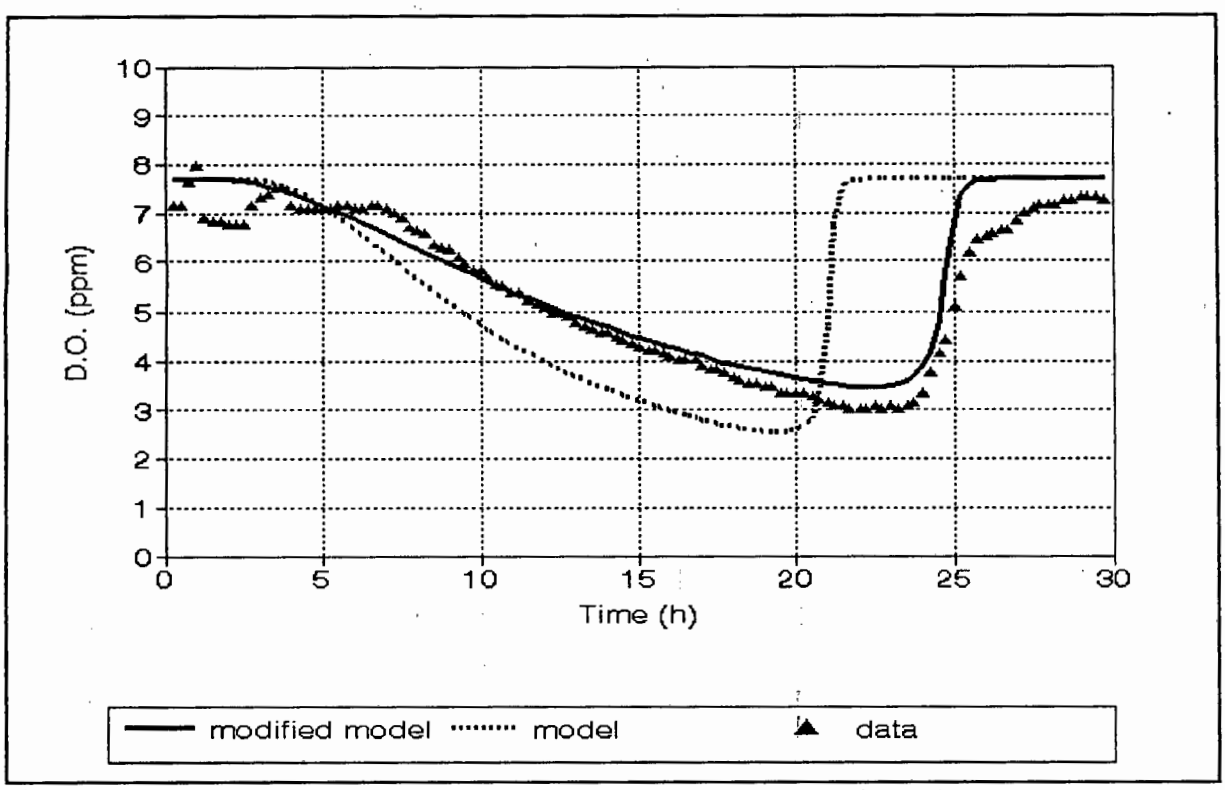

Figure 6.13 Comparison of 150 gl-1 dissolved oxygen profile with modified model

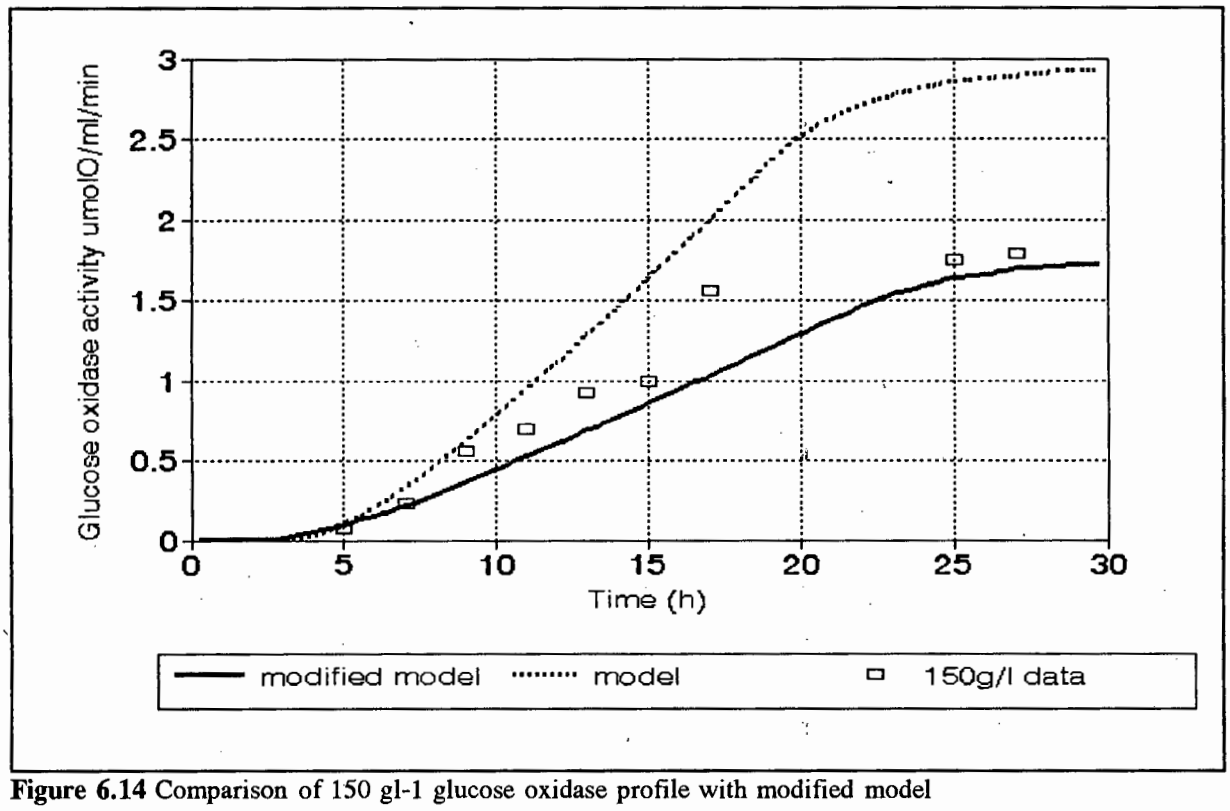

Figure 6.14 Comparison of 150 gl-1 glucose oxidase profile with modified model

6.5 Validation and limitations of the glucose induction model

The glucose induction model has been seen to model glucose oxidase induction, gluconic acid production and dissolved oxygen profiles for initial glucose concentrations below or equal to 100 gl^{-1}. At glucose concentrations above 100 gl^{-1}, the production of glucose oxidase is inhibited. The basic model does not include this effect. While a correction has been implemented by altering the mRNA production rate, the process of inhibition has not been understood well enough to offer a mechanism.

6.5.1 Sensitivity analysis

The sensitivity of the model to changes in the parameters was measured by varying each parameter by 10% and noting the percentage increase in the squared error on the sodium hydroxide addition profile. Table 6.4 contains the sensitivity results.

The rate of translation of mRNA into glucose oxidase and the transcription rate to form mRNA had the greatest effect on the model. This is to be expected as the final glucose oxidase concentration directly affects the rate of conversion of glucose to gluconic acid. Any changes to the production rate of the enzyme will significantly change the production profile.

The repressor threshold level has the next most significant effect on the model. The repressor threshold is a dominant term as it determines when the enzyme induction is switched on and how long the induction window remains open.

The sensitivity analysis shows that parameters closest to the production of glucose oxidase affect the product profile the most. Parameters further down the reaction chain that lead up to glucose oxidase production affect the profile less.

6.6 Conclusions

The *A.niger* system model describes the batch experimental results. The dissolved oxygen, gluconic acid and glucose oxidase profiles can be fitted by the model at an initial glucose concentration of 100 gl^{-1}. Furthermore the model can predict the 50gl^{-1} glucose experimental profiles. The 150 gl^{-1} profiles can only be predicted by decreasing the mRNA production rate parameter. This inhibition could be due to osmotic stress.

7. EXTENDED MODEL DEVELOPMENT OF *A. NIGER* SYSTEM AND GLUCOSE OXIDASE INDUCTION BY GLUCOSE AND OXYGEN

Glucose oxidase is known to be induced by both glucose and oxygen. The previous two chapters have illustrated that the glucose induction effect at constant oxygen can be modelled using the gene operon model and simple balance equations for the *A. niger* subprocesses. This section demonstrates an extension to the gene operon model to include induction by oxygen and glucose by means of two specialised repressors - one for glucose and one for oxygen. The operator is assumed to have binding sites in series for each repressor. The production of the mRNA is proportional to the product of the difference between the threshold and repressor levels for both inducers.

7.1 Oxygen and glucose induction system

Glucose oxidase system is induced by both glucose and oxygen. Minimum levels for both glucose and oxygen required for induction have been recorded but the interaction effects have not been quantified. The nine base experiments which straddle the induction ranges of both inducers show interaction trends. It can be seen that glucose and oxygen interact positively in the range from 50 to 100gl^{-1}. Increasing glucose and increasing oxygen at the same time results in a greater increase in glucose oxidase rate than produced by only increasing glucose or oxygen separately. At a point above 100gl^{-1}, glucose inhibition occurs and this mechanism is not well understood but can be modelled by a decreased mRNA production rate postulated to result from osmotic stress regulation. The interaction between glucose and oxygen in the induction system must therefore include a positive interaction.

The oxygen induction system is based on the glucose induction system. Oxygen is assumed to permeate the cell membranes freely. Thus the oxygen concentration is the same on the interior of the cell as in the bulk environment. The oxygen can combine with a repressor in

the cell to form a complex. The free repressor can combine with a binding site on the DNA inhibiting mRNA production. Positive interaction can be achieved by modelling two independent repressors for glucose and oxygen respectively and using two operator binding sites in series. The probability of passing one of the repressor binding sites is proportional to the difference between the concentration of the free repressor and a minimum threshold repressor concentration before binding occurs. When two of these binding sites follow in series, the mRNA production rate is proportional to the product of the two binding site probabilities. The production of the intracellular enzyme from this mRNA is the same as in the previous induction model.

7.2 Modification to model equations

Modifications to the induction kinetic system included:

a) An extra state variable for the oxygen repressor

b) A balance equation for the reversible oxygen repressor system

c) Extension of the equation for the production of mRNA to include a threshold level for both the glucose and oxygen.

The final balance equations are as follows:

Model equations

1) Dissolved oxygen [O_2] balance :

$$\frac{d[O_2]}{dt} = k_l a(C^* - [O_2]) - \frac{[GO_{ex}]r_{max}}{1 + \frac{\beta_g}{[G_{ex}]} + \frac{\beta_O}{[O_2]}} \qquad (7.1)$$

Dissolved oxygen increase	= bubble film bulk transfer	- rate for oxygen used in gluconic acid production.

2) Extracellular glucose [G_{ex}] balance :

$$\frac{d[G_{ex}]}{dt} = -\frac{[GO_{ex}]r_{max}}{1 + \frac{\beta_g}{[G_{ex}]} + \frac{\beta_O]}{[O_2]}} - U_g[X]\left[\frac{G_g[G_{ex}]}{K_{sg} + [G_{ex}]} - [G_{int}]\right] \qquad (7.2)$$

Extracellular glucose increase	= rate of glucose used in gluconic acid production	-rate of glucose transport into cell.

3) Intracellular glucose [G_{intra}] balance :

$$\frac{d[G_{int}][X]}{dt} = U_g[X]\left[\frac{G_g[G_{ex}]}{K_{sg} + [G_{ex}]} - [G_{int}]\right] - k_1[R][X][G_{int}] + k_2[R\text{-}G][X] \qquad (7.3)$$

Intracellular glucose increase	= rate of glucose transfer into cell	- rate of repressor complex formation	+ rate of complex breakdown.

4) Repressor glucose complex [R-G] balance :

$$\frac{d[R_g\text{-}G][X]}{dt} = k_1[R_g][X][G_{int}] - k_2[R_g\text{-}G][X] \quad (7.4)$$

Repressor glucose increase	= complex formation rate	- complex breakdown rate.

5) Repressor oxygen complex [R-O] balance :

$$\frac{d[R_{O_2}\text{-}G][X]}{dt} = k_1[R_{O_2}][X][O_2] - k_2[R_{O_2}\text{-}G][X] \quad (7.5)$$

Repressor oxygen complex	= complex formation rate	- complex breakdown rate.

6) Glucose oxidase mRNA balance:
If $[R_{oxygen}] < r_{oxygen\text{-}crit}$ **AND** $[R_{glucose}] < r_{glucose\text{-}crit}$ then

$$\frac{d[m\text{-}RNA][X]}{dt} = k_3(R_{O_2crit}\text{-}R_{O_2crit})(R_{g\text{-}crit} - R_g)[X] - k_4[m\text{-}RNA][X] \quad (7.6)$$

increase in glucose oxidase mRNA	= production rate	- natural decay rate

ELSE

$$\frac{d[mRNA][X]}{dt} = - k_4[mRNA][X] \quad (7.7)$$

increase glucose oxidase mRNA	= - natural decay rate

7) Intracellular glucose oxidase formation:

$$\frac{d[GO_{int}][X]}{dt} = k_5[mRNA][X] - U_{go}[X]\left[\frac{G_{GO}[GO_{int}]}{K_{sgo}+[GO_{int}]} - [GO_{ex}]\right] \quad \textbf{(7.8)}$$

Intracellular glucose oxidase increase	= production rate from mRNA	- rate of export out of cell.

8) Extracellular glucose oxidase formation:

$$\frac{d[GO_{ex}]}{dt} = U_{go}[X]\left[\frac{G_{GO}[GO_{int}]}{K_{sgo}+[GO_{int}]} - [GO_{ex}]\right] - \frac{[GO_{ex}]Km_{go}[GO_{ext}]}{[O_2]+Km_{go}} \quad \textbf{(7.9)}$$

Extracellular glucose oxidase increase	= rate of export out of cell	- oxygen deactivation

9) Gluconic acid formation:

$$\frac{d[G.A.]}{dt} = \frac{[GO_{ex}]r_{max}}{1+\frac{\beta_g}{[G_{ex}]}+\frac{\beta_O}{[O_2]}} \quad \textbf{(7.10)}$$

Gluconic acid production rate	= glucose oxidase enzyme kinetic rate

10) Biomass formation from logistic equation:

$$\frac{d[X]}{dt} = k_x[X](1-\beta_x[X]) \quad \textbf{(7.11)}$$

7.3 Model fit and predictive behaviour

Initial conditions were chosen to be similar to those in the model described in Section 6.3.1. Table 7.1 shows the initial conditions. The model parameters were optimised using the sodium hydroxide addition profile, for the initial glucose concentration of 100 gl^{-1} at 0.21 atm oxygen experiment, as the least squares objective function. Table 7.2 contains the near optimal parameters.

Table 7.1 Initial values of state variables for glucose and oxygen induction of glucose oxidase

State variable	Unit	Initial 100 gl^{-1} value
Biomass	(gl^{-1})	0.1651
Extracellular glucose	(M)	0.556
Intracellular glucose	(M)	0.2 E-3
Glucose repressor	(mole g^{-1}_{cell})	0.10
Oxygen repressor	(mole g^{-1}_{cell})	1 E-3
Glucose repressor complex	(mole g^{-1}_{cell})	1 E-8 ≡ 0
Oxygen repressor complex	(mole g^{-1}_{cell})	0
m-RNA	(mole g^{-1}_{cell})	0
Intracellular glucose oxidase	(U ml^{-1} g^{-1})	0
Extracellular glucose oxidase	(U ml^{-1})	0
Gluconic acid	(M)	0
Dissolved oxygen	(ppm)	7.7
Time	(h)	0

The model has been shown to predict the production of glucose oxidase and gluconic acid in the *A.niger* system based on glucose induction alone. The profiles for glucose oxidase induction by the extended model based on both glucose and oxygen induction are shown in Figures 7.1 to 7.3. At the 0.21 atm and 0.75 atm oxygen levels, the experiments at an initial glucose concentration of 50 and 100 gl^{-1} are modelled satisfactorily.

Table 7.2 Near optimal parameters used in glucose and oxygen glucose oxidase model

Parameter	Symbol	Near optimal value	Units
Glucose mass transport coefficient	U_s	50	h^{-1}
Glucose Michaelis-Menten saturation value	G_g	1 E-3	Mg^{-1}
Glucose Michaelis-Menten rate	Ks_g	0.0965	Mg^{-1}
Repressor + glucose formation rate	k_1	14300	$gh^{-1}M^{-1}$
Glucose repressor glucose destruction rate	k_2	0.37	h^{-1}
Glucose repressor threshold level	Rg_{gcrit}	2.1 E-4	Mg^{-1}
Oxygen + repressor formation rate	k_6	1.69	h^{-1}
Oxygen repressor destruction rate	k_7	0.245	h^{-1}
Oxygen repressor threshold level	Ro_{2crit}	0.076	Mg^{-1}
mRNA natural destruction rate	k_4	0.018	h^{-1}
mRNA induction rate	k_3	1.6 E-4	h^{-1}
glucose oxidase formation rate	k_5	5600	$UM^{-1}h^{-1}$
mass transfer coefficient	k_la	450	h^{-1}
Logistic biomass growth rate	μ_{max}	0.231	h^{-1}
Maximum cell mass	X_{max}	2.624	gl^{-1}

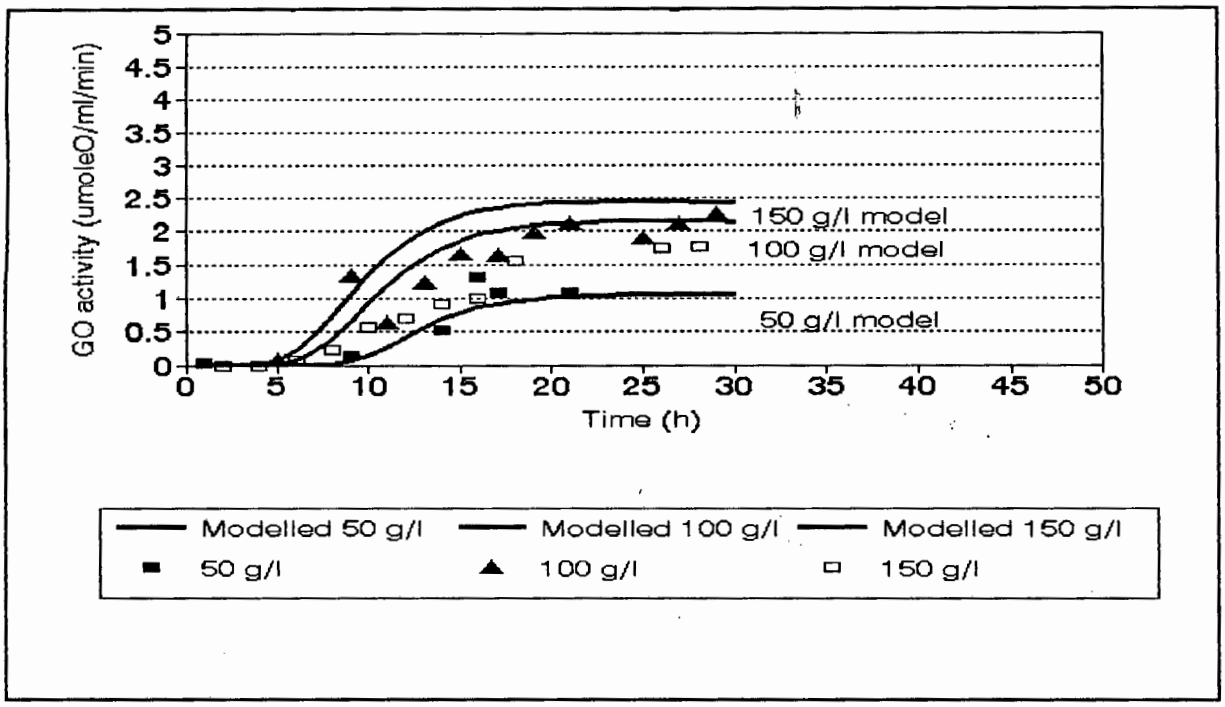

Figure 7.1 Comparison of predicted glucose oxidase and measured levels in 0.21 atm oxygen experiments

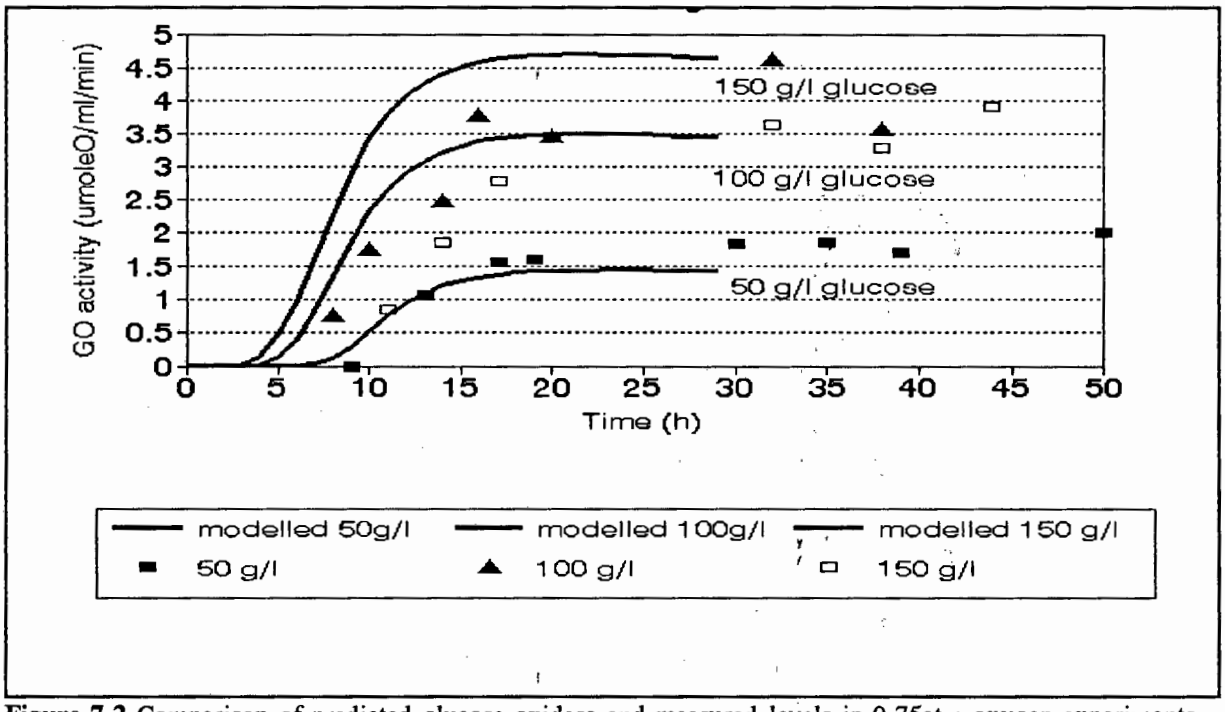

Figure 7.2 Comparison of predicted glucose oxidase and measured levels in 0.75atm oxygen experiments

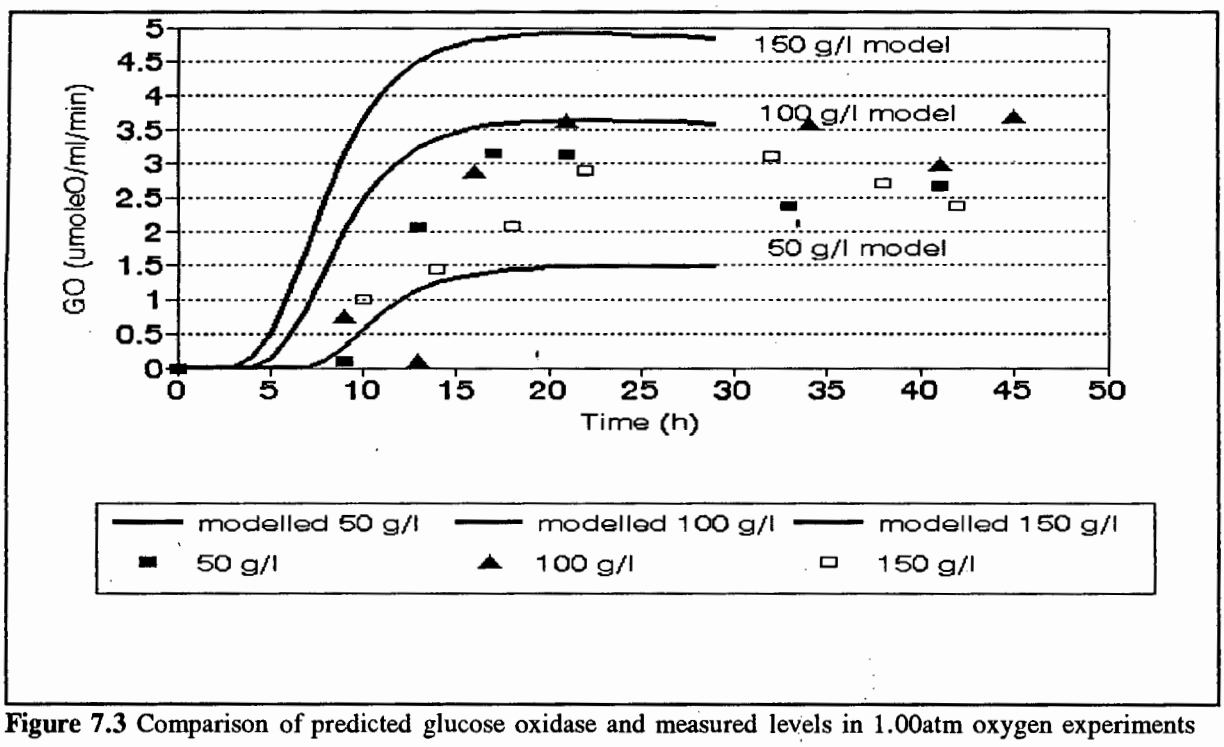

Figure 7.3 Comparison of predicted glucose oxidase and measured levels in 1.00atm oxygen experiments

The extended model over-predicts the glucose oxidase profiles resulting from an initial glucose concentration of 150 gl^{-1} at all three oxygen levels as did the model in Section 6.4.2. The decrease in production of glucose oxidase can again be accounted for by a decrease in mRNA production rate hypothesised to be associated with an osmotic stress reaction or regulation. A decrease in the mRNA activity to 73% of its original activity was used in the modified model. The prediction of glucose oxidase induction resulting from the modified model are shown in Figures 7.4 to 7.6. The glucose oxidase induction is modelled satisfactorily under atmospheric oxygen conditions and at 0.75 atm oxygen over the 50 to 150 gl^{-1} glucose range using the mRNA modification at high glucose concentration. In experiments carried out at 0.75 atm oxygen, the 100 gl^{-1} glucose experiment is under-predicted. This could be due to unmodelled factors of oxygen effects on glucose oxidase induction or inaccuracies in the optimisation of parameters to predict on increasing oxygen levels. In experiments conducted at 1.00 atm oxygen, glucose oxidase profiles are only modelled satisfactorily at initial concentrations of 100 and 150 gl^{-1} glucose. The 50 gl^{-1} glucose experiment is greatly under-predicted. The model will predict a spread in glucose oxidase activity with varying glucose level at a constant oxygen level. This is due to the length of time that the culture is in the induced state owing to the presence of glucose and oxygen. The induction window of glucose oxidase increases with increasing glucose

concentration as does the time to convert all the glucose

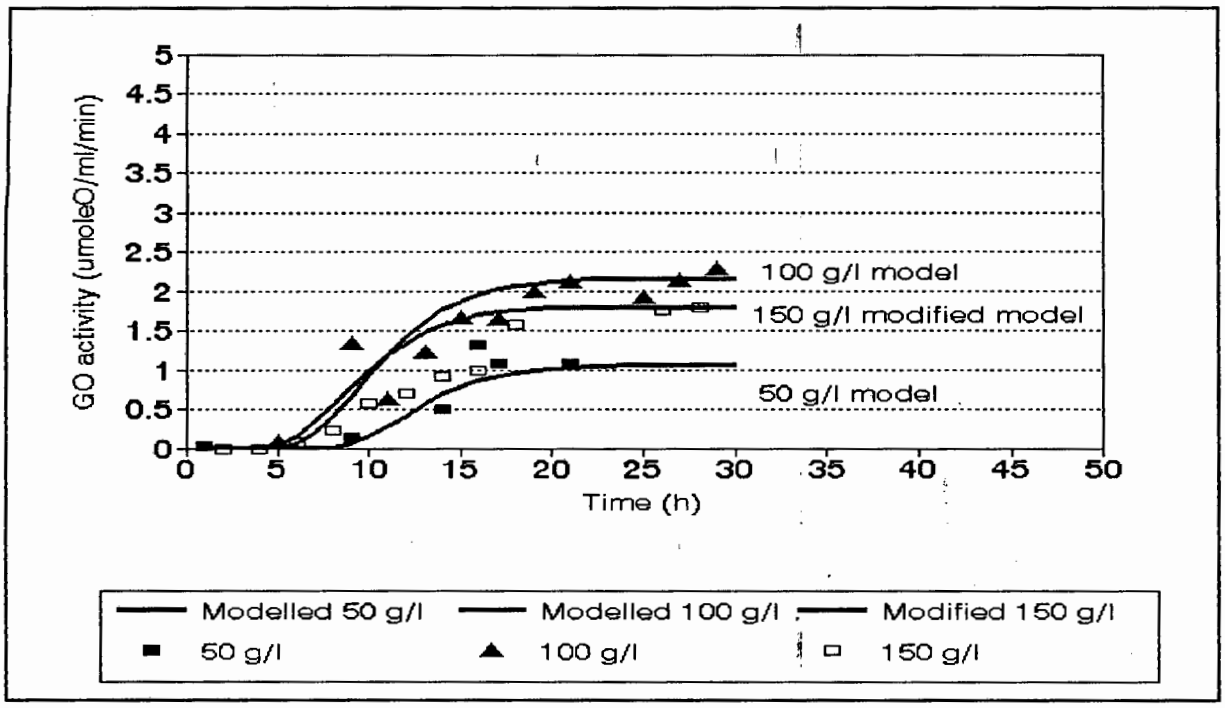

Figure 7.4 Comparison of glucose oxidase profile with modified model at 0.21 atm oxygen

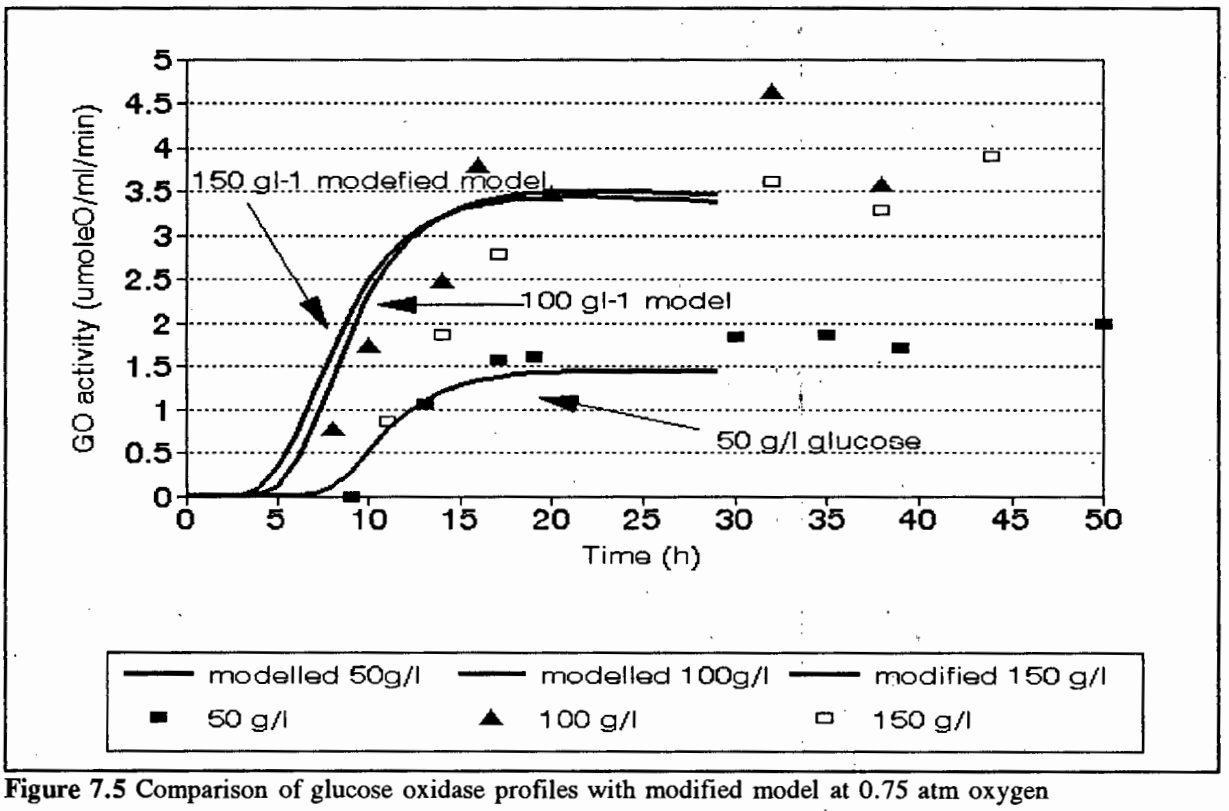

Figure 7.5 Comparison of glucose oxidase profiles with modified model at 0.75 atm oxygen

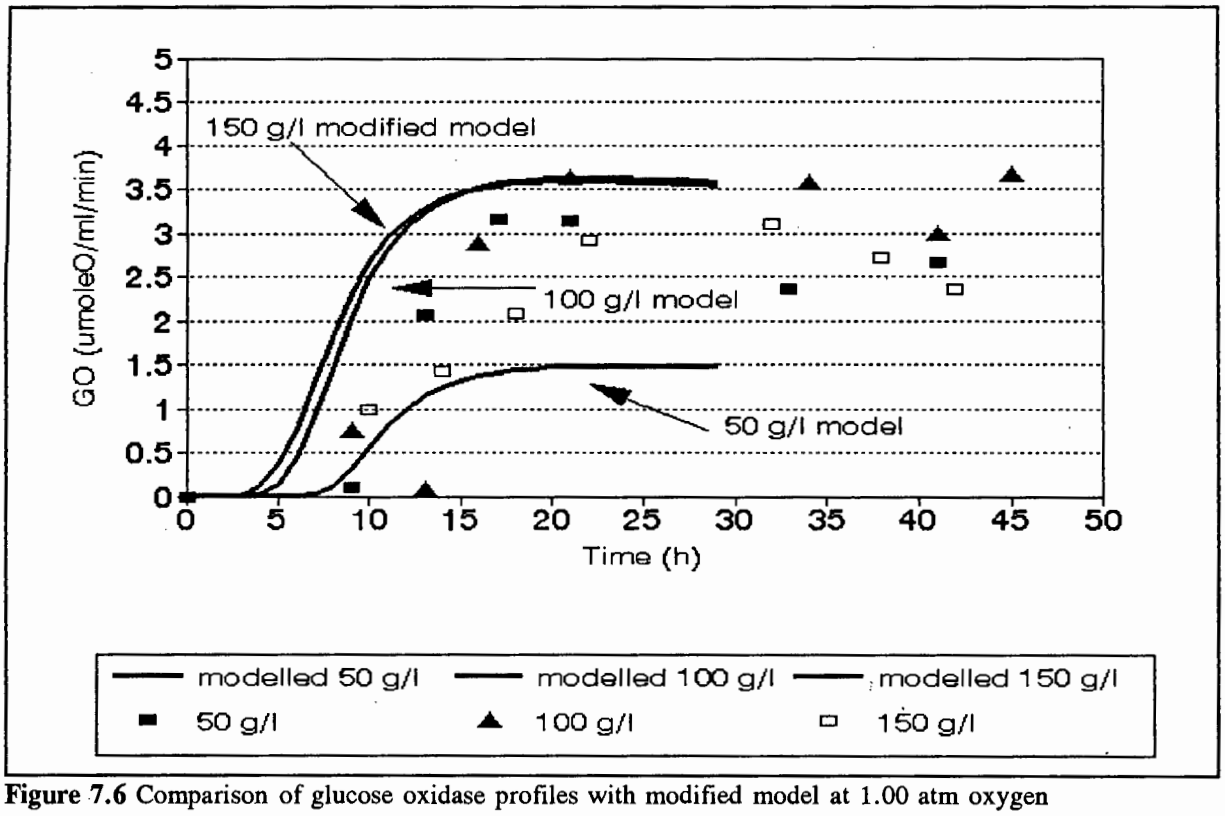

Figure 7.6 Comparison of glucose oxidase profiles with modified model at 1.00 atm oxygen

In prediction of the sodium hydroxide profile at 0.75 atm and 1.0 atm oxygen conditions using the model fitted at atmospheric experiments it became apparent that the rate of production of gluconic acid predicted by the model was much higher than the observed rates (Figures 7.7 to 7.9.). Figure 7.10 shows that rate of gluconic acid formation is only increasing at the same rate as the maximum glucose oxidase activity with increasing oxygen level. The rate of gluconate formation should be increased by two factors: firstly, the increased activity of the glucose oxidase and secondly, the increase in rate determined by the enzyme kinetics dependence on oxygen concentration. This indicates that the oxidation reaction is proceeding optimally. It is suggested that at the higher oxidation rates diffusion within the mycelial pellets may become dominant. There are three different components that may be diffusion-limited in the oxidation of glucose to gluconic acid: glucose, oxygen or hydroxyl ions. Glucose does not appear to be diffusion-limiting as the rates predicted by the model at elevated glucose levels are correct. Oxygen diffusion in *A.niger* pellets has been modelled by Kobayashi *et al.* (1973). Calculations based on their model (Appendix H) show that the diffusion resistance with respect to oxygen decreases with increasing dissolved oxygen concentration even with the inflated oxygen flux. Thus the transport of hydroxyl ions may be limiting the hydrolysis of glucono-δ-lactone to sodium gluconate.

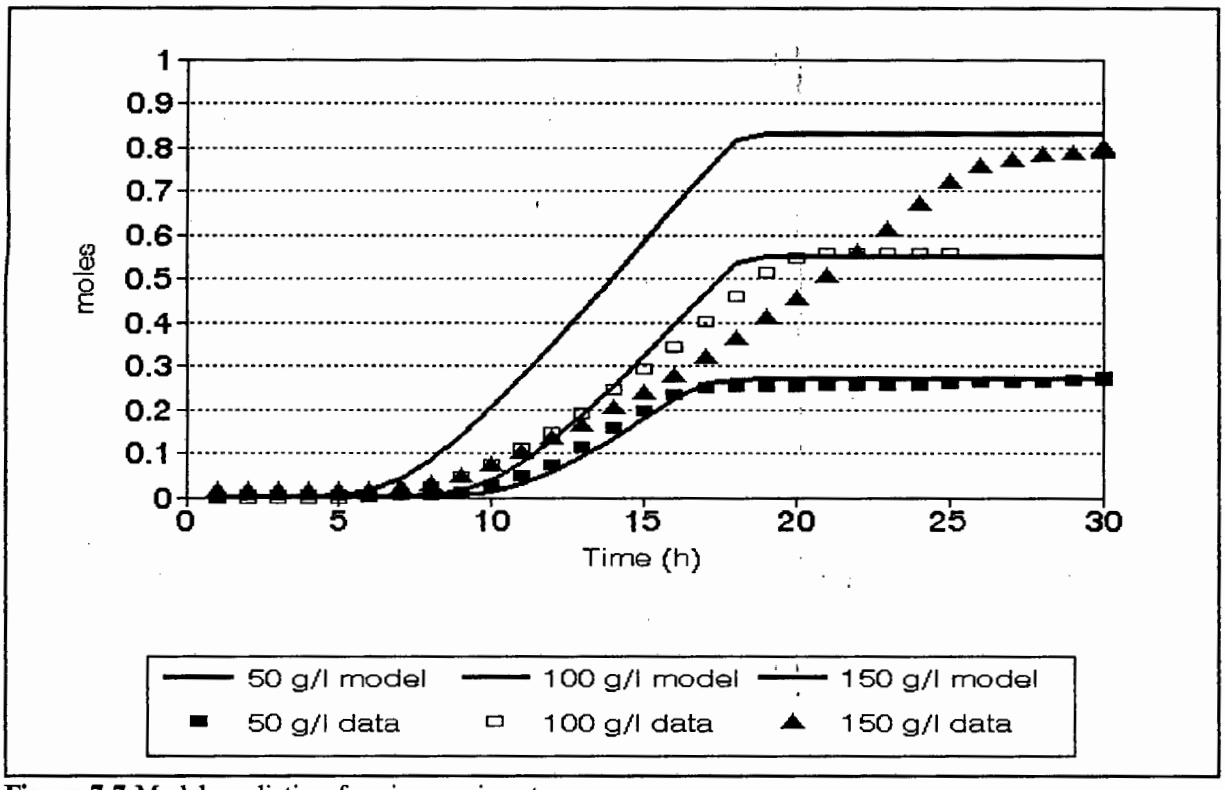

Figure 7.7 Model prediction for air experiments

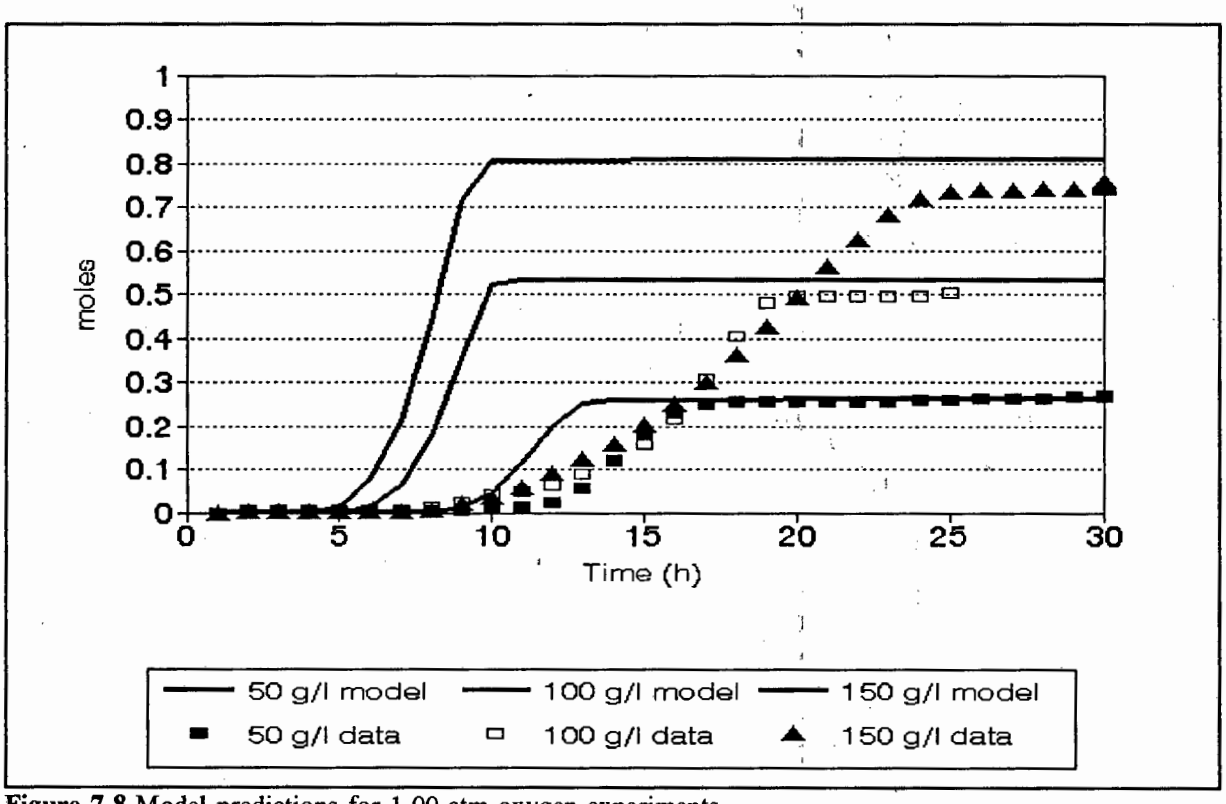

Figure 7.8 Model predictions for 1.00 atm oxygen experiments

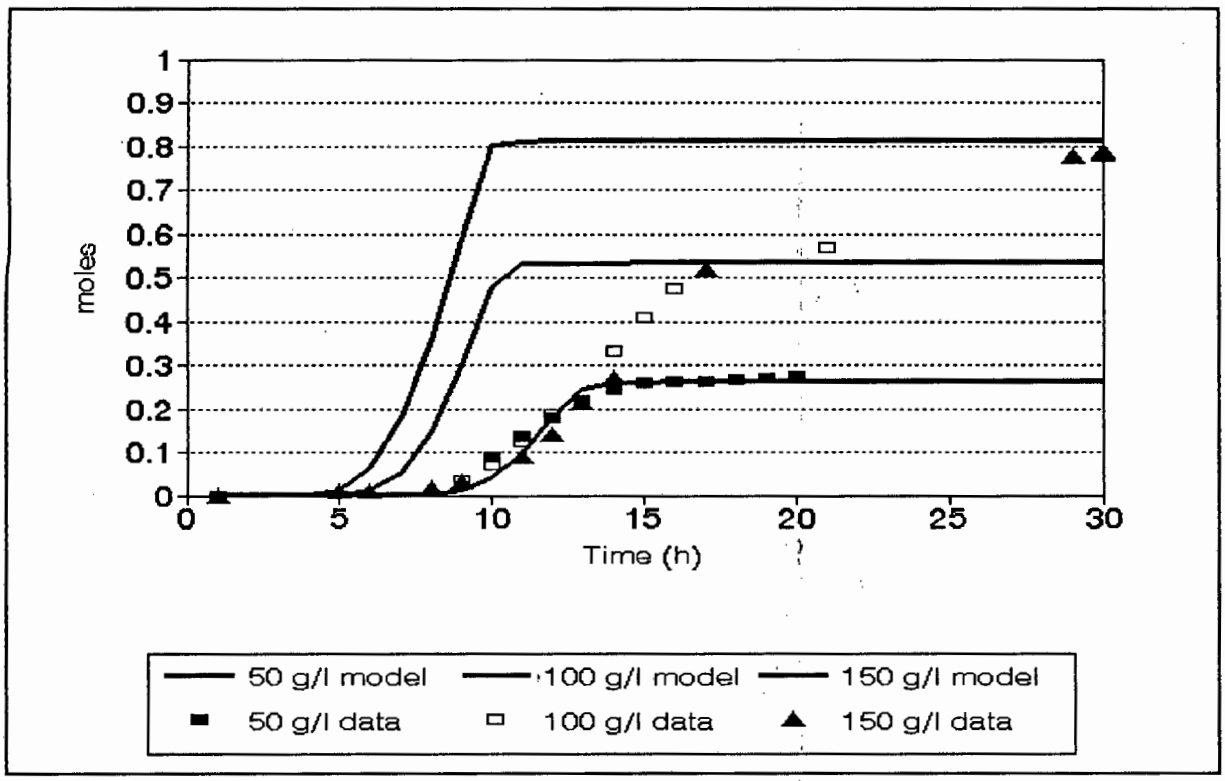

Figure 7.9 Model predictions for 0.75 atm fermentation

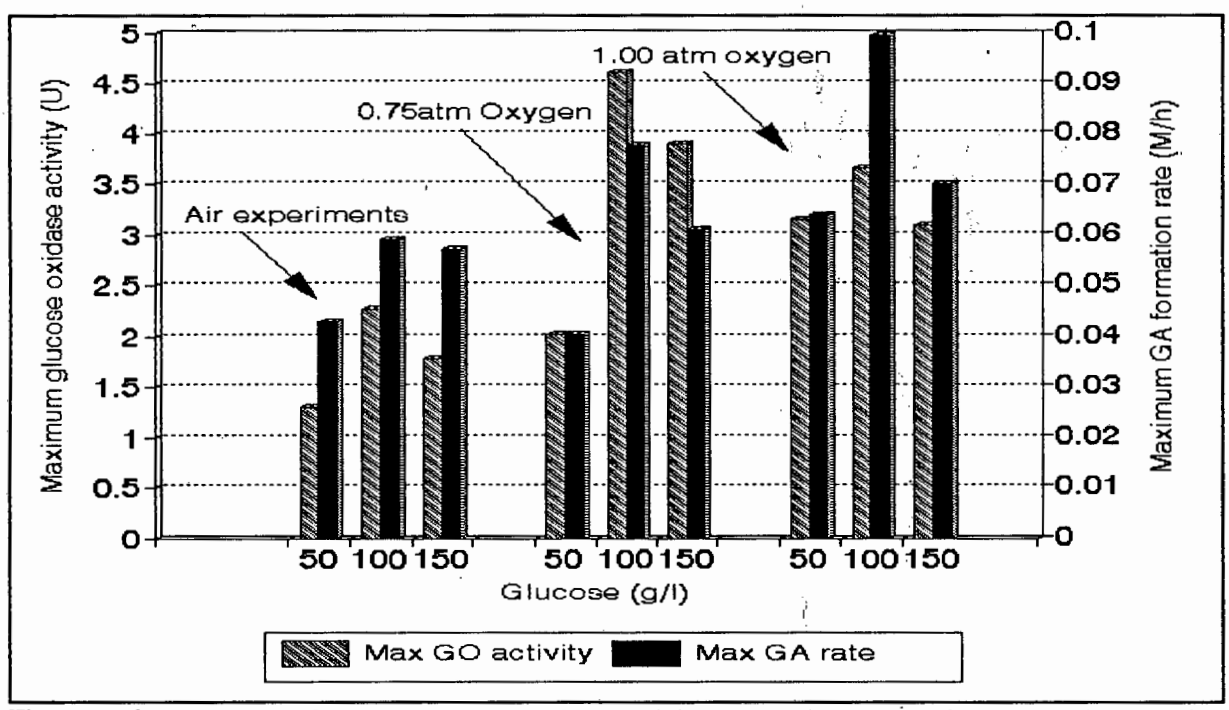

Figure 7.10 Comparison of maximum glucose oxidase activity and maximum rate of gluconic acid formation

7.4 Limitations of the extended model

The model proposes a simple positive glucose and oxygen interaction on the glucose oxidase induction kinetics. The model has an in built saturation level for glucose oxidase induction; hence a continued increase of glucose and oxygen concentration does not result in a continued increase in the rate and extent of the glucose oxidase production.

The following specific limitations are highlighted:

a) The effect of glucose on the level of glucose oxidase induced

Increasing the level of glucose at a constant oxygen level will always cause an increase the final level of glucose oxidase induced as predicted by the model. This is because the presence of both glucose and oxygen required for an inducing environment will always last longer with increased glucose level.

b) Diffusion limitation with microbial pellets

The pelleted nature of the system is not explicit in the model. Thus once diffusion resistances within the pellet become dominating, the model over predicts the rate of gluconic acid production. To account for diffusion within the pellet, concentration profiles of oxygen, glucose and pH as a function of pellet radius are required.

c) Effect of morphology on the model

The model was developed for a pelleted morphology which is reaction rate limited and not diffusion rate limited. Variation of experimental conditions to result in larger pellets will require the inclusion of a diffusion limitation within the pellet. Should a filamentous morphology be used, mass transfer parameters must be modified.

d) The model breaks down above 0.75 atm oxygen.

The model over-predicts the glucose oxidase induced above 0.75 atm oxygen. *A.niger* may experience oxygen toxicity at the elevated oxygen levels that inhibit the glucose oxidase production.

7.5 Conclusions

1. The gene operon model can be extended to include two inducers, glucose and oxygen. This was demonstrated by using two independent repressors for glucose and oxygen respectively and two specific repressor binding sites in series on the operator. Induction of the mRNA was proportional to the probability of both repressor binding sites being free at any one time.

2. Positive interaction was achieved with the extended model between the oxygen and glucose effect on glucose oxidase induction.

3. The model parameters were fitted to a base case experiment at 100 gl^{-1} glucose at 0.21 atm oxygen. The parameters were then used to predict the glucose oxidase and gluconic acid profiles at varying glucose and oxygen concentrations. The glucose oxidase produced using an initial glucose concentrations of 50 and 100 gl^{-1} at 0.21 and 0.75 atm oxygen were predicted satisfactorily.

3. At all oxygen concentrations, initial glucose concentrations of 150 gl^{-1} predicted higher glucose oxidase activities than observed experimentally. The observed lower glucose oxidase activities were postulated to be caused by osmotic stress and corrected by a 73% decrease in mRNA activity.

4. At 1.00 atm oxygen the model over predicts the rate of glucose oxidase formation. The gluconic acid production rate is over-predicted due to diffusion limitation within the mycelial pellets.

5. The over-prediction of glucose oxidase induction at 1.00 atm oxygen may be caused by an oxygen toxic effect.

8. CONCLUSIONS

The main aim of this project was to determine the process factors involved in simultaneous production of glucose oxidase and gluconic acid using *Aspergillus niger* in submerged cultivation. From the results of the previous sections the following conclusions can be drawn:

Literature

1. The *A.niger* bioprocess contains two kinetic areas, the induction kinetics of glucose oxidase and the production kinetics of gluconic acid by the enzyme glucose oxidase. The second area is well understood and optimum conditions for the production of gluconic acid catalysed by glucose oxidase are pH 5.5, above 0.3M glucose and above a dissolved oxygen concentration of 40ppm oxygen.

2. Glucose oxidase induction is affected by pH, glucose and oxygen concentration. Optimum pH was found to be between 5 and 6 by Roukas and Harvey (1988). Quantitative descriptions of the effect of glucose and oxygen on the induction of glucose oxidase have not been found in literature.

Experimental results

1. Gluconic acid can be produced at a concentration of 149gl^{-1} from glucose with a 94% mole/mole yield. Glucose oxidase can be produced with a maximal activity of 4.6 U at a glucose concentration of 100 gl^{-1} and 0.75 atm oxygen.

2. The biomass formation was not affected by the glucose or oxygen concentration. The logistic equation was found to describe the biomass growth under nitrogen limitation. Typical growth rates ranged from 0.2 to 0.3 h^{-1}.

2. At the three levels of oxygen used, (0.21, 0.75 and 1.00 atm oxygen), the rate of glucose oxidase induction was increased with increasing glucose concentration from

50 to 100gl^{-1}. Further increase in glucose concentration to 150gl^{-1} resulted in no further increase in glucose oxidase formation rate. A maximum initial glucose oxidase induction rate of 0.34 U/h was achieved at an initial glucose concentration of 100gl^{-1} and 1.00 atm oxygen.

3. Increasing the oxygen concentration from 0.21 atm to 1.00 atm using an initial glucose concentration of 50gl^{-1} increased the glucose oxidase induction rate from 0.12 to 0.26 U/h. Similar increases were observed using initial glucose concentrations of 100gl^{-1} and 150gl^{-1}.

4. Final levels of glucose oxidase follow similar trends to the initial glucose oxidase induction rate. Increasing glucose concentration from 50 gl^{-1} to 100 gl^{-1} results in an increased glucose oxidase level at all three oxygen levels used, 1.4 U to 2.3 at 0.21 atm oxygen, 2.0 U to 4.6 U at 0.75 atm oxygen and 3.1 U to 3.6 U at 1.00 atm oxygen. Further increase in glucose concentration to 150 gl^{-1} results in no further increase in glucose oxidase level. Increasing the oxygen from 0.21 atm to 0.75 atm increases the glucose oxidase final level at all three glucose concentrations. Further increase in oxygen concentration to 1.00 atm oxygen results in a further increase in the 50 gl^{-1} case and no further increase in level in the 100 and 150 gl^{-1} case. A maximum glucose oxidase final activity of 4.6 U was found at a glucose concentration of 100 gl^{-1} and 0.75 atm oxygen.

5. For each concentration of glucose there is an optimum oxygen concentration for maximum production rate of glucose oxidase. The dissolved oxygen can be controlled to the optimum level for corresponding glucose concentrations as the bioreaction proceeds.

Bioprocess model

1. The *A.niger* bioprocess system can be modelled mechanistically. Plant control and planning strategies can be developed on the model before implementation. The

model is based on simple species balances incorporating models of the mechanisms of subprocesses. The subprocesses included are:

Oxygen transfer using the two film theory.
Gluconic acid production using glucose oxidase enzyme kinetics.
Biomass growth using logistic equation.
Glucose oxidase induction using gene operon model.
Active glucose transport into cell.

2. The effect of glucose on glucose oxidase induction can be modelled using a single glucose repressor in the gene operon model. Prediction in the 50 to 100 gl^{-1} glucose range was satisfactory. Prediction of 150 gl^{-1} glucose experiment resulted in over-prediction of glucose oxidase which was postulated to be caused by an osmotic stress response at high glucose concentration. The effect could be modelled satisfactorily by decreasing the mRNA production rate.

3. The combined effect of glucose and oxygen on the induction of glucose oxidase could be modelled by including 2 specific repressors for glucose and oxygen. The bioprocess system could still be modelled satisfactorily and prediction of glucose oxidase activities in the 0.21 atm to 0.75 atm oxygen range over 50 to 150 gl^{-1} glucose including the osmotic effect modification were satisfactory. Gluconic acid production rates at 0.75 atm oxygen were over-predicted. This was attributed to an inhibition caused by diffusion limitations within the mycelial pellets at high conversion rates.

Prediction into the 1.00 atm oxygen range resulted in over-prediction of glucose oxidase levels and over-predicted gluconic acid production rates. The low glucose oxidase levels were attributed to an oxygen toxicity effect and the low gluconic acid formation rates to diffusion resistances in the mycelial pellets.

4. The model has several limitations:

a) The model does not take into account the decreased glucose oxidase induction rate observed at glucose concentrations above 100 gl^{-1}. An osmotic response has been proposed to be initiated above this concentration.

b) Oxygen concentrations above 0.75 atm oxygen appear to cause a reduced glucose oxidase induction rate. The mechanism is unknown but it has been hypothesised that oxygen toxicity may occur.

c) Diffusion within the mycelial pellets is not taken into account. Diffusion limitation occurs at high glucose oxidase activities causing a reduction in the gluconate formation rate.

5. Optimisation of pellet diameter and level of filamentous growth needs to be investigated to provide a balance between adequate oxygen transfer within the pellets and acceptable bulk oxygen transfer.

9. REFERENCES

Anderson, J.G., Blain, J.A., Drivers, M. and Todd, J.R., (1980), "Use of the disc fermenter to examine production of citric acid by *Aspergillus niger*", *Biotechnol. Lett.*, **2**, 99-104.

Aspinall, D., and Paleg, L.G., (1981), In "*Physiology and Biochemistry of Drought Resistance in Plants*", Eds., Paleg, L.G and Aspinall, D., Academic Press, New York, 205-241.

Atkinson, B. and Lester, D.E., (1974), "An enzyme rate equation for the overall rate of reaction of gel-immobilized glucose oxidase particles under buffered conditions. I. Pseudo-one substrate conditions", *Biotechnol. Bioeng.*, **16**, 1299-320.

Baig, M.A., (1987), "Calcium gluconate fermentation of maize gur (hydrol) in stirred 50l. fermenter", *Pakistan J. Sci. Ind. Res.*, **30**, 942-4.

Blom, R.H., Pfeifer, V.F., Moyer, A.J., Traufler, D.H, and Conway, H.F., (1952), "Sodium gluconate production fermentation with *Aspergillus niger*", *Ind. Eng. Chem.*, **44**, 435-40.

Bright, H.J. and Appleby, M., (1969), "The pH dependence of the individual steps in the glucose oxidase reaction", *J. Biol. Chem.*, **244**, 3625-34.

Bright, H.J. and Gibson, Q.H., (1969), "The oxidation of 1-deuterated glucose by glucose oxidase", *J. Biol. Chem.*, **242**, 994-1003.

Carroad, P.A. and Wilke, C.R., (1977), "Studies of lignin-degrading fungi and enzymatic delignification of cellulose materials", *Appl. Environ. Microbiol.*, **33**, 871.

Clark, D.S., Ito, K., Horitsu, H., (1966), "Effect of manganese and other heavy metals on submerged citric acid fermentation of molasses", *Biotechnol. Bioeng.*, **8**, 465-71.

Cochrane, V.W., (1976), "Glycolysis", In "*The Filamentous Fungi*", eds. J.E. Smith, D.R. Berry, Academic Press, London, 65-92.

Cohen, G.N., Monod, J., (1957), "Bacterial permiases", *Bacter. Rev.*, **21**, 169-194.

Csonka, L.N., (1989), "Physiological and genetic responses of bacteria to osmotic stress", *Microbiol. Rev.*, **53**, 121-147.

Csonka, L.N., Hanson, A.D., (1991), "Prokaryotic osmoregulation: genetics and physiology", *Ann. Rev. Microbiol.*, **45**, 569-606.

Davis, L.L and Baudoin, A.B.A.M, (1986), "Effect of osmotic potential on *Geotrichum candidum*: growth, polygalacturonase production, and polygalacturonase action", *Physiol. Mol. Plant Pathol.*, **28**, 53-60.

Davis, L.L. and Baudoin, A.B.A.M., (1987), "Effect of osmotic potential on synthesis and secretion of polygalacturonase and cellulase by *Geotrichum candidum*", *Can. J. Microbiol.*, **33**, 138-141.

De Baetselier A, Dohet P., De Beukelaer M., Ha-Thi V., Hanotier J., Frederick K., Rosenberg S. and Vasavada, A., (1992), "A new production method for glucose oxidase", *J. Biotechnol.*, **24**, 141-148.

Doeppner, T., and Hartmeier, W., (1984), "Glucose oxidation by modified mould mycelium", *Starch*, **36**, 284-7.

Edgley, M. and Brown, A.D., (1978), "Response of xerotolerant and non-tolerant yeasts to water stress", *J. Gen. Microbiol.*, **104**, 343-345.

Edgley, M. and Brown, A.D., (1983), "Yeast water relations: Physiological changes induced by solute stress in *Saccharomyces cerevisiae* and *Saccharomyces rouxii*", *J. Gen. Microbiol.*, **129**, 3453-3463.

Elnaughy, M.A. and Megalla, S.E., (1975), "Gluconic acid production by *Penicillium puberulum*", *Folia Microbiol.*, **20**, 504-8.

Fiedurek, J., Rogalski, J. and Ilczuk, Z., (1990), "Investigation of glucose oxidase synthesis with *Aspergillus niger* by way of multistage mutagenisation", *Acta Biotechnol.*, **10**, 371-376.

Fiedurek, J., Rogalski, J., Ilczuk, Z., and Leonowicz, A., (1986), "Screening and mutagenis of molds for improvement of glucose oxidase production", *Enzyme Microb. Technol.*, **8**, 734-6.

Frank, W., Eichhorn, G., Mochel, L., Bertram, L., (1963), "Zur Kenntnis der sogenannten Glucose-oxidase. V. Zur Physiologie und Enzymatik der Gluconsaure-Garung durch *Aspergillus niger*", *Arch Microbiol.*, **46**, 96-116.

Frederick, K.R., Tung, J., Emerick, R.S., Masiarz, F.R., Chamberlain, S.H., Vasavada, A. and Roseberg, S., (1990), "Glucose oxidase from *Aspergillus niger*", *J. Biol. Chem.*, **265**, 3793-3802.

Gervais, P., Marechal, P.A. and Molin P., (1992), "Effects of the kinetic of osmotic pressure variation on yeast viability", *Biotech. Bioeng.*, **40**, 1435-1439.

Gibson, Q.H., Swoboda, B.E.P. and Massey, V., (1964), "Kinetics and mechanism of action of glucose oxidase", *J. Biol. Chem.*, **239**, 3927-34.

Gbewonyo, K. and Wang, D.I.C., (1983), "Enhanced gas-liquid mass transfer rates in non-newtonian fermentations by confining mycelial growth to microbeads in a bubble column", *Biotechnol. Bioeng.*, **25**, 2873-87.

Kirk-Othmer, (1984), "Encyclopedia of Chemical Technology", John Wiley, New York, **14**, 596.

Kisser, M., Kubicek, C.P. and Rohr, M., (1980), "Influence of manganese on morphology and cell wall composition of *Aspergillus niger* during citric acid fermentation", *Arch. Microbiol.*, **128**, 26-33.

Koga, S., Burg, C.R. and Humphrey, A.E., (1967), "Computer simulation of fermentations systems", *Appl. Microbiol.*, **15**, 683-689.

Konig, B., Schugerl, K. and Seewald, (1982), "Strategies for penicillin fermentation in tower-loop reactors", *Biotechnol. Bioeng.*, **24**, 259-280.

Hatzinikolaou D.G., Macris B.J., (1995), "Factors regulating production of glucose oxidase by *Aspergillus niger*", *Enzyme Microb. Technol.*, **17**, 530-534.

Hayashi, S. and Nakamura, S., (1981), "Multiple forms of glucose oxidase EC 1.1.3.4. with different carbohydrate composition", *Biochim Biophys. Acta.*, **657**, 40-51.

Heck, J. and Onken, U., (1987), "Hysteresis effects in suspended solid particles in bubble columns with and without draft tube", *Chem. Ing. Tech.*, **24**, 259-80.

Heinrich, M. and Rehm, H.J., (1982), "Formation of gluconic acid at low pH-values by free and immobilized *Aspergillus niger* cells during citric acid fermentation", *Eur. J. Appl. Microbiol. Biotechnol.*, **15**, 88-92.

Huggett, A.S.Y. and Nixon, D.A,. ,(1957), "Use of glucose oxidase, peroxidase and o-dianisidine in determination of blood and urine glucose", *Lancet*, **273**, 368.

Imanaka T., Kaieda T., Sato K., Taguchi H., (1972), "Optimisation of α-galactosidase production by mold I", *J. Ferment. Technol.*, **50**, 633-646.

Imanaka T., Kaieda T., Taguchi H., (1973), "Unsteady-state analysis of a kinetic model for cell growth and α-galactosidase production in mold", *J.Ferment. Technol.*, **51**, 423-430.

Imanaka T., Kaieda T., Taguchi H., (1973), "Optimisation of α-galactosidase production in multi-stage continuous culture of mold.", *J. Ferment. Technol.*, 1973, **51**, 431-439.

Ishimori, Y., Karube, I. and Suzuki, S., (1982), "Continuous production of glucose oxidase with *Aspergillus niger* under ultrasound waves", *Enzyme Microb. Technol.*, **4**, 85-8.

Jacob F. and Monod J., ,(1956), "Genetic regulatory mechanisms in the synthesis of proteins", *J. Mol. Biol.*, **3**,318-358.

James, T.L., Edmondson, D.E., Husain, M., (1981), "Glucose oxidase contains a di-distributed phosphorous residue. Phosphorous-31 NMR studies of the flavine and nonflavine phosphate residues", *Biochem.*, **20**, 617-21.

Jung, K.H., Kim, J.J., Jeon, J. and Lee, J.H., (1993), "Production of high fructo-oligosaccharide syrup with two enzyme system of fructosyltransferase and glucose oxidase", *Biotechnol. Lett.*, **15**, 65-70.

Kisser, M., Kubicek, C.P. and Rohr, M., (1980), "Influence of manganese on morphology and cell wall composition of *Aspergillus niger* during citric acid fermentation", *Arch. Microbiol.*, **128**, 26-33.

Kobayashi, T., Van Dedem, G. and Moo Young, M., (1973), "Oxygen transfer into mycelial pellets", *Biotechnol. Bioeng.*, **15**, 27-45.

Lakshminarayana, K., Modi, V.V. and Shah, V.K., (1969), "Studies on gluconate metabolism in *Aspergillus niger*", *Arch. Mikrobiol.*, **66**, 396-405.

Lee, H.W., Sato, S., Mukataka, S. and Takahashi, J., (1987), "Studies on the production of gluconic acid by *Aspergillus niger* under high dissolved oxygen concentration", *Hakkokogaku*, **65**, 501-6

Lloyd, J.B. and Whelan, W.J., (1969), "Enzymatic determination of glucose in the presence of maltose", *Anal Biochem.*, **30**, 467.

Lockwood, L. B., (1975), "Organic acid production", In "*The Filamentous Fungi: Industrial mycology*", eds. Smith, J.E., Berry,D.R., Edward Ardon, London, **1**, pp. 140-157.

Markwell, J., Frakes, L.G., Brott, E.C., Osterman, J., and Wagner, F.W., (1989), "*Aspergillus niger* mutants with increased glucose oxidase production", *Appl. Microbiol. Biotechnol.*, **30**, 166-9.

Mattey, M., (1992), "The production of organic acids", *Critical Reviews in Biotechnol.*, **12**, 86-132.

Mischak, H., Kubicek, C.P., and Rohr, M., (1985), "Formation and location of glucose oxidase in citric acid producing mycelia of *Aspergillus niger*", *Appl. Microbiol. Biotechnol.*, **21**, 27-31.

Miura, Y., Tsuchiya, K., Tsusho, H. and Miyamoto, K., (1970), "Kinetic studies of gluconic acid fermentation using *Aspergillus niger*", *J. Ferment. Technol.*, **48**, 795-803.

Moo-Young, M., (1985), "Comprehensive Biotechnology: the principles, applications and regulations of biotechnologt in industry, agriculture and medcine", Pergamon Press, Oxford, **3**, 681-699.

Moresi, M., Parente, E. and Mazzatura, A., (1991), "Effect of dissolved oxygen concentration on repeated production of gluconic acid by immobilized mycelia of *Aspergillus niger*", *Appl. Microbiol. Biotechnol.*, **36**, 320-3.

Muller, H.M., (1985), "Utilization of gluconate by *Aspergillus niger*. I Enzymes of phosphorylating and non-phosphorylating pathways", *Zbl. Mikrobiol.*, **140**, 475-84.

Muller, H.M., (1986a),"Gluconate accumulation and enzyme activities with extremely nitrogen limited surface cultures of *Aspergillus niger*", *Arch. Microbiol.*, **144**, 151-7.

Muller, H.M., (1986b), "Utilization of gluconate by *Aspergillus niger*. II Enzymes of degradation pathways and main end products", *Zentralbl. Mikrobiol.*, **141**, 461-9.

Munk, V., Paskova, I and Hanus, J., (1963), "Factors influencing glucose oxidase activity in submerged cultivation of *Aspergillus niger*", *Folia Microbiol.*, **3**, 203.

Nakamatsu, T., Akamatsu, T. and Miyajima, R., (1975), "Microbial production of glucose oxidase", *Agr. Biol. Chem.*, **39**, 1803-11.

Omken, U. and Weiland, P., (1983), "Airlift fermenters: construction, behaviour and uses" In *Advanced Biotechnology Processes*, Hizraki,A., von Wezel, A.L. and Liss, A.R. (ed.)I.Alan R.Liss Inc., New York.

Oosterhuis, N.M.G., Groesbeek, N.M., Olivier, A.P.C. and Kossen, N.W.F., (1983), "Scale-down aspects of gluconic acid fermentation", *Biotechnol. Lett.*, **5**, 141-6.

Pace, G.W., (1980), "Rheology of mycelial fermentation broths", in *Biotechnology*, eds. Smith, J.E., Berry, D.R. and Kristiansen, B., Academic Press, London, 95-110.

Pazur, J.H., Kleppe, K. and Cepure, A., (1965), "A glycoprotein structure for glucose oxidase from *Aspergillus niger*", *Arch. Biochem. Biophys.*, **111**, 351-7.

Press, W.H., Flannery, B.P., Teukolsky, S.A and Vetterling, W.T., (1986), In "*Numerical recipes*", Cambridge University Press, Cambridge.

Prior, B.A. and Kenyon, C.P., (1980), "Water relations of glucose-catabolizing enzymes in Pseudomonas fluoresens", *J. Appl. Bacteriol.*, **48**, 211-222.

Quadeer, M.A., Baig, M.A. and Yubus, O., (1975), "Production of calcium gluconate by *Aspergillus niger* in 50-L fermenter", *Pakistan J. Sci. Ind. Res.*, **18**, 227-8.

Richter, G., (1983), "Glucose oxidase", In "*Industrial Enzymology*", eds. Godfry, T. and Reiche, J., The Nature Press, Bew York, **4**, 428-437.

Roels J.A., (1983), "Relaxation times and their relevance to the construction of kinetic models", In "*Energetics and Kinetics in Biotechnology*", Elsevier Biomedical Press, New York, **8**, 205-221.

Roels J.A., (1982), "Mathematical models and design of biochemical reactors", *J.Chem. Tech. Biotechnol.*, **32**, 59-72.

Rogalski, J., Fiedurek, J., Szczordrak, J.,Kapusta, K. and Leonowicz, A., (1988), "Optimization of glucose oxidase synthesis in submerged cultures of *Aspergillus niger* G-13 mutant", *Enzyme Microb. Technol.*, **10**, 508-11.

Roukas, T. and Harvey, T., (1988), "The effect of pH on production of citric and gluconic acid from beet molasses using continuous culture", *Biotechnol. Lett.*, **15**, 35-40.

Le Rudulier, D., Strom, A.R., Dandekar, A.M., Smith, L.T. and Valentine, R.C., (1984) "Molecular biology of osmoregulation", *Science*, **224**, 1064-1068.

Sakurai, H., Lee, H.W., Sato, S., Mukataka, S. and Takahashi, J., (1989), "Gluconic acid production at high concentrations by *Aspergillus niger* immobilized on a nonwoven fabric", *J. Ferment. Bioeng.*, **67**, 404-8.

Shah, D.N. and Kothari, R.M., (1993), "Glucose oxidase rich *Aspergillus niger* strain, cost effective protocol and an economical substrate for the preparation of tablet grade calcium gluconate", *Biotechnol. Lett.*, **15**, 35-40.

Takamatsu, T., Shioya, S. and Furuya, T., (1981), "Mathematical model of gluconic acid fermentation by *Aspergillus niger*", *J. Chem. Tech. Biotechnol.*, **31**, 697-704.

Tan, K.H., Ferguson, L.B. and Carlton, C., (1984), "Conversion of Cassava starch to biomass, carbohydrates and acids by *Aspergillus niger*", *J. Appl. Biochem.*, **6**, 80-90.

Tanner, R.D., Merk & Co., Inc., Rahway, N.J., (1970), "An enzyme kinetic model for describing fermentation processes", *Biotech. Bioeng.*, **12**, 831-843.

Traeger, M., Qazi, G.N., Onken U. and Chopra, C.L., (1989), "Comparison of airlift and stirred reactors for fermentation with *Aspergillus niger*", *J. Ferment. Bioeng.*, **68**, 112-6.

Traeger, M., Qazi, G.N., Onken, U. and Chopra, C.L., (1991), "Contribution of ante- and exocellular glucose oxidase to gluconic acid production at increased dissolved oxygen concentrations", *J. Chem. Tech. Biotechnol.*, **50**, 1-11.

Traeger, M., Qazi, G.N., Buse, R. and Onken, U., (1992), "Influence of constant and oscillating dissolved oxygen concentration on *Aspergillus niger*", *J. Ferment. and Bioeng.*, **74**, 282-7.

Vassilev, N.B, Vassileva, M.C and Spassova, D.I., (1993), "Production of gluconic acid by *Aspergillus niger* immobilized on polyurethane foam", *Appl. Microbiol. Biotechnol.*, **39**, 285-8.

Venugopal R. and Saville B.A, (1993), "The effect of oxygen upon the kinetics of glucose oxidase inactivation", *Can. J. Chem. Eng.*, **71**, 917-924.

Weiland, P., (1984), "Influence of draft tube diameter on operation behaviour of air loop reactors", *Ger. Chem. Eng.*, **7**, 374-85.

Witteveen, C.F.B., van de Vondervoort, P.J.I., van den Broeck H.C., van Engelenburg, F.A.C., de Graaff, L.F., Hillebrand, M.H.B.C., Schaap, P.J., Visser J., (1993), "Induction of glucose oxidase, catalase, and lactonase in *Aspergillus niger*", *Curr. Gen.*, **24**, 408-416.

Witteveen, C.F.B., van de Vondervoot, P., Swart, K. and Visser, J., (1990), "Glucose oxidase overproducing and negative mutants of *Aspergillus niger*", *Appl. Microbiol. Biotechnol.*, **33**, 683-6.

Witteveen, C.F.B., Veenhuis, M. and Visser, J., (1992), "Localisation of glucose oxidase and catalase activities in *Aspergillus niger*", *Appl. Environ. Microb.*, **58**, 1190-4.

APPENDIX A

GLUCOSE OXIDASE MEASUREMENT

Glucose oxidase activity is defined under the following controlled conditions to be 1 unit: pH 5.5, glucose in excess (0.5M), oxygen at 7.7ppm, oxygen consumption rate in the presence of peroxidase of 1μmole O_2 per ml per minute.

There are two main methods of measuring glucose oxidase activity. One method uses the coupled oxidative reaction of O-dianisidine with hydrogen peroxide (Muller 1986) and the other uses the oxygen utilisation rate method (Miura 1970). In each method the following operating conditions are controlled: temperature, glucose concentration, oxygen concentration and pH.

A.1 Oxygen utilisation method

Principle:

Glucose oxidase catalyses the reaction shown in equation A.1.

glucose oxidase reaction alone:

$$H_2O + glucose + O_2 \xrightarrow{GOD} gluconic\ acid + H_2O_2 \qquad \textbf{(A.1)}$$

When peroxidase is present, the hydrogen peroxide formed is broken down into molecular dissolved oxygen shown by equation A.2.

peroxidase reaction alone:

$$2\ H_2O_2 \xrightarrow{POD} H_2O + O_2 \qquad \textbf{(A.2)}$$

When glucose oxidase is combined with peroxidase as in the *A. niger* system (Wittiveen 1993) the overall reaction is shown in equation A.3.

overall reaction of glucose oxidase and peroxidase:

$$glucose + \frac{1}{2}O_2 \xrightarrow{GOD/POD} gluconic\ acid \qquad \textbf{(A.3)}$$

The oxygen consumption rate in the overall reaction under the controlled conditions refers to the equivalent glucose consumption rate and gluconic acid production rate. The μmolar glucose consumption rate per minute per ml of sample is the glucose oxidase activity.

Equipment

Magnetic stirrer

Yellow Springs dissolved oxygen probe fitted with groove and 'O' ring

Dissolved oxygen logging computer and software

125ml conical flask with custom made side port to fit the dissolved oxygen probe

Tightly fitting rubber stopper to fit the neck of the 125ml conical flask with 2 ports for the temperature probe and vent tube.

Thermometer

100ml conical flask

20 ml graduated pipette

Water bath and temperature controller

Chemicals

Solution A: 0.1M KH_2PO_4
0.5M glucose

Solution B: 0.1M K_2HPO_4
0.5M glucose

Method

In order to prepare a 0.5M glucose solution in a 0.1M phosphate buffer, pH 5.5, prepare solutions A and B in a 5:1 ratio based on volume. Place A in a large container on a magnetic stirrer with a pH probe immersed in it. Add solution B slowly allowing solution B to neutralise solution A to the desired pH (5.5). A pH of 5.5 is chosen for maximal glucose

oxidase activity.

The experimental apparatus is shown in Figure A-1. Place the 'O' ring onto the grove on the dissolved oxygen probe. Moisten the 'O' ring and slide the electrode into the glass-blown side arm of the 125ml conical flask. Clamp electrode so that the flask is centrally above the magnetic stirrer. Place the magnet in the flask and add 100ml of the buffered glucose solution pH (5.5). Turn on the stirrer at full speed and saturate the solution with oxygen (8.1ppm at 25°C). Turn the stirrer down to 25% of full speed and add a further 18ml of buffer (the stirrer speed should be such that the buffer is well stirred but not splashing out the flask). Allow any entrained bubbles to disengage before adding 5ml of glucose oxidase sample. Immediately stopper the flask ensuring that no air bubbles remain entrapped and a small amount of solution leaks from the stopper. This is achieved by pinching the rubber stopper while carefully inserting it into the flask. Start the dissolved oxygen data logging system and monitor the dissolved oxygen concentration for 200s.

Once complete remove the stopper and D.O. probe. Rinse the flask and probe in tap water and dry with paper towelling. Reassemble and repeat. Each sample should be analyzed in triplicate.

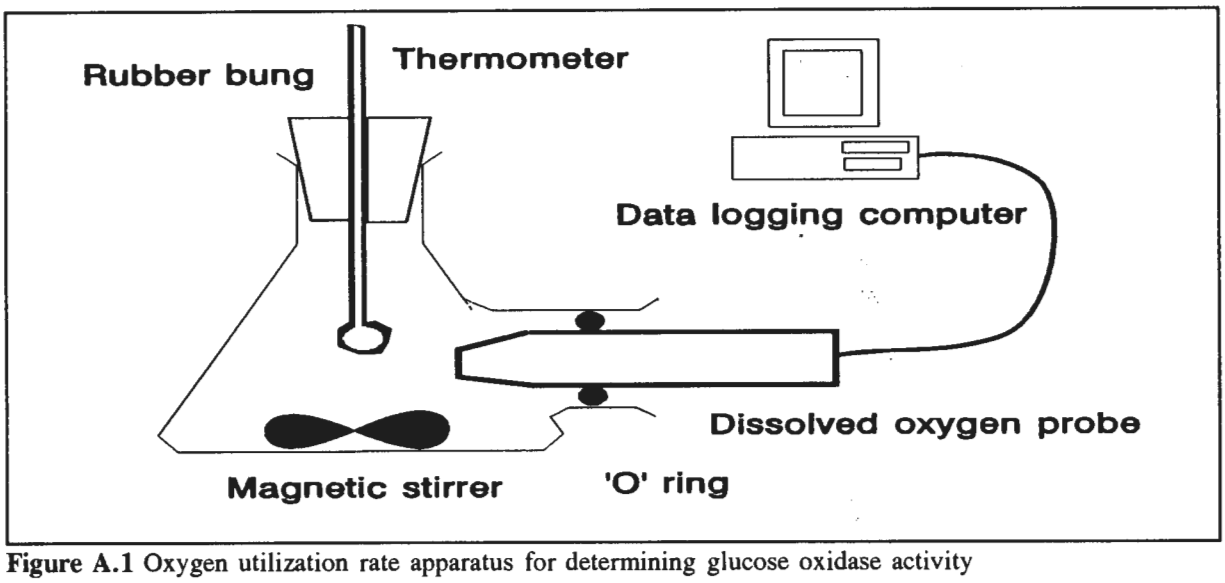

Figure A.1 Oxygen utilization rate apparatus for determining glucose oxidase activity

Once the data has been logged the profile can be regressed linearly. The slope represents the activity of the diluted sample in ppm/s. To convert this into glucose oxidase units, use

equation A.4.

$$G.O.activity \left[\frac{\mu mole\ glucose}{ml\ \min}\right] = slope[ppm/s] * dilution * 3.75 \qquad \textbf{(A.4)}$$

Typical results have a 5% error when diluted 1:120 and have a 2% error when dilute 1:24. Correlation coefficients on the linear regressions are in excess on 0.995.

Limitations and specificity

The oxygen utilisation method does not only measure the decrease in oxygen due to glucose oxidase activity but also any other oxygen utilisation. However the oxygen utilisation rate of *A.niger* from biomass formation and cell maintenance is small relative to the oxygen utilisation rate of the enzyme under the controlled conditions. Disrupted cells are used which have much lower oxygen utilisation rates than living cells.

The method assumes that peroxidase is induced at the same time as glucose oxidase. This has been shown to be true by Witteveen (1993).

The main advantage of the oxygen utilisation method over the o-dianisidine spectrophotometric method is that whole disrupted cells can be assayed. If filtered samples were used (as required by the o-dianisidine method), glucose oxidase activity associated with the membranes would not be measured.

A-2 O-dianisidine method

Principle:

The o-dianisidine method measures glucose oxidase activity by ensuring all hydrogen peroxide is broken down by peroxidase. The breakdown of hydrogen peroxide is coupled to the oxidation of o-dianisidine to a coloured complex, quinoneimine dye. The rate of increase in absorbance of the coloured complex shows the rate of breakdown of hydrogen peroxide and hence the activity of glucose oxidase. These reactions are shown in equations A.5 and A.6.

$$glucose + O_2 \xrightarrow{GOD} gluconic\ acid + H_2O_2 \quad \textbf{(A.5)}$$

$$H_2O_2 \xrightarrow{POD} H_2O + \frac{1}{2}O_2 \quad \textbf{(A.6)}$$

Chemicals

Solution A O-dianisidine dihydrochloride: 0.2ml of 6mg/ml solution added to 20ml of 0.1M pH7.0 phosphate buffer.

Solution B 10% (w/v) glucose in water.

Solution C 60ppg units/ml peroxidase in 0.1M pH 7.0 phosphate buffer.

Solution D 0.1M phosphate buffer pH 7.0.

Method

Pipette into glass tubes the solutions given in Table A.1.

Table A.1 Chemical volumes used in O-dianisidine assay method

	Blank (ml)	Sample (ml)
Solution A	1.20	1.2
Solution B	0.25	0.25
Solution C	0.05	0.05
0.1 M phosphate buffer	0.05	-
Sample	-	0.05

Mix solutions A,B and C and then add the sample or buffer. All samples should be run in triplicate. Incubate at 25°C for 5min and read the sample absorbance against the blank at 436nm every 5 minutes. To calculate the glucose oxidase activity, use equation A-7.

$$G.O.units = \frac{Absorbance}{Incubation\ time(\text{min})} \cdot 3.735 \cdot dilution\ factor \qquad \textbf{(A.7)}$$

Specificity and limitations

The method is extremely specific to glucose oxidase activity. However it cannot measure the activity of particulate suspensions as it is a spectrophotometric method. Reproducibility is also poor as the absorbance must be measured as a function of time. It was difficult to ensure the temperature remained at 30°C in the spectrophotometer and so samples were incubated in a water bath and withdrawn every 5 minutes to measure the absorbance.

APPENDIX B

COMPARISON OF CELL DISRUPTION METHODS

Overall aim:

In order to determine the best method of cell disruption of *A.niger* four methods of cell disruption were compared: the French Press, grinding of the biomass with Al_2O_3 in a waring blender, the high speed agitation of biomass with sand particles (bead mill) and ultrasonication.

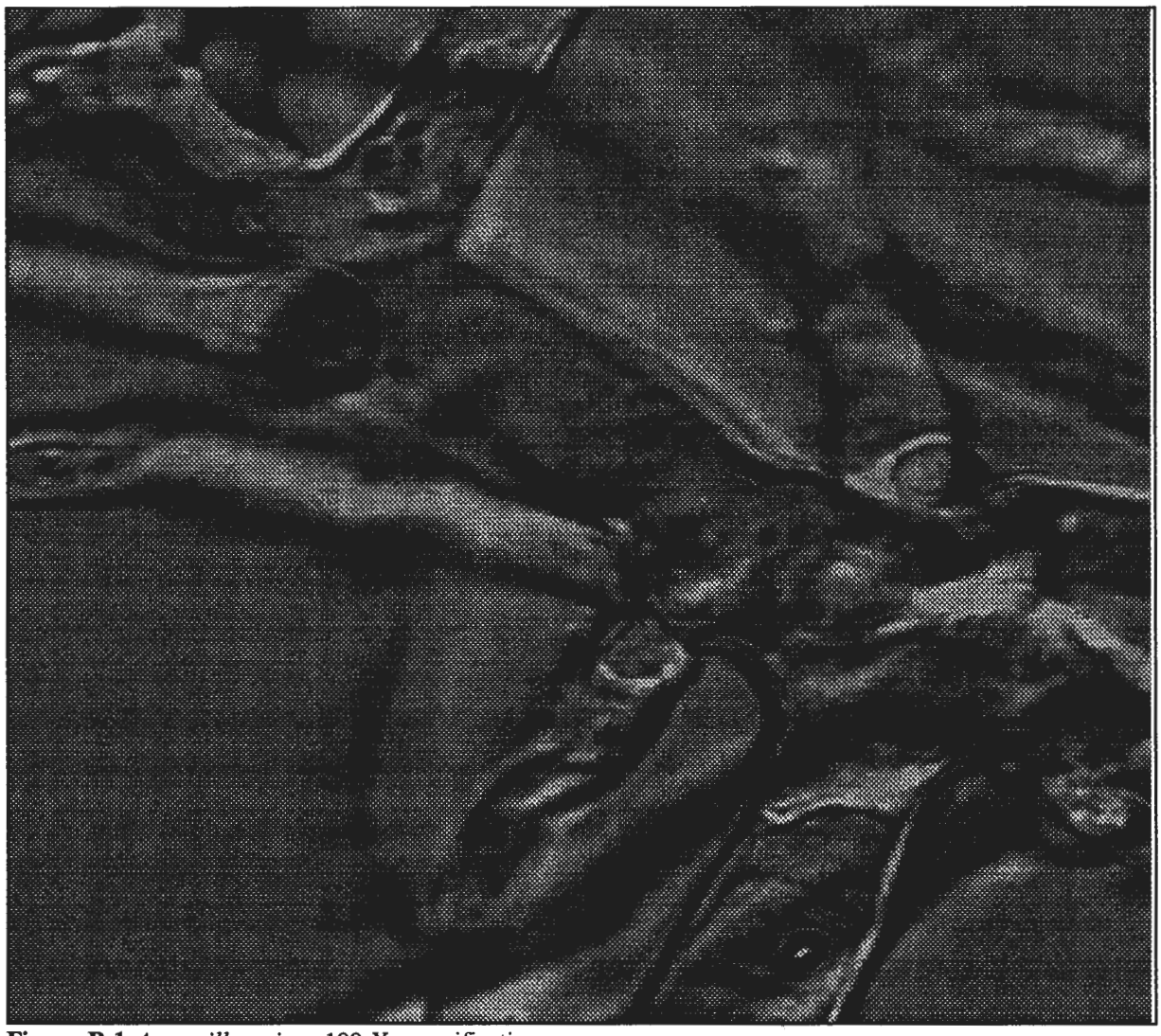

Figure B.1 *Aspergillus niger* 100 X magnification

B.1 French Press

Aim

To establish the number of passes required through the French press at chosen operating conditions to liberate the entire intracellular glucose oxidase content from *A.niger*, a sample was passed through the French Press four times. Release of glucose oxidase into the supernatant was measured at the end of each pass.

Method

1) Ensure that the French press apparatus is cleaned with 70% alcohol.
2) Moisten the 'O' ring of the plunger, open the valve at the base of the French press cell and insert plunger whilst turning. Ensure that the plunger is inserted in line with the cell.
3) Attach rubber tubing to the exit valve and draw in sample by pulling the plunger up 5cm, corresponding to 25ml of sample.
4) Close the exit valve and place French Press cell into the hydraulic press.
5) Place a collection container into an water/ice slurry. Connect exit tube into the container.
6) Carefully lower the press to contact the cell squarely on either side., Ensure that the cell is in line and concentrically placed.
7) Crank the hydraulic unit until the French Press cell is at 80 MPa.
8) Slowly open the exit valve and allow sample to leave until the pressure drops to 40 MPa.
9) Raise the pressure to 80 MPa and repeat steps 8 and 9 until all the sample as passed through the French Press.
10) Clean out the French Press cell with 70% alcohol.

Results

Figure B.2 shows the glucose oxidase activity of the French Press samples. The extracellular glucose oxidase is initially 1 unit per ml prior to any cell disruption. After a single pass most of the intracellular glucose oxidase is liberated and no significant change in glucose oxidase activity is observed with extra passes. Maximum liberation after a single pass indicates total cell disruption. Cells were viewed under the microscope to see the level of cell disruption. Figure B.3 shows that after a single pass, the cells are completely disrupted and broken into small fragments liberating intracellular contents and exposing membranes.

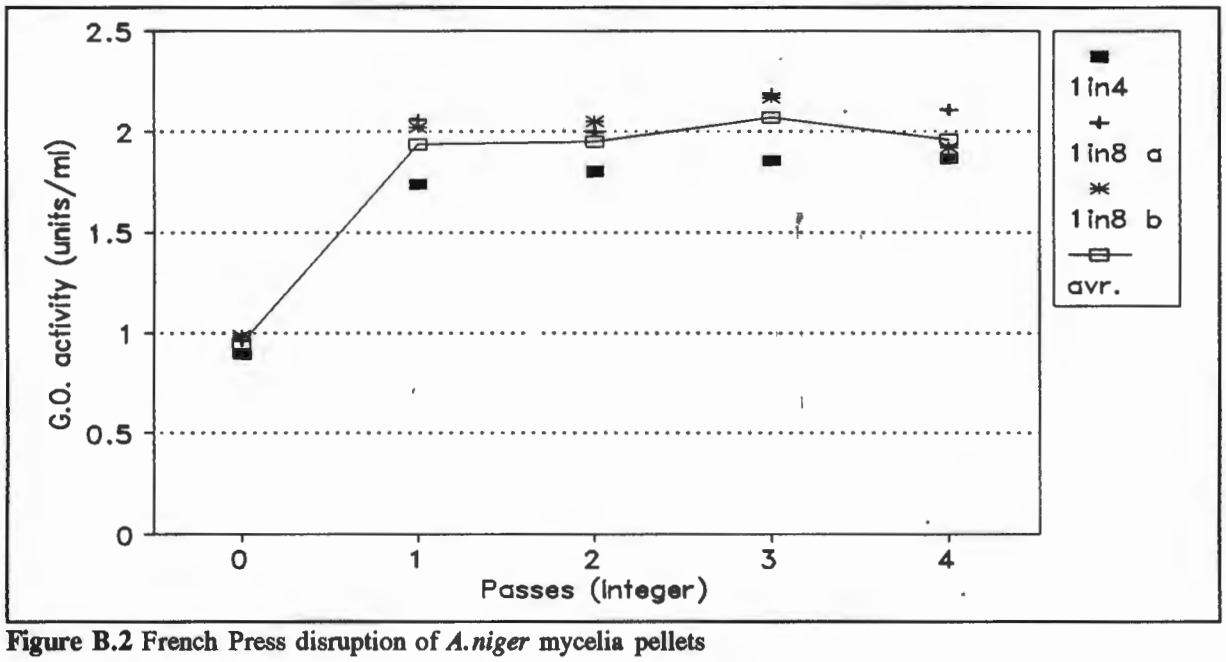

Figure B.2 French Press disruption of *A.niger* mycelia pellets

Figure B.3 ***A. niger*** **after French Press X100**

B.2 Al_2O_3 disruption

Method

2.5g powdered Al_2O_3 was added to 50ml of *A.niger* which was filtered and resuspended three times in a 0.1M pH 5.5 phosphate buffer. A commercial blender was used to disrupt the cells (Black and Decker hand held blender SB20 120W) for various times. In order to ascertain the level of disruption, the release of glucose oxidase using the blender was compared with the French Press.

Results

Figure B.4 shows the enzyme activity of the supernatant culture varying with residence time in the blender. It can be seen that after 6 minutes the enzyme activity is 88% of the entire glucose oxidase liberated by French Press. Figure B.5 shows the Al_2O_3 disruption of *A.niger* after 6 minutes. It can be seen that the cells are disentangled and broken into varying lengths. However there is less debri and the fragments are larger than disruption with the French press.

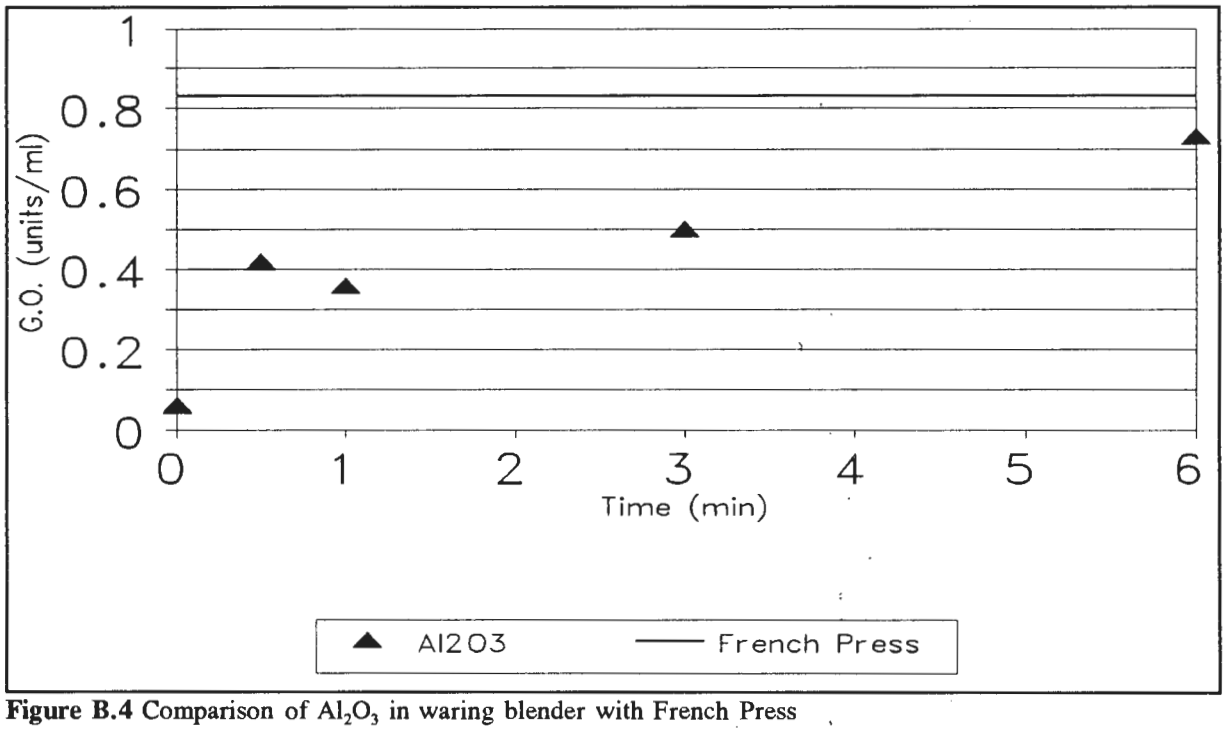

Figure B.4 Comparison of Al_2O_3 in waring blender with French Press

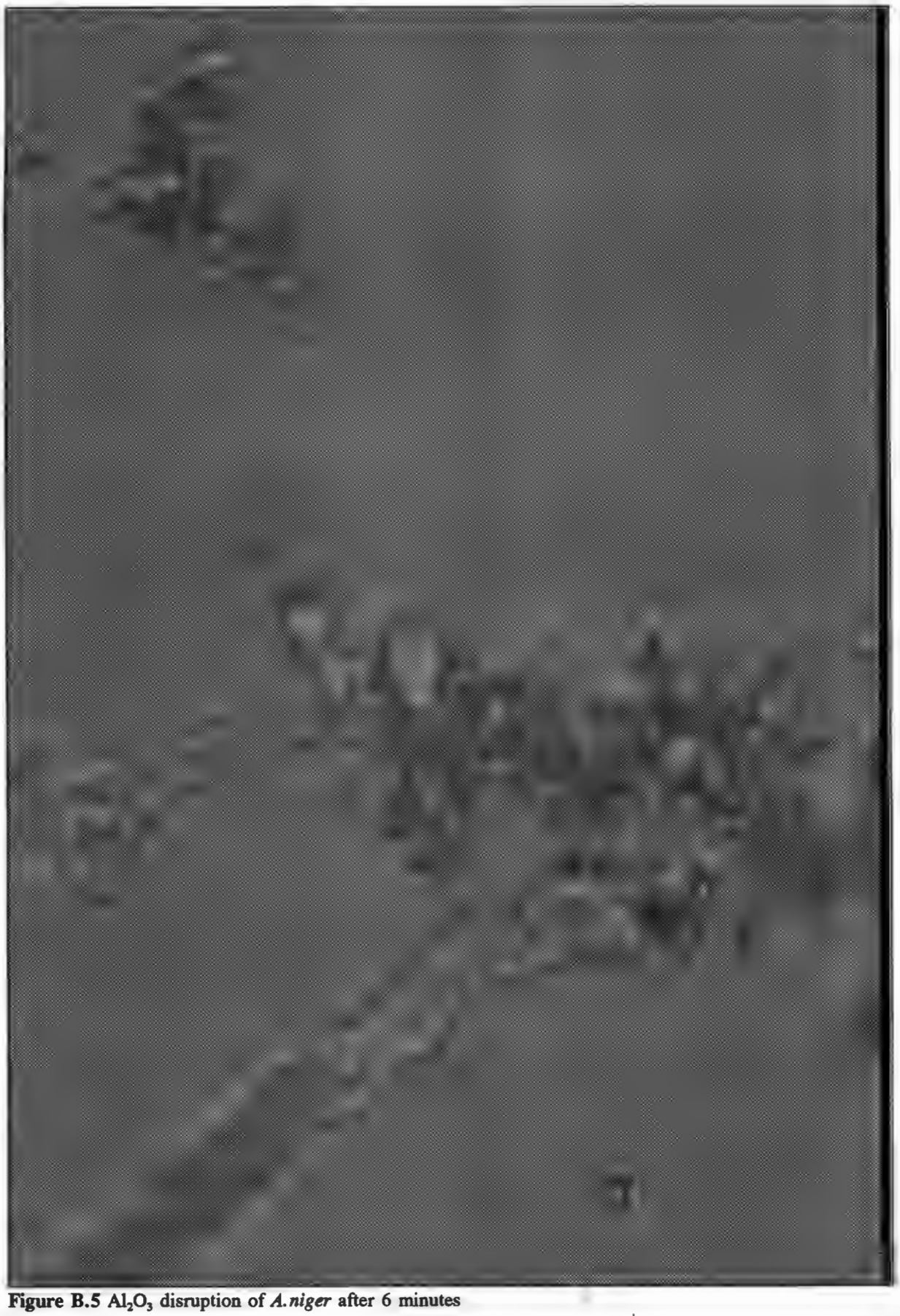

Figure B.5 Al_2O_3 disruption of *A.niger* after 6 minutes

B.3 Bead Mill Method

The aim of this experiment was to determine the time it takes to liberate all the glucose oxidase from *A.niger* cells. As the experiment was run on a different sample to the French Press, so final liberation values cannot be compared directly. Hence the times to reach a maximum steady value is determined. 200 gl^{-1} sand was used at 600 r.p.m. in a STR using a rushton turbine.

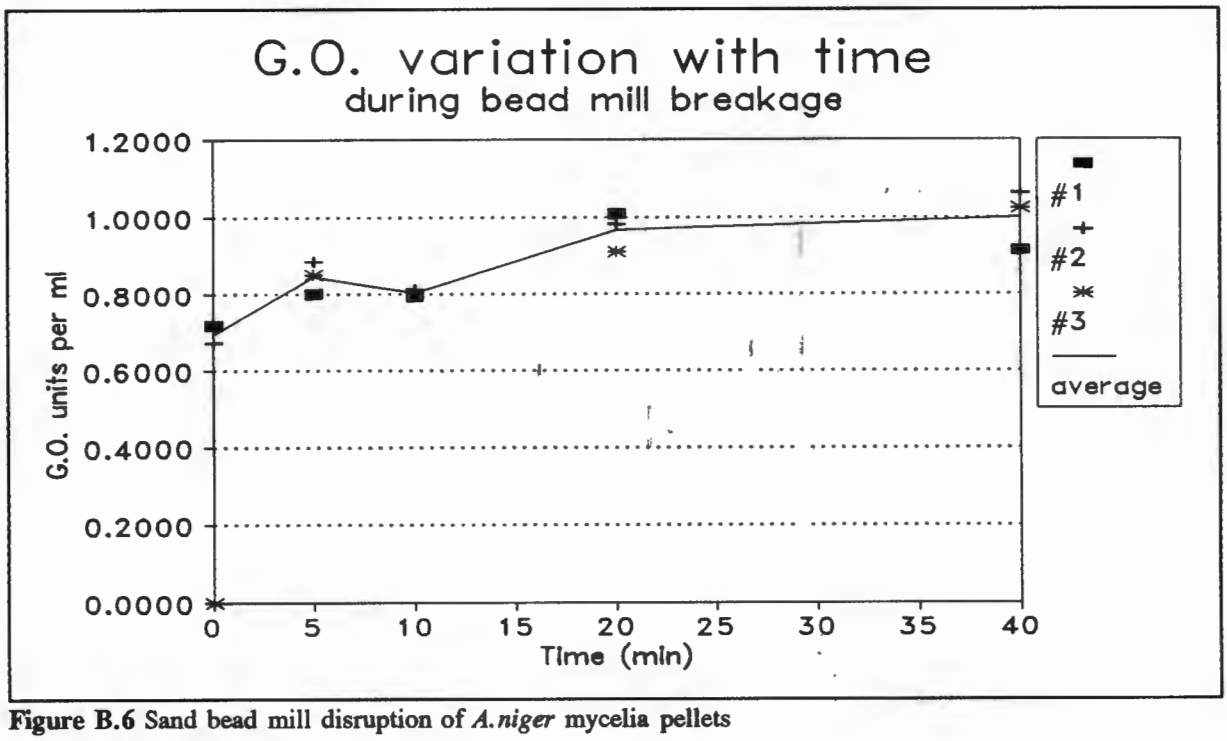

Figure B.6 Sand bead mill disruption of *A.niger* mycelia pellets

B.4 Ultra sound disruption

A.niger samples were placed in a sample container in a water/ice slurry and exposed to ultrasound for 30s at 22.8KHz or 22μm using a M.S.E. Soniprep 150. This procedure was repeated a number of times and samples were withdrawn for enzyme assay after each 30s dosage. The *A.niger* sample used was the same as that in the French Press experiment. It can be seen that even after a 150s exposure or 5 exposures to ultrasound, only 30% of the intracellular glucose oxidase liberated by the French Press was liberated. Continuous ultrasonication of growing *A.niger* systems has been investigated by Ishimori (1982) who and found that a 15W source in 80ml was able to liberate all the glucose oxidase from the cells. The difference can only be attributed to the power input of the ultrasound used.

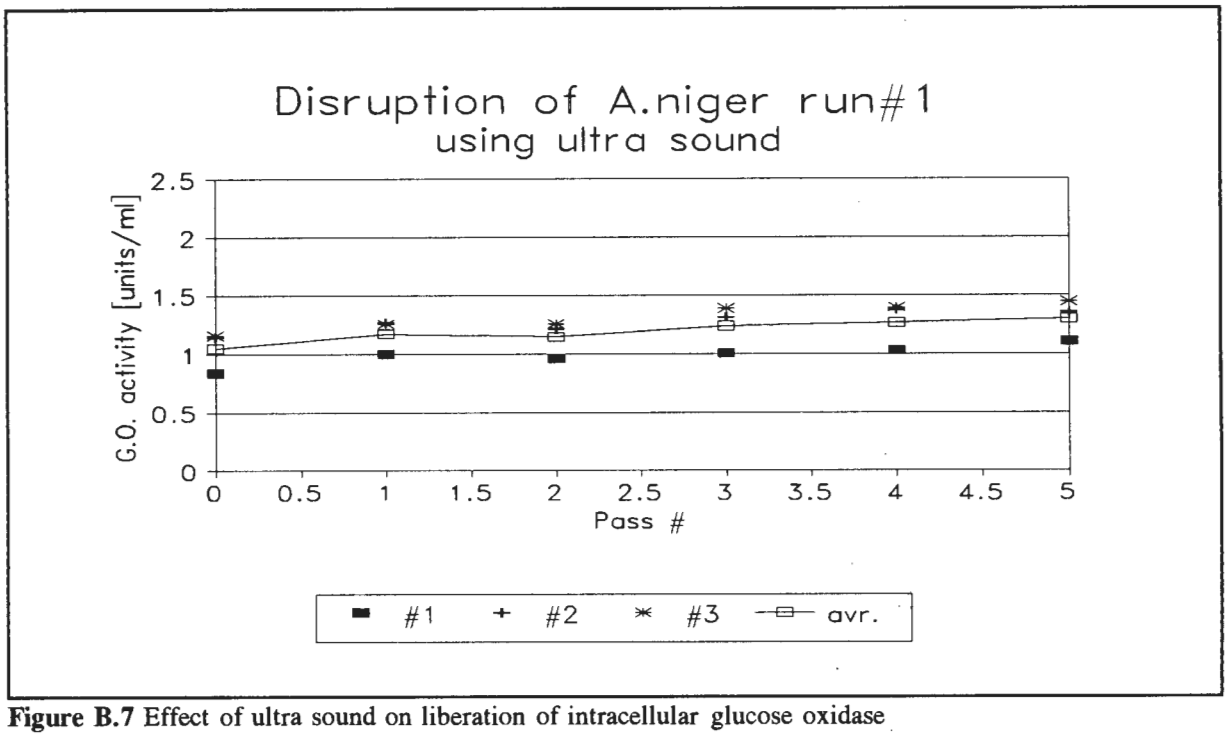

Figure B.7 Effect of ultra sound on liberation of intracellular glucose oxidase

B.5 Conclusion

Complete cell disruption is achieved by the French Press after a single pass. This is validated by observing the extent of disruption under the microscope. Agitation with aluminium oxide in a waring blender appears to be able to release the majority of the glucose oxidase after 6 min. The sand bead mill, however, shows unsatisfactory release of glucose oxidase.

APPENDIX C

GLUCONIC ACID ASSAY

Gluconic acid is measured using high performance liquid chromatography (HPLC). The equipment used was a Beckman model system gold. The column was a multipurpose organic acid column (Aminex HPX 87H) operating with a 0.01M H_2SO_4 as the single solvent at a flow rate of 0.6ml min^{-1}. The spectrophotometer was set to measure absorbance at 215nm. 25μl samples were injected. Standard gluconic acid samples had a residence time of 8.3 minutes and the calibration was 63 300 absorbance $\cdot s \cdot g^{-1}$ sodium gluconate injected

$$[Gluconate]\ (gl^{-1}) = \frac{Integral(abs \cdot s)}{0.0633 \cdot VOL(\mu l)}$$

(C.1) Calculation of sodium gluconate concentration

The method specificity was tested by injecting standards of oxalic and citric acid. The system was able to detect these acid at different peak positions to gluconic acid there by showing that the system is superior to titration methods and is able to identify the presence of other organic acids.

The assay was calibrated using a 10 gl^{-1} solution made from SAAR Chem grade sodium gluconate. The standard had an error of 2% at 25μl injections and over 20% at 10μl injection volumes.

APPENDIX D

IN SITU MEASUREMENT OF OXYGEN UTILISATION IN CHEMAP FERMENTATION

Measuring the oxygen utilization rate *in situ* during the course of a fermentation can only be achieved if the oxygen utilisation rate is low enough for the dissolved oxygen probe to respond to the change in concentration. The Ingold polagraphic dissolved oxygen electrode has a response time ($t_{1/2}$) of 20s. The oxygen utilisation rate (OUR) is measured as follows:

1) Turn the impeller to 50 rpm to minimise surface aeration but high enough to ensure homogeneous mixing.

2) Turn off the air supply

3) Start monitoring the time profile of the dissolved oxygen.

4) Return sparging and aeration to fermentation conditions.

5) Repeat 1-4 twice more to get the OUR profile in triplicate.

6) Dissolved oxygen concentration as a function of time in the absence of aeration is given by the following formula:

$$C(ppm) = C^*(ppm)[1-e^{-k_l a * t(s)}]$$

(D.1) Dissolved oxygen profile in OUR experiments

Plot $\ln((C^*/(C^*-C))$ vs time (s). The slope of the line is $k_l a$ ($ppms^{-1}$).

APPENDIX E

DRY CELL MASS MEASUREMENT

Aspergillus niger forms small pellets and filaments of low relative density. Conventional gravity settling in a 7600 g centrifuge does not separate out the cell mass so filtration techniques have to be used. In order to avoid loss of filaments 0.45μm membrane filters have to be used. The sample volume has to be fairly large to ensure representative sampling of the pellets and a significant dry mass increase (the dry weights are in the range of 0 - 3gl^{-1}).

Method

1) Pre-dry 0.45μm membrane filters placed on numbered aluminium boats in a 100°C oven for 24h.

2) Place dry membranes and boats into a desiccator to cool and weigh to 4 significant figures.

3) Note the number of the aluminium boat and place membrane on vacuum filter support.

4) Mix the culture broth and withdraw 30ml using a wide necked syringe.

5) Filter the 30ml aliquot through the membrane under vacuum and collect the filtrate for glucose, gluconic acid and enzyme analysis.

6) Wash the residue 3 times with distilled water.

7) Transfer the membranes onto the aluminium boats and dry for 48h at 80°C.

9) Place the aluminium boats in a desiccator to cool and weigh the combined boat,

membrane and cell mass to 4 significant figures.

10) Calculate the change in dry mass due to the sample and then divide this by the sample volume in (l) to give the dry mass in gl^{-1}.

A possible problem with the dry cell mass analysis is that the sample port withholds or hinders the passage of the pellets into the sample container. Selective sampling was investigated at the end of fermentation by withdrawing 100ml of sample and wasting 400ml to drain and then repeating six times. The 100ml samples were analyzed for dry weight in triplicate. This experiment checks for selective sampling and for the error in dry weight measurement at the end of a fermentation. The results (Figure E.1 and Table E.1) show that selective sampling does not occur at the end of the fermentation when the majority of the broth is pelleted. It also shows that the standard error on dry mass measurement is below 5%.

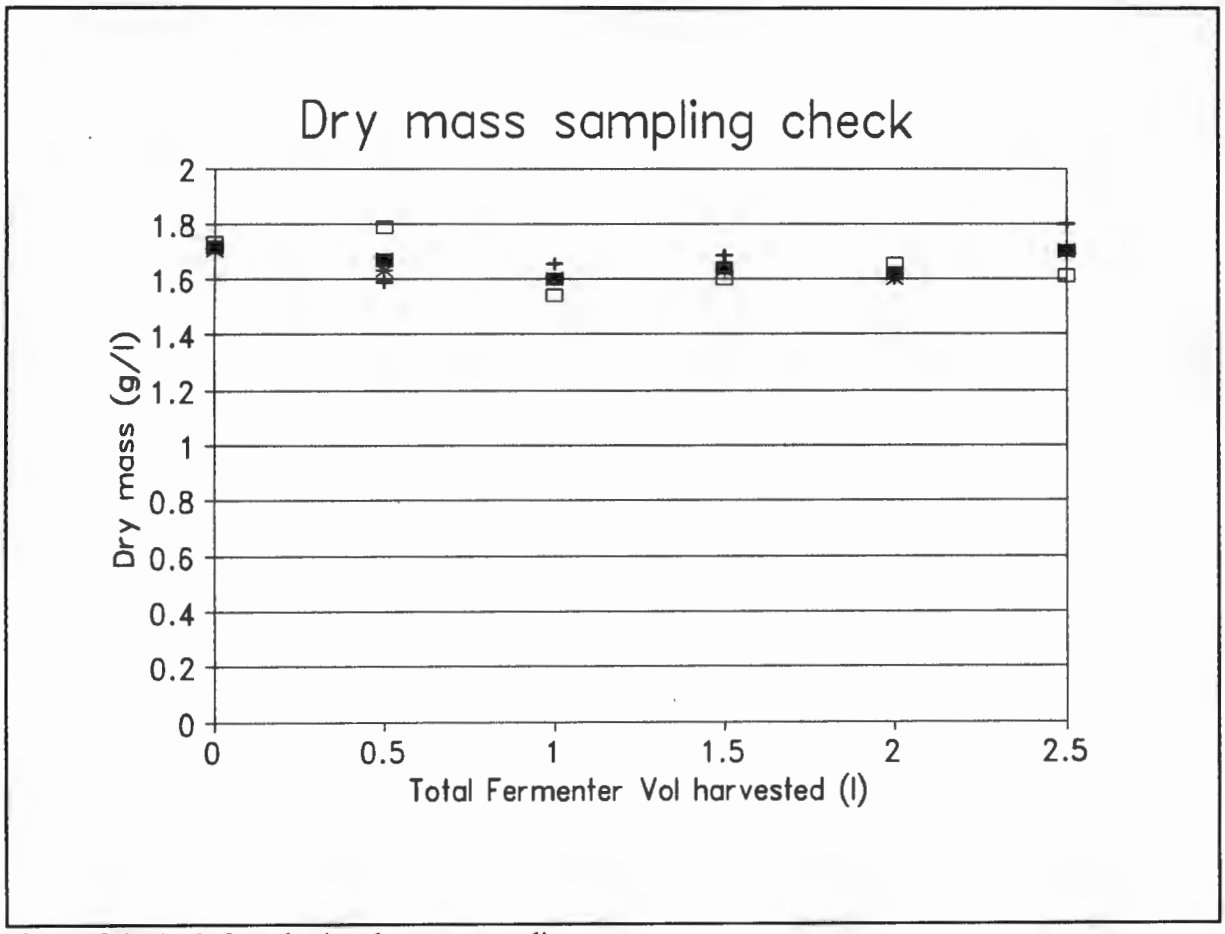

Figure E.1 Check for selective dry mass sampling

Table E.1 Dry weight data for selective sampling experiment

Vol. Broth withdrawn (l)	Average dry weight (gl^{-1})	Standard error %
0.1	1.7189	0.6
0.6	1.6700	5.1
1.1	1.6011	2.9
1.6	1.6867	2.2
2.1	1.6189	1.5
2.6	1.7033	4.5

APPENDIX F

PELLET SIZE DISTRIBUTION MEASUREMENT

Pellet size distributions were measured by placing 1ml sample volumes on a glass sheet and photographed the resultant image using a Joyce Loeble image analyzer. The digital image was eroded twice and dilated twice to remove the merging of adjacent pellets. The pellets were then counted and the area calculated. The area was scaled by calibrating a known area of graph paper. A representative diameter was calculated for each pellet by assuming the pellets to be spherical and the projected images to be circular. The diameters were grouped and a size distribution formed.

APPENDIX G

GLUCOSE ASSAY

The Boehringer Mannheim GOD-Perid Cat # 124 036 spectrophotometric method was chosen to measure glucose concentration. The method works on the coupled oxidation/reductive reactions between glucose and hydrogen peroxide and between hydrogen peroxide and a colourless dye ABTS (di-ammonium 2,2'-azino-bis(3-ethylbnenzothiazoline-6-sulfonate)). The reactions are as follows:

$$glucose + O_2 + H_2O \xrightarrow{GOD} gluconate + H_2O_2 \qquad \textbf{(G.1)}$$

$$H_2O_2 + ABTS \xrightarrow{POD} Coloured\ complex + H_2O \qquad \textbf{(G.2)}$$

GOD : Glucose oxidase

POD : Peroxidase

Method

Place 3ml of the buffered chromogen and enzyme solution (solution 2) into a series of test tubes. Dilute the glucose samples in to the 0 - 0.6gl^{-1} glucose range. Add 0.12ml of the diluted glucose sample to the test tubes. Make a blank using 0.12ml of water. Make a standard 0.6gl^{-1} solution and add 0.12ml to a test tube as a standard. Mix tubes and incubate out of sunlight at 20-25°C. After 25 - 50 minutes measure the absorbance of the resulting coloured complex at 610nm using 3ml disposable plastic cuvettes. Do not measure the absorbance after 50min. Calculate the glucose concentration as follows relative to the standard :

$$C_{(g/l)} = \frac{Sample\ Abs}{Std\ 0.6\ g/l\ Abs} * 0.6 \qquad \textbf{(G.3)}$$

The following calibration curve shows the linear range used for assays

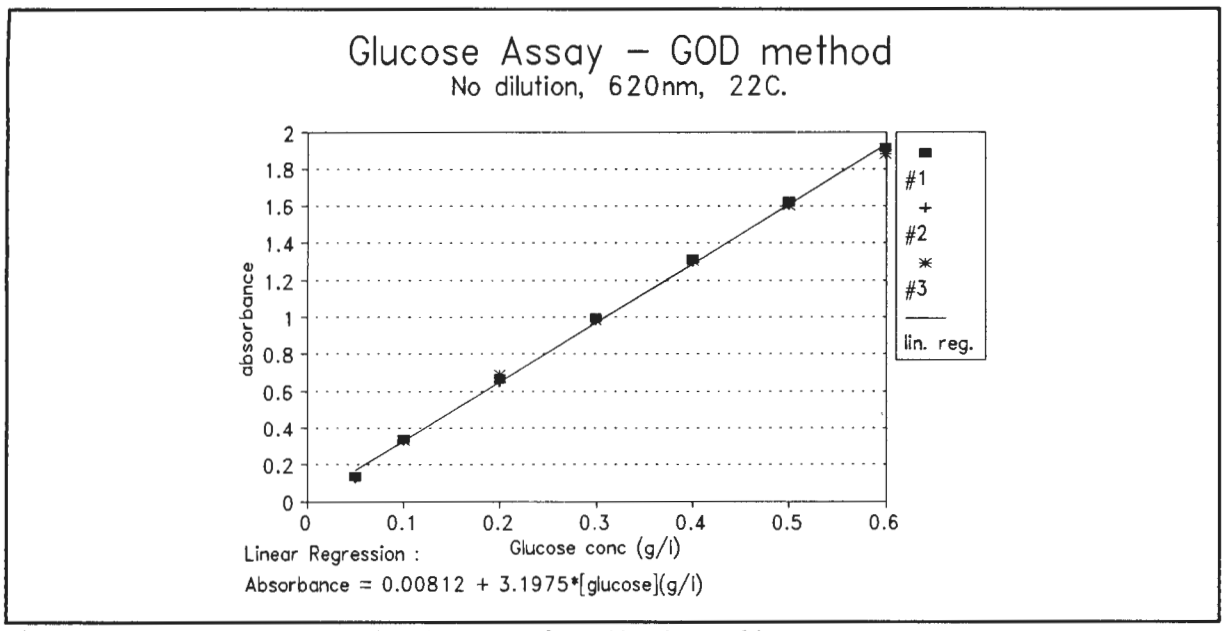

Figure G.1 Glucose standard calibration curve for GOD glucose kit

APPENDIX H

OXYGEN DIFFUSION INTO MYCELIAL PELLETS

In order to model the oxidation of glucose to glucose oxidase it is necessary to evaluate the effectiveness factor of the pellets used in fermentation in order to account for intraparticle diffusion. The effectiveness factor is defined as the ratio of activities of the pellet in a diffusion limiting environment under consideration and the activity of the pellet if diffusion constraints were removed. Pellet size distributions were generated using image analysis of samples taken from the fermentations in Appendix F and Section 4.1.5. The inoculum size distribution is bimodal. This is altered to a uni-modal distribution as the fermentation progresses. The uni-modal distribution has an average pellet diameter of 1.2mm. Kobayashi *et al.* (1973) have modelled the effectiveness factor of *A.niger* pellets by measuring oxygen utilisation rates of pellets and comparing them to filamentous utilisation rates.

The model equations follow:

$$Ef = \frac{E_0 + \alpha E_1}{1 + \alpha} \qquad \textbf{(H.1)}$$

$$E_1 = \frac{3}{m}\left[\frac{1}{\tanh(m)} - \frac{1}{m}\right] \qquad \textbf{(H.2)}$$

$$E_0 = \begin{cases} 1 & ; (0 < m \leq \sqrt{3}) \\ 1 - \left(\frac{1}{2} + \cos\left(\frac{\psi + 4\pi}{3}\right)\right)^3 & ; (m > \sqrt{3}) \end{cases} \qquad \textbf{(H.3)}$$

$$\alpha = \frac{K_m}{S_i} \qquad \textbf{(H.4)}$$

$$\xi = R\sqrt{\frac{\rho_m Q_i}{2DS_i}} \qquad \textbf{(H.5)}$$

$$m = \frac{\xi}{\sqrt{\left[(1+\alpha)\left(1-\alpha\ln\left(1+\frac{1}{\alpha}\right)\right)\right]}} \qquad \textbf{(H.6)}$$

$$\psi = \cos^{-1}\left(\frac{6}{m^2} - 1\right)$$

(H.7)

Table H.1 Constants for the *A.niger* system from T.Yano, T.Komadama, and K.Yamada, Agr. Biol. Chem., **25**, 580 (1961)

Parameter	Value	Units	Explanation
D	0.108	mm^2min^{-1}	diffusivity of oxygen in the mycelial pellets
K_m	3E-6	$\mu molO_2mm^{-3}$	Michaelis constant
Q_i	0.115	$\mu molO_2min^{-1}mg^{-1}$	Specific reparation rate at $S = S_i$
S_i	1.9E-4 ≡ 6.1 ppm	$\mu molO_2mm^3$	Dissolved oxygen in the bulk
ρ_m	$0.027(2R)^{-0.82}$	$mgmm^{-3}$	density of mycelial pellet

Effectiveness factors below 0.5 imply that diffusion starts to become significant (Kobayashi *et al.* 1973). Using these model equations H.1 to H.7 effectiveness factors of 0.52, 0.91 and 0.97 were obtained for 0.21, 0.75 and 1.00 atm oxygen conditions respectively at a pellet diameter of 1.2mm. This implies that the glucose oxidase reaction within the pellet may be mass transfer limited. It should be noted that approximately 50% of the total glucose oxidase is present in the supernatant and thus the only half of the glucose oxidase activity is subjected to the border line pellet diffusion resistance. Figure H1 shows the profile of effectiveness factor as a function of pellet diameter in the *A.niger* system.

It is important to understand the effect of oxygen on the effectiveness of pellets cultured. Varying oxygen demand and oxygen supply levels alter the effectiveness. Figure H.2 shows

the effect of dissolved oxygen on the effectiveness factor.

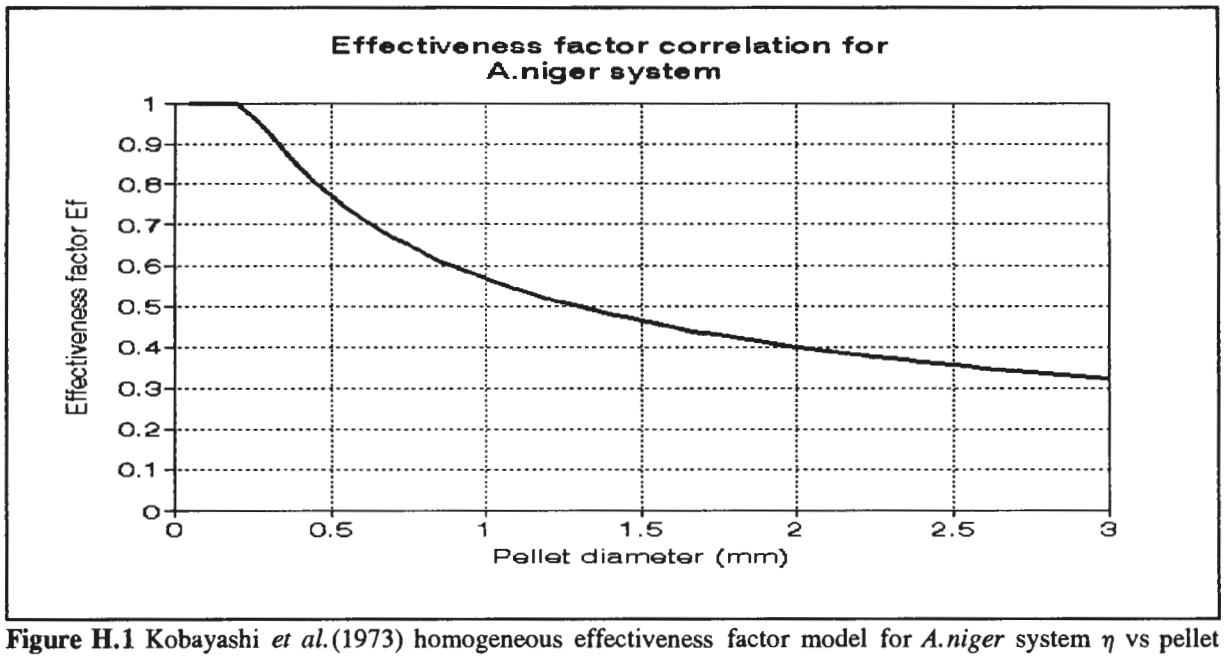

Figure H.1 Kobayashi *et al.*(1973) homogeneous effectiveness factor model for *A.niger* system η vs pellet diameter (2R)

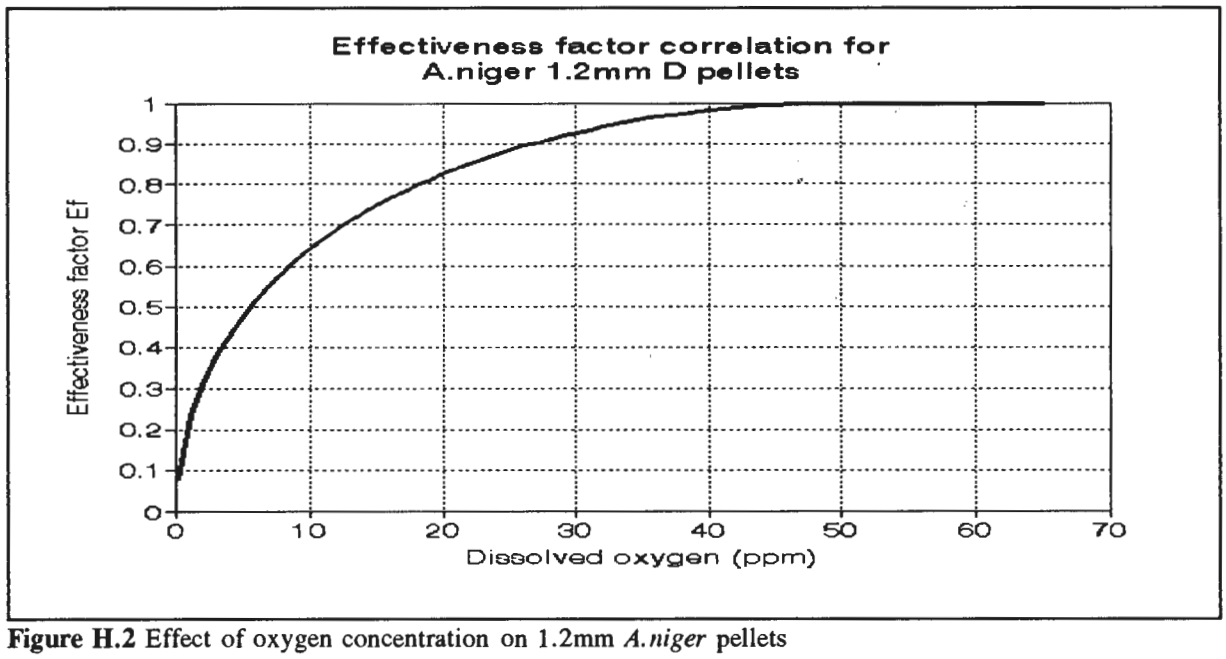

Figure H.2 Effect of oxygen concentration on 1.2mm *A.niger* pellets

APPENDIX I

CHEMAP FERMENTER STERILISATION PROCEDURE

1. Ensure the fermenter is clean and dry. Fit rubber seals on both sides of the glass tube into the fermenter base and lid. Place the 4 bars and nuts in place and tighten progressively moving from one bar to the next in a clockwise fashion.
2. Place glucose solution into the fermenter (usually glucose for 6.0l dissolved in 5.5l).
3. Ensure all ports have rubber seals and are screwed down tightly.
4. Calibrate the pH electrode at pH 7.0 at room temperature. This calibration point is independent of temperature. Adjust to pH 5.5 after sterilisation and salt addition to the glucose media. Place pH and D.O. probes onto their respective ports. The pH probe has a longer shaft than all the others and uses a longer injection port. Ensure that the air needle port is not used for any other probes. Place air condenser into the centre of the fermenter lid.
5. Ensure the boiler is filled with water to the maximum mark. Turn on the boiler and wait for 3 bar of steam to be generated.
6. Close the green cooling water valve on the fermenter.
   Open the red steam valve on the fermenter.
   Close the water reflux valve.
   Ensure the temperature controller is off.
   Place stirrer on maximum speed.
   Ensure the air supply is off.
7. Place the stainless steel shield around the fermenter.
   Wait until the fermenter reaches 100°C and steam just starts to spit out of the exhaust air group. Close the valve at the top of the air group.
8. When the fermenter has reached 1.5 bar, time the sterilisation process for 20min.

9. After 20min, close the red steam valve and open the green main water valve for cooling fully.

10. Turn the water for heating and cooling valve so that the flow is at the 0.7l/min mark. Once the fermenter pressure reaches 0.5bar prepare to place the air needle into the fermenter. Open and remove the air group valve to prevent a vacuum forming.

11. Cool to 95°C, close cooling valves and start to place needles for

    a) Air needle
    b) Acid control needle
    c) Base control needle
    d) Salt and inoculum transfer line needle

    into the ports as follows :

12. Unscrew and pull out the plunger in the port.

13. Ensure that you are wearing heavy duty boilerman gloves, goggles and a lab coat. Place 2ml of 96% alcohol onto the exposed rubber diaphragm and ignite.

14. Unwrap the needle from the sterilised sleeving and pass the needle through a bunsen burner flame before pushing the needle into the port and screwing the needle down firmly.

15. Repeat for other injection needles. Continue to cool to 30°C by opening the cooling valve.

16. Place air line onto the fermenter and allow air to slowly pass into the fermenter. Check that bubbles are leaving the base of the sparger at low flow rates and is not leaking by bypassing the air needle sparger seal.

17. Set the temperature controller to the desired temperature. The fermenter can be left in this state indefinitely - contamination is minimised by the low air flow causing a positive fermenter pressure.

Sampling procedure

1. Ensure the boiler is at maximum water height level by adding water.
2. Turn boiler on for 45 minutes before required sample.
3. Once boiler has reached 1.5, bar open the sample port steam valve with a plastic beaker below the port to catch condensate. Allow condensate to pass, followed by steam to sterilise the port.
4. Take a sample aseptically
5. Open sample port steam valve again to sterilise the valve.
6. Switch off boiler.

APPENDIX J

TURBO PASCAL 4TH ORDER RUNGE-KUTTA INTEGRATION PROGRAM

```
program integration_of_model;



uses crt,stdhdr,graph,worlddr,segraph;

const
   ndim = 3;                          {Simplex max dimensions }
   nmax = 3;                          {used in array declaration}

type
   vector = array[1..nmax] of real;    {}

var

{  This section contains explanation of variables used

   result
   rawdata      experimental data input file
   dout         modelled data output file
   serror
   state        contains the state values at a particular time
   dstate       contains the model differential of state
   ostate       contains the previous state value
   k1,k2,k3,k4  variables used in Runge-Kutta routine for integrating model
   rdatax       contains the time (h)                  values of the raw data
   rdata1       contains the dry mass (gl-1)           values of the raw data
   rdata2       contains the gluconic acid (tot moles) values of the raw data
   rdata3       contains the Dissolved Oxygen (ppm)    values of the raw data
   param        model parameters
   vparam
   verror
   vparam1
   vparam2
   i,j,k,l      integers used in FOR loops
   ii,jj,kk,ll  integers used in FOR loops
   ir
   numdat       QC number od data points to be plotted
   color        QC colour of plotted lines
   linestyle    QC line style
   perror
   minpos
   divisions
   optim
   nparam
   nstep
   outwin
   nrdata
   invh         # of integration steps between logging data
   jt
   h
   error
   cparam
   duration
   cstep
   plotdatax
   plotdatay
   mumax
   Yxs
   remainder
   rcrit
   slope
   temp1
   temp2
   tol
   est
   estwin
   iters                Total # of iterations done
}
   result,rawdata,dout,modelout      :text;
   filein                            :text;
   serror,header,stime,stemp,s       :string;
   filename,srawdata                 :string;
   state,dstate,ostate,k1,k2,k3,k4   :array [1..15] of real;
   temp                              :verylongvector;
   rdatax,rdata1,rdata2,rdata3       :verylongvector;
```

```
   plotx,ploty                      :verylongvector;
   param                            :array [1..21] of real;
   vparam                           :array [1..21] of real;
   verror                           :array [1..21] of real;
   vparam1,vparam2                  :verylongvector;
   i,j,k,l,numdat,color,linestyle,ir :integer;
   ii,jj,kk,ll,iters,m,perror       :integer;
   minpos,divisions,noptim,nparam   :integer;
   nstep,outwin,nrdata,invh,jt,ecode :integer;
   h,error,cparam,duration,vstep    :real;
   plotdatax,plotdatay              :verylongvector ;
   mumax,kmax,Yxs,remainder         :real;
   rcrit,dummy,csat                 :real;
   scope,temp1,temp2,tol            :real;
   est,estwin                       :verylongvector;
   px,ri                            :real;


   alpha,beta,gamma,itmax               : real;
   ftol,rtol                            : real;
   ypr,yprr,fac,rr                      : real;
   p                                    : array [1..ndim+1,1..ndim] of real;
   y                                    : array [1..ndim+1] of real;
   pr,prr,pbar                          : array [1..nmax] of real;
   iter,mp,np,mpts                      : integer;
   ilo,inhi,ihi,flag                    : integer;



procedure filedata;

{This procedure closes the state variables profile through time file}

begin
     close(dout);
end;

procedure initmodel;
{Initialise the parameters of the model by reading the input file}
begin

   assign (filein, 'kj3t5.inp'); { Open KJ1.INP - fileout name and state[0]}
   reset  (filein);

   readln   (filein,srawdata); {reads in the name of the raw data file}
   assign   (rawdata,srawdata);
   reset    (rawdata);

{This procedure reads raw data from a space delimited text file      }
{Each column is read into a separate verylongvector                  }
   i := 0;
   while not Eof(rawdata) do
      begin
      read   (rawdata,rdatax[i]);
      readln (rawdata,rdata1[i],rdata2[i],rdata3[i]);
{      writeln(rdatax[i],rdata1[i],rdata2[i],rdata3[i]);}
      rdata2[i] := rdata2[i]/10 ;
      rdata3[i] := rdata3[i]/10 ;
      i := i+1;
   end;
   nrdata := i;
   close(rawdata);

   readln  (filein, filename);
   assign  (dout, filename);
   rewrite (dout);
   writeln (dout,' TIME      BIOMASS _EX-GLUC _IN-GLUC _REPRESS  _COMPLEX _m-RNA    _IN-GO
_OUT-GO  _G.A.   _OXYGEN');

   for i := 1 to 11 do
   begin
      read(filein, state[i]); {read in initial conditions}
      read(filein, stemp);    {read in explaination in text file}
   end;
   for i := 1 to 20 do
   begin
      read(filein, param[i]); {read in model parameters}
      read(filein, stemp);    {read in explaination in text file}
   end;

   state[4]  :=param[16];     {set initial R0glucose}
   state[12] :=param[15];     {set initial R0oxygen }
   state[13] := 0;


{   read(filein,rcrit);     {rcrit}
{   read(filein,stemp);     {string}

{This procedure sets up all the variables and initial conditions    }
{It starts off with the model parameters stored in PARAM            }
{continues with the initial values of state                         }
{other variables for graphics settings etc are included             }
```

```
   read(filein,scope    ); {:= 10.0;                                    }
   read(filein, stemp   ); {read in explaination in text file           }
   read(filein,noptim   ); {:= 5;   # of optimisation runs              }
   read(filein, stemp   ); {read in explaination in text file           }
   read(filein,nparam   ); {:= 4;   # of parameters                     }
   read(filein, stemp   ); {read in explaination in text file           }
   read(filein,nstep    ); {:= 20;  # of intervals scan range is divided}
   read(filein, stemp   ); {read in explaination in text file           }
   read(filein,vstep    ); {:= 10;  The real equivelant of nstep!       }
   read(filein, stemp   ); {read in explaination in text file           }
   read(filein,h        ); {:= 0.004;                                   }
   read(filein, stemp   ); {read in explaination in text file           }
   read(filein,invh     ); {:= 250;                                     }
   read(filein, stemp   ); {read in explaination in text file           }
   read(filein,duration ); {:= 2;                                       }
   read(filein, stemp   ); {read in explaination in text file           }
   read(filein,iters    ); {:= 7500;                                    }
   read(filein, stemp   ); {read in explaination in text file           }
   read(filein,numdat   ); {:= 30;                                      }
   read(filein, stemp   ); {read in explaination in text file           }
   read(filein,color    ); {:= 1;                                       }
   read(filein, stemp   ); {read in explaination in text file           }
   read(filein,linestyle); {:= 5;                                       }
   read(filein, stemp   ); {read in explaination in text file           }

   csat := state[10];

   close (filein);

end;

procedure initgraph;
{This procedure sets up the graphics display of the graphs}

begin

   initSEGraphics('h:\pascal');
   settextstylexx(2,0,4);
   setcurrentwindow(1);
   setaxestype(0,0);
   defgraphwindow(0,0,480,450,1);
   bordercurrentwindow(1);
   setaxestype(0,0);
   scaleplotarea(0.0,-0.10,h*iters +1,1.001);
   setxyintercepts(0.0,0.0);
   setcolor(7);
   drawxaxis(10,1);
   drawyaxis(0.1,2);
   drawgrid(1);
   labelxaxis(1,0);
   labelyaxis(1,0);
   titleXaxis('Time (h)');
   titleYaxis('Intracellular (M)');

   setcurrentwindow(3);
   defgraphwindow(480,0,620,400,3);
   bordercurrentwindow(3);
   scaleplotarea(0,0,20,45);
   setxyintercepts(0.0,0.0);
   setcolor(7);

   SetCurrentWindow(4);
   defgraphwindow(480,400,620,450,4);
   bordercurrentwindow(4);
   scaleplotarea(0,0,1,1);

end;

procedure plotdata;

{This procedure plots the profile of the state vector through time       }

begin
   setcurrentwindow(1);
   Scatterplotdata(rdatax,rdata1,nrdata,1,0);
   Scatterplotdata(rdatax,rdata3,nrdata,2,0);
   Scatterplotdata(rdatax,rdata2,nrdata,2,1);
end;

procedure derrfunc;

{This procedure contains the model equations in derivative from (ODE's) }
{Each variable can be coupled and change its fromat depending on it's   }
{environment i.e. the from of the equation depends on the state vector  }

begin

                { BIOMASS (gl-1) }

   dstate[1] := param[11]*state[1]*(1.0-param[12]*state[1]);


                { EXTRACELLULAR GLUCOSE (M) }
   if state[2] > 1e-6 then
```

```
   begin
   dstate[2] := -state[8]*param[8]/(1+0.0797/state[2]
                +0.000443/(state[10]/1e3/32))
                -50.0*state[1]*(0.0007*state[2]/(2.4+state[2]
                )-state[3]);
   end
   else
   dstate[2] := 0.0;


                { INTRACELLULAR GLUCOSE (M/gram cell) }
   dstate[3] := +50.0*state[1]*(0.0007*state[2]/(2.4+state[2])-state[3])
                -param[1]*state[4]*state[3]*state[1]
                +param[3]*state[5]*state[1]
                -param[9]*dstate[1]
                {-0.03*dstate[1]};

                { REPRESSOR GLUCOSE /gram cell }
   if state[4] >0 then
   begin
   dstate[4] := -param[19]*state[4]*state[3]*state[1]
                +param[20]*state[5]*state[1];



                { REPRESSOR GLUCOSE COMPLEX /gram cell }
   dstate[5] := +PARAM[19]*STATE[4]*STATE[3]*STATE[1]
                -PARAM[20]*STATE[5]*STATE[1];

   end;

               { m-RNA /gram cell }
{  if state [6] < 0 then state[6] := 0.0;}

   if state[4]  < param[14] then
   begin
   if state[12] < param[13] then
   begin
                dstate[6] := -param[5]*state[6]
                             +param[6]*(param[13]-state[12])*
                             (param[14]-state[4])*100000;
   end
                else dstate[6] := -param[5]*state[6];
   end
                else dstate[6] := -param[5]*state[6];
```

```
                { INTRACELLULAR GLUCOSE OXIDASE / gram cell }
   dstate[7] := +param[7]*state[6]
                -50.00*((state[7])*(state[7]/(1.0e-4+state[7]))-state[8]);

                { EXTRACELLULAR GLUCOSE OXIDASE (U/ml/gram cell) }
   dstate[8] := +50.00*((state[7])*(state[7]/(1.0e-4+state[7]))-state[8])
                -(2.7e-3*0.363*22*0.363*state[8]*state[10])/
                 (state[10]+22*0.363);

                { GLUCONIC ACID (M) }
   dstate[9] := state[8]*param[8]/(1+0.0979/state[2] + 0.000443/
                (state[10]/1e3/32));

                { DISSOLVED OXYGEN (ppm) }
   dstate[10]:= param[10]*(csat - state[10]) - dstate[9]*1000*32;

                { T I M E }
   dstate[11]:= 1.0;

                { REPRESSOR OXYGEN /gram cell }
   if state[12] >0 then
   begin
   dstate[12]:= -param[18]*state[12]*state[10]*state[1]
                +param[17]*state[13]*state[1];

                { Repressor oxygen complex /gram cell}
   dstate[13]:= +param[18]*state[12]*state[10]*state[1]
                -param[17]*state[13]*state[1];
   end;

end;


procedure rungekutta;

{This procedure integrates the derrivative function using 4th order  }
{Runge-Kutta taken from Numerical methods for Engineers S.C.Chapra & }
{R.P.Canale McGrawHill 1989 New York p604                             }

begin
   for i := 1 to 13 do
   begin
      ostate[i] := state[i];
   end;
   derrfunc;
   for i := 1 to 13 do
```

```
   begin
      k1[i] := dstate[i];
      ostate[i] := state[i] + 0.5*h*K1[i];
   end;
   derrfunc;
   for i := 1 to 13 do
   begin
      k2[i] := dstate[i];
      ostate[i] := state[i] + 0.5*h*K2[i];
   end;
   derrfunc;
   for i := 1 to 13 do
   begin
      k3[i] := dstate[i];
      ostate[i] := state[i] + h*K3[i];
   end;
   derrfunc;
   for i :=1 to 13 do
   begin
      k4[i] := dstate[i];
      state[i] := state[i] +1/6*(k1[i]+2*k2[i]+2*k3[i]+k4[i])*h;
      ostate[i] := state[i];
   end;
derrfunc;

end;


procedure fmodel;

{This procedure generates the model profiles of the state vector     }
{It calculates a sqared error between the rawdata supplied and the   }
{model                                                               }

begin
   initmodel;
   error := 0.0;
   ir    := 1;
   for j:=1 to 10 do
      begin
         if param[j] <= 0.0 then param[j] := 0.0;
      end;
   for j := 1 to iters do
      begin
         rungekutta;
         if state[1] >= rdatax[ir] then
         begin
{           error := error + SQR(rdata1[ir]-state[9]);}
            ir    := ir + 1;
         end;
         if j mod invh = 0 then
         begin
            SetCurrentWindow(4);
            Setcolor(4);
            SettextStyle(0,0,3);
            Str(state[11]:4:1,s);
            s := s+'h';
            ClearWindow;
            LabelGraphWindow(500,200,s,1,0);
            writeln (dout,state[11]:9,' ',state[1] :9,' '
                         ,state[2] :9,' '
                         ,state[3] :9,' ',state[4] :9,' '
                         ,state[5] :9,' ',state[6] :9,' '
                         ,state[7] :9,' ',state[8] :9,' '
                         ,state[9] :9,' ',state[10]:9,' '
                         ,state[12]:9,' ',state[13]:9    );
         end
      end;
end;


procedure plotmodel;

{This procedure plots the data contained in the output file 5%out.txt    }
begin
   setcurrentwindow(1);
   settextstyle(2,0,4);

   for i := 1 to 12 do
   begin
      assign (modelout,filename);
      reset  (modelout);
      readln (modelout,header);

      j := -1;
      while not Eof(modelout) do
      begin
         j := j+1;
         read       (modelout,plotx[j]);
         for k:= 1 to 12 do
         begin
            read    (modelout,dummy);
            if k = i then ploty[j] := dummy;
         end;
```

```
    end;

    if i = 1 then fac := 0.1000;          { Biomass               }
    if i = 2 then fac := 1.0000;          { Extracellular glucose }
    if i = 3 then fac := 1000.0;          { Intracellular glucose }
    if i = 4 then fac := 1000.0;          { gluc Repressor        }
    if i = 5 then fac := 1000.0;          { G Repressor complex   }
    if i = 6 then fac := 1000.0;          { RNA                   }
    if i = 7 then fac := 0.1000;          { Intracellular GO      }
    if i = 8 then fac := 0.1000;          { Extracellular GO      }
    if i = 9 then fac := 1.0000;          { Gluconic acid         }
    if i = 10then fac := 0.0250;          { Dissolved oxygen      }
    if i = 11 then fac:= 10;              { Oxygen Repressor      }
    if i = 12 then fac:= 10;              { O Repressor complex   }

    for k:= 0 to j do
    begin
       ploty[k] := ploty[k] * fac;
    end;
    str(i,s);
    setcolor(i);
    rr := i/3;
    LabelPlotArea(20+rr,ploty[18],s,1,1);
    LinePlotData(plotx,ploty,j,i,1);

    close(modelout);
  end;

end;

procedure printparam;
begin
  SetCurrentWindow(3);
  SetTextStyle(2,0,3);
  SetUserCharSize(1 ,1 ,1,1);

  ri := 920.0;
  for i := 1 to 10 do
  begin
     s := 'p(';
     Str(i,stemp);
     s := s+stemp;
     Str(param[i]:4,stemp);
     s:= s+') = '+stemp;
     LabelGraphWindow (20,ri,s,0,1);
     ri := ri - 30;
  end;

  ri := 600;
  for i:= 1 to 10 do
  begin
     s := 's(';
     Str(i,stemp);
     s := s+stemp;
     Str(state[i]:5,stemp);
     s:= s+') = '+stemp;
     LabelGraphWindow (20,ri,s,0,1);
     ri := ri - 30;
  end;
  LabelGraphWindow (20,300,'1 - Biom  *0.10',0,1);
  LabelGraphWindow (20,270,'2 - Ex Gl *1.00',0,1);
  LabelGraphWindow (20,240,'3 - In Gl *1000',0,1);
  LabelGraphWindow (20,210,'4 - Repr  *1000',0,1);
  LabelGraphWindow (20,180,'5 - Compl *1000',0,1);
  LabelGraphWindow (20,150,'6 - m-RNA *1000',0,1);
  LabelGraphWindow (20,120,'7 - In GO *1000',0,1);
  LabelGraphWindow (20,90 ,'8 - Ex GO *1000',0,1);
  LabelGraphWindow (20,60 ,'9 - G.A.  *1.00',0,1);
  LabelGraphWindow (20,30 ,'10- D.O.  *0.10',0,1);
end;

{=============================================================================}

begin

initialise;             {Set up the model parameters and intialisations}
initmodel;
initgraph;              {Set up Graphs}
plotdata;               {Plot the experimental data}
printparam;

fmodel;                 {PERFORM INTEGRATION OF MODEL }

filedata;               { close up the model data out (dout) file }

plotmodel;              {Plot the model profiles}

{screendump(3,0,2,2.0,2.0,0,1,0,perror);}

writeln('finished');

readln;

end.
```